;

Department of Materials

Loughborough University

Development of Novel Bio-derived Polymer Composites Reinforced With Natural Fibres and Mineral Fillers

Doctoral thesis by

Abdul Shakoor

Submitted as partial consideration towards the award of
Degree of Doctor of Philosophy

Project Supervisor: Dr. Noreen .L.Thomas

School of Aeronautical, Automotive, Chemical and Materials Engineering,
Loughborough University, United Kingdom

ACKNOWLEDGEMENTS

Though only my name appears on the cover of this report, a great many people have contributed to its production. I owe my gratitude to all those people who have made this report possible and because of whom my research experience has been one that I will cherish forever.

First of all I would like to express my gratitude to Almighty ALLAH; the Most Merciful, and the Most Beneficent, for giving me the strength to complete this project.

I sincerely thank my supervisor, Dr. Noreen Thomas for her enthusiastic support, encouragement and understanding throughout my study at the Materials Department. She allowed me to work independently but was always available when I needed advice. Her extensive professional and research experience has contributed greatly to my work. It would be unfair not to mention the efforts, guidance and support of Dr. Andrew McLauchlin, Dr. Min Zhang and Dr. Jane Clarke during my experimental work.

I would like to thank all administrative and lab staff especially Ray Owens, Andy Woolley, Andrew Lau, Frank Page, Dr. Keith Yendall, Shawn Fowler, Sue Zhou, Faiz, Nik, Arshad, Riaz, Bilal, Asmat, Sajjad, Yasir and workshop Staff for their support, guidance and help.

I would like to thank University of Engineering and Technology Peshawar, Khyber Pakhtunkhwa Pakistan for sponsoring my PhD studies at Loughborough University.

Most importantly, none of this would have been possible without the love, patience and prayers of my brothers and sisters. My wife Sadaf Afsheen, a sweet daughter Kashmala and a lovely son Muhammad Salar Khan, all have been a constant source of love, concern and support all the time. I would like to express my heart-felt love for my daughter and son who always take away my apprehensions with their smiles.

A. Shakoor

Dedicated to

All those innocent people who lost their lives in the ongoing war in Afghanistan and Pakistan.

Table of Contents

LIST OF FIGURES

LIST OF TABLES

LIST OF ABBREVIATIONS

Abbreviations	Explanation
CP	*Copolymer*
DMTA	*Dynamic Mechanical Thermal Analysis*
DSC	*Differential Scanning Calorimetry*
DW	*Dried wood*
Endo	*Endothermic*
ENR	*Epoxidised Natural Rubber*
Exo	*Exothermic*
FTIR	*Fourier Transform Infra – Red (spectroscopy)*
MB1	*Masterbatch 1*
MB2	*Masterbatch 2*
MFI	*Melt Flow Indexer*
NDW	*Non-dried wood*
OM	*Optical Microscopy*
PCL	*Poly (caprolactone)*
PHB	*Poly (hydroxybutyrate)*
PHV	*Poly (hydroxyvalerate)*
PLA	*Poly Lactic Acid*
SEM	*Scanning Electron Microscopy*
T_c	*Crystallization Temperature*
TEM	*Transmission Electron Microscopy*
Tg	*Glass Transition Temperature*
TGA	*Thermal Gravimetric Analysis*
T_m	*Melting Temperature*
WF	*Wood flour*
wt %	*Weight Percent*
XRDA	*X-Ray Diffraction Analysis*

KEY WORDS

Biopolymers, Biodegradable Polymers, Bio-derived polymers, Bio-Composites, PLA, Wood, Flax, Silane, Talc, ENR, DSC, DMA, SEM, TEM

ABSTRACT

Biocomposites exhibit properties like many petrochemical-based polymers composites. They have the potentials be used in the automotive and decking industries and as biodegradable packaging. However, the high cost as well as, poor mechanical and thermal properties have restricted their widespread use. There are a number of technical issues that need to be addressed before bio-composites can be widely used.

In this research Polylactic acid (PLA) composites, reinforced with natural fibres (wood, flax) and mineral fillers (talc) were investigated. The thermal and mechanical properties of the composites were studied by means of Differential Scanning Calorimetry (DSC), Tensile Testing and Dynamic Mechanical Analysis (DMA), while morphology and crystallization processes of the composites were studied by hot stage optical microscopy. The experimental results are also compared with different theoretical models of the response of the composites.

PLA / wood composites were developed by mixing PLA with wood in different ratios using a melt compounding process. PLA/wood (90/10. 80/20, 60/40), PLA/wood/copolymers (85/10/05, 80/10/10, 75/20/05, 70/20/10, 55/40/05, 50/40/10) and PLA/wood/coupling agent (80/20/silane coating) were the three different composite systems that were developed. Adding increasing amount of wood into the PLA, the thermal properties remain unchanged but the mechanical properties increased significantly, bringing a stiffening effect to the composites. Tensile modulus increased from 4.1± 0.6 to 9.8 ± 1.2 (GPa) as the wood content increased from 0 to 40 (wt %), but the tensile strength at break reduced from 43.8 ± 3.1 to 31.8 ± 2.8 MPa. The experimental results of the PLA-wood composites were modelled according to the Halpin-Tsai equation.

The addition of copolymer affected the thermal properties considerably by decreasing the glass transition temperature of the composite. The glass transition temperature dropped from 54 ± 0.7 (^{o}C) to 48 ± 0.36 (^{o}C) when the content of copolymer was increased from 0 to 10 (wt %). The cold crystallization temperature also decreased

from 127 ± 1.41 (°C) to 103 ± 2.58 (°C) when the copolymer was incorporated into the PLA/wood composites. The significant aspect was the occurrence of a double peak in the melting endotherm. The degree of crystallinity also increased from 2 ± 0.83 (%) to 11 ± 1.23 (%) when the amount of copolymer was increased to 10 (wt %).

PLA, flax and expoidizied natural rubber (ENR) composites were also developed using a melt compounding process. The mechanical properties were affected significantly when the flax fibres were mixed with PLA in the ratios of 10, 20 and 30 (wt %). Addition of flax fibres increased the elastic modulus significantly but reduced the tensile strength and strain at break. To improve the toughness of the PLA- Flax composites, ENR was incorporated into the PLA- Flax composites.

In order to balance the modulus of the reinforcement and the matrix, the PLA- Flax and ENR composites were annealed above the glass transition temperature and the degree of crystallinity increased from 2 to 35 (%). The integral blending of PLA, Flax and ENR did not affect the brittle fracture but introducing a masterbatch of flax fibres and ENR into the PLA matrix during melt processing had a considerable effect on the fracture behaviour of the composites. The elastic modulus of the composites decreased due to the elastomeric content in the composites and there was an increase in elongation-to-break.

The effect of talc on the crystallinity and mechanical properties of a series of polylactic acid (PLA) / talc composites was investigated. PLA – talc composites were developed by incorporating different types of the talc into the PLA in the ratios of 10, 20 and 30 (wt %). The composites were prepared by melt blending followed by compression moulding. It was found that talc acted as a nucleating agent and increased the crystallinity of the PLA from 2% to 25%. There was significant improvement in Young's modulus of the composites with increasing talc addition and these results were found to fit the Halpin Tsai model. Thermo-mechanical tests confirmed that the combination of increased crystallinity and storage modulus leads to improvement in the heat distortion properties.

Chapter 1 INTRODUCTION

1.1 Background

The growing usage of synthetic polymers during earlier decades has led to apprehension about the environmental impact caused by plastic waste, which is of widespread concern[1-6]. The ecological aspect of both production and disposal of standard oil-based plastics is presently of concern worldwide[7, 8]. Because of this increased environmental consciousness and the demands of legislative authorities, traditional polymers are being critically considered. This has driven the search for alternatives that are bio-based and biodegradable [1, 2]. The persistence of plastics in the environment, the deficiency in landfill space, concerns over emissions during incineration, as well as entrapment and ingestion hazards of these materials have spurred efforts to develop biodegradable materials. In order to be a competitive alternative, bio-based plastics must have the same desirable properties as obtained in conventional plastics [3, 9].

Bioplastics are polymers that are derived from biological, renewable resources rather than fossil fuels. Some polymers occur in nature and are produced by plants, animals, and microorganisms through bio-chemical reactions [10, 11], whereas others are synthetically produced from renewable resources. For example, starch and cellulose are extracted from plants; Polyhydroxyalkanoates (PHAs) are made by bacterial fermentation, whereas poly (lactic acid) is chemically synthesized from lactic acid derived from corn starch [12]. Included in the category of bio-derived polymers are polyethylene made from bio-ethylene that is produced from ethanol derived from sugarcane.

Biodegradable polymers are polymers, which degrade by the action of microorganisms such as bacteria, fungi and algae. Biodegradable polymers are broken down by micro-organisms and hence become a part of the natural cycle [12]. Many bioplastics are said to be bio-degradable but they are not necessarily so. For

example, polyethylene derived from bio-ethylene is not biodegradable but behaves just like conventional polyethylene. However, most bioplastics are biodegradable. Most biodegradable polymers have oxygen or nitrogen atom in their polymer backbone that is the feature that is mainly responsible for their biodegradability. Synthetic polymers that have only carbon-carbon single bond in their backbone (e.g. polyolefin) are resistant to biodegradation [13-15].

Accordingly, biodegradable polymeric materials can be classified into two distinct groups. Polymers coming from natural/renewable resources like cellulose, starch, PHAs and PLA are grouped as natural biodegradable polymers. Polymers which are synthesized from petroleum sources such as polysteramide, poly (vinyl alcohol), etc. are classified as synthetic biodegradable polymers [8, 16].

Bioplastics have the advantage of lower carbon footprint compared with synthetic polymers. Different kinds of bioplastics exhibit different properties. Problems with bioplastics are lack of commercial availability, low thermal stability, poor mechanical properties (low toughness) and processability, high price and are hydrophilic. Due to poor durability, expensive manufacturing techniques and, in some cases, specialized composting facility requirements, bioplastics are not considered in the broad spectrum of applications [17]. Absorbable medical implants, compostable food packaging containers, bio-waste bags and agricultural mulch films are the major uses of bioplastics [4].

Examples of some important biodegradable aliphatic polyesters are poly lactic acid (PLA) derived from corn starch , polyhydroxybutyrate (PHB) , polyhydroxyvalerate (PHV) synthesized from micro organisms or plants , and polycaprolactone (PCL) derived from chemical synthesis of petroleum [18, 19].

Poly (lactic acid) (PLA) is commonly made from α-hydroxy acids. It is considered biodegradable and compostable. PLA is a thermoplastic, high strength, high–modulus polymer that can be made from annually renewable resources to yield articles for use in either industrial packaging or the biocompatible / bio-absorbable medical device market. PLA can be processed on standard plastic processing equipment to yield molded parts, film, or fibres [20].

The basic building block of PLA is lactic acid, which was first isolated in 1780 from sour milk by the Swedish chemist Scheele and first produced commercially in 1881 [21]. Lactic acid (2-hydroxy propionic acid) is the simplest hydroxyl acid with an asymmetric carbon atom and exists in two optically active configurations. The L (+)-isomer is produced in humans and other mammals, whereas both the D (-) – and L (+) - enantiomers are produced in bacterial systems. Figure 1-1 shows the two stereochemical isomers of lactic acid. The majority of the world's commercially produced lactic acid is made by the bacterial fermentation of carbohydrates [8].

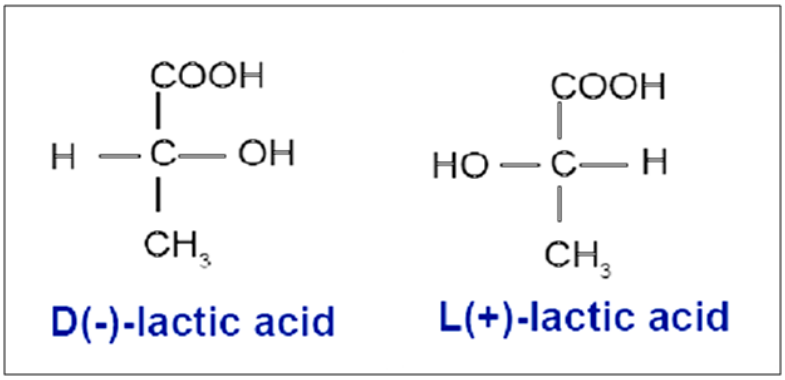

Figure 1-1: Stereochemical structure of lactic acid isomers [8]

The main process for synthesizing PLA is ring-opening polymerization (ROP). Lactic acid is first converted to lactide (dimer of lactic acid) as shown Figure 1- 2. There are three types of lactide dimers: D-lactide, L-lactide and meso-lactide which is then converted by ring-opening polymerisation to poly (lactic acid).

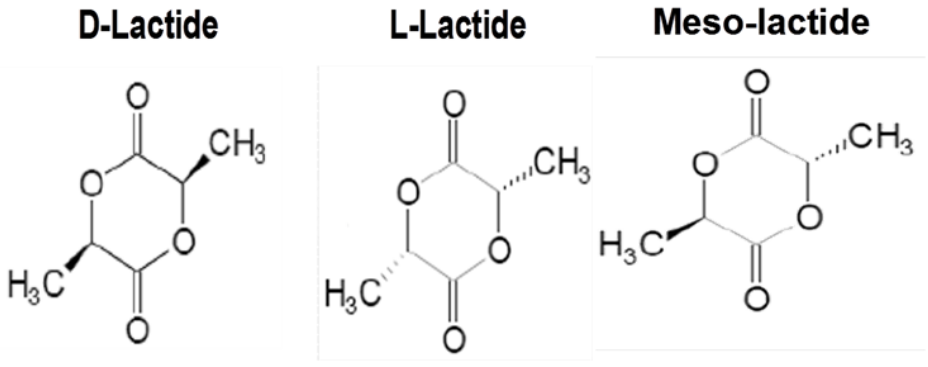

Figure 1- 2: Lactide dimers of Lactic acid [5]

Figure 1- 3 shows the ring opening polymerisation process for PLA. PLA is one of the few polymers in which the optical purity can be easily modified to alter the stereochemical structure on polymerization. Polymerizing a controlled mixture of the

L- or D- isomers yields high molecular –weight amorphous or crystalline polymers that can be used for food contact and are generally recognised as safe [22].

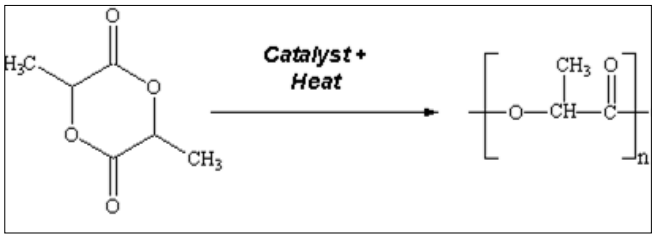

Figure 1- 3: Ring opening polymerization of lactic acid to PLA [5]

Processing PLA on large scale production lines such as injection moulding, thermoforming or extrusion etc., the polymer must have adequate thermal stability to prevent degradation and maintain the molecular weight and properties. PLA undergoes thermal degradation at temperatures above 200° C. Degradation of PLA is dependent on time, temperature, low-molecular-weight impurities and catalyst concentrations. Catalysts can also decrease the degradation temperature and increase the degradation rate of PLA and rheological changes during processing cause poor mechanical properties. Poly (lactic acid) homopolymers have glass transitions and melt temperature of about 55°C and 175°C respectively. PLA requires processing temperatures in excess of 180 - 190°C. At these temperatures, the chain scission reaction leads to loss of molecular weight as well as degradation. High molecular-weight poly (lactic acid) is a colourless, glossy, stiff thermoplastic polymer with properties similar to polystyrene and poly (ethylene terephthalate) (PET). The latter is a commonly used plastic in food packaging applications [21].

There are still a number of technical issues that need to be addressed before widespread use of biosustainable polymers is possible. A significant barrier to the widespread uptake of biosustainable polymers is that their mechanical properties tend to compare unfavourably with existing petroleum-based polymers. Poor mechanical properties and various processing problems restrain their extensive use. For example, strength values are lower than those of the synthetic plastics they would replace so that a component made from biopolymers would need to be accordingly thicker to compensate for lower mechanical properties, which is generally an adverse solution in practice.

Mechanical properties and processing of biopolymers are important parameters in respect of the design and product guarantee. Shortcomings in mechanical properties of different biopolymers may be overcome and sustained by several means like blending and reinforcement. In the past few decades research and engineering interests have been shifting from monolithic materials to fibre-reinforced or particulate filled polymeric composite materials [17]. Generally composites consist of two (or more) distinct constituents or phases. The resulting material has entirely different properties from those of the individual components [13]. Composites combine polymers and fibres, such as aramid, carbon or glass fibres. Natural fibres like wood, flax, jute, hemp etc. are progressively getting more attention [23]. The carbon dioxide neutrality of natural fibres is particularly attractive. Numerous attempts have been made to use natural fibre composites to replace glass fibre composites in non-structural applications. One recent example is automotive components previously made with glass fibre composites are now being manufactured using natural fibre composites [14].

One of the other most important types of composites is that reinforced with mineral fillers and additives. As mentioned above that PLA is considered as an alternative to petrochemical polymers, there is strong demand for extending the range of properties of PLA. For applications of PLA, it is important to enhance some specific properties like rigidity, heat deflection temperature (HDT), tensile strength and processability. If the transparency of the materials is not an issue for an application of PLA, then reinforcement with natural minerals can be a feasible option to address these properties. Different kinds of mineral fillers could be incorporated into with PLA to develop particulate filled PLA composites with improved properties [24]. Despite several advantages of polymers, important properties of the polymers are that possibility to modify the intrinsic physical or mechanical properties by incorporation of certain fillers and additives like talc or calcite in particular. Mechanical properties of the composites can be predicted based on basic principles by adding additives and fillers of various particle shapes [25]. Talc is known as one of the widely used mineral fillers to alter the properties of thermoplastic by developing particulate composites, which could also reasonably improve the properties of polymers such as PLA [26]. This should be studied in order to develop composite technologies and thereby bring

bioplastics into more widespread applications for which they have been identified as being suitable and desirable.

1.2 Rationale and objectives of the study

This thesis investigates reinforcing commercially available polylactic acid (PLA) with natural fibres (wood, flax) and mineral filler (talc), to develop novel biocomposites with improved thermal and mechanical properties. Initial studies have focussed on addition of different levels of wood flour to PLA, followed by addition of copolymers into the matrix to develop novel PLA composites. The effect of silane coupling agent on wood flour was also studied.

In the second stage of the project, flax fibre was incorporated into the PLA to develop composite materials. In order to improve the toughness of the PLA, blends of flax and epoxidised natural rubber (ENR50) were incorporated into the PLA matrix and investigated. Later on, some textile concepts based on sustainable materials were also studied.

In the (later part) of the thesis, talc based particulate PLA composites were developed. All the materials were melt processed and the thermal properties, mechanical properties and morphology of the composites have been studied.

The overall aim was to address some core issues related to PLA i.e. poor mechanical properties and poor thermal stability, by developing composites. The outline of the research plan to achieve these goals is as follows:

- To develop novel PLA composites reinforced with natural fibres and mineral fillers
- Measurement of composite properties.
- Studies on the effect of fibre properties, fibre content, and processing methods on the performance of composites in particular tensile, thermal, viscoelastic properties and morphology.

- Studies on the relationships between fibre characteristics, fibre treatments and composite properties.
- Comparison of the experimental data with the theoretical model for mechanical properties of the composites.

1.3 Structure of the thesis

The layout of this thesis is that of a conventional academic report presenting experimental results. It consists of eight chapters. The graphical story board of the structure of the thesis is given in Figure 1- 4.

In this thesis, Chapter 1, a general introduction to the subject is presented, in addition to the rationale and research goals, and the outline of the report.

Chapter 2 presents relevant literature review in support of the remainder of the thesis. This chapter provides a general understanding of polymers based on renewable resources and their different types. The later part of this chapter is focussed on a specific polymer made from annually renewable resources, polylactic acid (PLA), its composition, chemistry and an overview of its general characteristics.

Chapter 3 presents a relevant generic literature review of bio-composites and their properties. This chapter describes a broad range of biocomposite materials, description of reinforcing natural fibres, their composition and properties. In addition, this chapter contains a brief review of recent work on natural fibre and mineral filler reinforced PLA composites and their properties. Also included is the description of different theoretical models used for prediction of composite properties i.e. mechanical properties in particular.

Chapter 4 covers the details of the materials, methodology and composite processing, preparation of test samples, techniques for characterisation and testing of PLA and PLA composites.

The experimental results of this research are presented in three consecutive chapters (namely Chapters 5, 6 and 7). Chapter 5 covers the results and discussion of the

mechanical analysis using tensile testing, thermal analysis using Differential Scanning Calorimetry (DSC) and Dynamic mechanical thermal analysis (DMTA) for PLA – wood composites and the effect of the copolymer and a silane-coupling agent. The morphology of the tensile fractured samples of the composites is also discussed. The analysis of wood structure is also studied. The results are correlated with the predicted response of the Halpin-Tsai and Lewis & Neilson models.

Chapter 6 presents the results and discussion of the PLA/flax fibre and natural rubber composite properties. This includes results of the tensile properties, flexural properties, DMTA and DSC analysis. SEM images are included to support the above results. Also included are the applications of PLA/flax composites in textile applications of sustainable materials. The experimental results are also compared with the theoretical response based on the rule of mixtures.

Chapter 7 encompasses the results of tensile properties, as well as DMTA and DSC for PLA/Talc composites. Different grades of the talc are used to see the effect of particle size on the mechanical, thermal and viscoelastic properties of PLA/talc composites. Backscattered SEM and Transmission electron microscopy (TEM) images are presented to support the above results where appropriate. In addition to the above the measurements are compared with results predicted from the Halpin-Tsai model.

Chapter 8 summaries the main conclusions of this investigation and also suggests a number of points which are worthy of further investigation.

1.4 **Publications**

The following journal and conference papers have been prepared from this study.

1. **A. Shakoor** and Noreen.L.Thomas (2013), "*Talc as a Nucleating Agent and Reinforcing Filler in Poly Lactic Acid (PLA) Composites*", Journal of Polymer Engineering and Science (Accepted for publications).

2. **A.Shakoor**, M. Carandente, N.L.Thomas and L.Masica, "*Toughening of Polylactic (Acid) composites with flax fibres and Epoxidised Natural Rubber (ENR)*" Written up for submission in Journal of Advances in Polymer Technology.(In preparation)

3. **A. Shakoor**. R. Muhammad, N.L.Thomas and V.V Silberschmidt, "*Mechanical and Thermal Characterisation of Poly (L- Lactide) Composites reinforced with Hemp Fibres*", Submitted to Dynamic Deformation and Fracture of Advanced Materials Conference (D2FAM 2013), Loughborough University, 9-11 Sep, 2013 (Accepted for publications).

4. F. Kane, **A. Shakoor**, D. Vardy, N.L. Thomas (2012), "*The Significance of Craft in the Development of Sustainable Textile Materials: Localism, Digital Technologies and Emotional Durability*" Making Futures Conference Journal, Volume 2, P 90-100 (ISSN 2042-1664), Plymouth College of Art (Published).

5. F. Kane, **A. Shakoor**, D. Vardy, N.L. Thomas (2011), "*Essamplaire: An approach to working on the technology, art and design interface in Textile*", Ambience'II, Boras Sweden, 28-30 Nov (ISBN 978-91-975576-7-2 (56-59) (Published).

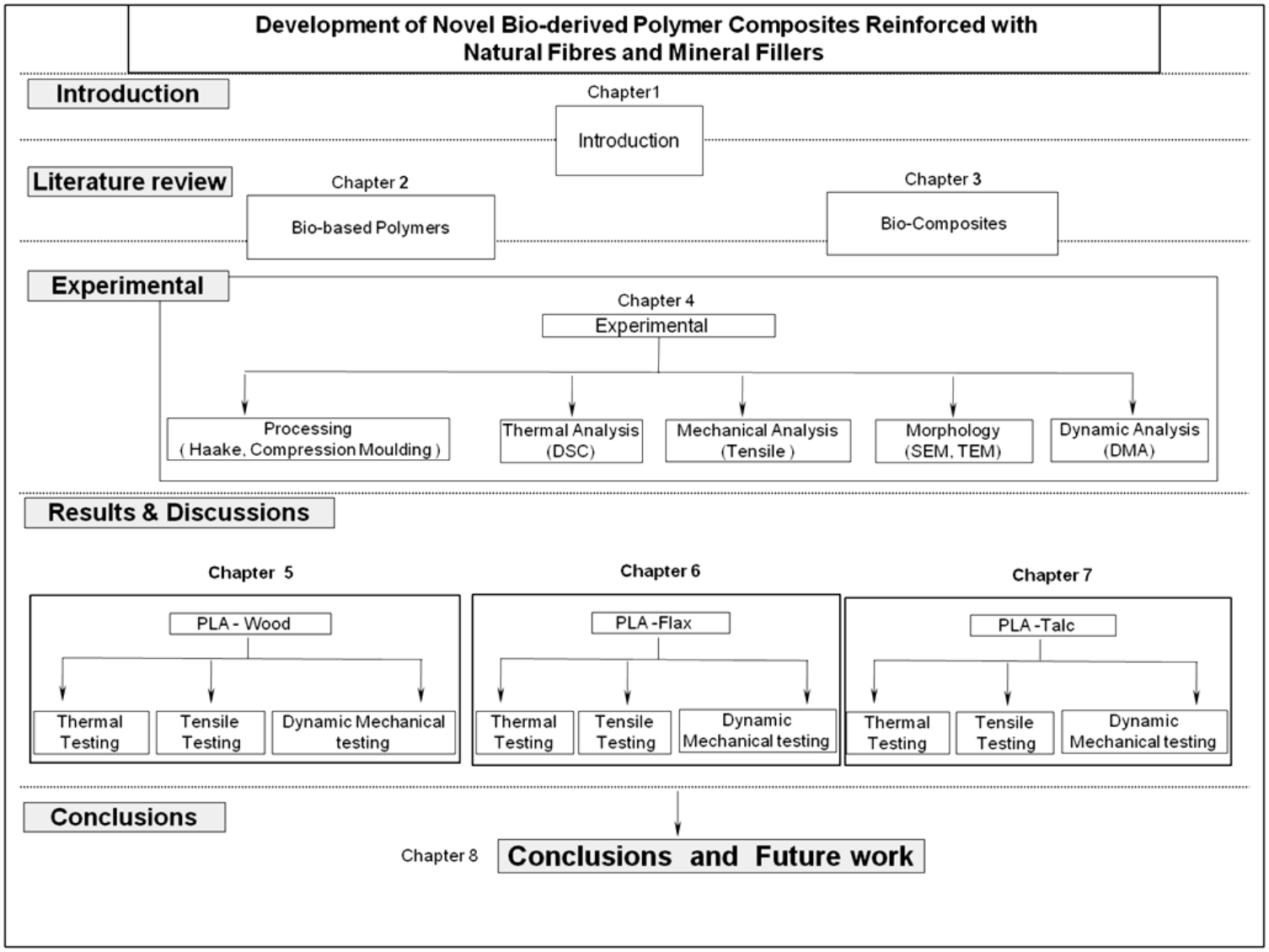

Figure 1- 4: Structure of the thesis

Chapter 2 BIO-BASED POLYMERS

2.1 Introduction

Research is underway around the world on commercial development of 'greener' polymer technologies. There has been a growing search for new materials with high performance at affordable costs in recent decades. The principle of 'going green' has diverted this search towards eco-friendly materials. Words like renewability, recyclability and sustainability have become the particular focus of growing environmental awareness. The divergence from non-renewable to renewable materials is becoming the centre of interest for research in industrial communities around the world. The development or selection of materials to meet the structural and design challenges calls for a compromise between conflicting objectives. These efforts have led to the development of materials adhering to the green philosophy. The fact is that environmental legislation is the driving force behind the development of these materials [13]. Originally plastics were designed to be durable and were synthesized from petrochemical resources, mainly crude oil. But nowadays focus has shifted to polymers originating from bio-based renewable sources, which may be biodegradable [27]. The shortage of synthetic raw materials and the depletion of petroleum resources has forced the world market to hit the highest prices ever [28]. The shortage and rise in price of petrochemical resources have resulted in the strong demand for plastics based on renewable resources i.e. bio-based materials. Bio-based materials should ease disputes on eco- pollution and reliance on fossil resources [28, 29].

Currently, there is considerable interest in bio-based polymers which seems to be a potential alternative to traditional plastics, thus reducing the environmental impact caused by plastic wastes. Industrial ecology, eco-efficiency and green engineering are guiding the next generation of products and processes [30]. Bio-based polymers are moving into the mainstream applications changing the dynamics of 21st century materials. Biopolymers, bio-based and biodegradable are the words which are becoming more important in the world of industrial plastics. These materials have

not only been a motivating factor for the materials scientists but also it provides potential opportunies for improving the standard of living of people around the world [12]. Before going into details these words need to be distinguished with respect to their meaning.

Bio-based polymer is the term used to describe a variety of materials. However they generally fall into two principal categories [22].

a. **Biopolymers** are polymers that are produced by biological systems such as microorganism, plants, and animals.
b. **Bio-derived polymers** are polymers that are synthesized chemically but their monomers are derived from biological starting materials such as amino acids, sugars, natural fats or oils.

2.2 Biopolymers

Polymers that are produced by plants, animals and microorganisms through metabolic reactions are called natural or nature's polymers. They are also called biological polymers or simply biopolymers. Carbohydrates such as cellulose and starch, and proteins like keratin and enzymes are therefore counted as biopolymers [10]. The Structure of the biopolymer affects its functional nature. The functional capability of biopolymers is mostly dependent on the crystalline nature of the materials. Hence, cellulose or poly (beta-D-glucose) is a structural polymer whose properties arise in part from its crystalline nature. But, in contrast, starch or poly (alpha-D-glucose) is an energy storage polymer. Starch is an important food (energy) source for humans, but physical or chemical treatment can transform it into a useful structural material for packaging applications [23]. Also chemically modified celluloses (e.g. Cellulose acetate) are found in a wide range of applications. Modified cellulose is used in the manufacture of paint, plaster, adhesives, cosmetics and pharmaceutical film coating and numerous other products [10].

A family of compounds known as polyhydroxyalkanoates have received much attention as biosustainable materials because they are produced more easily in quantity by fermentation of carbon–rich substrates by microorganisms particularly bacteria. Poly (beta-hydroxybutrate) or PHB is important in this group.

2.3 Bio-derived Polymers

Polymers that are derived from renewable resources are considered as bio-derived materials. This category excludes fossil carbon sources such as crude oil and coal. Bio-derived materials means materials derived from replenishable natural resources. Inherently bio-derived material has the principal that supply will always meet the demand, a situation that is unlikely ever to occur in the case of fossil carbon. Bio-derived polymers include aliphatic polyesters, the centre of interest nowadays. Poly (lactic acid) or PLA is the most promising polymers in this group. PLA is an important example of a bio-derived polymer. The monomer, lactic acid, is derived from fermentation of sugar.

2.4 Biodegradable Polymers

Biodegradable materials are those that will degrade completely by the action of microorganisms like fungi or bacteria. Accordingly, many researchers have discussed biodegradable polymers, but a standard definition of biodegradable materials has not yet been established. All the definitions already in place correlate the degradability of a material to a specific disposal environment [31]. One well accepted definition reads "*materials obtained from nature or by a synthetic route, whose chemical bonds are cleaved at least in one step by enzymes from a biosphere" [27].* In addition, we can add to this "according to required conditions". Thus, specific environmental conditions such as favorable pH, humidity and temperature must be met for satisfactory degradation to take place. These factors affect the rate of biodegradation. According to Albertson and Karlsson, biodegradation is defined as "*an event which takes place through the action of enzymes and / or chemical decomposition associated with living organisms (bacteria, fungi, etc.) and their secretion products*"[32].

The basic requirements for a material to be declared compostable are based on[13];

1. Complete biodegradability of a material, measured by a respirometric test like ASTM D5338-92, ISO/CD 14855 and corresponding CEN draft or modified strum tests ASTM D5209, in a time compatible with composting technology.

2. No adverse effects on compost quality and in particular any toxic effects of compost and leachates on the aquatic and terrestrial organisms.

3. Disintegration of the material during the fermentation phase

4. To be described as compostable, a plastic must conform to international standards EN13432 and ASTM D6400 and biodegrade within 180 days.

If a material is composed of carbohydrates, it will degrade into carbon dioxide (CO_2) and water (H_2O) ultimately which is the end product of any organic material comprising only carbon, oxygen and hydrogen.

2.5 Classification of Bio-based Polymers

Polymeric materials come from a variety of renewable and non-renewable sources such as plants (cellulose, chitin, vegetable oils, etc.), bacteria, as well as petroleum (aliphatic /aliphatic –aromatic co-polyester[9, 33]. Biodegradable materials have been classified accordingly as natural or synthetic depending on their origin. But bio-based polymeric materials can be divided into three main categories according to their origin.

Category 1: Biopolymers directly extracted /removed from biomass. Examples are polysaccharides such as starch and cellulose and proteins like casein and gluten.

Category 2: Polymers produced by classical chemical synthesis using renewable bio-based monomers. A good example is the poly lactic acid, a biopolyester polymerized from lactic acid monomers. The monomers themselves may be produced via fermentation of carbohydrate feedstock.

Category 3: polymers produced by microorganisms or genetically modified bacteria. To date, this group of bio-based polymers consist mainly of the polyhydroxyalkonoates, but developments with bacterial cellulose are in progress.

A summary of bio-based polymers is shown in Figure 2- 1, which is a generic overview of bio-based materials [9, 34].

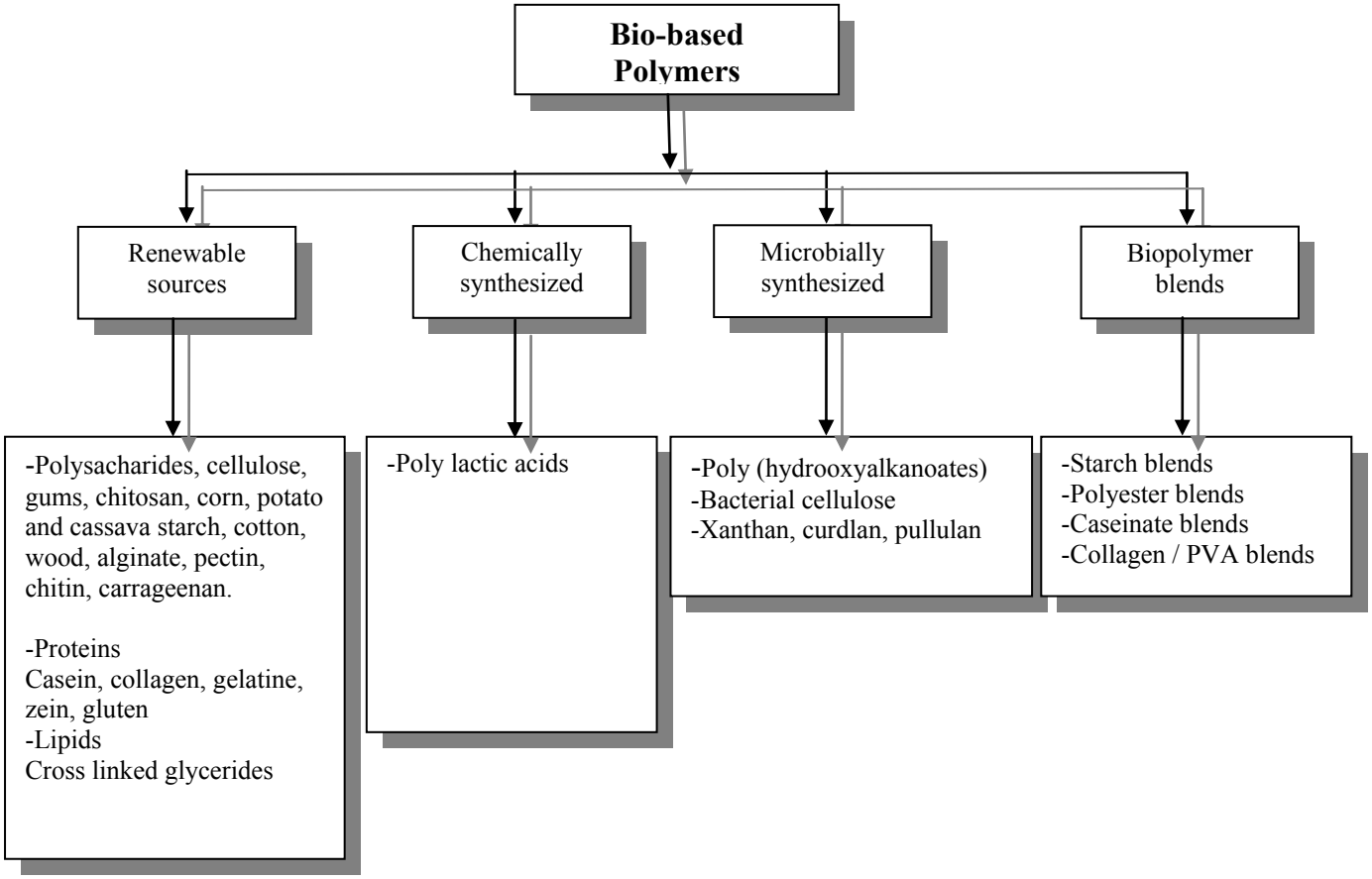

Figure 2- 1: Classification of bio-based polymers and nomenclature [7]

2.6 Properties of Bio-based Polymers

Various properties of bio-based polymers reviewed from a number of research articles are given below in Table 2- 1. The table describes the comparative range of various physical, mechanical and thermal properties of different bio-based materials. Upper and lower limit of density, tensile strength, modulus of elasticity, percentage strain, glass transition and melting temperature are presented in the table.

It is clear from the table that densities of all bio-based polymers lie between 1.2 to 1.8 (g/cm^3). The table also summarizes the thermal properties; the glass transition and melting temperatures are listed. There is not much difference in the glass transition temperatures for most of the bio-based polymers. PLA, the most common bioplastic, has a glass transition around 50 ~ 60 ^oC and most of the polymers in the same category lie in the range between 45 ^oC (lower limit) to 65 ^oC (upper limit), while the melting range lies between 150 and 200 ^oC, depending on molecular weight and structure. One bioplastic, PCL (Poly-ε-Caprolactone) has a low glass transition temperature (-60 to -65 ^oC) and a melting temperature between 58 and 65 (^oC).

The table also lists the comparative analysis of different mechanical properties like tensile strength, elastic modulus and percent strain. It is clear from the table that percent strain is low for most of the polymers except PCL which has quite high percentage tensile strain. The elastic moduli of the bioplastics listed in the table are quite high and it seems that these materials are brittle in nature. The exception again is PCL with a much lower modulus.

Table 2- 1: Mechanical, thermal and physical properties of various bio-derived polymers [5]

Properties	**Limits**	**Type of Biopolymer**							
		Poly-Lactide (PLA)	**Poly (L)-Lactide (L-PLA)**	**Poly(DL)-Lactide (DL-PLA)**	**Poly-Glycolide (PGA)**	**DL- PLA/PGA 50/50**	**DL- PLA/PGA 75/25**	**Poly-ε-Caprolactone (PCL)**	**Polyhydroxy-butyrate. (PHB)**
Density , ρ (g/cm^3)	L.L / U.L	*1.21 / 1.25*	*1.24 / 1.30*	*1.25 / 1.27*	*1.50 / 1.707*	*1.30 / 1.40*	*1.3 / --*	*1.11 / 1.46*	*1.18 / 1.262*
Strength, σ (MPa)	L.L / U.L	*21 / 60*	*15.5 / 15.0*	*27.6 / 50*	*60 / 99.7*	*41.4 / 55.2*	*41.4 / 55.2*	*20.7 / 42*	*40 / --*
Elastic Modulus, E (GPa)	L.L / U.L	*3.45 / 3.83*	*2.7 / 4.14*	*1 / 3.45*	*6.00 / 7.00*	*1 / 4.34*	*1.38 / 4.13*	*0.21 / 0.44*	*3.5 / 4*
Strain, ε (%)	L.L / U.L	*2.5 / 6*	*3 / 10*	*2 / 10*	*1.5 / 20*	*2 / 10*	*2.5 / 10*	*300 / 1000*	*5 / 8*
Glass Transition Temperature, Tg (^{0}C)	L.L / U.L	*45 / 60*	*55 / 65*	*50 / 60*	*35 / 45*	*40 / 50*	*50 / 55*	*-60 / -65*	*5 / 15*
Melting Temperature, Tm (^{0} C)	L.L / U.L	*150 / 162*	*170 / 200*	*am*	*220 / 233*	*am*	*am*	*58 / 65*	*168 / 182*

Note: am: amorphous polymers and thus no melting point, U.L: Upper limit, L.L: Lower limit

2.7 Polylactic Acid (PLA)

Materials based on renewable resources are proving to be a viable alternative to petrochemical-based plastics for many applications [35]. Of these materials poly lactic acid (PLA) has received enormous attention. PLA was the first commodity bioplastic and seems to be a potential substitute to replace synthetic polymeric materials for a number of applications. The manufacture of PLA is claimed to be highly versatile, and derived from completely renewable resources [36].

PLA belongs to the family of aliphatic polyesters commonly made from α-hydroxy acids and is considered biodegradable and compostable. PLA exists in a helical configuration with an orthorhombic unit cell. It is a thermoplastic, having high strength and modulus, produced from natural resources to use in industrial packaging or biomedical applications. It can be easily processed on standard plastic equipment to yield molded products [21]. In spite of its excellent balance of properties, its commercial viability has historically been limited by high production cost. Because of this PLA has enjoyed little success in commodity applications and is mostly used in biomedical applications. The significant intention of bringing down the production cost, will definitely place PLA as a widely used polymer in future [7, 37]. PLA is a unique polymer that in many ways behaves like PET, but also can perform like polypropylene (PP). Ultimately, it may be the polymer with the broadest range of applications because of its ability to be stress or thermally crystallized and its capability to be processed on most common plastics processing equipment. It can be formed into transparent films, fibres or injection molded. Figure 2- 2 shows comparison between PLA and polypropylene (PP) properties. High modulus indicates that PLA is comparatively brittle compared with PP. The modulus for PLA is significantly higher, but the PP seems to be tougher compared with PLA.

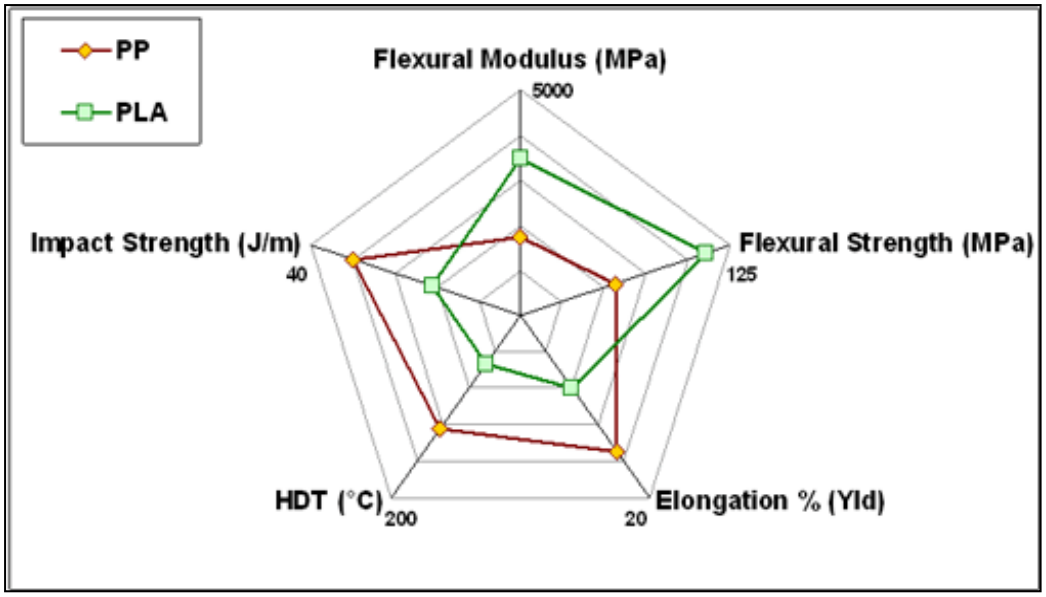

Figure 2- 2: Comparative analysis of properties of PLA and PP [4]

2.8 Synthesis of PLA

The basic building block of PLA is lactic acid. Synthesis of PLA is a multistep process which starts from the production of lactic acid and ends with its polymerization. Lactic acid (2-hydroxy propionic acid) is the simplest acid with an asymmetric carbon atom and exists in two optically active configurations. The L (+) and D (-) are the two enantiomers that are produced in bacterial systems. The majority of the world's lactic acid is made by bacterial fermentation of carbohydrates [10, 21]. PLA is synthesized by following three methods:

1. Polycondensation of Lactic acid
2. Dehydration Condensation
3. Ring –opening –Polymerisation (ROP) of lactides

This is illustrated in Figure 2- 3. Firstly lactic acid can be condensation polymerized to yield the low- molecular- weight, brittle polymer which for most of the products is unusable. Condensation polymerization is the least expensive route, but it is difficult in a solvent-free system to obtain high molecular weights and modifier (coupling agent or esterification) is required to increase chain length, which causes additional

cost and complexities. The second route is the azeotropic dehydration condensation of lactic acid. It can yield high molecular weight PLA without employing any chain extender or special additives. The third and main process is the ring-opening-polymerisation (ROP) of lactide to obtain high molecular weight PLA, patented by Cargill Dow (US) in 1992 [11].

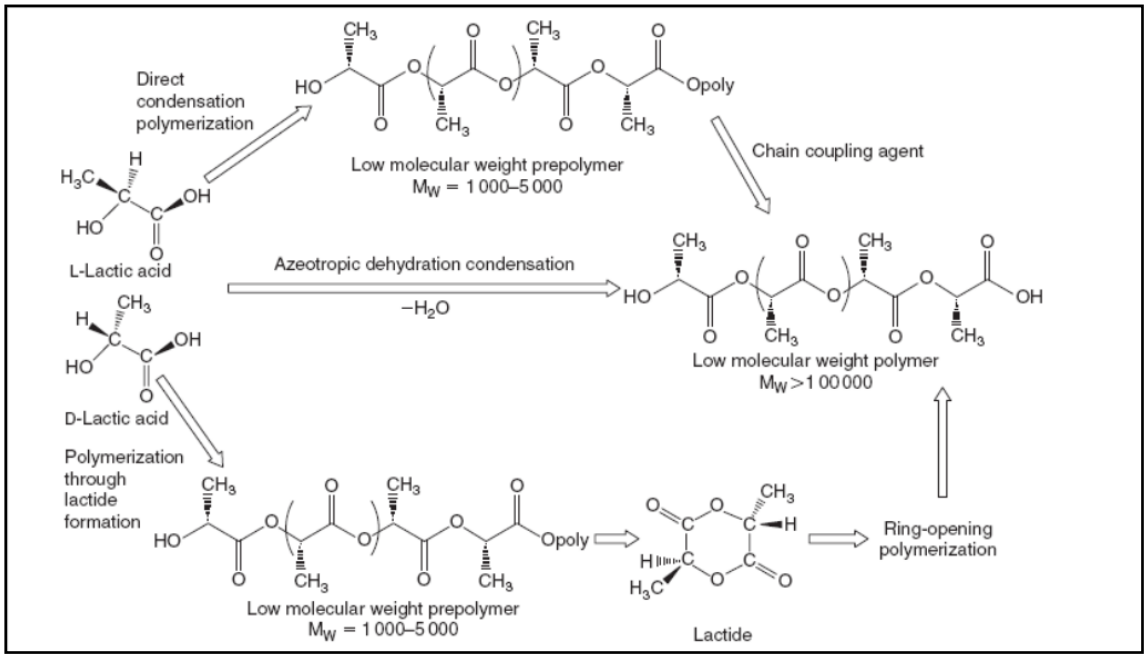

Figure 2- 3: Synthesis method for obtaining high molecular PLA [10]

2.9 Life Cycle Analysis

Recently products, processes and technology have been evaluated generally for their sustainability. Technologies utilized to produce different products or to process various materials, which use more energy, deplete natural resources, pollute the environment or emit greenhouse gases, are considered as less sustainable. The best way to measure the sustainability of the product or process is to do a life cycle analysis (LCA).

Figure 2- 4 shows the fossil energy requirements for some petroleum based polymers and polylactides. The figure shows that first generation Poly lactide production

system (PLA) uses 22-55 % less fossil energy than petroleum based polymers. The key finding is the potential for environmental benefits for polymers made from renewable resources [3].

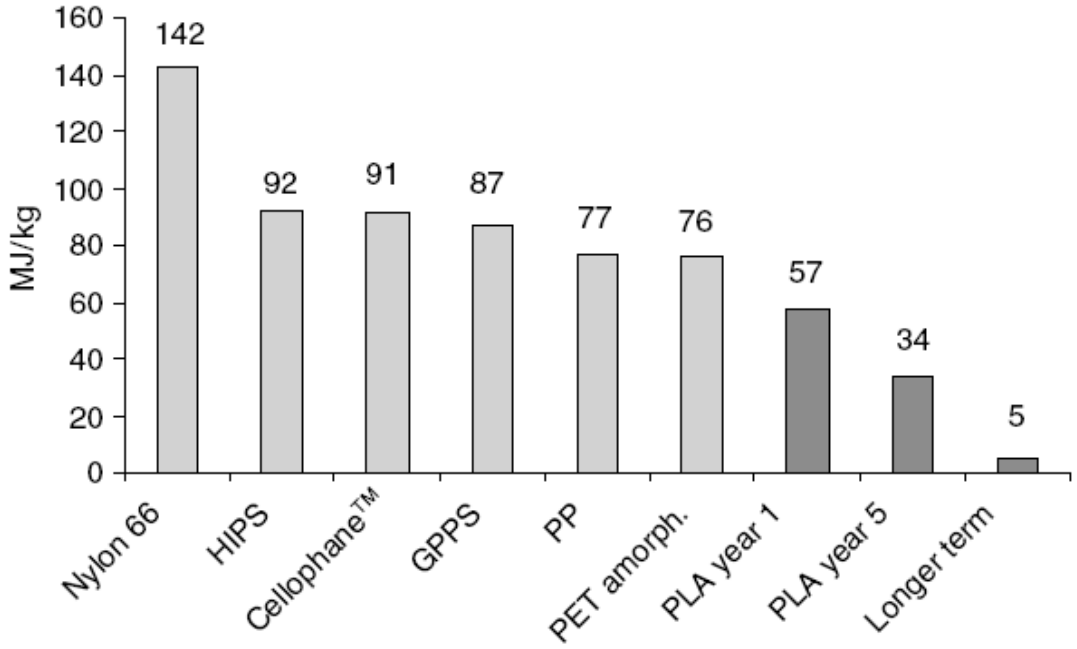

Figure 2- 4: Energy requirements producing various polymers [8]

PLA has a low greenhouse emission compared with other thermoplastic polymers. Cargill Dow has undertaken a comparative analysis of the contributions to global climate change for a range of petrochemical-based polymers and three different PLA systems. Figure 2- 5 shows the contribution to green house gas emission for some petrochemical polymers and the three polylactide polymer systems [3].

PLA is also a low-impact, greenhouse gas polymer because the CO_2 generated during PLA biodegradation is balanced by an equal amount taken from the atmosphere during the plant feedstock's growth. While in contrast petrochemical-derived plastics contribute to volatile organic compound (VOC) emission and CO_2 generation when incinerated. LCA calculations indicate that PLA has a greenhouse gas emission rate of 1600 Kg CO_2 / metric ton, while PP, PS, PET and nylon have greenhouse gas values of 1850, 2740, 4140 , and 7150 Kg CO_2 / metric ton respectively [2, 3, 38].

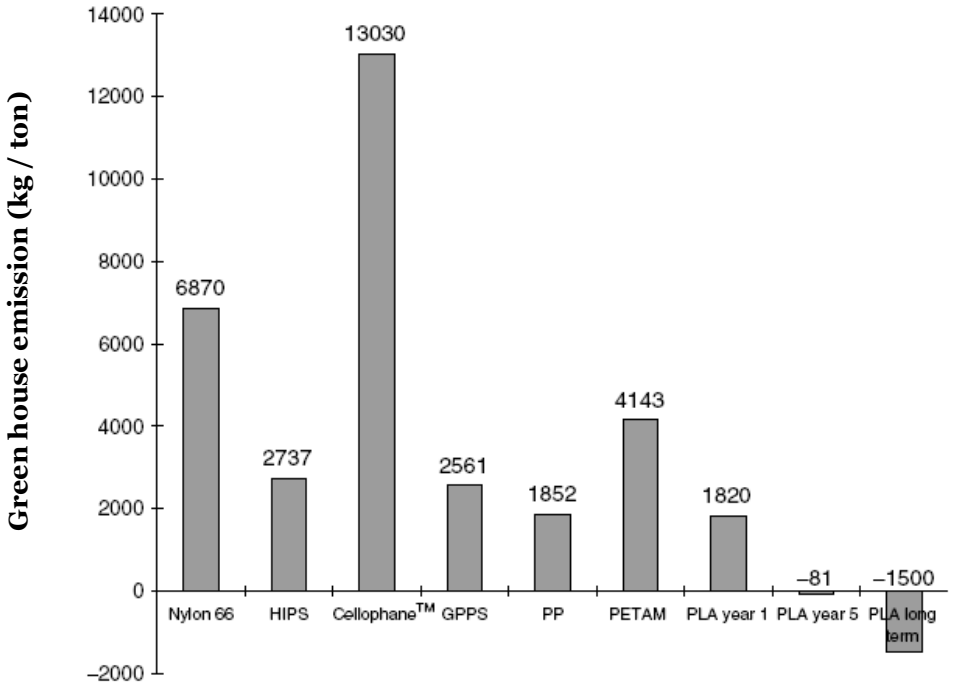

Figure 2- 5: Green-house emissions of various polymers [3]

Apart from composting or biodegradation, PLA can also be recycled chemically and can be utilized to form lactide and convert into PLA again. Figure 2- 6 shows the different steps involved in the process of chemically recycling by converting PLA into lactic acid and then back to PLA by ring opening polymerization.

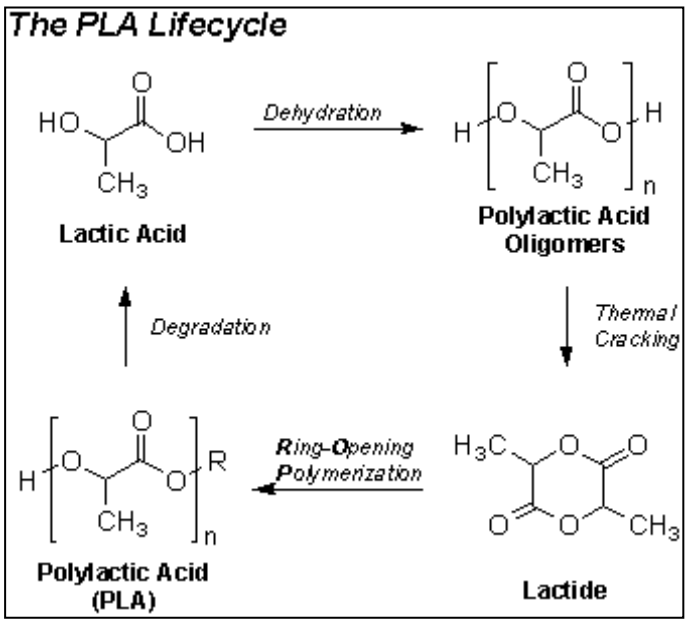

Figure 2- 6: Process chain of chemical recycling of PLA [1].

2.10 **Stereoisomeric nature of PLA**

Lactic acid (2-hydroxy propionic acid) is the simplest hydroxy acid with an asymmetric carbon atom and exists in two optically active configurations. One is L (+)-isomer and second is D (-)-isomer. The L (+)-isomer is produced in humans and other mammals, while the D (-) - and L (+) - enantiomers are produced in bacterial systems[21]. Figure 2- 7 shows the lactides of lactic acid. When L (+) & D (-) isomers of lactic acid, same or different isomers are combined with each other, they form lactide. When L & L (+) combine they form L (+)-Lactide, D & D (-) form D (-)-Lactide and when L (+) and D (-) combine they form meso-Lactide. There are three different lactides of PLA. Lactide is then converted via ring opening polymerization (ROP) to poly lactic acid [2].

The stereoisomeric nature of PLA and the existence of three different lactides makes the structure completely isomerism dependent. The stereochemical make up of the lactide monomer stream determines the stereochemical composition of the resulting polymer [4, 7] . Due to the steroisomeric nature of lactic acid, several distinct forms of Polylactide exist: poly-L-Lactide (PLLA) the product resulting from polymerization of L and L-lactides; poly-D-Lactide (PDLA) the product resulting from polymerization of D and D-lactides; poly-DL-Lactide (PDLLA) the product resulting from the polymerization of a racemic mixture of L- and D-lactides [39]

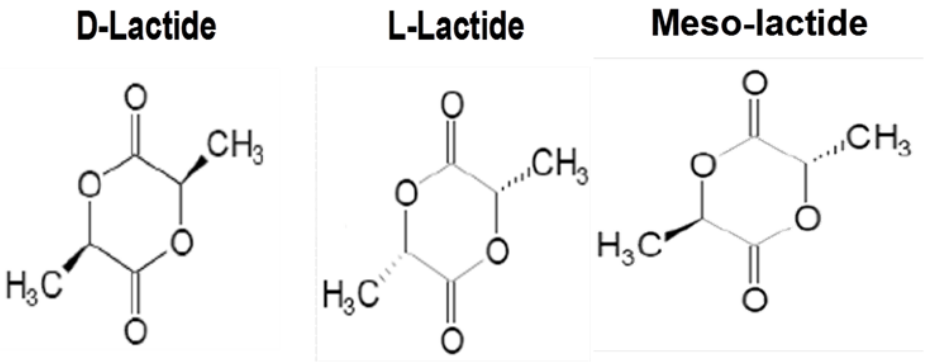

Figure 2- 7: Sterioisometric Lactides of Lactic acid [2]

The optical purity of the monomer has a great effect on physical, mechanical properties and biodegradability of PLA. PLA polymers may be either amorphous or semicrystalline at room temperature, depending on the L-to D lactic acid ratio. The

homopolymer PLA resulting from polymerization of pure L, L- or D, D-lactic acid and high L, L-or D, D-Lactic acid copolymers have very regular structures to form a crystalline phase. For example, PLLA is a hard, transparent and crystalline polymer having a crystallinity of 37 (%), a melting temperature of about 170-180^{o}C and a glass transition temperature of 50-60 ^{o}C [40]. PLA polymers containing more than 93 (%) of L, L-lactic acid are semicrystalline, while PLA with 50-93 (%) L, L-lactic acid is amorphous. The presence of both meso-and D-lactide forms produces imperfections in the crystalline structure, reducing the percent crystallinity [35].

2.11 **Physical properties of PLA**

A review has been published which includes details of the properties and characteristics of PLA. Physical properties of PLA polymers as well as other polymers depend on their molecular characteristics as well as ordered structures such as degree of crystallinity, the size of the spherulite, morphology and degree of chain orientation. These reviews discussed the variety of structures and their thermal and mechanical behaviour. In the solid state PLA can be either amorphous or semicrystalline depending on the stereochemistry and thermal history [4].

Above *Tg,* amorphous PLA transforms from glassy to rubbery states and will behave as a viscous fluid upon further heating. Below *Tg,* PLA behaves as a glass with the ability to creep until its β transition temperature of approximately -45^{o} C. Below this temperature PLA will only behave as a brittle polymer [41]. For amorphous PLAs, the glass transition (*Tg)* determines the upper use temperature for most commercial applications. For semicrystalline PLA, both the *Tg* (~ 58 ^{o}C) and melting point (T_m), 130 -180 ^{o} C (depending on stereochemical structure) are important for determining the use temperature across various applications [21] . Both of these transitions, *Tg and* T_m, are strongly affected by overall optical composition, primary structure, thermal history and molecular weight [41].

2.11.1 Amorphous PLA

For amorphous PLA, the glass transition temperature (*Tg)* is one of the most important parameters as dramatic changes in polymer chain mobility take place on and above the *Tg*. The behaviour of amorphous PLA is shown in Figure 2- 8 , as a representative case of high molecular weight amorphous polylactide [6]

The figure shows that below the β-relaxation temperature T_β, PLA polymers are completely brittle. Between the T_β and *Tg* the amorphous polylactide undergoes physical aging and can show a brittle or ductile fracture. In transition between 110–150^{o}C, PLA changes from rubbery to viscous which is mainly dependent on the molecular weight and shear stress [4]. Amorphous PLA can be processed within the range of *Tg* and viscous liquid (58 -215 ^{o}C) [4, 42]. Processing PLA above 215^{o}C, decomposition of PLA starts and finally, amorphous PLA decomposes between 215 and 285^o C. Properties of amorphous PLA depend in part on how far below the *Tg* the product is used or stored [6, 43] . Figure 2- 8 shows how the metastable state of high molecular weight PLA responds to different temperatures.

2.11.2 Semicrystalline PLA

PLA resin containing more than 93 % of L-Lactic acid is semicrystalline. For semicrystalline polylactide, both the *Tg* and melting temperature (Tm) are important physical parameters for predicting PLA behaviour. For semicrystalline polylactide, the melting temperature is a function of the processing conditions and the stereochemistry of the polymer. Typical high molecular weight semicrystalline PLA is shown in Figure 2- 9.

The crystalline melting temperature, Tm, depends on the presence of meso-lactide in the structure. For semicrystalline PLA, *Tg* indicates the transition between brittle and ductile fracture. The maximum practically obtainable melting point of stereochemically pure Polylactide (either L-or D-) is around 180 ^{o} C with an enthalpy (heat of fusion (ΔH_m)) of 40-50 J.g^{-1} (crystallinity is 42 -53 %).

The processing window is narrower due to the crystallinity of semicrystalline PLA. Semicrystalline PLA can be processed between 130 and 207 ^{o}C when PLA is behaving as a viscous liquid. Above ***Tg*** and below 130^{o} C, PLA exists in ductile (leathery or tough) condition. Like amorphous PLA, semicrystalline PLA also undergoes decomposition between 215 and 285 ^{o}C [4, 6, 43]. Figure 2- 9 shows how the metastable state of high molecular semicrystalline PLA depends on temperature [6].

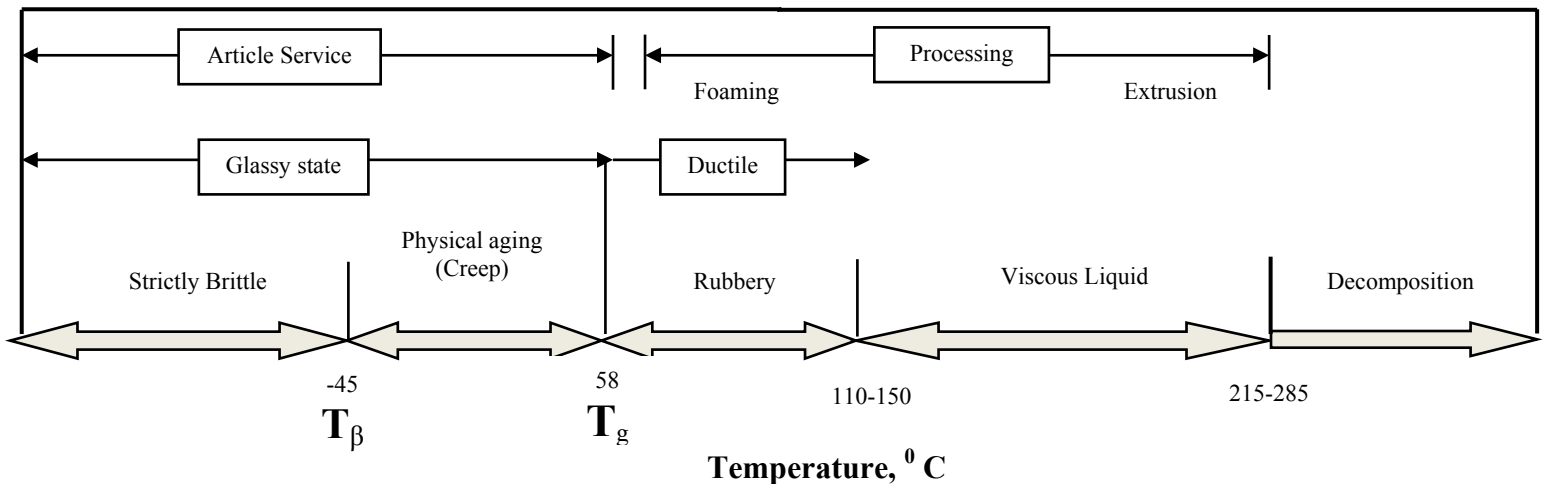

Figure 2- 8: Metastable state of high molecular weight amorphous Polylactides [4]

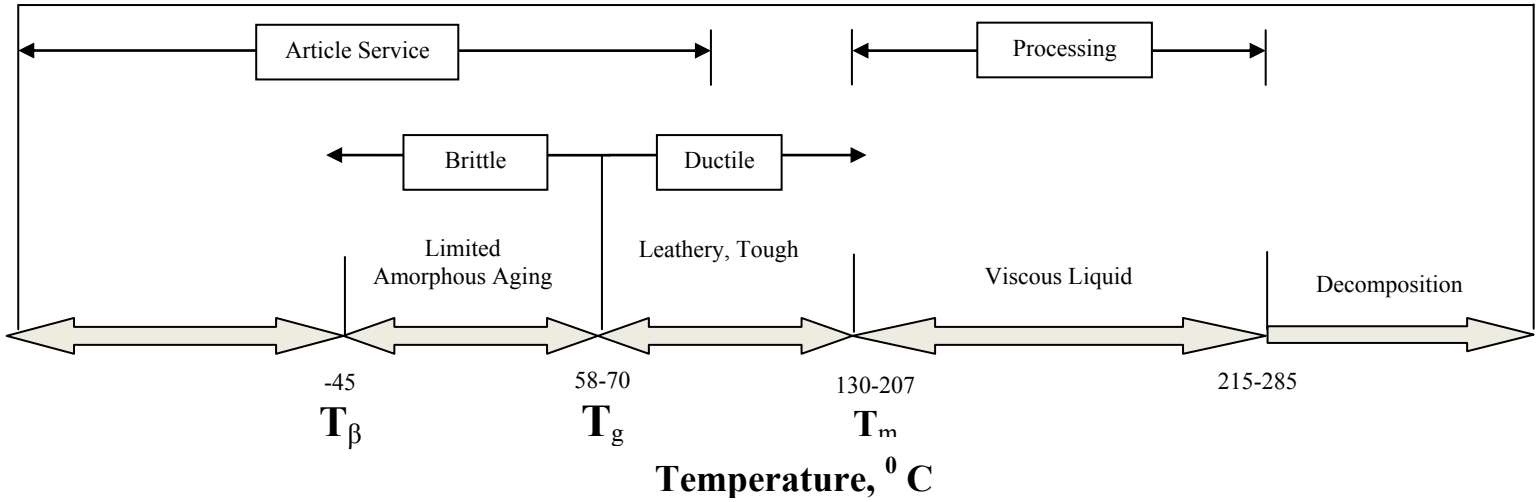

Figure 2- 9: Metastable state of high molecular weight semcrystalline Polylactides [4]

Qualitative and quantitative analysis and understanding of the transition temperature along with other polymer properties are important to identify polymer applications. Polymer melting temperature increases with a rise in molecular weight M_w but on the other hand the crystallinity of the samples decreases with increasing M_w [38]. The glass transition temperature is also determined by the proportion of the different lactides present. This results in PLA polymer with a wide range of hardness and stiffness values. Typical PLA glass transition temperature (*Tg)* ranges from 50°C to 80°C while the melting temperature ranges from 130°C to 180°C [6, 44]. Glass transition temperature (***Tg***), melting temperature (T_m) and enthalpy of fusion (ΔH_m) for two grades of PLA , PS and PET films are given below in Table 2- 2, measured according to ASTM D 3418-9 and ASTM D 3417-97 [45].

Table 2- 2: Physical properties of PLA (98 % L-lactide), PLA (94% L-Lactide), PS and PET

	PLA (98 % L-Lactide)	**PLA (94 % L-Lactide)**	**PS(atactic)[b]**	**PET**
Tg (°C)	*71*	*66*	*100*	*80*
Relaxation enthalpy **(J.g^{-1})**	*1.4*	*2.9*	*N/A*	*N/A*
T$_m$ (°C)	*163*	*140*	*N/A*	*245*
Relaxation enthalpy **(J.g^{-1})**	*37*	*21*	*N/A*	*47.7*
Crystallinity (%)	*40*	*25*	*N/A*	*38*

***b**: PS used in packaging is actatic, so it does not crystallize. Since it is an amorphous polymer, it does not have a defined melting point but it gradually softens through a wide range of temperatures [4, 45].*

2.11.3 Crystallinity

Poly (lactic acid) is a slow-crystallizing material, similar to poly (ethylene terephthalate). A review can be found on the crystallization kinetics of polylactides. It has been found that poly (L-Lactide-co-meso-lactide) ranging from 0 % to 9 % meso-lactide showed that crystallization kinetics are strongly dependent on the stereochemical (copolymer) composition [46]. PLLA can crystallize in the presence of D-Lactide. However, as the structure becomes more disordered, the size of spherulites and the time for crystallization increases [44].

Degree of crystallinity of PLA depends on different factors which strongly affect the crystallization like;

- *Morphology*
- *Crystallization kinetics*
- *Stereocomplex*
- *Stress induced crystallization*

The morphology of PLA crystals is influenced by the chemical composition and thermal history. The spherulitic growth is decreased due to decrease in nucleation density, which leads to larger spherulites with increasing crystallization temperature [2, 47]. Melt-crystallized polymers are never 100 % crystalline because of chain entanglements in the melt. The degree of crystallinity is of technological importance [47]. PLA literature shows the enthalpy of fusion for 100 (%) crystalline PLLA or PDLA homopolymers is ($\Delta \mathbf{Hm^0} = \mathbf{93.1}\frac{\mathbf{J}}{\mathbf{g}}$) and Equation **2- 1**, shown below, is used to calculate the percent crystallinity for DSC scans [13, 21]:

$$Crstallinity(\%) = \left[\frac{\Delta H_m - \Delta H_c}{93.1}\right] * 100$$

Equation 2- 1: Percent Crystallinity of PLA

Where ΔH_m , is the measured heat of fusion and ΔH_c , is enthalpy of cold crystallization.

The optical purity is a common nomenclature to describe the polymers of this variety. The crystallinity is affected when there is any change in optical purity (OP). As the optical purity decreases, the crystallization becomes eventually impossible and the polymer is amorphous. Crystallization is essentially nonexistent when OP < 0.78 [2, 4, 47]. Crystallization kinetics of PLA is strongly dependent on the copolymer composition. Degree of crystallinity, nucleation rate and spherulite growth rate decrease drastically with a decrease in optical purity (OP).

For PLA the highest rate of crystallization occurs between 110 and 130°C. The literature shows a rough estimate of about 40 (%) increase for every 1 (wt %) increase in meso-lactide [46] . The melting point (Tm) and enthalpy of fusion ($\Delta \mathbf{H_m}$) of the stereocomplex is dependent on the ratio of L-lactide–rich polymer and D-lactide-rich polymer. In the case of constant optical purity (OP) of the polymers, the T_m varies only by a few degrees across the possible blend ratios where the $\Delta \mathbf{H_m}$ is directly related to the blend ratio. Lorenzo [51] also studied the crystallization behaviour of PLA and reported that PLA crystals are present in three different structural confirmations (α, β, γ) that can develop under different processing or treatment conditions.

Many authors have reported interesting findings and researched the crystallization kinetics of PLA. Celli and Scandola [52] have studied the thermal properties and physical aging of poly (L-lactide). They reported that thermal history strongly affects the properties of PLA by inducing changes in crystalline and amorphous ratio as well as aging effects on the glassy amorphous phase. It can be seen from their DSC results that above *Tg*, PDLLA exhibits an aging peak in the interval of 65–90(°C), with an enthalpy of 8 (J/g), indicating a typical amorphous polymer aging. The longer the aging time or closer the aging temperature to the *Tg,* the more intense is the peak with a higher enthalpy. But on the other hand it is also clear from their report that initially amorphous PLA presents a broad exothermic crystallization peak in the range of 100 – 160 (°C) centred about 132 (°C) with enthalpy (ΔH_C) of 38 (J/g), followed by melting at 182 (°C) with melting enthalpy (ΔH_m) of 38 (J/g). Kalb and Pennings [53] have reported that providing favourable crystallization conditions exist during the polymerisation process, all the samples in the DSC first scan display a high crystallinity between 50 (%) and 70 (%) depending on their molecular weight.

Enhancement of the overall crystallization rate of PLA is a matter of concern when PLA is under consideration for industrial applications. Badrinarayanan et al.[54] have studied the comparative analysis of crystallization behaviour for melt and cold crystallized PLA. They have reported the crystallization rate of PLLA by mixing it with nucleating agents such as talc. Saintis et al. [55] have studied the nucleation and crystallization kinetics of PLA and reported that talc can be used as a nucleating agent to accelerate the crystallization rate of PLA.

Partially during processing, PLA has a low crystallization rate because of high cooling rate. Therefore for this reason different kind of nucleating agent and plasticizers have been introduced during polymer processing. Ke and Sun [56] have studied the melting behaviour and crystallization kinetics of talc and PLA composites. They reported that by using 1 % talc, the crystallization half time can be reduced to less than 1 minute. Li et al. [57] have also studied the effect of nucleation and plasticization on the crystallization of PLA. They reported that other nucleating agents such as montmorillonite are less effective than talc. Saeidlou et al. [58] have also studied the crystallization kinetics of PLA and reported that addition of 1 % calcium lactate induced crystallization in a 90: 10 L to D copolymer.

2.11.4 Mechanical Properties

Generally when PLA is characterized it displays good mechanical properties, with elastic modulus of 3000-4000 (MPa) and tensile strength of 50-70 (MPa). Mechanical properties of polylactides PLLA produced and processed under different conditions reported in a number of reports are shown in Table 2- 3 [4]. The variation is seen because of differences in molecular weight and degree of crystallinity. The mechanical properties of PDLLA produced under different conditions and with different molecular weights are presented in Table 2- 4 [11].

From the analysis of mechanical data presented in Table 2- 3 and Table 2- 4, it is evident that in the selected range of molecular weights, the tensile and flexural properties of PDLLA and amorphous PLLA are quite different. Tensile strength for PLLA typically ranges from about 50 to 70 MPa while for PDLLA it ranges from 40 to

53 MPa. This different behaviour is mainly related to the stereoregularity of the polymer chains. It has been observed that after annealing at 105 (°C) for 20 minutes, PLLA samples showed a crystallinity ranging from 45% to 70%, as revealed by DSC analysis. Tensile strength of these PLLA samples ranged from 47 to 70 MPa in the same range of molecular weights. The effect of molecular weight on tensile and flexural properties is more evident in annealed PLLA than non-annealed PLLA and PDLLA specimens, with an increase of tensile strength from 47 to 66 MPa in the range of molecular weight between 20,000 and 70,000 g/mol (viscosity-average molecular weight (Mv). In the case of PDLLA, the relationship between the increase in tensile and flexural properties with molecular weight becomes less pronounced when the molecular weight is higher than 45,000–50,000. A similar phenomenon is observed for amorphous PLLA.

The dependence of Mechanical properties of PLA on its molecular weight has been investigated by other authors. Engellberg and Kohn [60] have studied the physico-mechanical properties of biodegradable polymers and characterised PLA with different molecular weights. They have reported 20 % rise in tensile strength when the molecular weight increases from 107,000 to 550,000 g/mol. Grijpma et al.[61] have studied the effect of annealing and orientation on microstructure and mechanical properties of polylactic acid. They have reported a comparable tensile strength of 47 MPa, elongation at break of 1.5 % and elastic modulus of 3650 (MPa) for an unoriented PDLLA with weight average molecular weight of 241,000 g/mol. Glauser et al. [62] have studied the effect of crystallinity on the deformation mechanism and bulk mechanical properties of PLLA. They have reported an elastic modulus of 1151 (MPa), with a yield stress of 62 (MPa) and strain at break of 14.5 (%).

The impact resistance of PLA is significantly affected by notching. Perego et al. [63] have studied the effect of molecular weight and crystallinity on poly (lactic acid). They have reported the values of Izod impact resistance of PLLA fall in the range of 2.0–3.0 (kJ/m^2) for low-crystallinity (3–9%) samples. The values obtained with more crystalline PLLA (45–70%) are in the range of 3.0–7.0 (kJ/m^2). Impact properties were observed by Grijpma et al. [61], who reported that the values of impact strength decreased from 2.2 to 1.2 kJ/m2 when the notch radius decreased

from 1.00 to 0.10 (mm). Material processing has a considerable effect on the impact resistance of PLA. Grijpma et al. [64] have studied the impact strength of polymerised PLLA. Very high molecular weight PLLA (Mv - 780,000 g/mol) shows impact strength values that decrease significantly from 47 (kJ/m^2) for as-polymerized polymer to 12 (kJ/m^2) for compression molded samples of the same material. This behaviour is clearly due to the loss of crystallinity associated with the fast cooling during the compression molding process.

It is very apparent from the thermal analysis of the data presented in Table 2- 3 and Table 2- 4 that the original manufactured articles from injection moulding grade PLLA are generally amorphous due to its slow crystallization kinetics. It is clear from the table that annealing promotes crystallization and increases the impact resistance. The effect of annealing on the fracture toughness of PLLA has been investigated in material samples quenched and annealed in the work of Park et al. [65] . They reported that PLLA samples prepared by a quenching procedure show Tg of 64 ^{o}C Tm of 168 ^{o}C, and crystallinity (Xc) of 2.7 (%), while the annealed samples are characterized by *Tg* of 66 ^{o}C, T_m of 169 ^{o}C, and Xc of 48(%).

As evidenced by these data, Tg and Tm slightly increased due to the annealing treatment, which results in crystallization. Generally, the annealed material has a higher degree of crystallinity (Xc) ranging from 45 (%) to 70(%), as determined by DSC analysis, depending on its molecular weight. Park et al.[65] have also reported that the toughness of PLLA under impact loading is therefore significantly increased by annealing. It is also clear from table 2-3 that impact resistance of PLLA is significantly increased from 13 to 35 (kJ/m^2) when annealed depending on the molecular weight.

Table 2- 3: Mechanical properties of PLLA with different molecular weights and processing conditions [11, 55].

Sample	**PLLA I**		**PLLA II**		**PLLA III**	
Annealing at 105^{0}C	***No***	***Yes***	***No***	***Yes***	***No***	***Yes***
Molecular weight (M_V, D_a)	23, 000	20, 000	58, 000	47, 000	67,000	71,000
T_m (^{0} C)	178	178	179	180	181	178
Crystallinity (%)	9	70	9	52	3	45
Tensile Properties						
Yield Strength (MPa)	-	-	68	68	70	70
Tensile Strength (MPa)	59	47	58	59	59	66
Yield Elongation (%)	-	-	2.3	2.2	2.2	2.0
Elongation at Break (%)	1.5	1.3	5.0	3.5	7.0	4.0
Elastic Modulus (MPa)	3550	4100	3750	4050	3750	4150
Flexural Properties						
Flexural Strength (MPa)	64	51	100	113	106	119
Maximum Strain (%)	2.0	1.6	4.1	4.8	4.7	4.6
Elastic Modulus (MPa)	3650	4200	3600	4150	3650	4150
Impact Resistance						
Izod, notched (KJ/m^2)	1.9	3.2	2.5	7.0	2.6	6.6
Izod, unnotched (KJ/m^2)	13.5	18.0	18.5	34.0	19.5	35.0
Heat resistance						
HDT (^{0}C)	57	66	-	-	55	61
Vicat penetration (^{0}C)	60	157	59	163	59	165
Hardness						
Rockwell Hardness (scale H)	85	84	83	84	88	88

Table 2- 4: Mechanical properties of PDLLA specimens with different molecular weights [53, 55].

Sample	PDLLA I	PDLLA II	PDLLA III
Molecular weight (M_V, D_a)	47, 500	75, 000	114,000
Tensile Properties			
Yield Strength (MPa)	49	53	53
Tensile Strength (MPa)	40	44	44
Yield Elongation (%)	1.7	1.4	1.5
Elongation at Break (%)	7.5	4.8	5.5
Elastic Modulus (MPa)	3650	4050	3900
Flexural Properties			
Flexural Strength (MPa)	84	86	88
Maximum Strain (%)	4.8	4.1	4.2
Elastic Modulus (MPa)	3500	3550	3600
Impact Resistance			
Izod, notched (KJ/m^2)	1.8	1.7	1.8
Izod, unnotched (KJ/m^2)	13.5	14.0	15.0
Heat resistance			
HDT (^0C)	51	50	50
Vicat penetration (^0C)	52	53	52
Hardness			
Rockwell Hardness (scale H)	78	72	76

Chapter 3 BIO-COMPOSITES

3.1 Introduction

Sustainability is changing the dynamics of the materials industry, offering new opportunities, prospects and challenges to materials scientists. Industrial ecology and eco-efficiency are driving the materials industry to develop the next generation of materials, products and processes. Innovations in the bio-plastic industry are providing a portfolio of sustainable and eco-efficient products to compete in the market presently dominated by synthetic plastics. The production and use of synthetic plastics have given rise to concerns about the depletion of natural resources and disposal issues, as previously discussed. These two main concerns have driven efforts to develop alternatives to fossil fuel based products. Development of bio-composites is one of these initiatives, where opportunities exist to explore the 'green' materials and develop sustainable products. Bio-composites combine bio-based fibres with resins and polymers. Bio-composites have enjoyed a considerable growth over the past decade or so. The main markets are packaging, automotive and decking products [66].

3.2 Bio-composites

A composite consists of two (or more) distinct constituents or phases when one or more of the discontinuous phases (reinforcements) are dispersed in another continuous phase (matrix) in order to obtain tailor-made characteristics or properties. When composite materials comprise one or more phase(s) derived from a biological origin, they are described as bio-composites [11, 67]. A broad definition of bio-composites is composite materials made from natural / bio fibres and either petroleum derived non-biodegradable polymer (PP, PE) or bio-derived polymers (PLA, PHA) [66]. Fully sustainable bio-composite made from bio/natural fibres and biodegradable polymers termed as green composites, are the centre of focus due to environmental concerns and legislation. The most common form of reinforcement is fibre; this could include plant fibres such as cotton, flax, hemp or more likely fibres from recycled wood or waste paper, or even by-products from food crops. Cellulose

fibres (viscose/rayon) are also included in this category as they come from renewable resources. In fibre- reinforced polymer composite materials, fibres are used to carry the load while the polymeric matrices are used to bind the fibres together, transfer the stresses from one fibre to the next and keep them in a desired orientation [11]. Biobased materials that are derived from renewable resources having an accepted level of recyclability and a triggered biodegradability, along with commercial and environmental viability, are described as sustainable bio-based products. It means that the materials would remain stable in their intended lifetime but would degrade after disposal in suitable composting conditions. The bio-composites that are more specifically "green composites" consist of bio-fibres and biopolymers and are expected to be biodegradable [1]. This concept of sustainability is shown in Figure 3- 1.

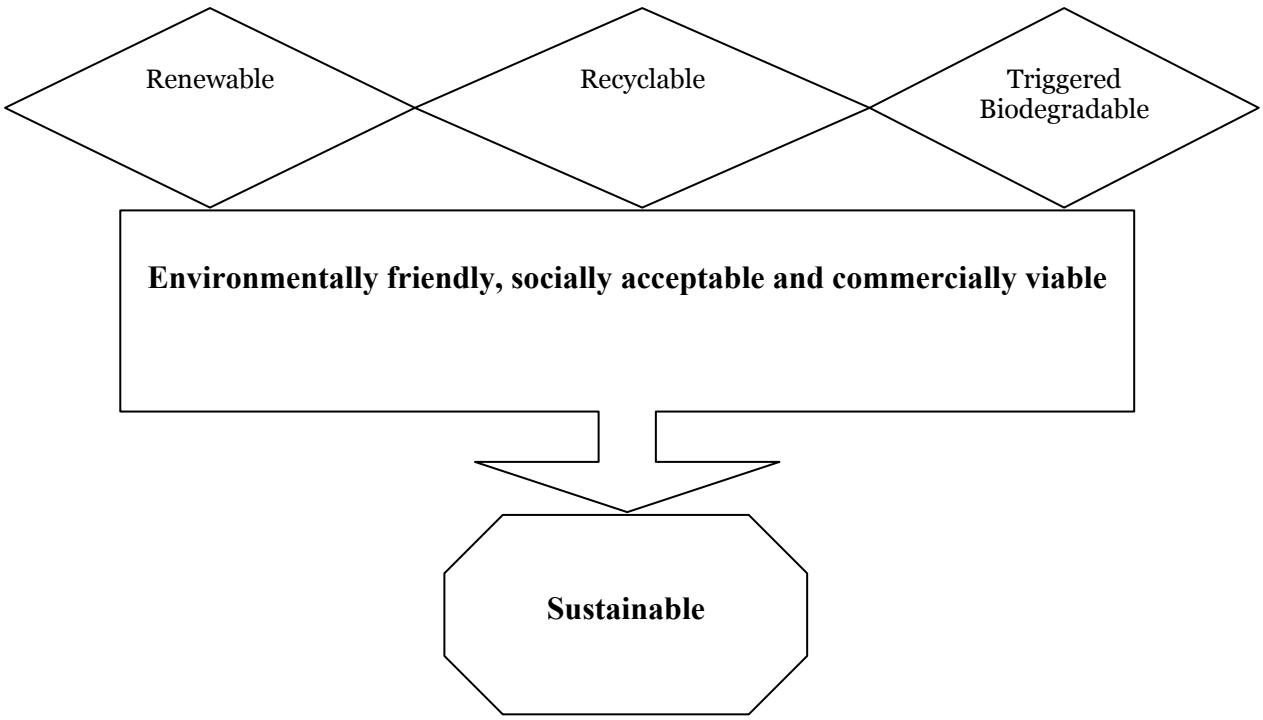

Figure 3- 1: Concept of "Sustainable" bio-based products [1]

3.3 Biofibres and their Classification

Combining natural reinforcing fibres (e.g. wood, hemp, flax, ramie, jute, etc.) into a bio-polymeric matrix made of derivatives of cellulose and starch (PLA, PHAs, etc.) produces reinforced materials which are termed biocomposites. Biocomposites consist of biodegradable polymer as matrix and usually biofibres as a reinforcing agent. Since both components are biodegradable, the composite as the integral part is also expected to be biodegradable [13, 68]. These biofibres enhance the strength and stability of the resulting composite structures depending on their origin as well as physical, chemical and structural composition [69]. Synthetic fibres like carbon, glass, aramid etc. can be produced with a desired range of properties whereas characteristic properties of biofibres vary significantly[66, 67]. The properties of the biofibres depend whether it's taken from plant stem or leaf, the quality of plant locations , age of the plant and preconditioning etc. [70, 71]. Natural fibres have the advantages of being low cost and bio-degradable.

Natural fibres are classified according to their source. One type is animal based, another is plant based and a third one is mineral based. The animal based fibres are subdivided into hair based fibres (wool), silk fibre (bugs) and avian fibres (birds). Plant based fibres are subdivided into fruit based, stalk based and leaf based. Stalk based fibres are mainly divided into flax, jute, hemp and wood fibres. Wood is further divided into hardwood or softwood based, depending on its origin [67, 72]. Flax, jute, hemp and wood are the most popular plants based natural fibres used as reinforcing natural fibres. Leaves of some plants like sisal, pineapple, banana and agave are also used as plant based natural fibres. Some of the fruit-based fibres are also used as hard reinforcing fibres like coconut, cotton and coir. Mineral-based reinforcing materials like asbestos are also used in altering the properties of thermoplastic materials. Mineral-based reinforcing materials will be discussed later in detail. Figure 3- 2 shows the generic classification of natural fibres.

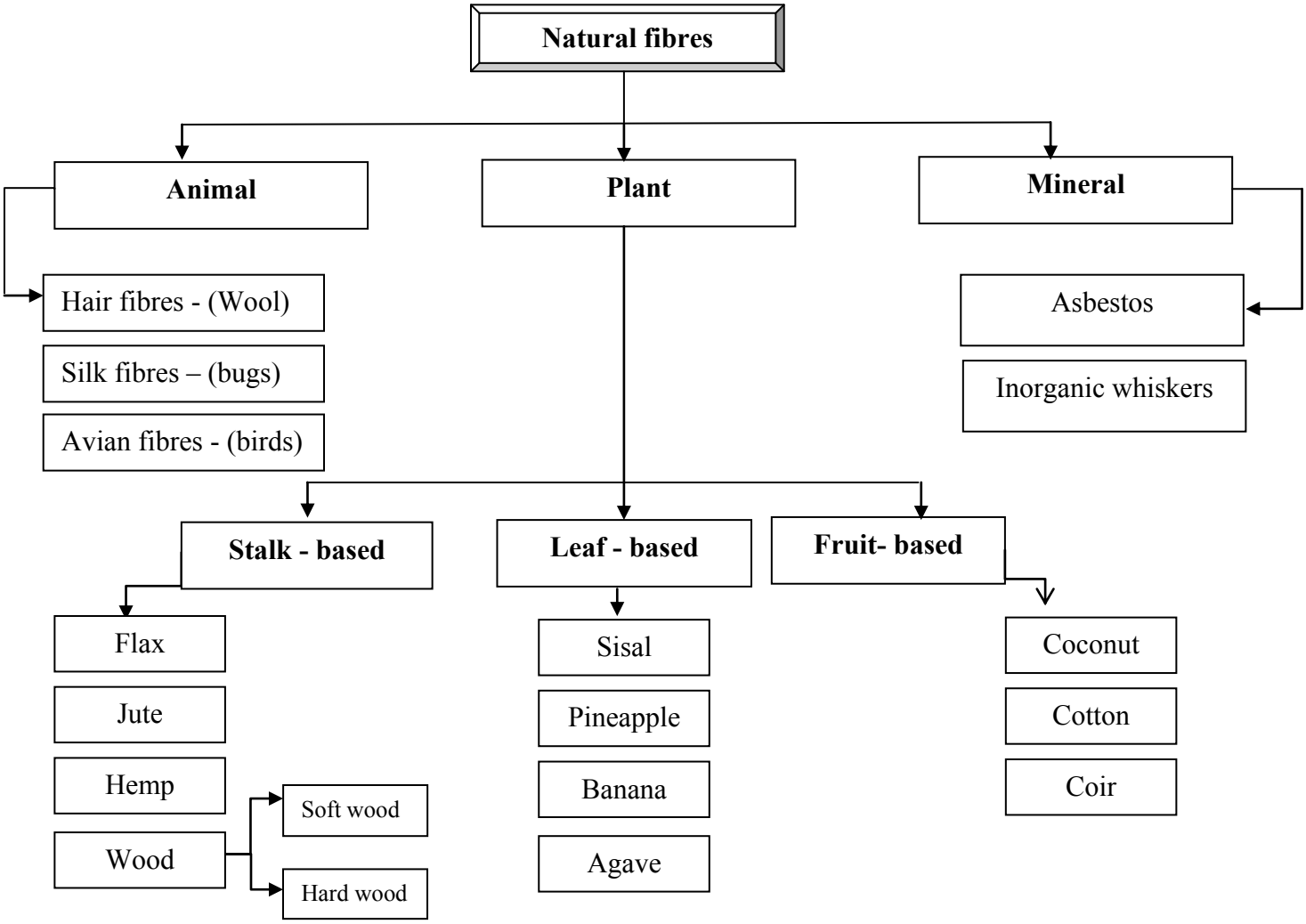

Figure 3- 2: Natural fibres classification [14].

Plant-based natural fibres are lignocellulosic in nature. Lignocellulosic materials are the most abundant renewable biomaterial. Major constituents of biofibres are cellulose, hemicelluloses and lignin, which is a kind of natural composite itself. Hemicelluloses act like a matrix to keep cellulose and lignin together [1, 73]. The amount of cellulose, in lignocellulosic systems, can vary depending upon the age of the plant/species. Chemical structures, physical and mechanical properties are reported in literature. Chemical compositions and structural parameters of various natural fibres are represented in Table 3- 1 showing that all three major constituents vary significantly. Such variation may be due to the origin, age, retting treatment or other processes adopted. Table 3- 2 compares the properties of some natural fibres with conventional man-made fibres.

Table 3- 1: Chemical composition and structural parameters of natural fibres.

Type of fibre	Cellulose (wt %)	Lignin (wt %)	Hemicellulose (wt %)	Pectin (wt %)	Wax (wt %)	Moisture Content (wt %)	Reference
Stalk							
Jute	61 - 71.5	12 - 13	13.6 – 20.4	0.2	0.5	12.6	[1, 13]
Flax	71	2.2	18.6 – 20.6	2.3	1.7	10.0	[1, 13, 67]
Hemp	70.2 – 74.4	3.7 – 5.7	17.9 – 22.4	0.9	0.8	10.8	[67, 72]
Ramie	68.6 – 76.2	0.6 – 0.7	13.1 – 16.7	1.9	0.3	8.0	[67, 72]
Kenaf	31 - 39	15 - 19	21.5	--	--	--	[1, 72]
Leaf							
Sisal	67 - 78	8.0 – 11.0	10.0 – 14.2	10.0	2.0	11.0	[1, 72]
Seed							
Cotton	82.7	--	5.7	--	0.6	--	[1, 13, 67]
Fruit							
Coir	36 - 43	41 -45	0.15 – 0.25	3 - 4	--	8.0	[67, 72]

Table 3- 2: Comparative properties of some natural fibres with conventional man-made fibres.

Fibre	Density (g/cm^3)	Diameter (µm)	Tensile strength (MPa)	Young's modulus (GPa)	Elongation at break (%)	Reference
Cotton	1.5 – 1.6	--	287 – 800	5.5 -12.6	7.0 -8.0	[1, 13]
Jute	1.3 -1.45	25 – 200	393 – 773	13 – 26.5	1.16 – 1.5	[1, 13, 67]
Flax	1.50	--	345 – 1100	27.6	2.7 – 3.2	[67, 72]
Hemp	--	--	690	--	1.6	[67, 72]
Ramie	1.5	--	400 – 938	61.4 – 128	1.2 – 3.8	[1, 72]
Sisal	1.45	50 - 200	468 – 640	9.4 – 22.0	3 – 7	[1, 72]
Coir	1.15	100 - 450	131 – 175	4 - 6	15 – 40	[1, 13, 67]
E-glass	2.5	--	2000 – 3500	70	2.5	[67, 72]
S-glass	2.5	--	4570	86	2.8	[67, 72]
Aramid	1.4	--	3000 – 3150	63 – 67	3.3 – 3.7	[1, 13]
Carbon	1.7	--	4000	230 - 240	1.4 – 1.8	[1, 13, 67]

3.4 Factors affecting composite properties

A composite is a combination of two or more component engineered materials which, when combined, retain their identities and properties. Typically the composite, would consist of reinforcing fibres which are the hardest, strongest and stiffest component, embedded in a continuous matrix [74]. Fibres increase the strength of the material and serve as reinforcement, where the PLA (matrix) is acting as a binder or adhesive. The properties of the composites are strongly influenced by the proportion and the properties of the matrix and reinforcement. The desired properties of fibres depend upon the desired stiffness and strength behaviour of the composites. Appropriate fibre reinforcement depends on different selection parameters [6, 15], like;

a. Thermal and Mechanical properties
b. Adhesion between fibres and matrix
c. Dynamic behaviour
d. Long-term behaviour
e. Price and processing costs

All these factors combine to affect the properties of composite materials but the properties of composites are controlled by the intrinsic properties of the constituents. The two most important properties to influence the mechanical properties of the composites are given below [67]:-

- ***Fibre architecture***
  (Geometry / Aspect ratio, Orientation, Packing arrangement, Volume fraction)

- ***Fibre-matrix interface***

3.4.1 Fibre volume fraction

Fibre volume fraction is one of the most important factors controlling the strength, stiffness and many other physical / mechanical properties of the composites. For a composite system where matrix failure strain is greater than fibre failure strain, two possible failure regimes exist depending on whether the fibre volume fraction (V_f) is above or below a minimum value (V_{min}). When $V_f < V_{min}$, the polymer matrix is able to carry the applied load after fibre fracture. Failure of the fibres does not lead to composite failure but merely increases the stress in the matrix. The failed fibres, which now carry no load, can be regarded as holes in the polymer matrix. When $V_f > V_{min}$, failure of the fibres leads to failure of the whole composite, since the polymer matrix is unable to support the additional load which is transferred into the matrix of the fibres. Thus, the critical volume fraction (V_{crit}) for the composite system is the amount of fibres necessary to ensure the composite strength is at least greater than that of the matrix. At very high volume fractions, the strength of composites starts to decrease due to the insufficient loading by the matrix material [75].

3.4.2 Fibre Aspect ratio

Fibre aspect ratio (length/diameter or thickness) is an important parameter in composite materials. A critical fibre aspect ratio is necessary for efficient strengthening and stiffening of the composites. This critical fibre length is defined as the minimum length of the fibre required for the stress to reach the fracture stress of the fibre. Fibres shorter than the critical length will not carry the maximum possible load and are thus unable to function efficiently [75, 76].

3.4.3 Fibre Orientation

The orientation of the fibre is of equal importance to the length of the fibres. The fibre orientation depends on the processing route. When continuous fibres are used, the orientation can be controlled to give predictable end properties for the composite in terms of strength and stiffness. Short fibre reinforced injection molded composites have fibres that are randomly oriented but commonly show

preferential fibre alignment in the matrix flow direction or a layered structure with distinct fibre alignment in different layers. Changes in fibre orientation are related to a number of factors, such as viscoelastic properties of the fibre filled matrix, mold design and the change in shape of the material produced by the processing operation[76].

3.4.4 Composite (fibre –matrix) interface

The most important phenomenon in composite theory is “composite interface”, which is a region of significantly changed chemical composition that constitutes the bond between the matrix and the reinforcement [76]. This interface region plays a key role in transferring the load to the fibres from the matrix. Fracture behaviour of the composites is also dependent on the strength of the interface. Generally a weak interface results in low strength , stiffness and less resistance to fracture, whereas a strong interface leads to high strength and stiffness and a high resistance to fracture , but often low impact resistance because of embrittlement [76]. Another phenomenon of importance is the bonding mechanism at the interface. Once the matrix and reinforcement are exposed to each other, different types of bond may be formed, of which some might occur at the same time. Five different principle mechanisms involved in the interfacial bonding mechanism are inter-diffusion, electrostatic attraction, chemical bonding, reaction bonding and mechanical bonding [74].

Apart from these, several other factors need to be considered to maximize the benefits of fibre reinforcement. These include the homogeneous dispersion of fibres into the matrix and optimizing the processing parameters (i.e. throughput rate, temperature, rpm, etc.) [17].

3.5 Modelling Composite properties (Predictions of Tensile Properties)

Several theories have been proposed to model the tensile properties of composite materials in terms of different parameters [77]. Some of the differentiation can be

made in terms of the incorporation of rigid or non-rigid particulate or fibrous reinforcement into rigid or non-rigid polymer matrices [78]. Some of these models are discussed here briefly.

3.5.1 Einstein and Guth Equation

Einstein equation is used mainly for theoretical prediction of the properties of particulate (spherical) –reinforced polymer composites [77, 79].

$$\boldsymbol{E_c = E_m(1 + 1.25\emptyset_f)} \qquad \text{(3.1)}$$

Where E_c and E_m are the Young's modulus for composite and matrix respectively, $\emptyset_f$ is the volume fraction of the fillers / particles. Guth derived a modified version of the same equation for considering the effect of the reinforcement which is given below.

$$\boldsymbol{E_c = E_m(1 + 2.5\emptyset_f + 14.1\emptyset_f^2)} \qquad \text{(3.2)}$$

It is observed from the literature that the Einstein and Guth equation seems accurate at low concentration of the reinforcement but drops far behind the experimental data at higher contents of the reinforcement specifically for spherical reinforcement materials , because of their geometric constraints [80].

3.5.2 Rule of Mixture

The effect of strong reinforcement on the matrix can also be investigated by the rule of mixtures. The rule of mixtures is a mathematical equation that relates to the property of the composite to properties of each component and their volume fractions in the composite. Using the rule of mixtures, the modulus of the composite product can be estimated using the following equation [81].

$$\boldsymbol{E_c = E_f V_f + E_m V_m} \qquad \text{(3.3)}$$

Where E_c , E_m and E_f is the modulus of the composite, matrix and fibre respectively, and the V_f and V_m are the volume fractions of fibres and matrix respectively.

When a composite is the simplest arrangement of two-phase materials containing continuous fibres and matrix, the composites properties can also be predicted on the basis of the upper and lower limit. Reuss and Voigt have modified the rule of mixture into the series and parallel models giving the relationship between the modulus of the composite and volume fraction of the fibres. This is often given the name of the Voigt – Reuss upper and lower bounds for composite properties. The Voigt model gives the linear relation between the composite properties and fibre volume fraction; the same as the rule of mixtures as given in equation 3.3. The upper –bound can be derived from the rule of mixtures as [82]

$$\boldsymbol{E_C^{upper} = E_f V_f + E_m(1 - V_f)} \quad \text{----------(3.4)}$$

The lower-bound for the composite modulus, described as the Reuss model which is given as follows.

$$\boldsymbol{E_C^{Lower} = E_f E_m / [E_f(1 - V_f) + E_m V_f]} \quad \text{-----(3.5)}$$

The modulus of composites lies between these two bounds. These upper and lower bounds are applicable to most particulate micro and nano-composites. Generally, the modulus of the composites should be lower than the upper - bound and higher than the lower – bound, however it is possible for a composite to violate the Voigt-Reuss bounds due to the fibre-matrix interface and reinforcement effect [83].

3.5.3 Halpin-Tsai Model

Different theories described earlier to predict the stiffness of the composites imply that the reinforcement effect of the filler is independent of its geometry but that the volume fraction of the filler / fibre is a crucial variable. Therefore, the

effectiveness of these mathematical models is restricted to low filler concentrations and seems useful at a low amount of filler.

The Halpin-Tsai equation is useful in predicting the effect of reinforcement geometry on the modulus of composite materials as it takes the geometry of the filler into account [80, 84]. The Halpin - Tsai equation is as follows;

$$\frac{\boldsymbol{E_c}}{\boldsymbol{E_m}} = \frac{(\mathbf{1} + \boldsymbol{AB\, V_f})}{(\mathbf{1} - \boldsymbol{B\, V_f})} \qquad ----------(\mathbf{3.6})$$

Where $\mathbf{A} = 2\left(\frac{L}{D}\right)$, $\mathbf{B} = \frac{(R-1)}{(R+A)}$ and $R = \left(\frac{E_f}{E_m}\right)$. *Ec, Em, E_f and V_f* are defined as the modulus of the composite, matrix, filler and volume fraction of the filler respectively. $\left(\frac{L}{D}\right)$ is known as the aspect ratio of the filler, where L= Length and D= Thickness or diameter.

3.5.4 Lewis & Neilson Model

Lewis & Neilson suggested an improvement in the Halpin – Tsai model, to bring a closer agreement with experimental data. The Halpin- Tsai equation is modified by taking into account the maximum packing fraction of the filler and introducing a new factor into the equation which is follows as

$$\frac{\boldsymbol{E_c}}{\boldsymbol{E_m}} = \frac{(\mathbf{1} + \boldsymbol{AB\, V_f})}{(\mathbf{1} - \boldsymbol{B\psi\, V_f})} \qquad ----------(\mathbf{3.7})$$

Where $\psi = 1 + \left(\frac{1-\phi_{max}}{\phi_{max}}\right)V_f$, and ϕ_{max} is the maximum packing fraction of the filler, which is defined as true volume of the filler to the apparent volume occupied by the filler [85]. Lewis and Neilson reported different values of the maximum fraction based on the aspect ratio and the geometry of the filler, which ranges from 0.1 to 1 [85].

3.5.5 Volume Fraction

The volume fraction of the filler in the composite can be calculated from the weight fraction of the filler by using the following equation [86].

$$V_f = 1 \Big/ \left[1 + \frac{\rho_f}{\rho_m}\left(\frac{1 - w_f}{w_f}\right)\right] \quad -----(3.8)$$

Where ρ_f , ρ_m are the density of the filler and matrix respectively, and w_f is the weight fraction of the filler.

3.5.6 Coefficient of Determination, R^2

The accuracy between the experimental and the theoretical responses can be verified by the multiple coefficient of determination, R^2 , which is the most popular indicator to determine the performance of data fitting in the best possible manner. It is given as [87, 88].

$$\left[R^2 = 1 - \frac{\sum (Y_{actual} - Y_{Pred})^2}{\sum (Y_{actual} - \frac{\Sigma Y_{actual}}{N})^2}\right] ----(3.9)$$

Where, Y_{actual} = Experimental response value, Y_{pred} = Predicted theoretical value, and N = total number of readings in the data. The closer the value of R^2 to one (unity), the better the correlation between the target and the output.

3.6 Overview of Poly (lactide) – composites

PLA composites have been used for several years now, and their market share is increasing. Fibre reinforced polymer composites are being successfully used because of their combination of very high mechanical strength and low weight. This section gives a brief overview of the PLA matrix and different fillers and fibres used as reinforcement.

I. PLA – Natural fibre reinforcement
II. PLA - Synthetic fibre reinforcement
III. PLA – Mineral filler reinforcement

3.6.1 PLA- Natural Fibre Reinforcement

Organic fibres are less abrasive comparable with inorganic counterparts which offer a competitive advantage during processing [89]. Therefore in the recent past, natural fibres are preferred over man-made fibres because of their sustainability, low cost, competitive specific mechanical properties, CO_2 sequestration and much lower production of ash during incineration [33].

The most widely known and used organic fillers are wood fillers or fibres and derivatives. Apart from wood derivatives other natural fillers like cellulose, cotton, jute, flax and hemp etc., are also used in many applications. Further to this discussion "environment – friendliness" can also be achieved by using recycled polymers in place of virgin polymer matrix [90].

Lignocellulosic - PLA composites have been presented in a number of research publications. Satyanarayana *et al.* [91] published an overview of biodegradable composites based on lignocellulosic fibres. They presented an overview of the developments made in the area of plant-based bio-composites, in terms of market dynamics, processing methods, matrix–reinforcement systems, morphology, properties and product development.

Different kinds of lignocellulosic fibres have been employed to produce PLA composites. A number of studies have shown quite a good improvement in developing biodegradable PLA composites. Most of the studies carried out regarding PLA-natural fibre reinforced composites are hemp-PLA [92] , kenaf-PLA [92] , flax-PLA [17, 67], jute-PLA [15, 38], PLA-Wood (fibres or flour)[15, 93].

There are still challenges related to plant-fibre reinforced PLA composites because of their incompatibility. Some of these challenges are listed below [11, 91];

a. Difficulties in mixing due to poor interfacial adhesion between hydrophilic fibre and hydrophobic PLA matrix.

b. Processing temperature of plant fibre composites is restricted to less than 200^{o}C or below as plant fibre undergoes degradation at higher temperatures.

c. High moisture absorption of natural fibres leading to swelling and the presence of voids at the interfaces, which results in poor mechanical properties and reduces dimensional stability of composites.

d. Nonuniformity in dimensions and in mechanical properties (even between individual plants in the same cultivation).

Some animal based fibres have also been employed to develop PLA composites but very limited research work has been done in this area so far. For example, chicken feather and gelatine based animal fibres have shown no significant improvement compared with neat PLA [10].

Wood flour is the most widely used organic filler reinforcement with PLA , as well as other organic fillers like starch, rice hulls and sugar beet [38].

Wood is the cheapest source of lignocellulosic fibres. The use of wood flour can reduce the materials costs and provide specific properties like low density, high specific stiffness and biodegradability. Wood is used as filler in many developing thermoplastic composites. Being the cheapest biodegradable filler source, wood is also a suitable choice to develop PLA composites. It has been studied and has shown good results [6, 15, 93] . Huda *et al.* [93] studied PLA-wood composites in more detail and compared the results with PP-wood composites. They reported that tensile and flexural properties of PLA-wood composites were significantly higher when compared with the virgin resin. The flexural strength increased from 98.8 to 114.3 (MPa) when wood content increased from 0 to 40 (wt %). Similarly

the flexural modulus increased from 3.3 to 10.3 (GPa) with increasing wood content from 0 to 40 (wt%) which was comparable to that of traditional PP-wood composites [93].

Huda *et al.* [93] also reported the decrease in tensile strength of PLA from 62.8 to 58.7 (MPa) when wood contents increased from 0 to 40 (wt %). But on the other hand tensile modulus increased significantly from 2.7 to 6.3 (GPa) bringing total of about 133 % improvement in tensile modulus. Similarly the flexural strength also reported to be reduced from 98 to 75 (MPa) when wood fibre's contents increased from 0 to 30 (wt%) but flexural modulus increased from 3.3 to 8.6 (GPa) bringing a significant improvement in modulus [28]. But application of potential coupling agent has been reported to improve the tensile properties of PLA-wood composites up to some extent. Huda *et al.* [93] have reported maleated polypropylene coupling agent (MAPP) which improved the flexural and impact properties of PLA-wood composites.

Auras *et al.* [11] have reported that tensile strength is increased from 41.0 to 56.0 (MPa) when wood content increased from 0 to 20 (wt%), changing Young's modulus from 1.66 to 2.7 (GPa). Pilla et al [114] have studied the effect of coupling agent (silane) on PLA/wood composites and reported an improvement in the tensile properties of the composites.

Literature shows that comparative studies of mechanical and thermal analysis of PLA based composites containing different amount of wood (fibres or flour) are limited. The properties of these bio-composites are greatly influenced by the fibre and fibre –matrix adhesion. In order to improve the adhesion between the matrix and fibres, research is conducted to address this issue. In most cases the surfaces are incompatible, therefore some chemical treatment (coating) of fibres is done prior to mixing or a compatibilizing agent is used. Bledzki *et al.* [94] studied the reinforcement and treatment of cellulose based natural fibres. It was concluded that mechanical properties of composites are mainly influenced by the adhesion between matrix and fibres. Chemical treatment and surface modification methods were developed to improve the mechanical adhesion and surface compatibility by resistance to moisture and environmental effects. These treatments have proved

encouraging in natural fibre reinforcement in plastics and bioderived polymers [94].

Table 3- 3 shows the mechanical properties of PLA composites. This data has been taken from a number of different studies and is summarized in the table.

Table 3- 3: Mechanical properties of PLA Composites [11]

Composite	*Process Route*	*Tensile strength (MPa)*	*Young's modulus (GPa)*	*Elongation at Break (%)*	*Impact Strength (kJ/m²)*
PLA-neat	***C.M***	41.06	1.66	4.2	11.00
PLA-hemp (40 %)	***C.M***	57.5	8.1	1.2	9.5
PLA-Lyocell (40 %)	***C.M***	82	6.8	4.1	39.5
PLA-hemp (20 %) /Llyocell (20 %)	***C.M***	71.5	7.0	1.7	24.7
PLA –Kenaf (40 %)	***F. S***	52.8	7.1	1.05	8.9
PLA- flax (40 %)	***I.M***	46.4	7.9	--	11.0
PLA-flax (40 %)	***C.M***	99	6.0	--	--
PLA-jute (40 %)	***C.M***	100	9.4	--	14.3
PLA-cotton (40%)	***C + C.M***	41.2	4.2	2.9	28.7
PLA-RWF (20%)/silane (0.5%)	***I.M***	56.1	2.7	--	--
PLA-$CaCo_3$ (5%)	***E***	55.3	2.3	2.7	--

RWF = Recycled wood fibres, **C.M** = Compression Molding, I.M = Injection Molding

F.S = Film stacking**, C** = Carding, **E** = Extrusion, M= Mixing

Table 3- 3 shows clearly that tensile strength and elastic modulus are considerably increased when the amount of hemp fibres increased from 0 to 40 (wt %). Tensile strength increased from 41.0 to 58.0 MPa and modulus increased from 1.66 to nearly 8.0 (GPa) compared to neat PLA. But on the other hand the elongation at break and impact strength decreased significantly as the contents of hemp fibres increased from 0 to 40 (wt %) [92, 112] . Similar properties were observed with PLA-loycell composites. The tensile strength increased from 41.0 to 82.0 (MPa) and the Young's modulus increased from 1.6 to 6.1 (GPa) as the loycell content increased from 0 to 40 (wt%) as reported by Grapuner *et al.[92].* It is also shown that the impact strength is improved quite significantly from 11.0 to nearly 40 (KJ/m²). The hybrid reinforcement of hemp and loycell into PLA brings an

improvement in tensile strength and modulus. Tensile strength increased from 41 to 71 (MPa) and elastic modulus increased from 3.2 to 7.1 (GPa) compared to neat PLA when contents of hemp/loycell changes from 0/0 to 20/20 (wt %). Similarly the impact strength also improved distinctly from 11.0 to 25.0 (KJ/m^2).

Grapuner *et al. [92]* have also reported the incorporation of kenaf fibres into a PLA matrix. It is clear that tensile strength and Young's modulus increased while elongation at break and impact strength decreased when the contents of hemp fibres increased from 0 to 40 (wt %). Tensile strength increased from 41 to 53 (MPa) and young's modulus increased from 2.8 to 7.1 (GPa). While elongation at break decreased from 11.0 to 1.0 (%) and impact strength reduced to 8.9 (KJ/m^2).

There is also significant improvement reported for PLA-flax composites. Compression molded PLA-flax composites have improved mechanical properties compared with neat PLA. The tensile strength of PLA-flax composite increased from 42.0 to 54.0 (MPa) and Young's modulus increased from 3.9 to 6.31 (GPa) as flax content increased from 10 to 30 (wt %) [113].

The largest improvement comes when PLA is mixed with jute fibres. Plackett *et al.* have reported that the tensile strength and Young's modulus increased significantly as the jute fibres increased from 0 to 40 (wt%). Tensile strength increased from 55.0 to 98 (MPa) and modulus increased from 3.5 to 9.4 (GPa) which is quite a significant improvement [27].

Cotton did not show significant improvement when cotton contents increased from 0 to 40 (wt %). Tensile strength doesn't change. However, Young's modulus increased from 1.66 to 4.2 (GPa) and impact strength increased from 11 to 28.7 (KJ/m^2).

3.6.1.1 **Silane Treatment**

Silane coupling agents are a unique class of organic silicon compounds. A typical general structure is

$$(RO)_3\,SiCH_2CH_2CH_2\text{-}X$$

Where RO is a hydrolyzable group, such as methoxy, ethoxy or acetoxy, and X is an organofunctional group, such as amino, methacryloxy, epoxy. These chemicals are hydrophilic compounds with different groups appended to silicon, such that one end will interact with hydrophilic groups and the other end will react with hydrophobic groups. Therefore, hydrophilic and hydrophobic materials can be coupled together with silane coupling agent acting as a bridge between them. A simplified coupling mechanism scheme of silane treated fibre and polymer matrix is shown in Figure 3- 3.

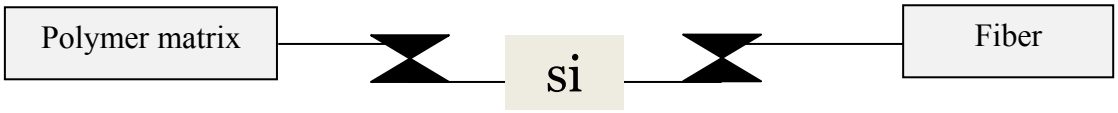

Figure 3- 3: Schematic analysis Silane treatment of PLA and fibres mixing [59]

Silane coupling agents are generally applied to fibres to improve the overall performance of fibre reinforced composites. Although this type of treatment is well established with glass fibre, its effect on natural fibre has also been reported [69]. Silane uptake is very dependent on a number of factors including hydrolysis time, organofunctionality of silane, temperature and pH. Beg [74] studied the effect of silane coupling agents (γ-amino-propyltriethoxysilane and dichlorodiethylsilane) on radiata pine wood fibre. It is found that the fibre treatment improved the strength of polyethylene and wood fibre composites due to better adhesion. Li *et al.* [95] also used silane coupling agents to modify the surface of sisal fibres. They found that the silane treatment did not affect the fibre strength significantly. On the other hand, 3-aminopropyltriethoxy silane was found to react only with the fibre but not the matrix, so that interfacial strength was not improved significantly.

Coupling agents are used quite regularly in natural fibre composites. Huda *et al.* [93] also used maleated polypropylene coupling agent (MAPP) and have shown improvement in the flexural and Izod impact properties of wood fibre reinforced composites. Lee *et al.* [96] also studied the effect of coupling agent (silane) in PLA - wood - talc composites. The properties of PLA-wood composites improved considerably with the use of 1 (wt%) silane [96]. Pilla et al.[97] have reported that

no crystallization peak was observed in cooling scans for PLA and wood flour composites and observed no significant change in degree of crystallinity of the composites.

Starch is another biodegradable polymer which is abundantly available in nature. Research efforts have been made to develop and optimize PLA-Starch composites mainly for short term single-use applications [94]. Reduced cost is one aspect of using starch as filler. Also starch is used to act as a nucleating agent for PLA, thus improving the crystallinity of PLA and improving mechanical and thermal properties of PLA [11, 67, 93, 94] . Compatibilization of Starch with PLA is another important factor which affects the PLA-starch composite quality because interfacial adhesion plays a vital role in mechanical properties of polymeric composites. Manjula Dilkushi Silva et al.[98] have investigated the effect of coupling agent on mechanical and thermal properties of PLA/wheat starch composites. They reported that coupling agent like methyldiphenyldiisocynate (MDI) and stearic acid (SA) have shown improvement in thermal and mechanical properties. It is also reported that MDI behaves as a coupling agent and glycerol and SA behave more like plasticisers.

Literature shows that various methods have been adopted to improve the PLA-starch compatibilization. To achieve compatibilization of starch with PLA, various methods have been adopted including use of maleic anhydride grafting system, addition of compatible polymers such as polyvinyl alcohol and polycaprolactone [11, 94]. Zhang and Sun [99] have studied the effect of the compatibilizing agent on mechanical properties of PLA-starch composites, showing significant improvement in interfacial adhesion between PLA and starch. Mechanical properties increased markedly with addition of 1 wt% maleic anhydride (MA) compared to neat PLA-starch composites. Tensile strength increased from 30.2 to 52.4 (MPa) with 1 wt % MA treatment of starch compared to PLA-starch [93, 99].

3.6.2 Synthetic Fibre Reinforcement

Apart from biofibre reinforcement, synthetic fibres are also employed to develop PLA composites. Synthetic fibre reinforcement is commonly used to reinforce polymer matrices to develop structural composites with improved properties (i.e. Mechanical). Structural bio-composites always need to have good mechanical durability for structural applications. Therefore synthetic fibre reinforced PLA composites need to have favourable characteristics like [11, 100] ;

- High strength to weight ratio
- Good dimensional stability
- Good resistance to heat
- Resistance to moisture and corrosion
- Good electrical insulation
- Good processability

Research in the use of glass and carbon fibres have shown promising results in improve the mechanical properties of PLA to become suitable for some non-packaging applications. M.S Huda *et al.* have studied the effect of glass fibres and recycled newspaper cellulose fibres (RNCF), mixed with PLA and found that tensile strength increased from 62.9 to 80.2 (MPa) when glass fibres increased from 0 to 30 (wt %) [100] .

Other researchers have also investigated the effect of glass fibre reinforcement on poly (lactide) composites. The elastic modulus increased from 2.7 to 6.7 (GPa) when glass fibre increased from 0 to 30 (wt %) bringing about 145 (%) improvement compared with neat PLA [100]. Ahmad *et al.* have also studied the effect of glass fibre on PLA composites [101]. It is found that flexural strength increased from 50 to nearly 90 (MPa) as fibre content increased from 0 to 14 (vol %) and modulus was also seen to increase from 2.5 to 5.0 (GPa) [101]. Hu *et al.* [102] have also investigated the effect of glass beads on mechanical and thermal properties of poly L-lactide (PLLA). They found improvement in the tensile modulus and reported an increase from 3.5 ± 0.15 to 3.7 ± 0.3 (GPa) when the content of glass beads increased from 0 to 15 (wt %). Impact strength was also

reported to be increased from 2.3 ± 0.04 to 2.9 ±0.05 (J/m^2). They also reported an improvement in mechanical properties with addition of coupling agent. Improvement in thermal properties was also investigated and increase in the degree of crystallinity was observed.

3.6.3 PLA – Mineral filler reinforcement

Utilization of mineral fillers as a reinforcement is one of the approaches used to improve the mechanical properties of thermoplastics in the development of particulate composites. Fillers or additives are used to produce particulate composites to modify properties like flexural modulus, temperature resistance and warpage of the virgin material. Therefore these fillers are often called functional fillers, mineral additives or reinforcing agents.

Mineral additives- matrix composites are made of two very dissimilar materials. The matrix or resin is covalently bonded organic in nature, and the filler is inorganic in nature with ionic interactions between the atoms. Differences in the nature of the matrix and fillers can be exploited to develop composites for specific desired properties by blending various amounts of different components.

Mineral fillers are also used to reinforce bio-based polymeric materials and show promising results in the enhancement of desired properties. However, there may be a negative effect on other properties.

There are certain issues that need to be considered during the use of mineral filler as a reinforcement material. Processing of the mineral additives is critical to the end-use performance; having the best filler and then dispersing or processing it poorly into the resin will not lead to desired results. Therefore the addition of mineral fillers into the resin is often considered as an art rather than science. In general the physical properties of the fillers, like average particle size, particle size distribution, particle shape and surface properties have the greatest influence on the mechanical response of the composites.

Different types of functional fillers can be used to improve the mechanical performance, but calcium carbonate ($CaCo_3$), mica, kaolin, glass beads and talc are the most common and are frequently incorporated into thermoplastics to reduce

the end-product cost and improve mechanical properties like strength, rigidity, and hardness of the virgin material [80]. Interests in using talc as reinforcing filler is mounting due to its unique properties and it is one of the most common fillers used in polypropylene (PP). Some of the non-plastic market applications are in ceramics, paints and paper industries but significant amounts are also used in cosmetics, insecticides and roofing materials.

Talc is a hydrated magnesium silicate with the formula $Mg_3SiO_{10}(OH)$ [103]. Structure of talc is given in Figure 3- 4. Morphology of the talc is also given. Talc has a plate-like structure held together by weak Van der Waal's forces, so that the talc platelets can be disseminated at low shear stresses and are easy to disperse [104].

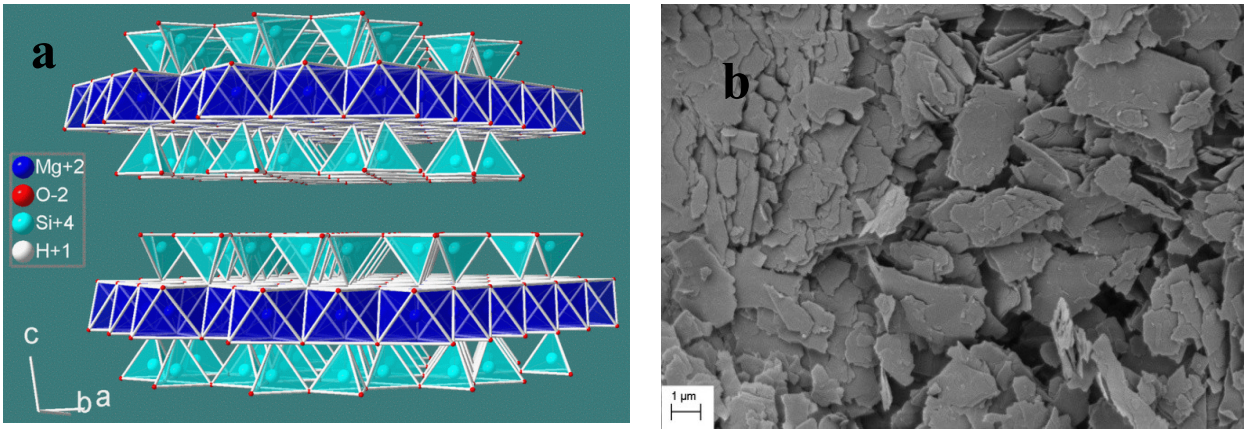

Figure 3- 4: (a)Structure of the talc tetrahedral surface plane [105]; (b) microscopy

Most commonly, talc is added as filler to isotactic poly (propylene) (PP). At low concentrations (less than 3 weight %) it acts as a nucleating agent, reducing spherulite size and shortening processing time [106]. At higher loadings (10 – 40 weight %) it acts as a reinforcing filler, increasing tensile modulus and stiffness, but reducing strain-to-break and impact strength [107].

Talc is also incorporated into bio-based plastics like poly (hydroxyalkanoate) (PHAs), poly (3-hydroxybutyrate) (PHB) and PLA to improve the mechanical performance [108]. Inclusion of higher content and finer size talc into bioplastics

has also shown a significant effect on the mechanical properties. Fowlks and Narayan reported significant effect in elastic modulus and improvement in overall crystallinity of PLA-talc composites with a talc content of 40 (wt %) compared to pure PLA [109]. Other researchers have also reported considerable improvement in Young's modulus with the incorporation of talc into neat PLA and observed a slight decrease in overall crystallinity [80, 110] .

The addition of 2(%) talc was found to reduce crystallisation half-times and resulted in a significant increase in crystallinity and decreased processing time [111]. Jain et al.[84] investigated adding talc (1 – 5 weight %) to blends of PLA and PCL. It was found that talc improved the miscibility and adhesion between the PCL bulk phase and the PLA domains. Values of tensile and storage modulus increased linearly with the talc loading.

It is a well established fact that particulate fillers improve the mechanical and physical properties of polymers in different ways. In literature it is reported frequently that mechanical properties of particulate filler - polymer composites are strongly dependent on particle size, particle –matrix interface adhesion and loading amount [82].

3.7 Applications of PLA-Composites

PLA biocomposites offer a significant non-food market for crop-derived fibres and resins. Considerable growth has been seen in the development of PLA composites but still there are some technical and commercial issues which affect its growth. PLA is mainly used in biomedical applications. PLA composites produce partial degradable bone plates. The development of PLA composite-based biodegradable porous structure represents a promising alternative for bone grafting [66, 68]. PLA composite device materials are also being developed for the replacement of metal plates, screws, pins and nails for fracture fixation. PLA based biocomposites are fully biodegradable and biocompatible and have shown potential growth for developing polymeric scaffolds for tissue engineering applications[13].

Another area where PLA is making good improvement and seems to have good prospects in the future, is packaging. As a packaging material, PLA is attractive

because it exhibits a tensile strength comparable to that of petroleum-derived thermoplastics, degrades under commercial composting conditions, and can be sealed at low temperatures.PLA is mostly used in short-term packing products but research efforts are continuing to overcome some of the issues related to PLA packaging [4].

Another development is applications of biodegradable composites in the automotive industry. Developing biodegradable composites for interior and exterior uses in the automotive sector has gained a lot of momentum. There are a lot of potential benefits of using the PLA-based composites in car design, as a concept of “green car” is appealing from both the consumer and manufacturer point of view [91]. Automotive manufacturers are exploring various applications of PLA composites but still there are technical issues which need to be resolved first.

Recently another PLA-based composite has been developed to be used in the electronic industry which is still in the developmental phase[14].

While numerous opportunities exist for PLA composites to enter into new markets, the future growth and sustainability of PLA composite is reliant on continued research, which will help in producing technically viable and economically feasible PLA composites in the future to widen its application spectrum.

Chapter 4 EXPERIMENTAL

Three different reinforcement materials (fillers), wood , flax and talc were incorporated into PLA to develop PLA composites

4.1 Materials

All raw materials used in this project with their trade name and supplier of each are listed in Table 4- 1.

Table 4- 1: List of raw materials

Ingredients	Supplier	Trade name	Comments	
			Median Diameter (Particle size)	Relative density
Polylactic acid (PLA)	Hycail, BV (Now Tate & Lyle)	HM1010 (Granules)	-----	1.24 g/cm^3
Wood Powder	A & O filmpack Ltd. UK.	Wood flour	150 'micron' (110 mesh size)	0.22 – 0.26 g/cm^3
Copolymer	Robinson Brothers, Ltd. UK	Not a commercial product	N/A	N/A
Silane Coupling Agent	Sigma- Aldrich Co. Ltd. UK.	Dow Corning® Product Z-6020	----	1.03 g/ml @ 25^{o}C
Flax Fibre	TRG, De-Montfort University Leicester, UK	Agatha & Electra	16 "micron" (SEM Analysis)	1.5 g/cm^3 (literature)
Epoxidized Natural Rubber (ENR)	TARRC,UK	ENR50	50 mol % epoxidation	---
Talc 1	Luzenac Inc. USA / Canada	JetFine 3CC	0.9 'micron'	2.78 g/cm^3
Talc 2		JetFL 625C	2.2 'micron'	2.7 – 2.8 g/cm^3

PLA granules (HM1011) were supplied by Hycail BV (now Tate & Lyle, London, UK) in the form of semi- transparent pellets. The weight average molecular weight (M_w) of the PLA was found to be 224 x 10^3 g/mol as determined by gel permeation chromatography (GPC). Its specific gravity was 1.24 g/cm3

The dry wood was supplied in powder form sourced from european timber yards, typically in Scotland or the Nordic Countries.

The Copolymer was supplied by Robinson Brothers Ltd UK. It is a low molecular weight (2,000) polymer. It is a star shaped polymer made from reacting ethoxylated pentaerithratol with lactide. It is therefore compatible with PLA.

Coupling agent based on silane, [3-(2-Aminoethylamino) propyl] trimethoxy silane, molecular weight 222.36 (g/mol) was used to improve the interfacial adhesion and properties of PLA - wood composites.

Two different grades of mineral filler, Talc 1 and Talc 2 were chosen to incorporate into the PLA matrix. They consist of > 99 (wt %) talc and < 2 (wt %) Magnesite.

Flow chart of development and processing of PLA composites and characterization methodology used, is shown in Figure 4- 1 below.

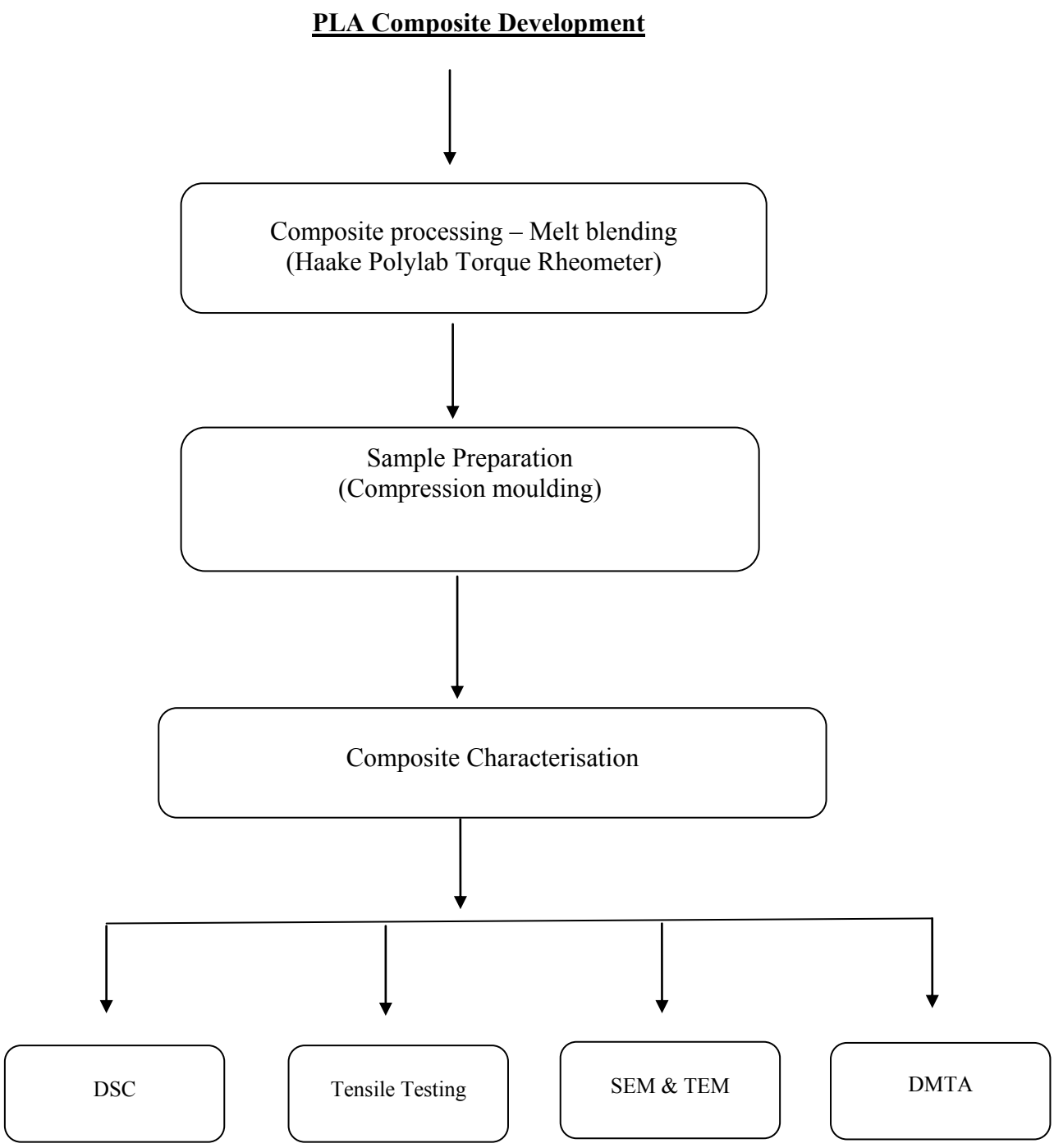

Figure 4- 1: Flowchart for experimental procedures

4.2 Mixing and processing of composites

PLA was pre-dried at 60°C for 16 hrs in a de-humidified oven prior to processing. All composites were processed in a Haake Polylab mixer (Thermo Electron Corporation Waltham, MA) to achieve melt blending with different reinforcement materials in various ratios. For each shot, the total mass was about 60 (g). Figure 4- 2 shows the Haake polylab mixer. The formulations and compounding conditions to develop different PLA composites are listed in Tables 4-2, 4-3, 4-4, 4-5 and 4-6.

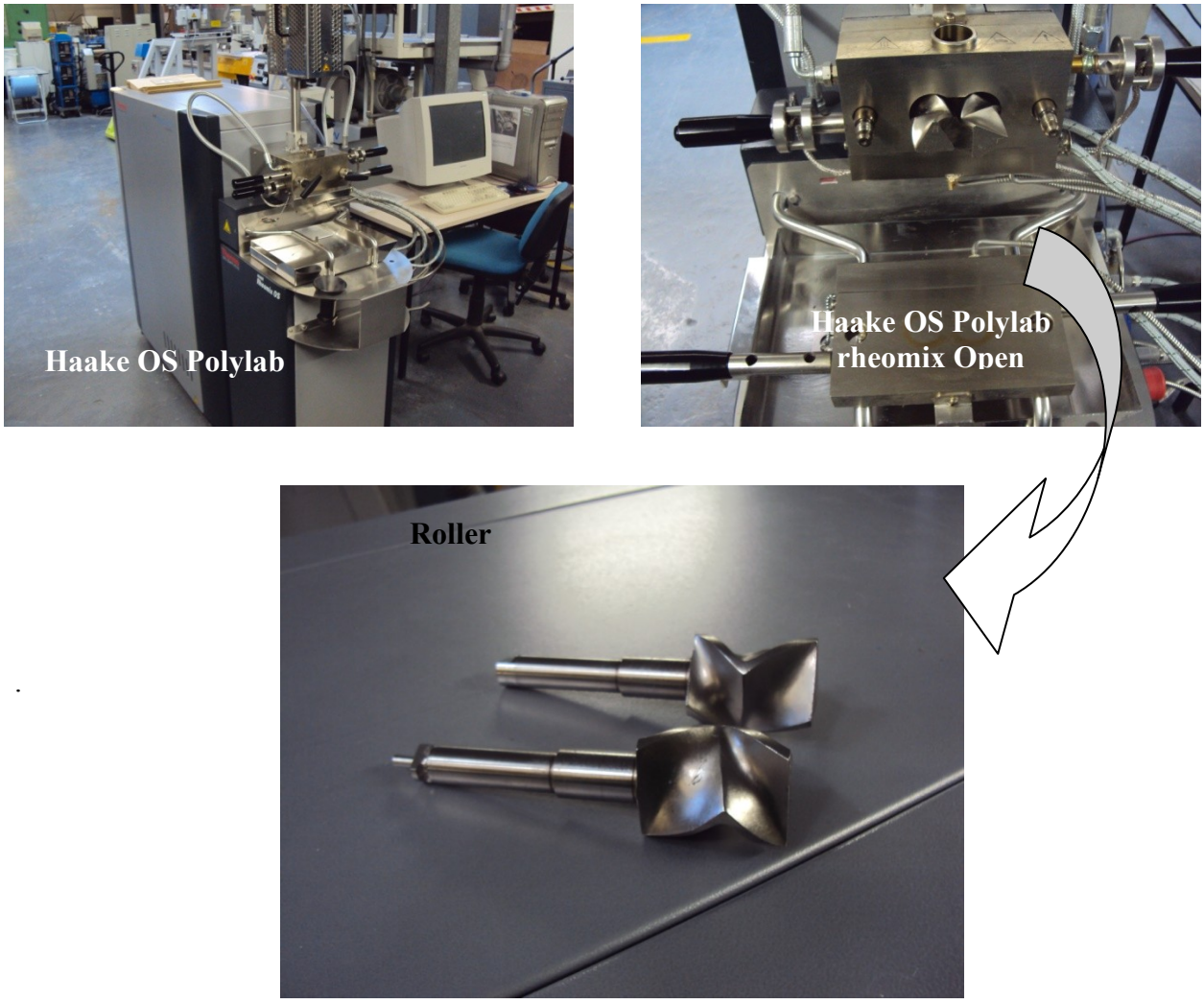

Figure 4- 2: Haake Polylab rheomix and rotors

4.2.1 Mixing protocol

For PLA/wood composites, PLA was melted first in a Haake mixer and then the wood was incorporated into PLA. For PLA/Wood/Copolymer composites, the copolymer was melt blended first in a Haake mixer with PLA and then the wood is mixed into PLA/copolymer mixture in the mixer.

In order to improve the interfacial adhesion of the matrix and the fibre, wood fibres were treated with silane based coupling agent. [3-(2-Aminoethylamino) propyl] trimethoxy silane coupling agent was used for surface treatment of wood. To see the effect of surface treatment on the mechanical and thermal properties of the composite, only one formulation of reinforcement was chosen. For this reason PLA composites were made only with 20 (wt %) silane treated wood fibres. Two different procedures were used to coat the wood fibres with silane.

1. Integral mixing of the matrix, fibres and silane described as pre-mixed samples.

2. Treatment of fibres with silane based solution prior to mixing with the matrix described as pre-treated samples.

4.2.1.1 **Pre-mixing**

First, the wood was fed into the kinetic mixer (K-mixer) and then 3 (wt %) of silane i.e. (0.35 g silane) was added into the wood contents. The amount of silane 3 (wt %) employed in this study was a percentage relative to the wood fibre content in the formulations; thus the higher the wood fibre content, the higher the silane content. The K-mixer was turned on, on slow speed (60 rpm), and left running for about 5~10 minutes. This helped to properly disperse the silane within the wood fibre. After silane coating, the wood fibres were melt blended with PLA in the Haake Rheometer to produce composites.

4.2.1.2 **Pre-treatment**

Figure 4- 3 shows the wood fibres when treated with silane coupling agent. The following procedure was used: 11.8 g (20 wt %) of wood fibres were placed in a flask, containing 100 (ml) of acetone and 0.34 - 0.36 g (3 wt %) of [3-(2-Aminoethylamino) propyl] trimethoxy silane relative to the weight percentage of wood. The mixture was refluxed at room temperature for 3 hours in a fume cupboard. This was followed by filtering the solution using a vacuum suction pump, and then the mixture was dried at room temperature for about 24 hours in a fume cupboard to evaporate the acetone solution. After that the mixture was dried in an oven at (60^{o}C) for 24 hrs. Then the pre-treated wood fibres were melt blended with PLA in the Haake.

Pure PLA was also treated with 3 (wt %) silane to see the interaction of silane with the matrix itself.

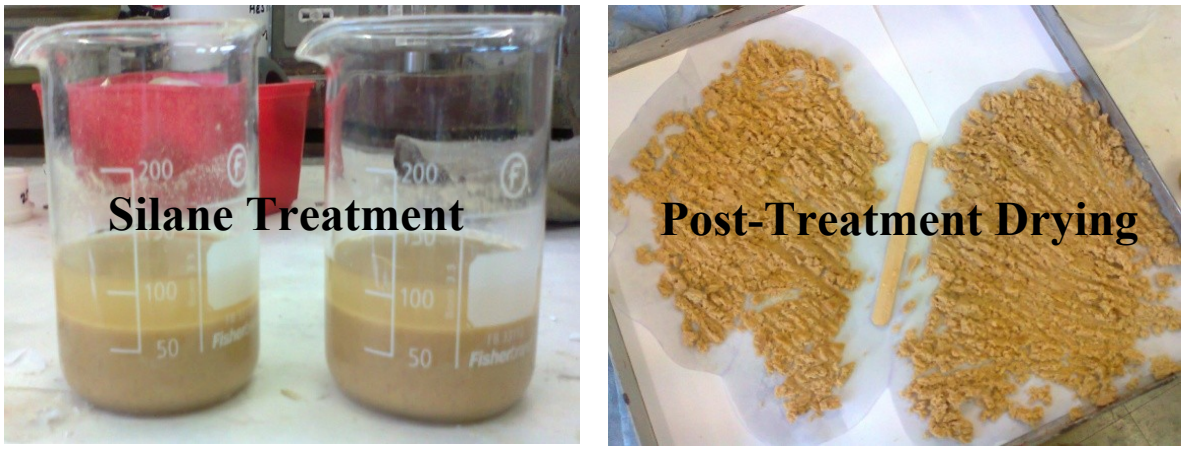

Figure 4- 3: Silane surface treatment of wood fibres

Table 4- 2, Table 4- 3, Table 4- 4, Table 4- 5 and Table 4- 6 show the formulations and compounding conditions of PLA - wood - copolymer, PLA - wood (Silane), PLA-Flax, and PLA - talc composites respectively.

Table 4- 2: Formulations and Compounding conditions for PLA, wood, Copolymer and coupling agent composites.

No	PLA/wood	Copolymer	Rotor Speed	Temperature	Time
	(wt %)	***(wt%)***	***(rpm)***	***(^{o}C)***	***(min)***
1	100/0	---	60	170	10
2	90/10	---	60	170	10
3	80/20	---	60	170	10
4	60/40	---	60	170	10
5	95/0	5	60	170	10
6	90/0	10	60	170	10
7	85/10	5	60	170	10
8	80/10	10	60	170	10
9	75/20	5	60	170	10
10	70/20	10	60	170	10
11	55/40	05	60	170	10
12	50/40	10	60	170	10

Table 4- 3: PLA- wood (silane treatment) compositions

No	***PLA (wt %)***	***Wood (wt %)***	***Silane (wt %)***
Pure PLA	100	---	---
Pure -Treated	100	---	3 (~ 3g)
Pre-Mixed	80	20	3 (~ 0.35g)
Pre-Treated	80	20	3 (~ 0.35g)

For PLA/flax composites the PLA is melted first in a Haake and then the flax fibres were mixed with PLA to develop the composites. Formulations and mixing conditions are given the Table 4- 4 below.

Table 4- 4: Formulations and Compounding conditions for PLA- Flax composites

No	PLA	Flax	Rotor Speed	Temperature	Time
	(wt %)	***(wt%)***	***(rpm)***	***(^{o}C)***	***(min)***
1	100	0	60	170	10
2	90	10	60	170	10
3	80	20	60	170	10
4	70	30	60	170	10

In a second stage composites based on the mixtures of PLA, flax fibres and ENR50 were prepared in three different formulations using masterbatches of ENR50 and flax.

I. Masterbatch 1 (MB1) was prepared with flax and ENR50 weight ratio of 1:1. Subsequently mixtures of PLA and MB1 at 60:40 weight ratios were prepared under the same mixing conditions. This gives composites of PLA/Flax/ENR at 60/20/20 weight ratios.

II. Masterbatch 2 (MB2) was prepared with Flax and ENR at weight ratio of 2:1, and the mixtures of PLA and MB2 were prepared at 70:30 ratio. This was then used to produce composites of PLA/Flax/ENR at 70/20/10 weight ratios.

Details of the formulations and weight ratio of masterbacthes to the PLA are described in Table 4- 5.

Table 4- 5: Formulations and Compounding conditions for PLA- Flax-ENR composites

No	PLA	Flax/ENR	Rotor Speed	Temperature	Time
	(wt %)	***(wt%)***	***(rpm)***	***(^{o}C)***	***(min)***
1	60	20/20	60	170	10
2	60	MB1 (40)	60	170	10
3	70	MB2 (30)	60	170	10

Note: MB1: Masterbatch 1, MB2: Masterbatch 2

For PLA/Talc composites the PLA is melted first in a Haake and then the talc filler was mixed with PLA to develop the composites. Formulations and mixing conditions are given Table 4- 6 below.

Table 4- 6: Formulations and Compounding conditions for PLA and Talc 1 & 2 cmposites.

No	PLA	Talc1	Rotor Speed	Temperature	Time
	(wt %)	***(wt%)***	***(rpm)***	***(^{o}C)***	***(min)***
1	100	0	60	170	10
2	90	10	60	170	10 ~12
3	80	20	60	170	10 ~12
4	70	30	60	170	10 ~12
		Talc2			
5	90	10	60	170	10 ~12
6	80	20	60	170	10 ~12
7	70	30	60	170	10 ~12

4.3 Compression Molding of PLA Composite

The PLA and its composites melt blended in the Haake OS-Polylab Rheomix were hot pressed at 180°C to mold samples for tensile testing and DMTA. The compression molding machine used was a 20 Ton Lab press C01123/1.

For all types of samples the compression molding process was as follows:

a. The mold was filled with PLA and its composites and placed between two plates with the protection of polyethylene teraphthalate (PET) film on both sides. The mold was sprayed with a mold release agent before being filled.

b. When the temperature reached 180°C, the assembly was put into the press, and the height adjusted until the assembly just touched the plates of the press. 5~6 minutes were allowed to melt the composite before applying the pressure.

c. Initially a pressure of 1~3 tons was applied for 5~10 seconds and then released. This process was repeated about 3~4 times to release any trapped steam and air and hence to prevent air bubbles.

d. A pressure of 10 tons was applied on sample mould of 5 x 5 (inches) and held for 3 minutes.

e. The mold assembly was moved to another press at room temperature applying the same pressure for about 3 minutes.

f. The assembly was cooled down to room temperature and the pressed sheet was extracted very carefully not to damage the samples and sheet.

Figure 4- 4 shows the dimensions and dog bone shapes of the compression molded samples for tensile testing. Thickness of the sample is 2(mm).

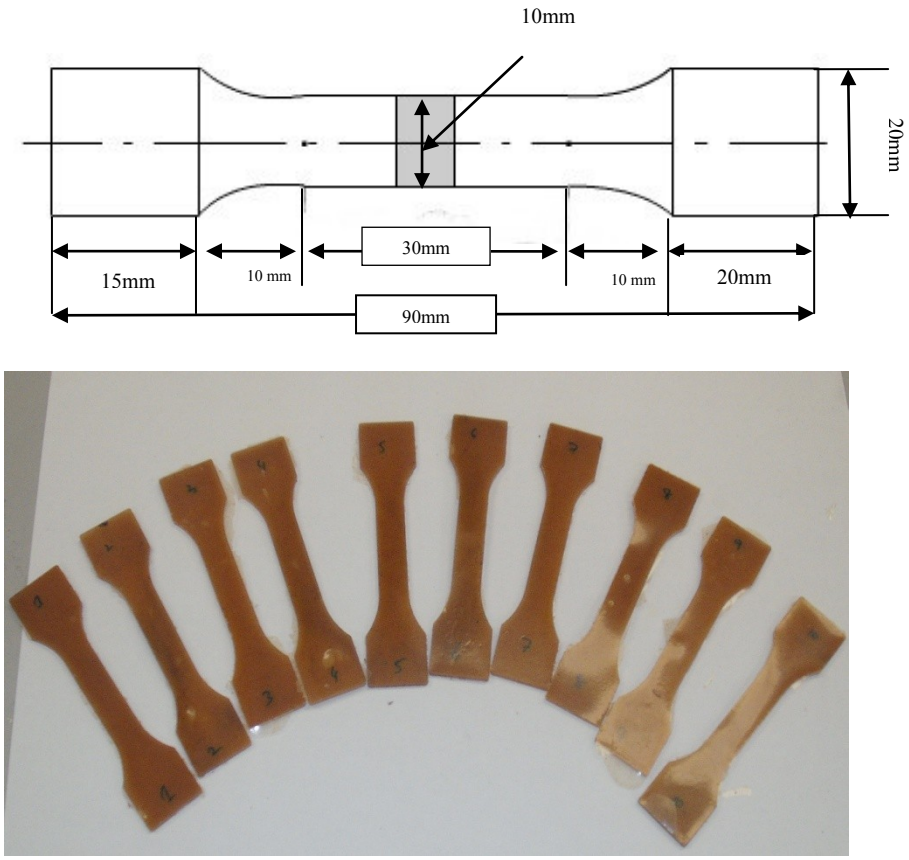

Figure 4- 4: Dimensions and shape of tensile test specimen

For DMTA, a sample of the size (64 x 12 x 3) mm was cut from a hot pressed sheet using a conventional sharp cutting saw according to the required size for dynamic thermo mechanical analysis. Figure 4- 5 shows the dimension and shape of the DMTA specimens.

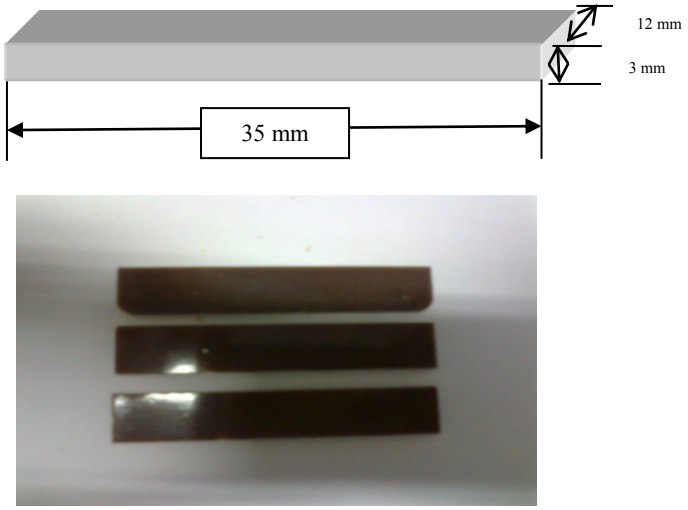

Figure 4- 5: Dimensions and shape of DMTA specimens

Figure 4- 6 shows the images of the 20 ton hot press and cold hydraulic press used for compression moulding of the samples.

Figure 4- 6: Hot & Cold Press Compression Moulding

4.4 Measurements

4.4.1 Thermal characterization

Differential Scanning Calorimetry (DSC)

Differential scanning calorimetry (DSC) was used to measure the thermal transition temperatures and crystallinity of all samples described in this research. The measurement was performed on a DSC Q200 apparatus fitted with samplers and mechanical cooler (TA Instruments, USA). Samples of approximately 10~15 mg in mass were placed in sealed aluminium pans and loaded into the sampler (furnace chamber). The machine was run on heat-cool-heat mode and the second run was considered for analysis. The samples were heated from 0°C to 200°C at 10°C / min to measure the melting point of the as-formed samples, then cooled down to 0°C at the same heating rate to determine the crystallinity. Then the

samples were reheated to 200°C at 10 °C/min to study the melting . Figure 4- 7 shows the Q200 DSC instrument along with the mechanical cooler unit.

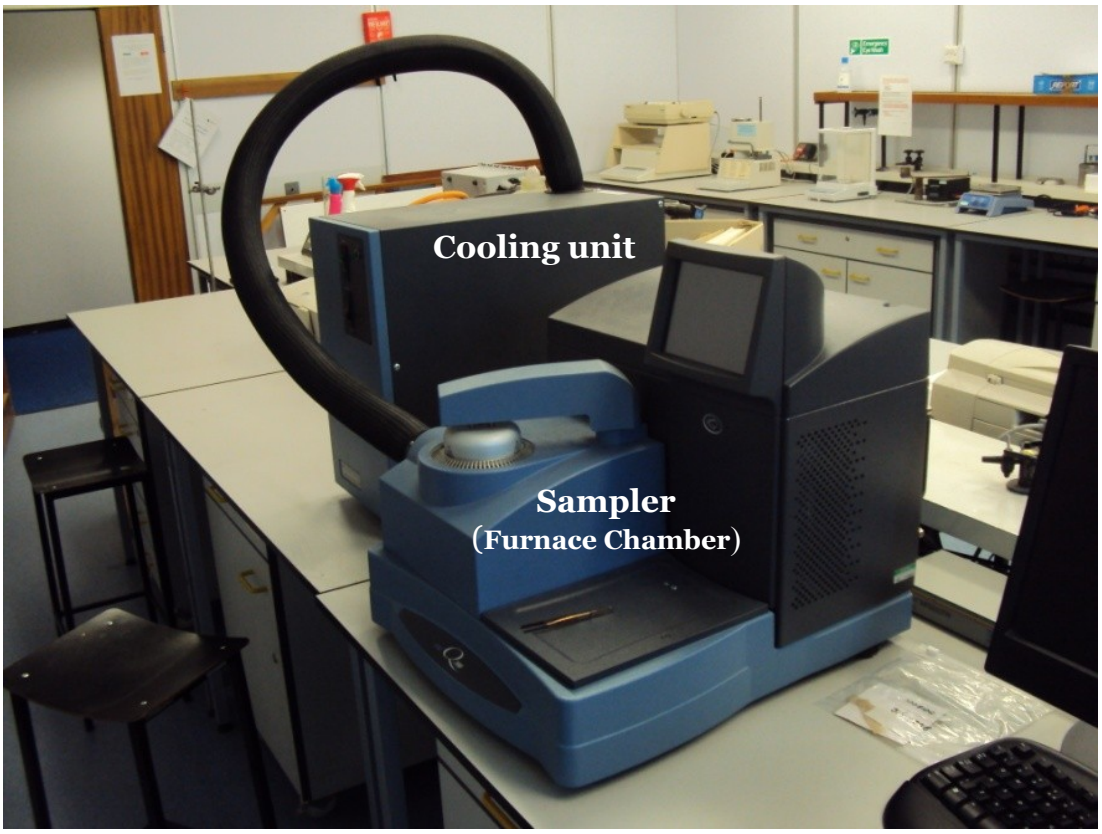

Figure 4- 7: DSC Q200 (TA Instruments) with mechanical cooler

Figure 4- 8 shows a generic diagram of PLA DSC scan indicating the glass transition, cold crystallization and melting points. The plot shows the heat flow as a function of temperature at a specified heating rate and signifies the different transitions. A significant change is observed when the sample goes from glassy to rubbery state and the step change is defined as the glass transition temperature. As the heat flow continues the sample undergoes an exothermic transition identified as the cold crystallization phenomenon. Similarly as the heat flow continues further, there is an endothermic peak, which is the melting process in the given sample. Analysis of the DSC scan was used to calculate the percent crystallinity for PLA and its composites. All calculations were based on the second heat scan.

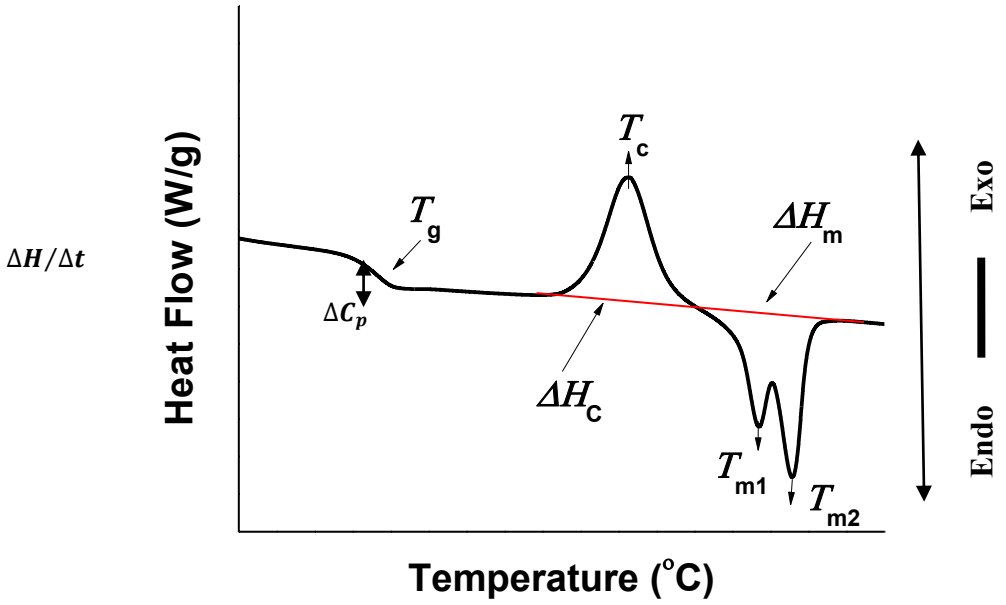

Figure 4- 8: Generic second heat DSC thermograph for PLA and its composites

The percent crystallinity for PLA composites was calculated using Equation 4- 1, where 93.1 is enthalpy of fusion for 100 % crystalline PLA, $\Delta\mathbf{H_m}$, is the measured heat of fusion and $\Delta\mathbf{H_c}$, is enthalpy of crystallization.

$$Crstallinity(\%) = \left[\frac{\Delta H_m - \Delta H_c}{93.1}\right] * 100$$

Equation 4- 1: Percent Crystallinity of PLA

Equation 4- 2 is used to calculate percent crystallinity for PLA Composites from DSC scan where *"w"* is the weight fraction of PLA in the sample [4, 117].

$$Crstallinity(\%) = \left[\frac{\Delta H_m - \Delta H_c}{93.1(w)}\right] * 100$$

Equation 4- 2: Percent Crystallinity of PLA Composites

4.4.2 Mechanical Testing

Tensile Testing

Tensile testing was used to measure the tensile properties such as Young's modulus, tensile strength, stress at break and elongation to break. Tensile testing was performed on a Lloyd LR50K tensile testing machine equipped with two different load cells 1kN and 50kN. Accuracy of the tensile modulus was checked by repeating the test using the Tinius Olsen H50 KS testing machine with a clip-on extensometer used to measure the extension more precisely.

For PLA and its composites, dumbbell – shaped tensile specimens (width ~3mm, thickness ~ 2mm, Lo =30 mm) were extended at a crosshead speed of 10 (mm/min). The Young's modulus, stress at break and strain at break were measured. Figure 4- 9 shows the Lloyds 50K tensile testing machine.

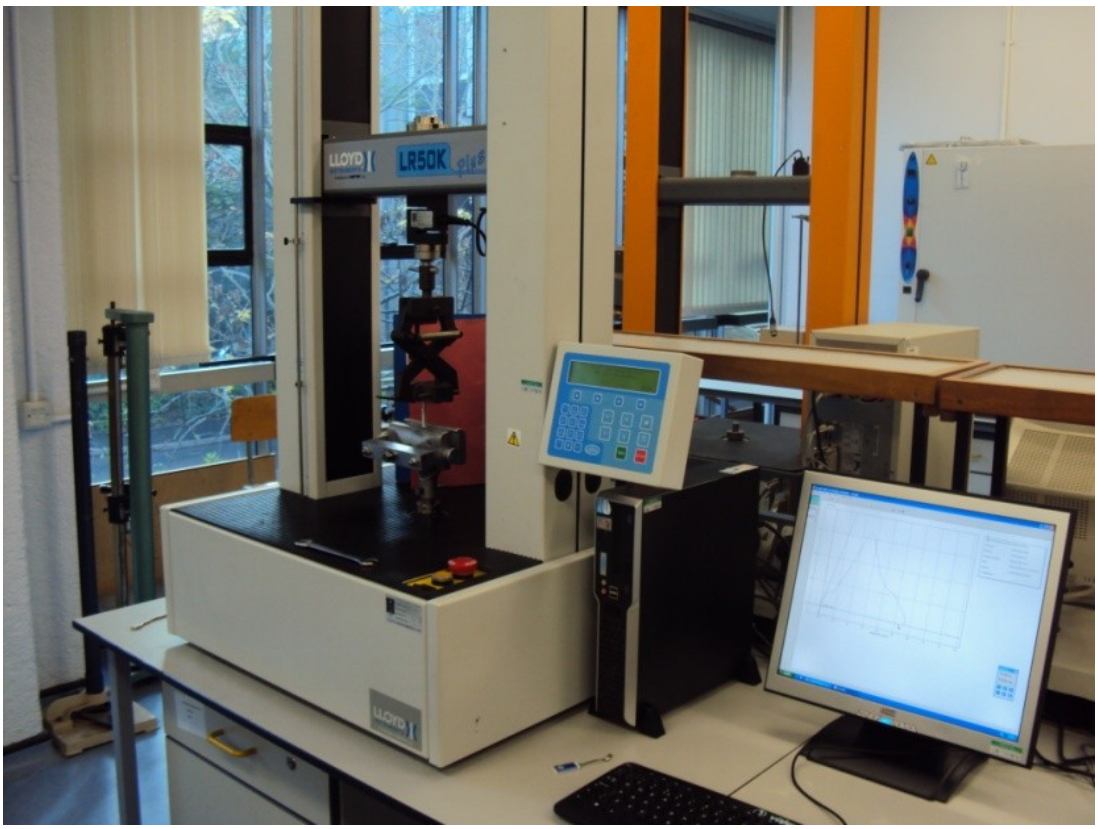

Figure 4- 9: Lloyd LR50 K Tensile testing machine

4.4.3 Morphological characterization

Scanning Electron Microscopy (SEM)

A scanning electron microscope (SEM), LEO 1530 VP, (Carl Zeiss – Leo Germany) was used to investigate the morphology of PLA and its composites, particularly the fracture surface of the tensile sample. The morphology of fibre reinforcement and filler were also analyzed. For wood and talc, a tiny sample was stuck to the aluminum stub and coated with gold to make it electrically conductive, thus preventing charging up and allowing it to be imaged and analyzed using this technique. Fracture surfaces of the tensile specimens of PLA and its composites were also analyzed. A small piece of the fracture surface was fixed with adhesive bonding to the aluminium stub and coated with gold, then imaged and analyzed using the SEM to investigate the fracture surface morphology. Backscattered SEM technique was also used to see the compositional contrast within the composite samples in order to analyze the distribution of the filler in the matrix. Figure 4- 10, shows the machine used for scanning electron imaging of the tensile fractured surface.

Figure 4- 10: LEo 1530 VP, Scanning Electron Microscope

Transmission Electron Microscopy (TEM)

The dispersion of talc in the PLA matrix was visualized by using transmission electron microscopy (TEM). The analysis was conducted on a JEOL 2000 FX Transmission Electron Microscope. In order to prepare the samples they were cut into small isosceles triangle shaped pieces. These pieces were then mounted in epoxy resin in a plastic container and kept in an oven at 60^{o}C for 24 hours. When the resin was cured, it was taken out of the container and the epoxy resin was cut to expose the embedded specimen. Samples were cut into thin sections with an ultra-microtome using a diamond knife at room temperature. Copper (Cu) grids were used to collect the sections and insert them into the microscope for analysis. The aspect ratio of the talc was then measured using image processing software. Figure 4-11 shows the machine used for transmission electron microscopy.

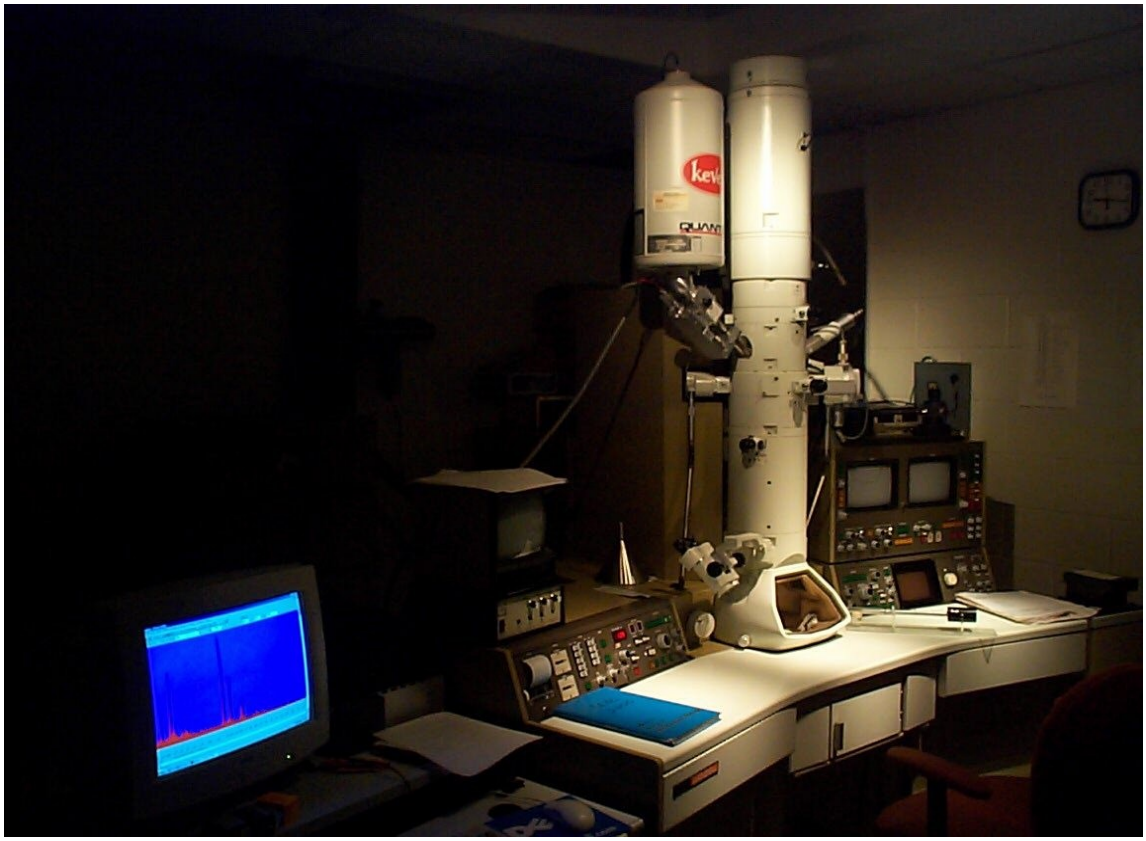

Figure 4-11: JEOL 2000 FX Transmission Electron Microscope

4.4.4 Dynamic Mechanical Thermal Analysis (DMTA)

Dynamic mechanical thermal analysis (DMTA) is a thermal analysis technique used to measure changes in the viscoelastic behaviour of a material as a function of temperature, time, or deformation frequency.

DMTA measurements of PLA and its composites were performed in three point bending (Flexure) mode (L_o = 35 mm) using the DMA Q800 apparatus (TA Instrument Inc, USA) as shown in Figure 4- 12. The rectangular specimens for PLA and its composites of (width ~12mm, thickness ~ 3mm, L_o =35 mm), were heated from room temperature to 140° C at 3° C / min, with a constant frequency of 1 Hz. The storage modulus (E'), Loss modulus (E''), and loss factor tan δ (where tan δ = E''/E', and δ is a phase angle) were recorded. DMTA data were analyzed using the TA data analysis package known as "Universal Analysis". Figure 4- 12 shows the DMA equipment and Figure 4- 13 shows the generic DMA analysis for PLA and its composites.

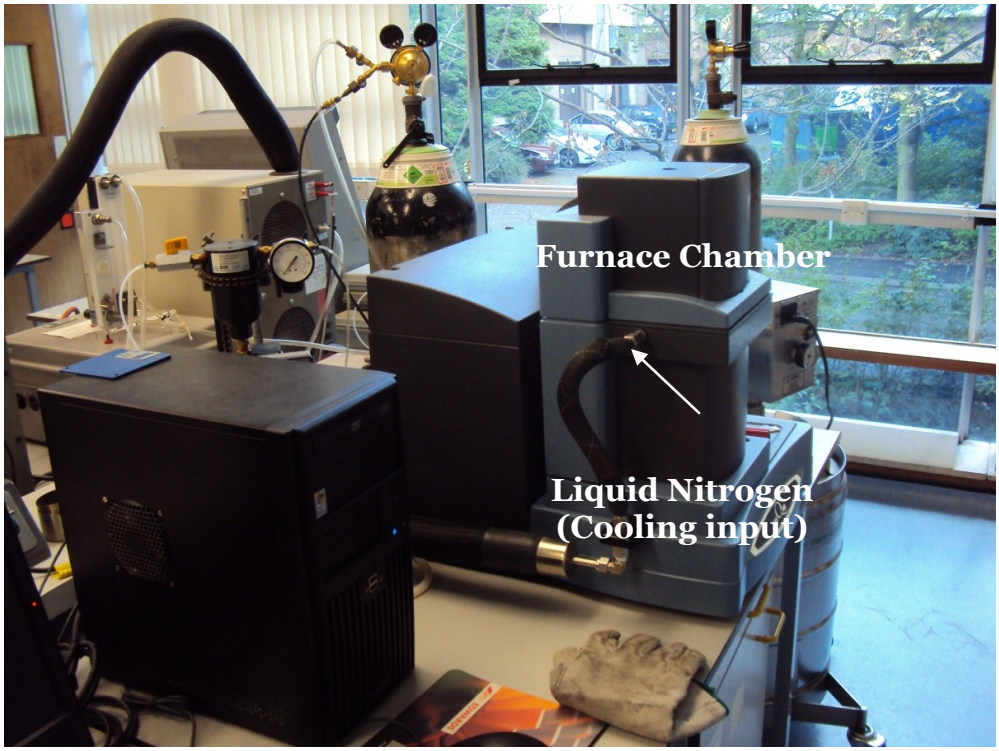

Figure 4- 12: DMA Q800 (TA Instruments, USA)

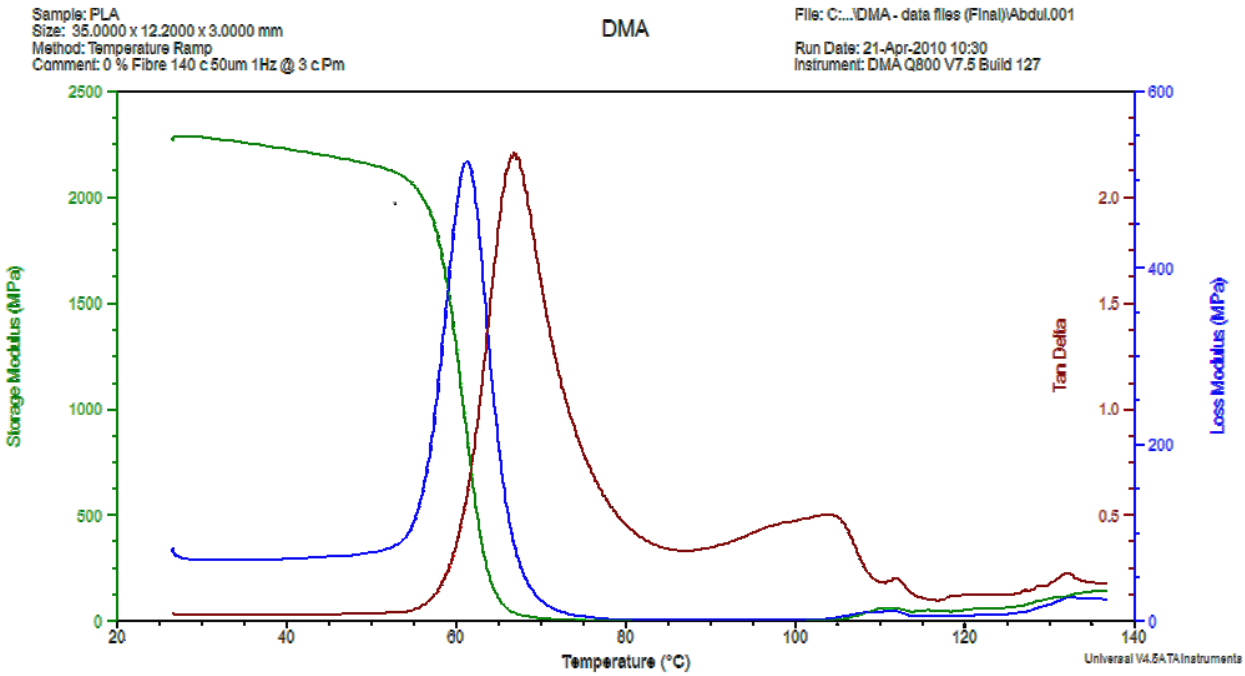

Figure 4- 13: Generic DMA analysis PLA and its composites)

RESULTS AND DISCUSSION

Chapter 5 PLA – Wood Composites

In this chapter, characterization of PLA was carried out to investigate its inherent properties . A series of experiments was also performed to study the thermal and mechanical behaviour of wood-based PLA composites. The main experimental results obtained are presented, with significant features indicated and interpreted and comparison between PLA and formulated composites was made to study the effect of reinforcement.

In the first phase of the project, PLA /wood flour composites were prepared with the following (weight %) of wood flour; 0, 10, 20, 40. The effect of moisture was also studied by developing PLA composites reinforced with dried and non-dried wood.

In the second phase, the PLA/wood flour composites were prepared with the same proportion of filler as described above but copolymer was added to plasticise the PLA and aid penetration of the matrix into the wood fibres. Two sets of samples were prepared; the first set with 5 (wt %) of copolymer (CP) and the second set with 10 (wt %) of CP.

In the third phase wood was treated with a silane based coupling agent to see the effect. Analysis and experimental results are described in detail below.

5.1 Differential Scanning Calorimetric Analysis (DSC)

The main purpose of this experiment was to characterize the thermal properties of PLA and PLA-Wood composites. The thermal properties of PLA (amorphous or semi-crystalline) are not only determined by its chemical structure, chain conformation and molecular weight distribution but also by the crystallization mechanism and kinetics. Apart from determining the melting point, DSC analysis

is also one of the most convenient ways to find out the crystallization behaviour of PLA and its composites.

Two samples of each formulation were tested to analyze the thermal properties. All the results were based on the second heat run.

5.1.1 PLA and Non-Dried Wood

DSC thermographs of pure (neat) PLA and PLA plus non-dried wood (NDW) composite are shown in Figure 5- 1. 0 (wt%) fibres represent neat PLA while the different fibre contents (10 %, 20 % and 40 %) show the weight % of non-dried wood in the composite.

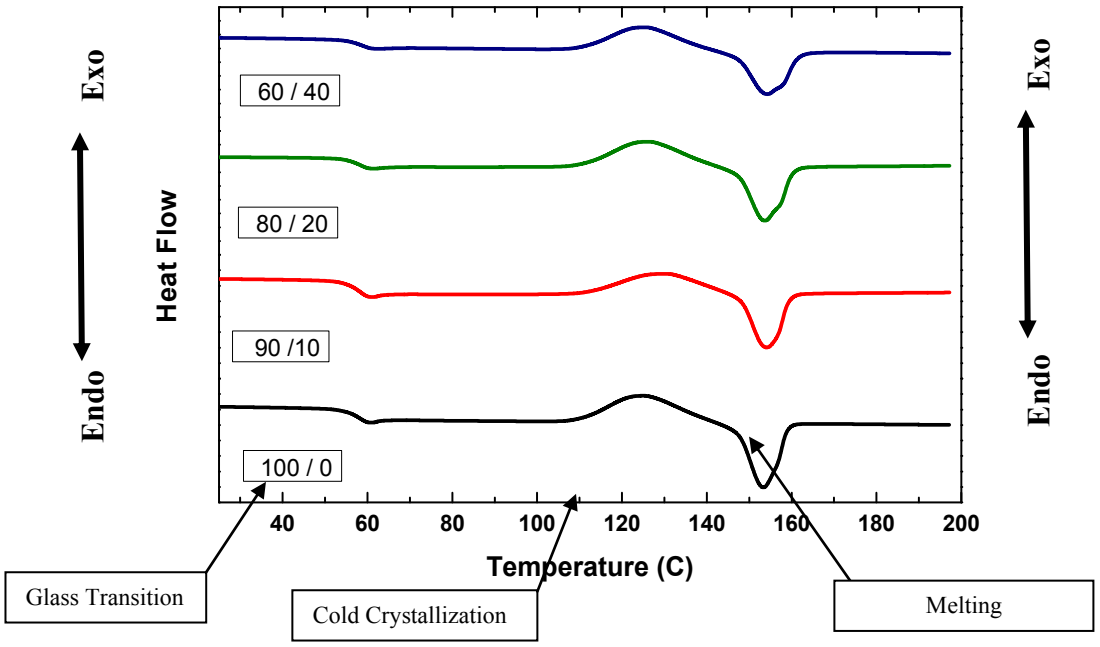

Figure 5- 1: DSC 2nd heat thermogram of PLA-non dried wood composites

As shown in Figure 5- 1 the transition (step change in DSC scan) where the sample changes from the glassy state to the rubbery state, takes place between 55°C and 60°C. Glass transition temperature for PLA and non-dried wood composites was also recorded at about 55°C. There is no significant difference in the glass transition with the addition of non-dried wood fibres into the PLA matrix. Table 5- 1 shows the thermal properties of PLA and PLA-non dried wood composites.

Table 5- 1: Thermal properties of PLA + non dried wood composite

PLA / Wood	*Tg*	T_c	T_m		Cold - Crystallization	Crystallinity
(wt%)	(^{o}c)	(^{o}c)	(^{o}c)		(%)	(%)
			α	β		
100/0	54 ± 0.7	127 ± 1.4	155 ± 1.5	---	22 ± 1.2	2.0 ± 0.8
90/10	55 ± 0.2	130 ± 0.3	155 ± 0.7	---	15 ± 0.8	2.0 ± 1.2
80/20	56 ± 1.3	127 ± 1.4	157 ±0.2	154 ± 0.2	22 ± 2.1	1.3 ± 0.4
60/40	56 ± 1.4	122 ± 2.6	157 ± 1.3	152 ± 1.4	24 ± 2.3	8.4 ± 1.2

As the heat flow continues the rubbery sate of PLA becomes less viscous but at some point the molecules of PLA get enough energy to obtain freedom of motion and suddenly arrange themselves into a crystalline form and this is the point where the cold crystallization takes place. Cold crystallization is a transition from an amorphous to a crystalline solid, which results in an exothermic peak in the DSC thermogram. For PLA and non-dried wood composite, cold crystallization takes place around 127^{o}C. There is no observation of a significant shift of the cold crystallization peak for wood levels of 10 and 20 (wt %). However 40 (wt %) addition causes a reduction in cold crystallization temperature to 122^{o}C, showing that the wood may be having a nucleating effect.

As the temperature increases, the sample starts melting and eventually reaches the melting point. The enthalpy of cold-crystallization changes with increase in wood content, which also causes corresponding changes to the enthalpy of melting. As shown in Table 5- 1 with increasing wood content the crystallinty of the samples increases. The crystallinity increased from about 2.0 ± 0.83 to 8.0 ± 1.2 (%) when 40 (wt %) non-dried wood fibre is incorporated into the PLA matrix. An increase in crystallinity indicates that the filler acts as a nucleating agent, but this only takes place for high wood contents of 40 (wt%).

This increase in crystallinity agrees with the findings from the literature that addition of wood as filler enhances the crystallinity of PLA also found by S.Pilla et al. and others [17, 97]. There is no crystallization peak observed in all the DSC cooling scans for PLA and PLA+WF composites. This was also observed by Pilla et al.[97].

During the melting process the most noticeable feature is the occurrence of a double melting peak with increasing amount of filler. It is not so evident in the addition of a low amount of filler but as the amount of wood fibre increases, this double peak becomes clearer. Research publications are available which show a similar kind of result, but no explanation has been found for the double peak melting endotherm behaviour [11, 93, 96, 97, 111].

The double melting peak could be because of the sample having two different spherulite forms or it could be two different crystalline forms but this is not yet clear. In the case of two different spherulite types one may be formed during the composite preparation and the second formed during sample preparation, because at both times the PLA composite is processed above its melting point. The peak appearing at the higher temperature represents a thermally more stable crystalline form, while the second peak represents a thermally less stable form. The double peak didn't appear in the neat PLA and this is also observed by Tabi et al.[118]. Generally the addition of wood fibres results in increasing crystallinity, producing two different melting endotherm peaks appearing at different temperatures.

5.1.2 PLA and Dried Wood

Figure 5- 2 represents the second heat DSC thermograms of neat PLA and PLA composites reinforced with dried wood fibres. Generally there is no significant difference as compared with PLA composites reinforced with non-dried wood fibres. The glass transition occurs in the same range, almost at the same temperatures.

The cold crystallization starts around 115 (^{o}C), with crystallization peaks between 123 (^{o}C) and 127 (^{o}C) followed by a melting endotherm. The most important

difference as compared with non-dried wood fibre reinforced PLA composite is the more significant occurrence of double melting endotherm peak. In NDW–PLA composites the double peaks are not so clear but in DW-PLA composites they become more distinct. There is no change in crystallinity of DW-PLA composites; they remain almost the same as NDW-PLA composites. Thermal properties of PLA-Wood composites obtained from DSC analysis like glass transition temperature (***Tg***), crystallization peak temperature (***T_c***), melting peak temperature (***Tm***), enthalpy of cold-crystallization (ΔH_c) , enthalpy of fusion (ΔH_m) and crystallinity ($\%\, x$) does not change significantly and remains almost the same for both types of composite samples (NWD & DW fibres with PLA).

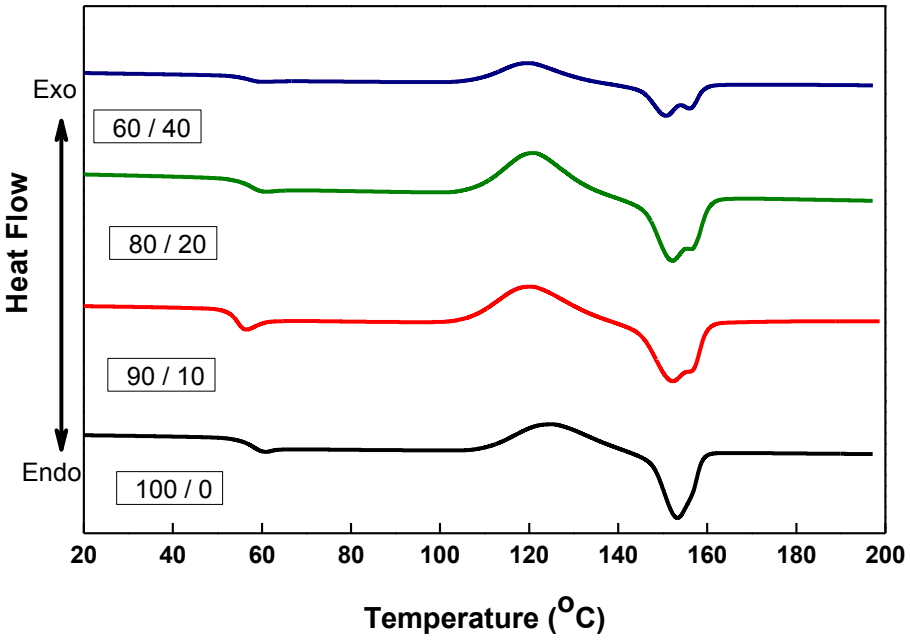

Figure 5- 2: DSC 2nd heat thermograph of PLA+ dried wood composites

Table 5- 2 shows the physical properties of PLA and PLA-dried wood composites. All the calculations are based on the second heat of the DSC run.

Table 5- 2: Thermal properties of PLA + dried wood composite

PLA / wood	Tg	T_c	T_m		Cold - Crystallization	Crystallinity
(wt%)	(°c)	(°c)	(°c)		(%)	(%)
			α	β		
100/0	54 ± 0.7	127 ± 1.4	155 ± 1.4	---	22.0 ± 1.2	2.0 ± 0.8
90/10	54 ± 1.2	122 ± 1.2	152 ± 0.4	152 ± 0.7	24.8 ± 2.8	2.6 ± 0.3
80/20	55 ± 1.4	121 ±0.8	152 ±0.2	156 ± 0.3	30.6 ± 2.1	3.8 ± 0.7
60/40	54 ± 1.1	120 ± 1.7	150 ± 1.2	155 ± 0.8	25.1 ± 1.7	5.5 ± 1.2

5.1.3 PLA and Copolymer

The effect of copolymer on PLA is shown in Figure 5- 3. When copolymer is added to pure PLA, the glass transition, crystallization temperature and melting temperature are affected by the copolymer.

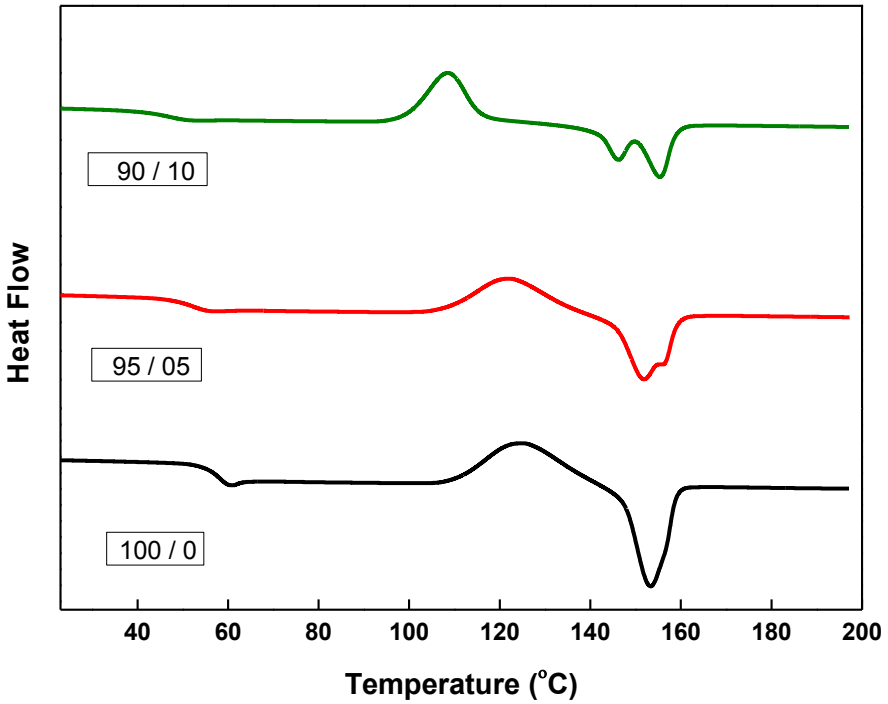

Figure 5- 3: DSC second heat thermogram of PLA+ Copolymer

The thermal properties of PLA and the effects of copolymer are shown in Table 5- 3. Analyzing the data presented in the table, it is clear that the glass transition temperature is reduced from 54°C to 47°C when the copolymer content increases from 0 to 10 (wt %). Crystallization temperature is also decreased from 126°C to 106°C. Degree of Cold crystallization is increased from 22 to 35 (%) when copolymer is increased from 0 to 10 (wt %). Copolymer also affected the crystallinity of pure PLA. Crystallinity increased from 2.0 (%) to 3.8 (%) to 5.8 (%) when the copolymer increased from 0 to 10 (wt %) content.

The reason for these results is that the copolymer is acting as a plasticizer for the PLA and hence creates more free volume in the PLA matrix. Hence the *Tg* of PLA is reduced, the cold crystallization temperature is reduced and there is an increase in the degree of cold crystallization and also in the crystallinity of PLA.

Table 5- 3: DSC properties of PLA + CP composite

PLA / CP	Tg	T_c	T_m		Cold Crystallization	Crystallinity
(wt %)	(°c)	(°c)	(°c)		(%)	(%)
			α	β		
100/ 0	54 ± 0.7	127 ± 1.4	155 ± 1.5	---	22 ± 1.2	2.0 ± 0.8
95/05	52 ± 0.55	121 ± 1.3	155 ± 0.3	151 ± 0.9	29 ± 3.2	3.8 ± 0.4
90/10	47 ± 0.20	106 ± 0.9	155 ± 0.2	146 ± 0.2	35 ± 0.7	5.8 ± 0.2

5.1.4 PLA + 10 (wt %) Wood flour + Copolymer

Figure 5- 4 shows the effect of 5 to 10 (wt %) content of copolymers on PLA + 10 (wt %) wood flour composite. The addition of 5 and 10 (wt %) copolymer has a significant effect on DSC properties of PLA and PLA-wood composites. From Figure 5- 4 , it is clear that when 10 (wt%) wood flour is added to PLA matrix, there is no apparent double peak in the melting endotherm, but when 5 to 10 (wt %) copolymer is added to the composite, the double peak becomes clearer. The

melting temperature of these double peaks can be found in the Table 5- 4 given above where **α** represent the more stable peak while **β** is the least stable.

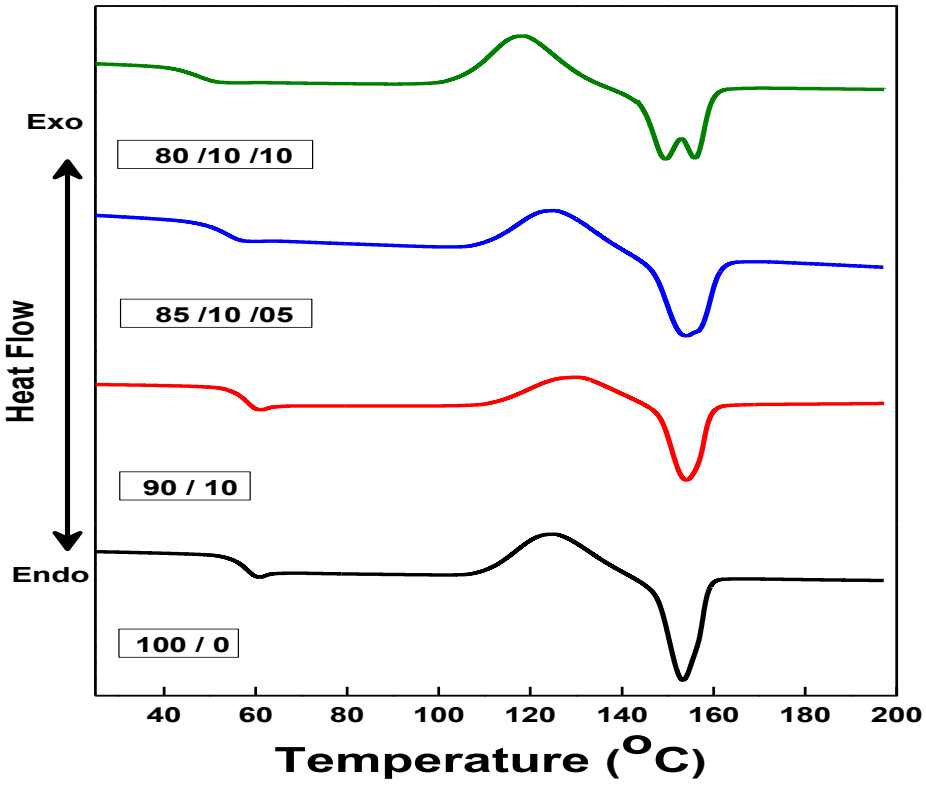

Figure 5- 4: DSC 2nd heat thermogram of PLA + 10 (wt %) wood + CP

DSC properties of PLA and PLA + 10 (wt %) wood composites are given in Table 5-4 Analyzing the DSC properties below, it is clear that the glass transition temperature goes down from 55°C to 51°C when 10 (wt %) copolymer is mixed with PLA + 10 (wt%) wood flour composite. Similarly crystallization temperature is also reduced from 130° C to 119° C when copolymer is increased from 0 to 10 (wt%). Cold crystallization of PLA + 10 (wt %) wood composite is increased from 15 to 33 % with the addition of copolymer although there is no significant change in overall crystallinity.

Table 5- 4: DSC properties of PLA and PLA + 10 (wt%)wood flour + Copolymer

PLA/ wood / CP	Tg	T_c	T_m		Cold - Crystallization	Crystallinity
(wt%)	(^{o}c)	(^{o}c)	(^{o}c)		(%)	(%)
			α	**β**		
100/0	54 ± 0.7	127 ± 1.41	155 ± 1.47	---	22 ± 1.21	2.0 ± 0.8
90/10	55 ± 0.1	130 ± 0.3	155 ± 0.7	---	15 ± 0.8	2.0 ± 1.2
85/10/5	53 ± 0.1	125 ± 0.2	156 ± 0.4	154 ± 0.1	27 ± 1.6	1.2 ± 1.3
80/10/10	51 ± 0.6	119 ± 0.2	157 ± 0.1	150 ± 0.7	33 ± 1.5	2.6 ± 1.4

5.1.5 PLA + 20 (wt %) wood flour + Copolymer

Figure 5- 5 shows the second heat DSC thermogram and the effect of copolymer on PLA + 20 (wt %) wood composite. The DSC thermogram suggests that the copolymer has affected the DSC properties of PLA + 20 (wt %) wood composites. The glass transition temperature is reduced from 56 ^{o}C to 49^{o}C when copolymer increases from 0 to 10 (wt %). Similarly the crystallization temperature reduces from 127 ^{o}C to 114 ^{o}C. The DSC thermogram also shows that the double peak in the melting endotherm becomes more evident with the addition of copolymer.

Thermal properties of PLA with 20 (wt %) wood along with copolymer are shown in Table 5- 5. The melting temperatures of the double endotherms are shown. The lower temperature peak (**β)** appears at 154 ~146 ^{o}C and the other peak (**α)** appears at 154 ~156 ^{o}C. Cold crystallization also increased from 22 to 39 (%) and there was an increase in crystallinity from 1.3 to 9.2 (%) when the copolymer content increased from 5 to 10 (wt %). Increasing the copolymer creates more free volume between the polymer chains and allow more crystallization.

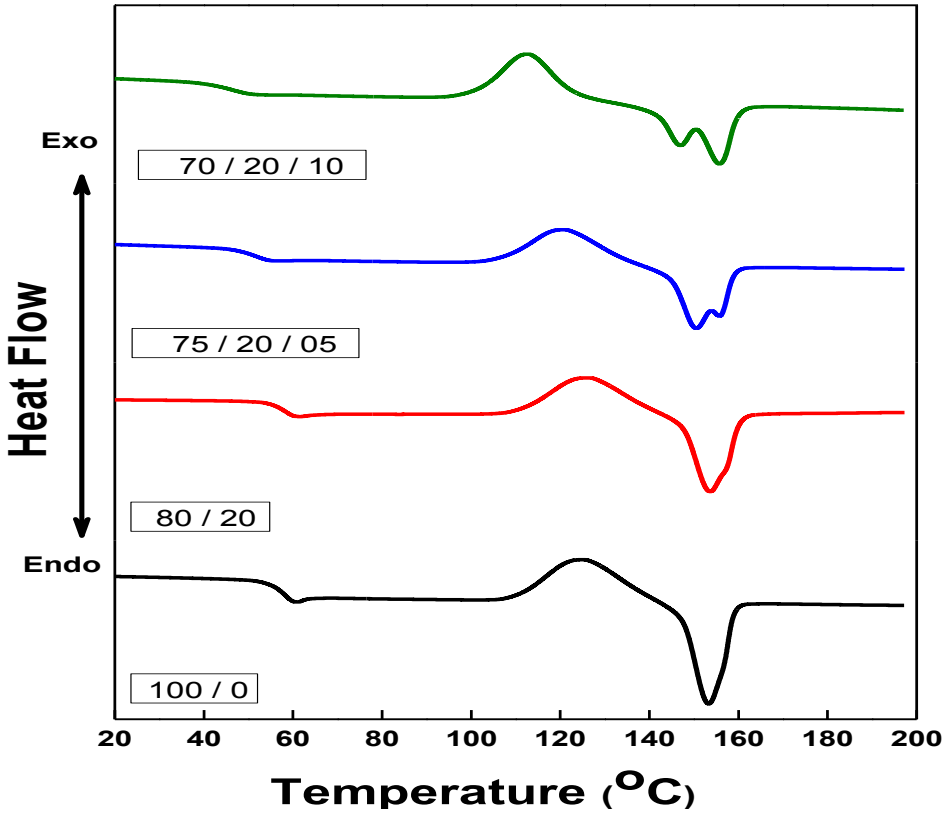

Figure 5- 5: DSC 2nd heat thermogram of PLA + 20 (wt%) wood + copolymer

Table 5- 5 shows the thermal properties of PLA and PLA- 20 (wt %) dried wood composites. All the calculations are based on the second heat of the DSC run.

Table 5- 5: DSC properties of PLA and PLA + 20 (wt%) wood flour + copolymer

PLA / wood / CP	Tg	T_c	T_m		Cold Crystallization	Crystallinity
(wt%)	(°c)	(°c)	(°c)		(%)	(%)
			α	**β**		
100/0	54 ± 0.7	127 ± 1.4	155 ± 1.5	---	22 ± 1.2	2.0 ± 0.8
80/20	56 ± 1.3	127 ± 1.4	157 ± 0.2	154 ± 0.2	22 ± 2.1	1.3 ± 0.4
75/20/5	51 ± 1.3	121 ± 0.3	156 ± 0.3	150 ± 0.6	35 ± 2.2	1.8 ± 0.2
70/20/10	49 ± 0.3	114 ± 1.5	156 ±0.5	146 ± 0.8	39 ± 1.8	9.2 ± 1.2

5.1.6 PLA + 40 (wt %) wood flour + copolymer

The effect of wood 40 (wt %) as filler together with copolymer on PLA is shown in Figure 5- 6. The figure indicates clearly that wood flour and copolymer both have a significant effect on the thermal properties of PLA.

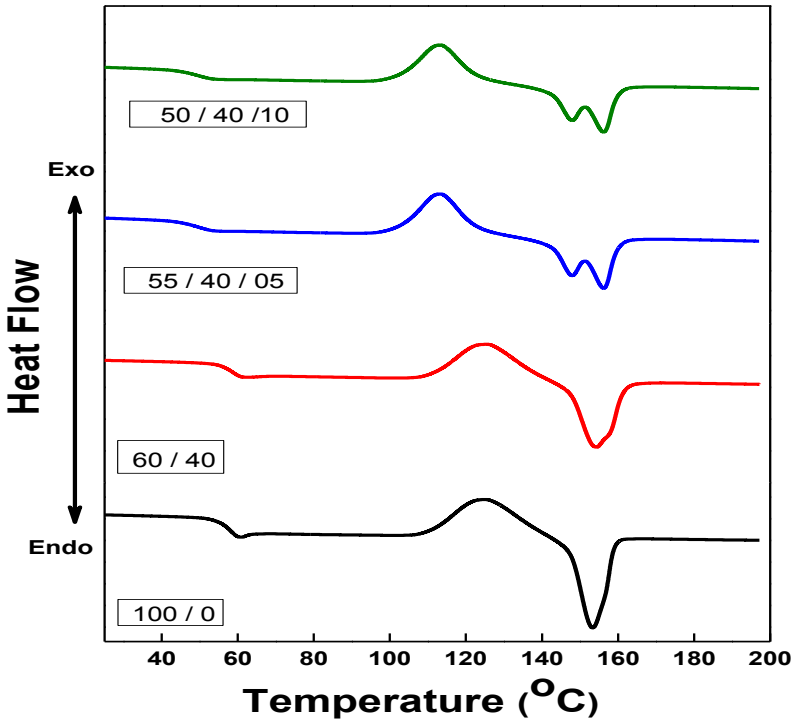

Figure 5- 6: DSC scan for PLA and PLA +40 (wt%) wood + copolymer composite

Table 5- 6 shows thermal behaviour from the DSC scan. It is clear that the copolymer has brought down the glass transition temperature from 56°C to 48°C as the copolymer increases from 0 to 10 (wt %). Secondly the crystallization temperature also reduced from 121°C to 104°C with 40 (wt %) wood flour as copolymer increased from up to 10 (wt %).

There are quite significant double peaks observed in the melting endotherm when 40 (wt %) wood floor is added to PLA. These double peaks become clearer as the amount of copolymer increases. These double melting peaks occur at different temperature compared to neat PLA. The stable peak melting temperature drops down from 157°C to 154°C while less stable peak melting temperature drops down from 152°C to 142°C. The addition of filler and copolymer has given significant increases in cold crystallization of PLA. Degree of Cold crystallization increased from 24 % to 38 % based on the enthalpy of crystallization when copolymer increased from 0 to 10 (wt %). The overall degree of crystallinity has also increased considerably. The addition of 5 (wt %) copolymer decreased the overall crystallinity but increasing the copolymer to 10 (wt %), the overall crystallinity increased significantly compared to neat PLA and PLA-wood composites.

Table 5- 6: Thermal characteristics of PLA and PLA +40 (wt%) wood + copolymer composite

PLA/ wood /CP	Tg	T_c	T_m		Cold Crystallization	Crystallinity
(wt%)	(°c)	(°c)	(°c)		(%)	(%)
			α	β		
100/0	54 ± 0.7	127 ± 1.4	155 ± 1.5	---	22 ± 1.2	2.0 ± 0.8
60/40	56 ± 1.4	121 ± 4.8	157 ± 1.3	152 ± 1.4	24 ± 2.3	8.4 ± 1.2
55/40/5	49 ± 0.9	114 ± 1.8	157 ± 0.7	149 ± 1.1	36 ± 2.6	4.4 ± 0.8
50/40/10	48 ± 0.4	103 ± 2.6	154 ± 0.4	142 ± 1.4	38 ± 3.7	11.0 ± 1.2

The overall conclusion is that the copolymer has a plasticising effect: reducing the *Tg*, reducing the cold crystallization temperature, reducing melting temperature and increasing crystallinity.

5.1.7 PLA –Wood composites (Silane Treated)

Figure 5- 7 shows DSC thermogram of pure PLA and PLA and wood based on the second heat of DSC.

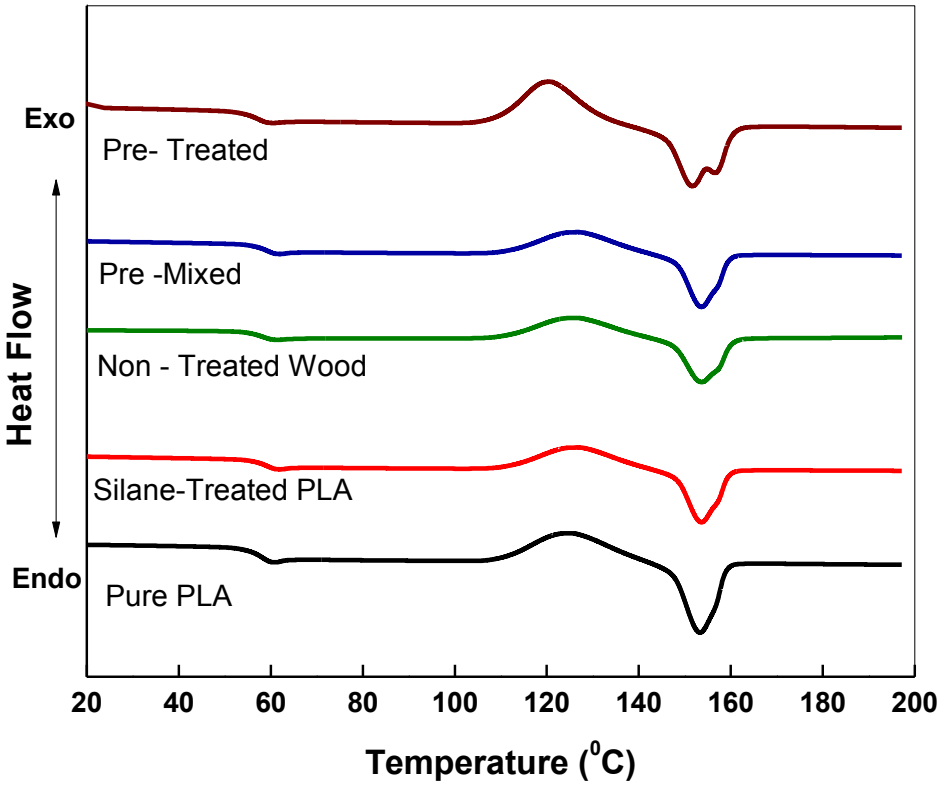

Figure 5- 7: DSC scans for PLA and PLA + 20 (wt%) wood (Silane Treated) composite

It is clear from the figure that the transition from the glassy state of the rubbery state, take place between 55 ^{o}C and 60 ^{o}C. Glass transition temperature for PLA and treated wood composites was also recorded at about the same range. The effect of silane treatment on the pure PLA was also recorded and no significant difference was observed. There was also no significant difference in the glass transition temperature with addition of silane treatment of wood fibres in the PLA matrix.

Table 5- 7 summarizes the thermal properties of PLA and silane treated wood composites. It is clear from the table that the glass transition, crystallization and

melting temperatures are not affected by the silane treatment. The treatment of pure PLA causes an increase in the cold crystallization temperature compared with the non- treated PLA. On the other hand, the incorporation of treated wood fibres into PLA causes the reduction in the degree of cold crystallization temperature compared with pure PLA and PLA wood composites. The overall crystallinity of the PLA and wood composites with silane treatment stays unchanged and no significant improvement is observed in crystalline contents of the composites, suggesting that no nucleation is taking place because of the silane treatment.

Table 5- 7: Thermal properties of PLA and treated wood composite

PLA / Wood	Tg	T_c	T_m		Cold - Crystallization	Crystallinity
(wt%)	(^{o}c)	(^{o}c)	(^{o}c)		(%)	(%)
			α	**β**		
100 / 0	54 ± 0.7	127 ± 1.4	155 ± 1.5	---	22 ± 1.21	2.0 ± 0.8
100/0 (Treated)	57 ± 0.2	128 ± 1.0	157 ± 0.1	152 ± 0.1	33 ± 1.9	2.6 ± 0.7
80/20 (Non-Treated)	56 ± 1.3	127 ± 1.4	157 ±0.2	154 ± 0.2	22 ± 2.1	1.3 ± 0.4
80 /20 (Pre-Mixed	55 ± 0.3	127 ± 0.9	157 ± 1.4	154 ± 0.2	15 ± 2.7	1.5 ± 0.4
80/20 (Pre-Treated)	56 ± 0.8	125 ± 1.2	156 ± 1.5	154 ± 0.8	19 ± 1.6	1.2 ± 0.2

5.2 Mechanical Properties

Tensile testing was performed on a Lloyd tensile testing machine. Five to seven samples of each specimen were tested to analyze the mechanical properties. Values for elastic modulus, tensile strength and elongation were recorded and are presented as a function of weight fraction of fibres in the composites.

5.2.1 PLA + Non-Dried Wood (NDW) Flour Composites

The tensile properties of the PLA and PLA -wood composites are summarised in Table 5- 8.

Table 5- 8: Tensile properties PLA + non-dried wood composites

PLA /wood (wt %)	Tensile Strength (MPa)	Tensile Modulus (GPa)	Elongation to break (%)
100 / 0	43.8 ± 2.1	4.1 ± 0.6	4.1 ± 0.6
90 / 10	28.2 ± 2.3	5.4 ± 0.7	2.3 ± 0.2
80 / 20	29.4 ± 2.5	6.3 ± 0.6	2.8 ± 0.3
60 / 40	31.8 ± 2.8	8.7 ± 0.3	2.3 ± 0.2

The tensile modulus (Young's modulus) of neat PLA obtained from tensile testing is 4.1 ± 0.62 (GPa). As the wood content increased, tensile modulus also increased. Tensile modulus increased from 4.1 ± 0.62 to 8.68 ± 0.26 (GPa) as the non- dried wood flour contents increased from 0 to 40 (wt %) (See Figure 5- 8). The improvement of Young's modulus brings a stiffening effect into the PLA-wood composite and also is indicative of mechanical adhesion between the matrix and fibres. A similar kind of result and trends was also been reported by other authors investigating PLA– natural fibre composites. For example Auras et al.[11] reported an increase in Young's modulus from 1.66 to 2.7 (GPa) when wood content is increased from 0 to 20 (wt %). M.S.Huda et al. [93] have also reported the significant increase in tensile modulus from 2.7 ± 0.4 to 6.3 ± 0.9 (GPa) when wood content increased from 0 to 40 (wt%) bringing a total of about 133 (%) improvement in tensile modulus.

It is clear from Table 5- 8 that the tensile strength (max stress at break) drops on the addition of wood flour. Tensile strength drops from 43.8 ± 2.1 (MPa) for PLA to 28.2 ± 2.2 (MPa) with the addition of 10 (wt %) non-dried wood flour. M.S.Huda *et al.*[93] have reported the decrease in tensile strength of PLA from 62.8 ± 4.9 to 58.7 ± 3.1 (MPa) when wood content increased from 0 to 40 (wt %). But Rafel *et al.* [11] have reported increase in tensile strength for PLA from 41 to 56 (MPa) when wood contents increased from 0 to 20 (wt%).

Figure 5- 8 shows the tensile modulus of PLA and its composites reinforced with non-dried wood as a function of weight fraction of wood present in the composite.

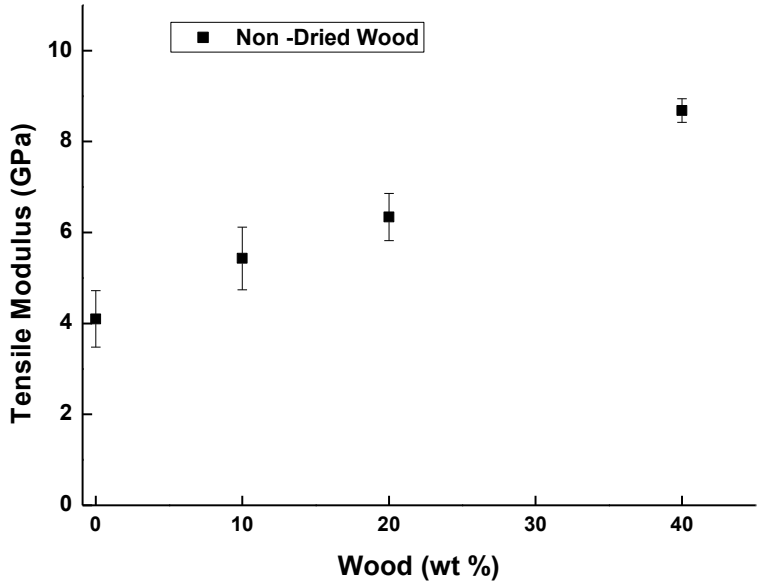

Figure 5- 8: Tensile Modulus of PLA and its composites with various concentrations

5.3 Comparison between theoretical and experimental tensile properties

Mechanical performance of composite materials can be predicted based on mathematical modelling. In this study, it is hoped that the combined experiment–modelling effect will allow for a better and deeper understanding of the structure–property relationship in the quest for wood fibre composites with the desired, optimized properties.

5.3.1 Modelling PLA – Wood Composites

It has been observed that Young's modulus of PLA is significantly improved when wood is incorporated along with other ingredients. In summary it is seen that there is a very significant increase in Young's modulus from a value of 4.1 (GPa)

for the pure PLA up to 8.7 (GPa) on the addition of 40 (wt %) of wood. This effect is due to the addition of a high modulus filler to a lower modulus polymer.

Different theoretical models can be applied to predict the reinforcing effect of Young's modulus of particulate composites. The geometrical parameters of the wood filler will affect the properties of the composite. Of particular importance is the aspect ratio (L/D) of the filler, which is the ratio of length (L) to a thickness (D) of the filler particles. The Halpin-Tsai equation (Eq. 3.6) given earlier, takes into account the effect of filler geometry in predicting the modulus of the composite materials.

In calculating the predicted value of the Young's modulus of the various PLA/wood composites from the Halpin Tsai equation, the following values have been used; the modulus of the matrix (PLA) is a 4.1 (GPa) as measured and modulus of the filler (wood) is taken as 10 (GPa) which is the elastic modulus of soft wood . The Halpin –Tsai equation is given below.

$$\frac{\boldsymbol{E_c}}{\boldsymbol{E_m}} = \frac{(\mathbf{1} + \boldsymbol{AB}\, \boldsymbol{V_f})}{(\mathbf{1} - \boldsymbol{B}\, \boldsymbol{V_f})} \qquad ---------- (\mathbf{3.6})$$

Where $\mathbf{A} = 2\left(\frac{L}{D}\right)$, $\mathbf{B} = \frac{(R-1)}{(R+A)}$ and $R = \left(\frac{E_f}{E_m}\right)$. *Ec, Em, E_f and V_f* are defined as the modulus of the composite, matrix, filler and volume fraction of the filler respectively

The volume fraction of the filler is calculated from the weight fractions of the wood using equation 3.8 explained in previous chapters. The value of the density of PLA is taken as 1.24 (g/cm^3), while the density of soft wood is 1.4 (g/cm^3) [119]. The aspect ratio of the wood was measured from the SEM morphology shown in the Figure 5- 9 using the Image J® software package, and the average value was found to be about 20 ~ 22. The particle size distribution in terms of percent frequency against the aspect ratio is shown in Figure 5- 10 below.

5.3.1.1 Procedure to use Aspect ratio using ImageJ® software

There are different steps involved to calculate dimensions of the particle using the SEM or TEM image.

Step 1: Open the Image J and select the "file > open"

Step 2: Set measurement scale based "scale bar" from the image directly.

Step 3: Crop the image by selecting the "rectangular tool" button on the menu bar.

Step 4: Adjust the "image brightness" from the menu bar "Image >Adjust>Brightness"

Step 5: Threshold the particles to remove the unwanted background information "Image>Adjust> Threshold"

Step 6: Measure the Particle dimension lengthwise using the "measure" button from the menu bar and add it to ROM manager list

Step 7: Repeat the step 6 to measure as many as possible particles dimensions to get the average value at the end.

Step 8: Repeat the whole process for measuring the thickness of the particles.

At the end the average value of length and thickness of the particles is calculated to determine the aspect ratio of the particle.

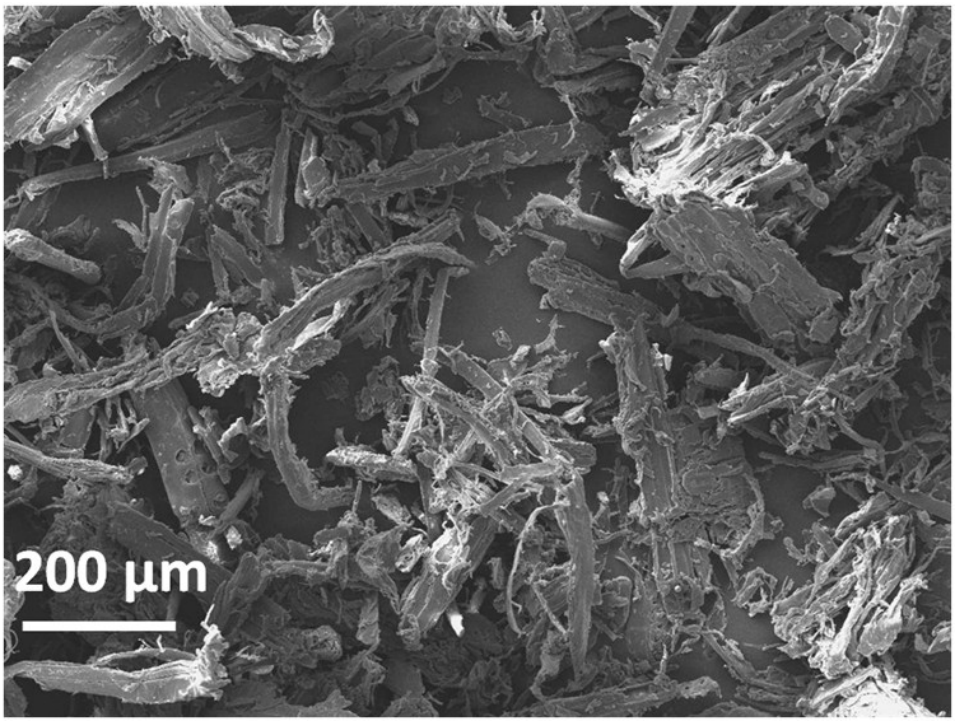

Figure 5- 9: SEM morphology of untreated wood surface

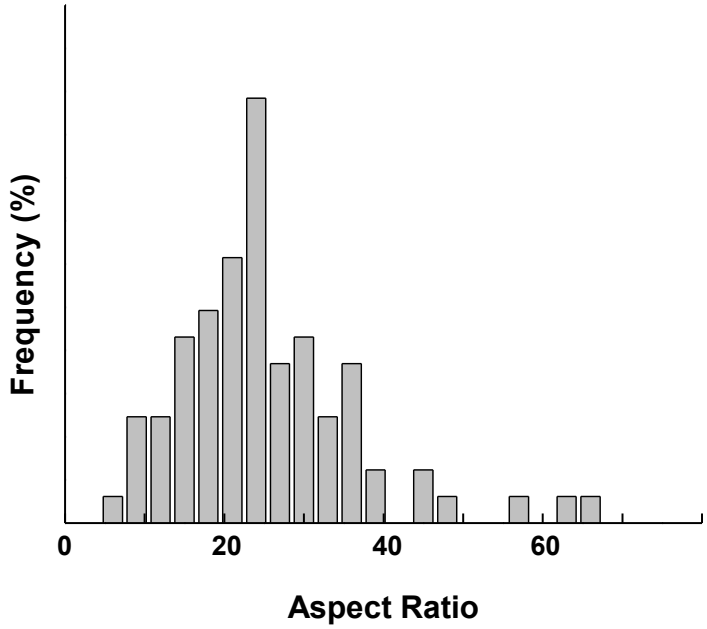

Figure 5- 10: Particle size distribution of wood fibres

Experimental measurements of the tensile modulus of the PLA and wood composites are plotted in Figure 5- 11 and superimposed on these data is the theoretical prediction of the Halpin Tsai model. The coefficient of determination is calculated using equation 3.9 described in previous chapters and found to be 0.91. There is seen to be a reasonable fit between the Halpin Tsai prediction and the experimental data when pure wood is added into the PLA matrix. The accuracy of the tensile testing can also be analyzed from Figure 5- 11 . The deviation of the composites experimental data from the theoretical response at 20 (wt %) may be because of reduced adhesion between the fibres and the matrix.

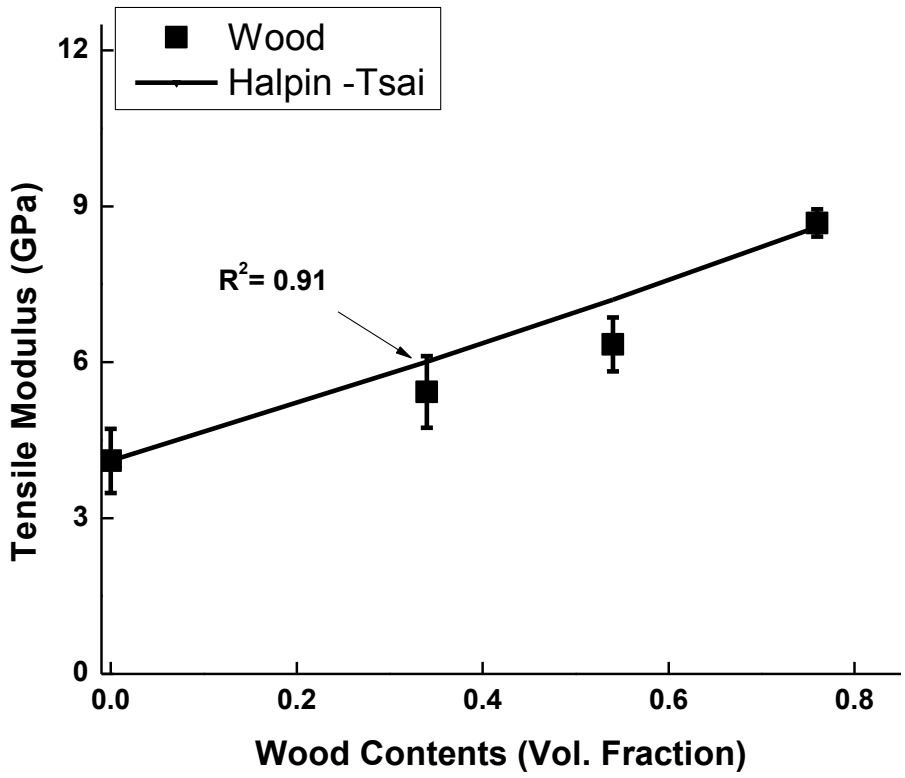

Figure 5- 11: Young's Modulus as function of wood volume fraction for PLA- wood composites.

5.3.2 PLA + Dried Wood (DW) Flour Composites

The tensile properties of PLA and its composites reinforced with dried wood are shown in Table 5- 9.

Table 5- 9: Tensile properties of PLA + dried wood composites

PLA /wood	Tensile Strength	Tensile Modulus	Elongation to break
(wt %)	(MPa)	(GPa)	(%)
100 / 0	43.8 ± 2.1	4.1 ± 0.62	4.1 ± 0.56
90 / 10	40.4 ± 1.4	5.5 ± 0.71	5.8 ± 0.5
80 / 20	36.9 ± 1.6	6.1 ± 0.92	4.3 ± 0.2
60 / 40	34.1 ± 1.3	9.8 ± 1.23	1.6 ± 0.4

Analysing the tensile properties presented in the table, it is clear that Young's modulus is increased as the wood content increases in the composite. Tensile modulus improved from 4.1 ± 0.62 to 9. 8 ± 1.23 (GPa) when the dried-wood flour content increased 40 (wt %) compared with neat PLA.

Comparing with tensile strength of PLA-non dried wood composites, it is clear that the drop in tensile strength is less for the 10 (wt %) wood content. But as the wood content increases, the tensile strength of the composites drops. The sample with 40 (wt %) dried wood flour has almost the same tensile strength as the sample with 40 (wt %) of non-dried flour and is indicative that pre- drying of wood flour does not have any significant effect.

Figure 5- 12 shows the tensile modulus of PLA and its composites reinforced with dried –wood.

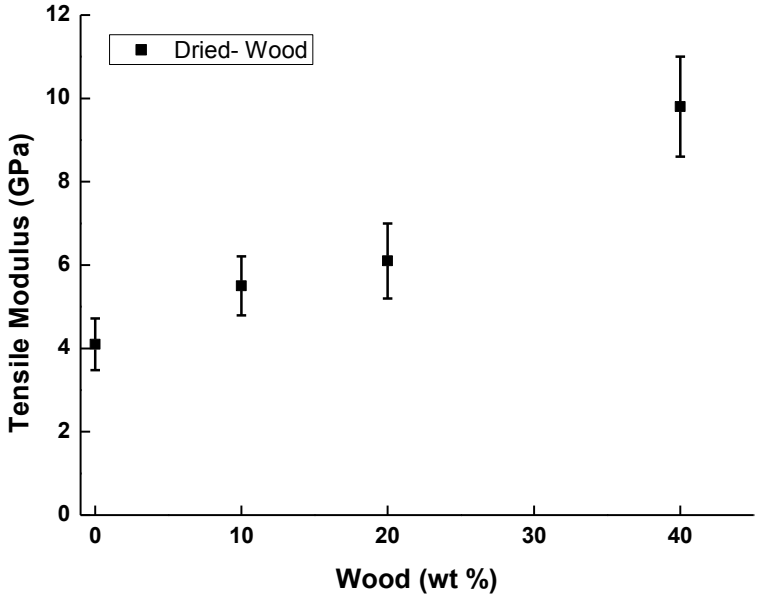

Figure 5- 12: Tensile Modulus of PLA and its composites with various concentrations of dried-wood

Analyzing Figure 5- 8 and Figure 5- 12 , it is clear that drying the wood flour does not have any significant effect on the tensile modulus. It is almost the same improvement as already observed. Hence pre-heat treatment of the wood is not making any significant difference to the modulus of the composites Improvement of modulus also indicates the homogeneous mixing of wood flour into the PLA matrix.

5.3.3 PLA + Wood Flour + Copolymer Composites

Table 5- 10 shows the tensile properties of PLA – wood composites with the addition of copolymer. It is clear from the table that the addition of wood into PLA gives a significant improvement in Young's modulus.

Table 5- 10: Tensile properties of PLA + wood + copolymer (CP) composites.

PLA /wood/CP (wt %)	Tensile Strength (MPa)	Tensile Modulus (GPa)	Elongation to break (%)
100/0/0	43.8 ± 2.1	4.1 ± 0.6	4.1 ± 0.56
95 /0 /5	28.4 ± 2.4	5.2 ± 0.8	1.8 ± 0.14
90/0/10	24.1 ± 3.1	5.6 ± 1.1	1.5 ± 0.31
85 /10/5	38.2 ± 1.4	5.8 ± 1.2	2.0 ± 0.4
80/10/10	33.4 ± 2.7	6.1 ± 0.9	2.7 ± 0.32
75 /20 /5	33.4 ± 2.3	6.6 ± 1.1	2.4 ± 0.37
70/20 /10	31.4 ± 2.8	6.9 ± 0.8	1.6 ± 0.29
55 /40/5	37.2 ± 1.5	8.9 ± 1.4	2.0 ± 0.23
50 /40 /10	30.6 ± 2.8	10.2 ± 1.8	2.1 ± 0.36

Figure 5- 13 shows the Elastic modulus of PLA and wood and copolymer composites as a function of weight fraction of wood present in the composite. It is clear from the figure that as the stiffness of the composites increased when the amount of copolymer increased from 0 to 10 (wt %). This is somewhat surprising because copolymer has a plasticizing effect but it does also increase crystallinity.

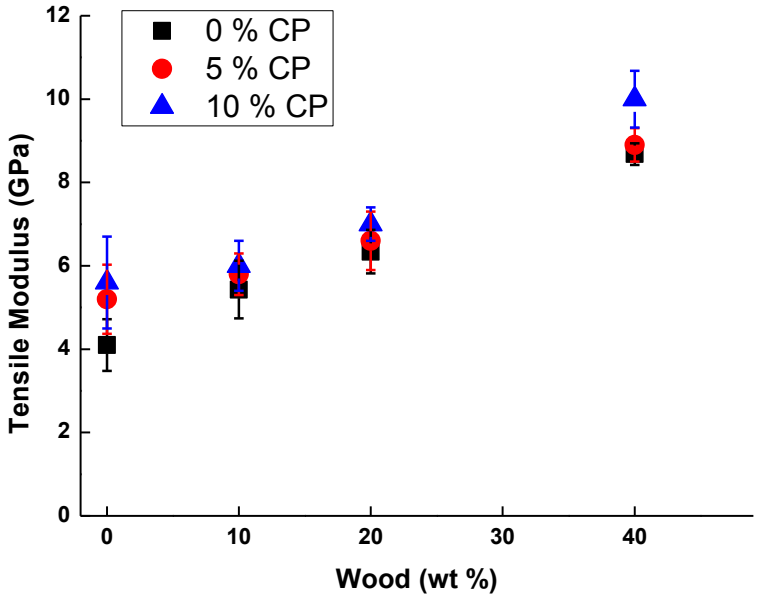

Figure 5- 13: Tensile Modulus of PLA and PLA-WF Composites

Figure 5- 14 shows the effect of copolymer on tensile strength of PLA and PLA/WF composites compared to neat PLA and its composite. It is very clear from the analysis that the tensile strength drops as the copolymer is added to pure PLA. There is improvement in tensile strength, when 5 (w %) copolymer is added to the PLA - wood composite compared to neat PLA-WF composite. But again tensile strength is decreased when 10 (wt %) copolymer is added to the PLA - WF composite. Resulting tensile strength of PLA-WF composite with 10 (wt %) copolymer is less than the 5 (wt %), but shows improvement when incorporated in 10 (wt %) wood compared to neat PLA- WF composite. The reduction in the tensile strength with the addition of copolymer is due to decrease in availability of the contents of matrix in presence of the copolymers. As the contents of copolymer increased, on the other hand the content of matrix is decreased while the content of the wood remain the same. Therefore it is believed that reduced content of the matrix causes reduction in adhesion of PLA and wood. This shows that the copolymer has improved the penetration of the PLA matrix into the narrow lumens' of wood particles resulting in a slightly stronger material.

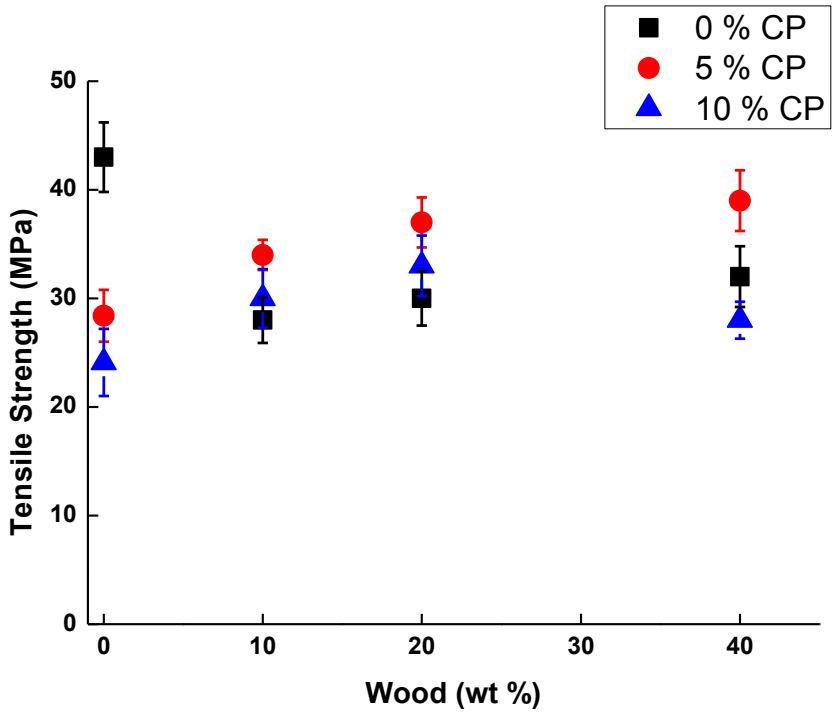

Figure 5- 14: Tensile strength of PLA and PLA- WF composites

From the analysis of the results it is clear that percent strain at break is decreased when wood is added to a PLA matrix. Reduced percent strain is an indication of the brittle behaviour of PLA-WF composites. Surprisingly the strain increased when 20 (wt%) wood flour was added to the PLA compared to 10 (wt%) wood flour mixed with PLA matrix, but again reduced when wood flour contents increased up to 40 (wt%), which is indicative of the increased brittle nature of PLA-WF composite.

Copolymer did not improve the ductile nature of PLA and PLA-WF composite. In fact it seems to have reduced ductility. When 5 (wt%) copolymer was added to PLA and PLA-WF composite, strain at break went down and kept going down when wood flour increased from 0 to 40 (wt%). When 10 (wt%) copolymer was added to the PLA and PLA-WF composite, percent strain at break reduced more compared with 5 (wt %) copolymer. Wood flour and copolymer do not seem to be compatible fillers to improve the ductile behaviour of the PLA matrix.

Experimental measurements of the tensile modulus of the PLA/wood and copolymer composites are plotted in Figure 5- 15 and superimposed on these data is the theoretical prediction of the Halpin Tsai model. The coefficient of determination is calculated using equation 3.9 described in previous chapters and found to be 0.78 for lower loading of copolymer and 0.67 for higher loading of copolymer. From the analysis of the Figure 5- 11 and Figure 5- 15, it is observed that a good fit could not be observed between the theoretically predicted composite modulus and that of the experimentally measured one.

Pilla et al. [97] have studied the effectiveness of PLA- wood composites and reported that there is no good fit observed between the experimental and theoretical value of the composites modulus. They reported that this might be due to, but not limited to, the following factors;

a. The model does not account for the interface between the wood and PLA.
b. The model does not account for the variation in the wood structure within the PLA matrix.

Therefore, to examine the effectiveness of the composites properties, the models should be further developed with the inclusion of the above mentioned factors.

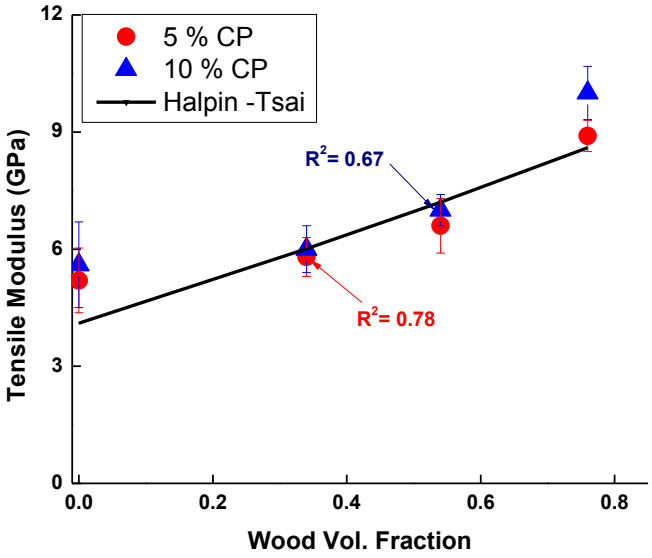

Figure 5- 15: Young's Modulus as function of wood volume fraction for PLA- wood-copolmers composites.

5.3.4 PLA –Wood Composites (Silane Treated)

The detailed tensile properties Pure PLA and PLA-wood treated with silane are given in Table 5- 11.

Table 5- 11: Tensile properties of PLA and silane treated wood composites.

PLA / wood (wt %)	Tensile Strength (MPa)	Tensile Modulus (GPa)	Elongation to break (%)
100 /0	43.8 ± 2.1	4.1 ± 0.6	4.1 ± 0.56
100 / 0 (pre-treated)	11.1 ± 2.8	0.8 ± 0.7	9.3 ± 2.6
80 /20	29.4 ± 2.5	6.3 ± 0.6	2.8 ± 0.2
80/20 (Pre-mixed with silane)	11.8 ± 3.6	2.1 ± 0.6	3.2 ± 1.4
80/20 (Pre-treated with silane)	13.5 ± 1.07	1.8 ± 0.5	5.1 ± 1.3

It can be seen that the pre-treatment of PLA and wood fibres with silane coupling agents showed a significant decrease in the tensile properties of the composites. Mixing of silane with pure PLA tends to reduce its tensile strength and Young's modulus significantly but the elongation to break is increased. A similar trend is also observed in the mechanical properties of the PLA-wood composites.

The tensile strength and tensile modulus both seem to be decreased by the addition of silane using two different methods. Pilla et al. [97] have also investigated the effect of silane surface coating on raw wood fibres and polylactide composites. They reported a significant improvement in mechanical properties with the addition of 0.5 (wt %) of silane coupling agent compared to neat PLA-wood composites. They have reported improvement in Young's modulus from 0.6 ± 0.10 to 2.8 ± 0.6 (GPa) when the contents of silane treated wood fibre increased from 0 to 20 (wt%), and no significant effect on tensile strength. Sun-Young Lee et al. have also studied the effect of 1 and 3 (wt %) silane coating on hybrid PLA composites reinforced with wood and talc fibres [96]. They also reported an improvement in tensile properties compared to neat PLA and PLA- wood composites.

Tensile properties (modulus and strength) seem to be dropping at a higher level of silane concentration. On the other hand, it is observed that elongation to break is increased slightly due to coating of wood fibres with acetone–silane solution indicating an improved behaviour of the composite. Figure 5- 16 shows that the tensile modulus of the pure PLA and PLA composites reinforced with 20 (wt %) silane coated wood fibres as a function of fibre volume fraction.

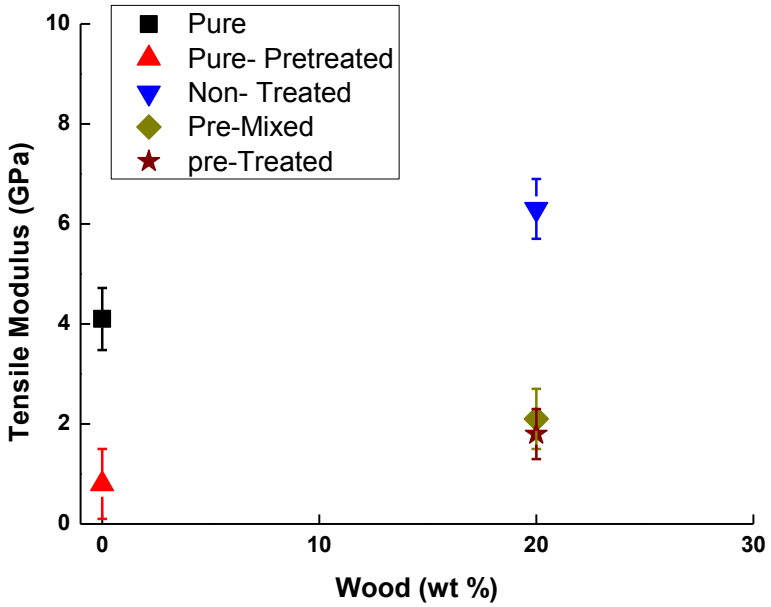

Figure 5- 16: Tensile Modulus of PLA and silane treated wood composites

Figure 5-17 shows the silane treated samples for pure PLA and PLA- wood composites. It is apparent that the addition of silane to the pure PLA seems to have degraded the sample. Discoloration of PLA is also observed. Therefore it is suggested that degradation tends to decrease PLA and PLA-wood composites properties. This still needs to be investigated.

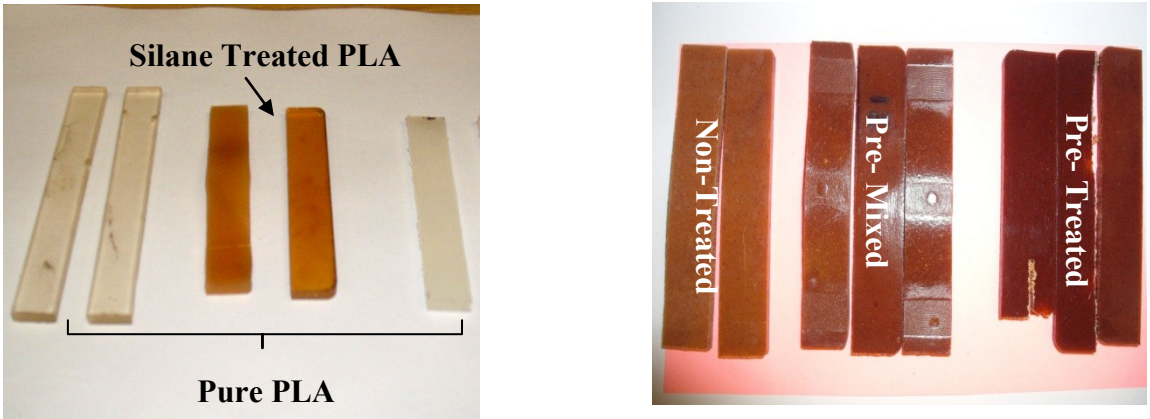

Figure 5-17: Silane Treated Pure PLA and PLA-20 (wt %) wood

5.4 **Morphological Properties**

Scanning Electron Microscopy (SEM) analysis has been carried out in order to study the fracture mode of the pure PLA and PLA–wood composites and to investigate the dispersion homogeneity of wood particles in the polymeric matrix. The micrographs have been taken on the tensile fracture surface at different locations and also at different magnification levels. Figure 5- 18 shows the morphology of the tensile fracture surface for pure PLA. SEM analysis shows that the PLA samples break homogeneously during the tensile testing. The micrograph clearly shows a brittle fracture surface.

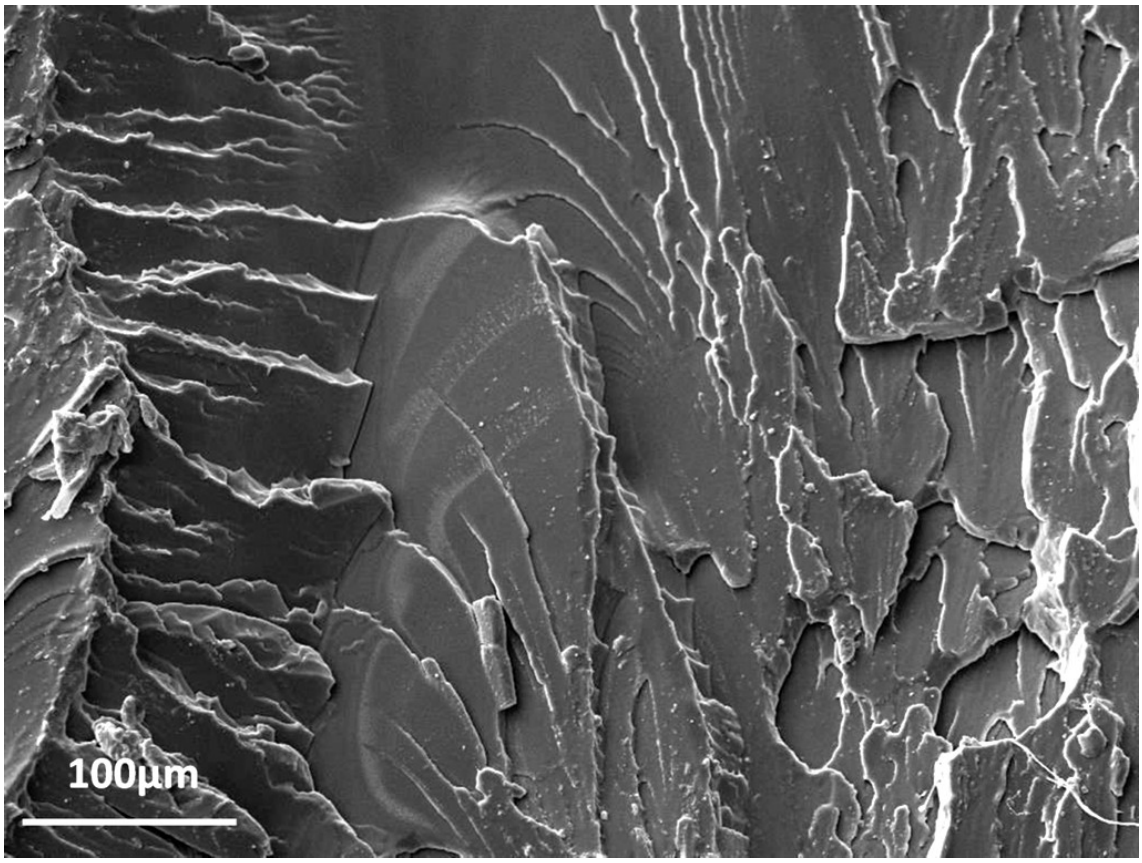

Figure 5- 18: SEM Micrograph of Tensile fractured surface of Pure PLA

SEM micrographs of the tensile fracture surface of the composites with PLA and wood flour contents from 10 to 40 (wt %) are shown in Figure 5- 19 and Figure 5- 20. These SEM images are recorded at various locations across the

fracture surfaces being tested under tensile loading. The images show that the compounding method led to a uniform distribution of wood flour (WF) in the PLA matrix and suggest good dispersion of fibres in the matrix, thus resulting in a homogeneous composite. SEM images Figure 5- 19 (a, b) shows the morphology of PLA-wood fibres when wood content increased from 10 to 20(wt %) respectively. It is clear from the analysis that fibres breakages, which are indicative of good interfacial adhesion between fibres and the PLA matrix can be seen.

Figure 5- 20 (a, b) shows the SEM micrographs of PLA-wood composites when wood content increased to 40 (wt %). As analysed, the fibre pullout is less compared with fibre breakages in the composites, thus in general signify good adhesion between the wood and the PLA matrix. Analyzing the fractured surface in more detail as shown in Figure 5- 20 (b) , indicates that the fibres which were pulled out left a distinct imprint on the wood fibre surfaces instead of a clean pullout of the matrix, suggesting good mechanical interlocking between wood fibres and the PLA matrix which was also observed recently by Mathew et al [115].

Fibre pullout and leaving imprints left on the PLA matrix is attributed to the surface roughness of the wood fibres. The fingerprints of the fibre breakages also indicate a hollow structure of the composites which could occur due to the poor dispersion between the matrix and the fibres. Probably this could give rise to poor mechanical behaviour of the composite materials.

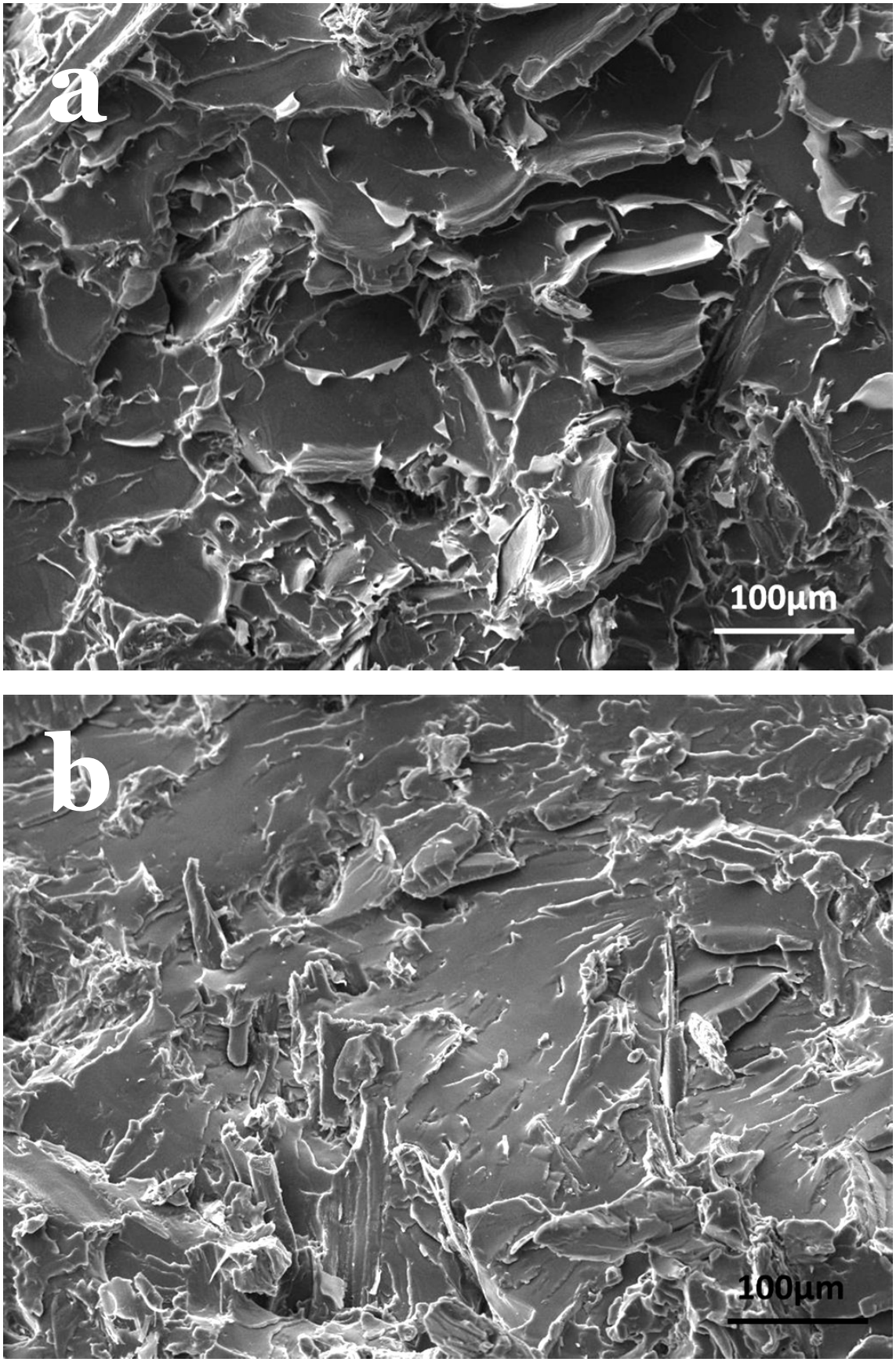

Figure 5- 19: SEM fractured surface analysis of PLA – wood Composites;(a) 10 % wood, (b) 20 % wood

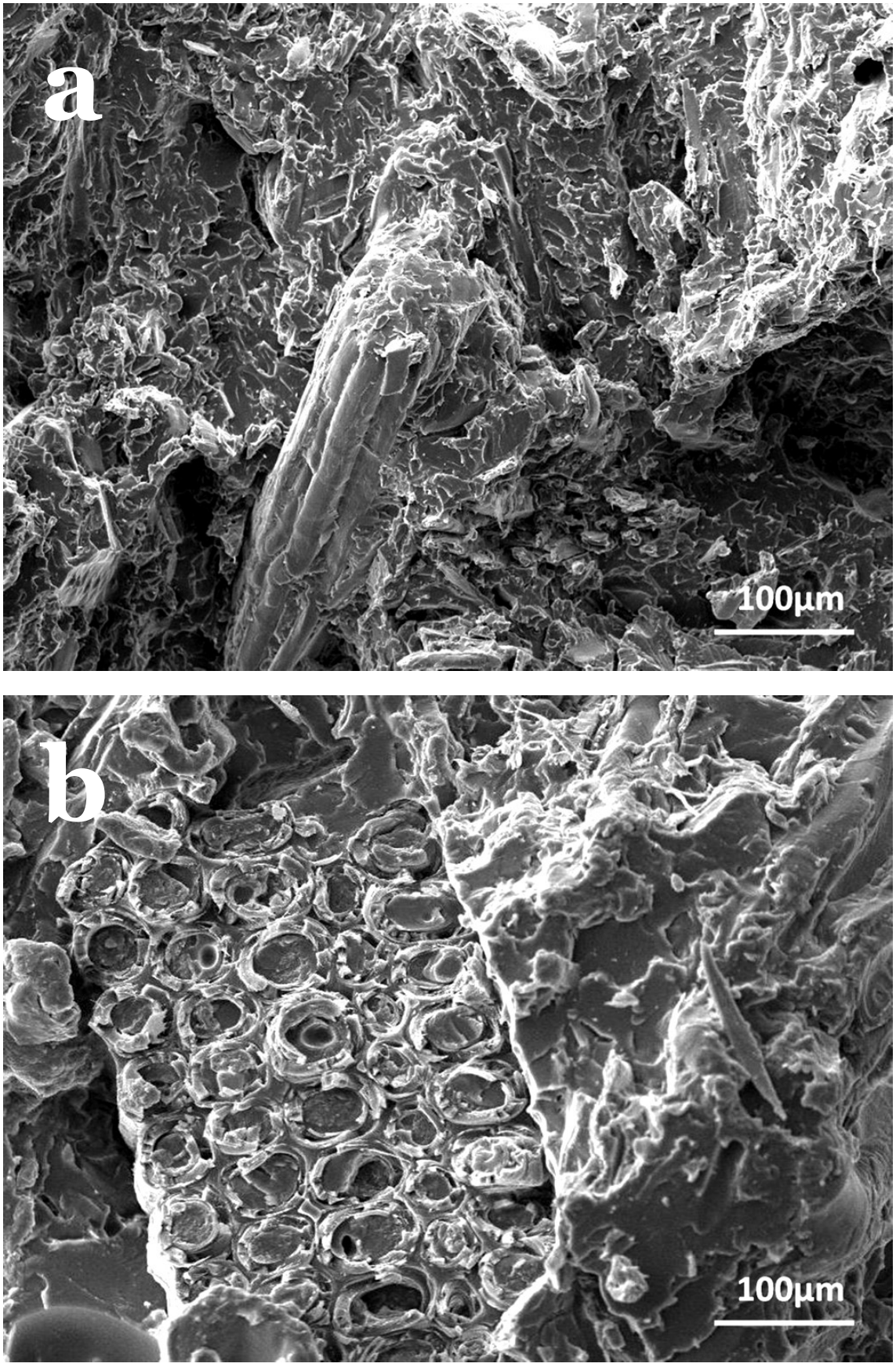

Figure 5- 20: SEM Micrographs of Tensile fractured surface of PLA + 40 % wood composites.

Figure 5- 21 (a, b) shows scanning electron images of pure wood fibres recorded at different locations and magnifications. The roughness of the wood surface is quite clear from these images. Micrographs showed in Figure 5- 21 (a), show narrow hollow channels, known as lumens of wood fibres. These kind of structural compositions are present in all plants and are responsible for water and nutrient ransportation to the other parts of the plants.

When such kind of substance is used as reinforcement material in composites, the penetration of the matrix into the structure of such a substance becomes one of the core factors to determine the mechanical properties of the composites. If the polymer matrix is able to flow and penetrate these hollow lumens of wood particles and fill them, this would add strength to the composite [118]. During the morphological analysis of the PLA- wood composites, presence of hollow structures was observed and the mechanical properties went down when the wood fibres were incorporated into the PLA. It was supposed that existence of these hollow lumens on composite surface and deficient mechanical interlocking are responsible for the drop in tensile properties (i.e. tensile strength, etc.) when wood is added to PLA matrix. It is also observed from the stress-strain relation of PLA-wood composites that the area under the stress-strain curve significantly reduced when wood was added to the PLA matrix. The reduction in area under the stress-strain curve is an indication of a drop in strain energy per unit volume which has direct impact on the toughness of the materials. It can be deduced that as the wood contents increased in the composites; the amount of PLA is reduced.

It is also suggested that PLA seems not to penetrate into the hollow lumens of wood particles resulting in poor adhesion in the composites. The composite loses its ability to withstand high stress and subsequently weaker composites are produced. If the viscosity of PLA is reduced, it might be possible to flow and penetrate into the hollow lumens of the wood particles and reduce the proportion of hollow regions in the composites. Existence of hollow regions in the composites, contribute to reduced toughness and tensile strength of the composite materials.

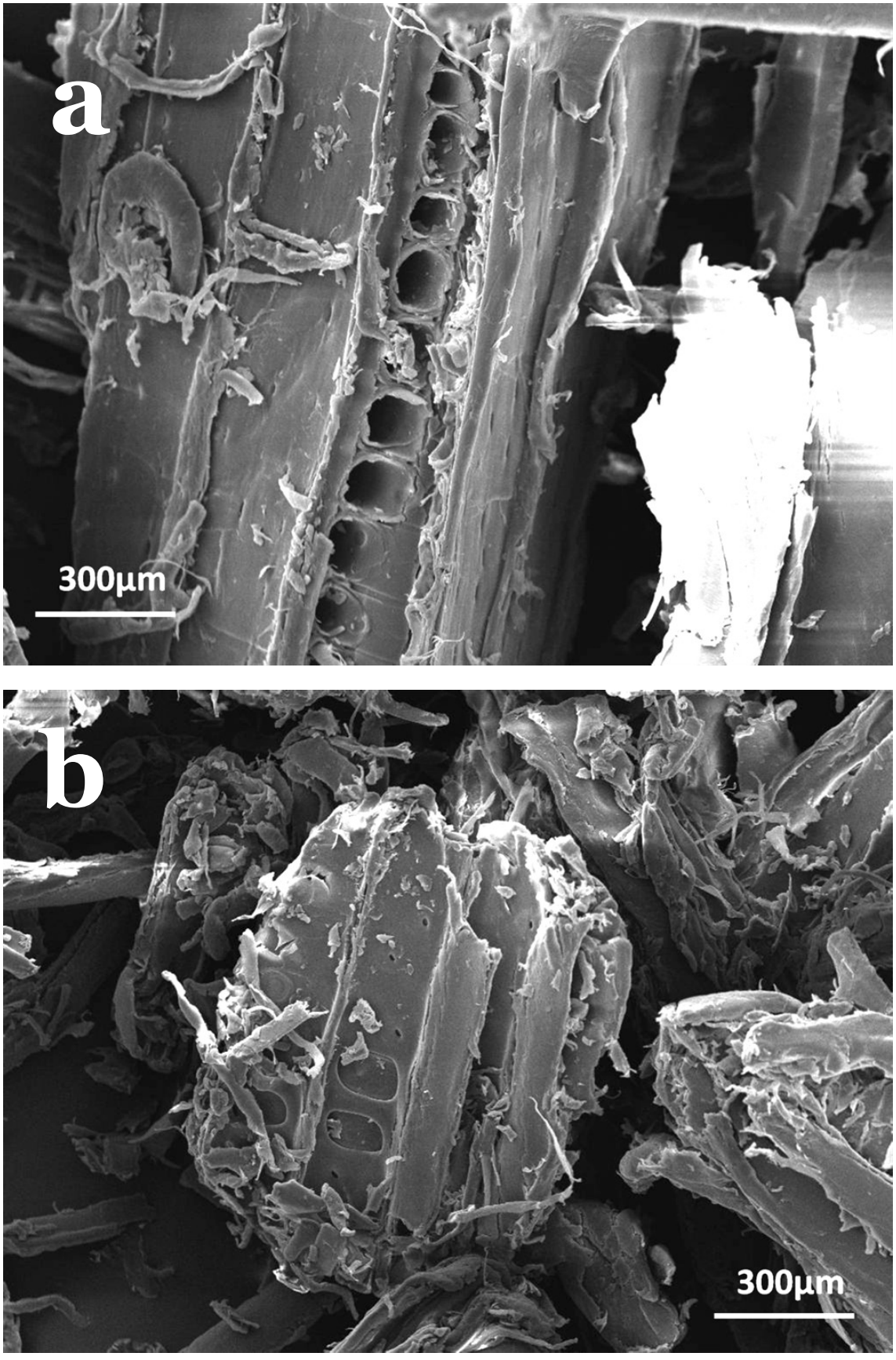

Figure 5- 21: Micrographs of the internal narrow channels of wood fibres /flour

To overcome the poor interfacial adhesion and improve the contact between the wood filler and the matrix, it was proposed to reduce the viscosity of PLA hence allowing the matrix to flow easily into the narrow hollow lumens' and fill the hollow regions in the wood structure. A copolymer compatible with PLA was mixed with PLA during the blending to reduce the viscosity, and to allow the PLA to penetrate easily into the wood structure. Observations made of the fracture morphology of the PLA- wood composites with copolymer are discussed below.

Figure 5- 22 and Figure 5- 23 shows morphological features of PLA- wood composites with copolymer. SEM analysis of PLA– wood composites with 5 (wt %) copolymer added is shown in Figure 5- 22 (a). The broken fibre's surface is observed when copolymer is added into the PLA–wood composite, which is indicative of reasonably good adhesion between the filler and matrix as compared to neat PLA-wood flour composite. Figure 5- 22 (b) shows SEM images when 10 (wt %) copolymer is added to PLA-wood composites. SEM analysis suggests that less broken fibres and comparatively higher fibre pull-out ratio were observed during tensile testing compared to Figure 5- 22 (a). This shows poor interfacial adhesion between the filler and matrix compared to 5 (wt %) copolymer addition. The amount of PLA in the composites decreases as the amount of copolymer is increased. With the decreased amount of matrix, while keeping the same wood content, filler will not be mixed homogeneously with the matrix. This is also indicated in terms of tensile strength which is increased with 5 (wt %) copolymer but reduced with 10 (wt %) copolymer.

Figure 5- 23 (a, b), it is clear that copolymer has affected the flow of the matrix into the wood particles. The narrow wood lumens seems more filled with the addition of copolymer. This indicates that the copolymer reduced the viscosity of PLA matrix and the penetration of matrix into narrow channels of wood particles is facilitated. Penetration of PLA matrix into wood particles showed improved tensile strength compared to neat PLA- wood composite. In fact, as previously discussed, the addition of copolymer increased the tensile stress but reduced the percent tensile strain at break, which is symptomatic of the brittle behaviour of PLA- wood

composite is enhanced with the addition of 5 (wt %) copolymer. It is suggested that the Copolymer showed some usefulness but did not show much improvement.

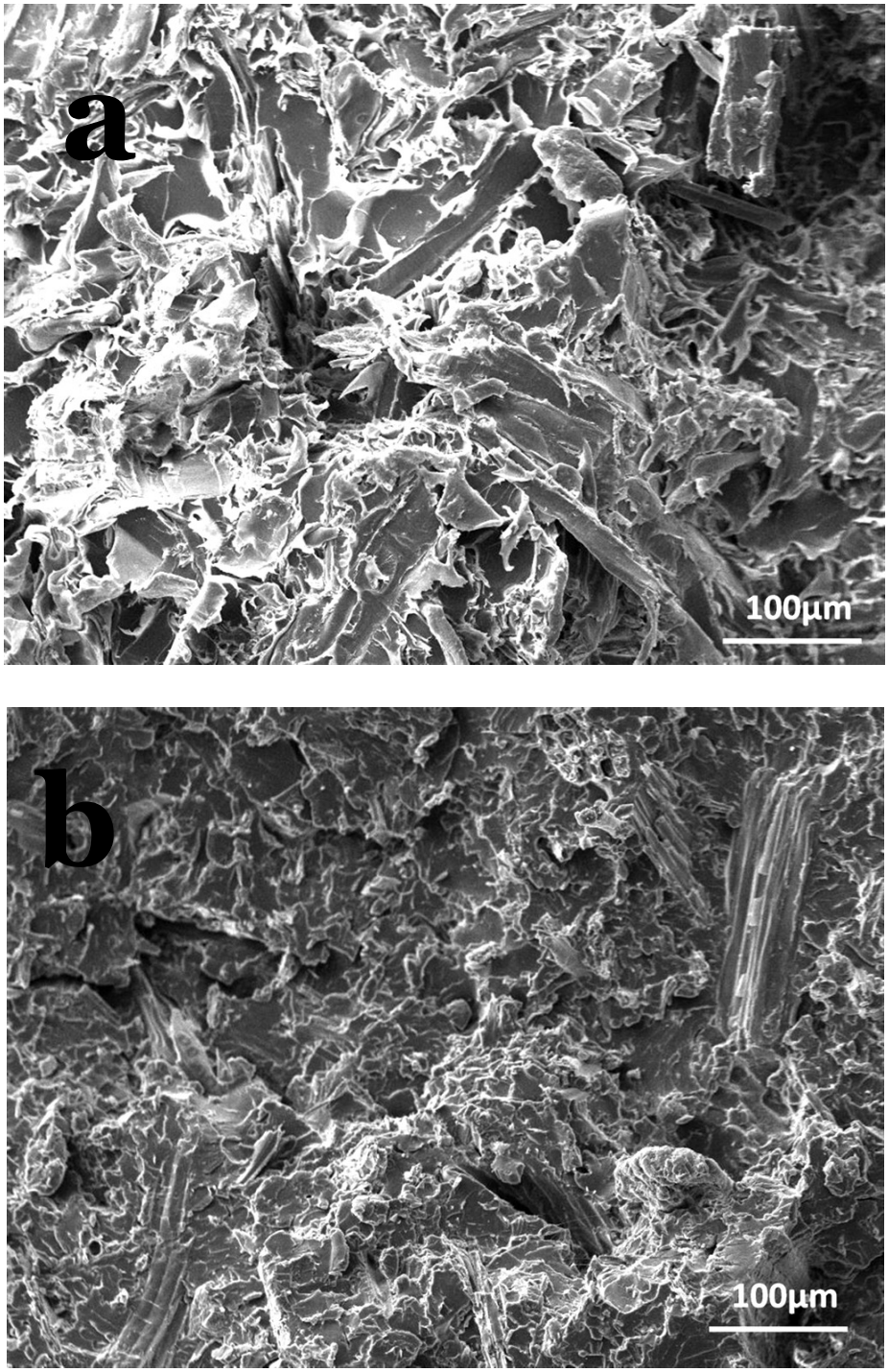

Figure 5- 22: SEM analysis of fractured PLA–Wood–Copolymer composites; (a) PLA + wood+ 5 (wt %) Copolymer, (b) PLA + wood+ 10 (wt %) Copolymer

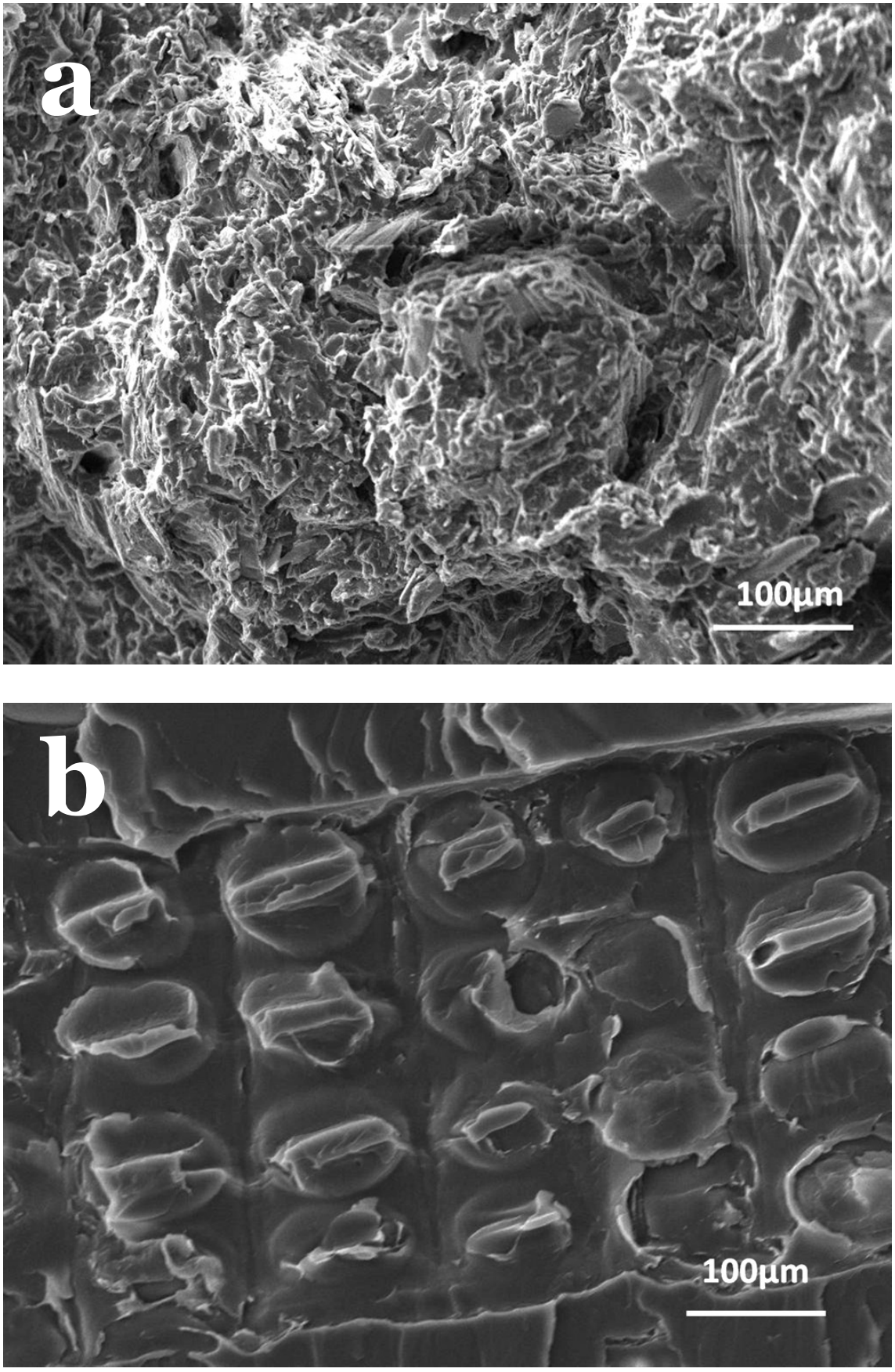

Figure 5- 23: SEM micrographs of PLA- wood –copolymer composites

To improve the adhesion between the wood and the PLA, in order to enhance the mechanical properties of the composites, wood fibres were coated with a silane based coupling agent. To see the effect of the coupling agent, the morphology of the fracture surfaces of coated tensile samples was studied under the SEM. Figure 5- 24 (a, b) and (c, d) shows the SEM micrographs of pure wood before and after the silane treatment respectively, recorded at different locations. The roughness of the wood fibres can be observed from the morphology and it seems that there is no significant difference between the pre and post-treatment morphology of the wood fibres. However the morphology suggests that the surface of treated wood fibres seems slightly smoother compared with the surface of pure wood fibres as shown in images Figure 5- 24 (c, d).

Figure 5- 25 shows the SEM micrographs of a fractured surface of coated tensile samples recorded at different locations for PLA- wood composites. Figure 5- 25 (a, b) shows the surface morphology of pure PLA and silane treated PLA respectively. It is apparent from these images that samples fractured quite cleanly with no fibrous indications were observed, suggesting quite brittle behaviour of booth samples. So presumably no significant difference from silane treatment can be inferred from the surface morphology of the treated PLA compared with the pure PLA. Figure 5- 25 (c, d) shows the fractured surface of PLA and silane treated wood fibre composites collected after tensile testing. The morphology implies uniform distribution of the wood fibres in the PLA matrix. It was clear that fracture at the surface is quite clean, indicating brittle morphology of the composites similar to pure PLA- wood composites. It was interesting to note that less fibre pullout was observed compared to neat PLA-wood composites, signifying improved compatibility between the wood fibres and the matrix. It was also believed that silane treatment lead to lesser fibres and matrix de-bonding ratio. It is suggested that silane treatment improves the adhesion between the PLA and the wood fibres. The drop in mechanical properties with silane treatment is supposedly due to the degradation of the silane at a higher temperature. The discoloration of the samples is indicative of degradation of one of the ingredients of the composites. The amount of silane using for coating, is a critical issue in surface coating which needs to be optimized.

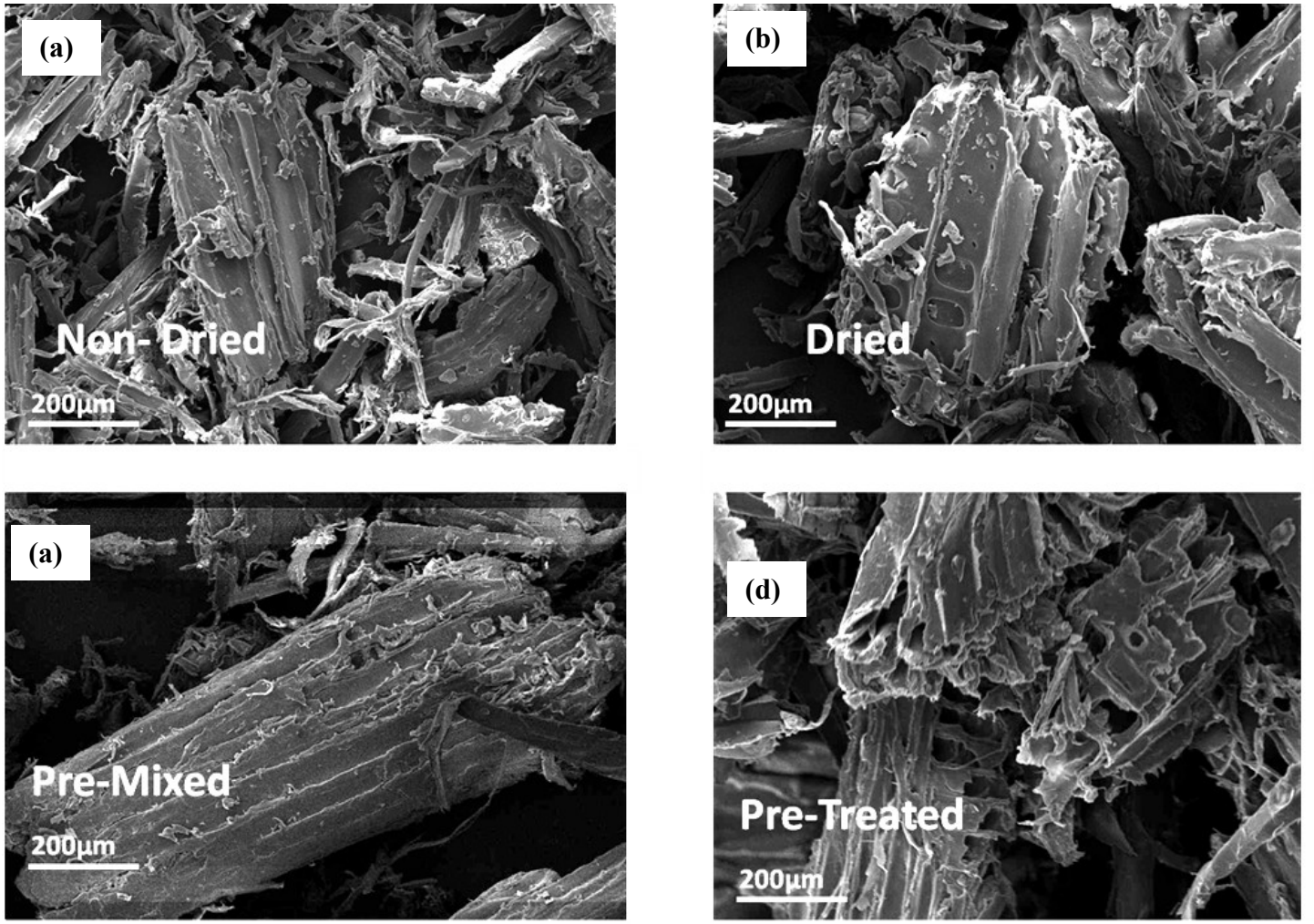

Figure 5- 24: SEM images of Pure wood (a) Non-dried, (b) Dried, (c) Pre-Mixed with silane , (d) Pre-Treated with silane

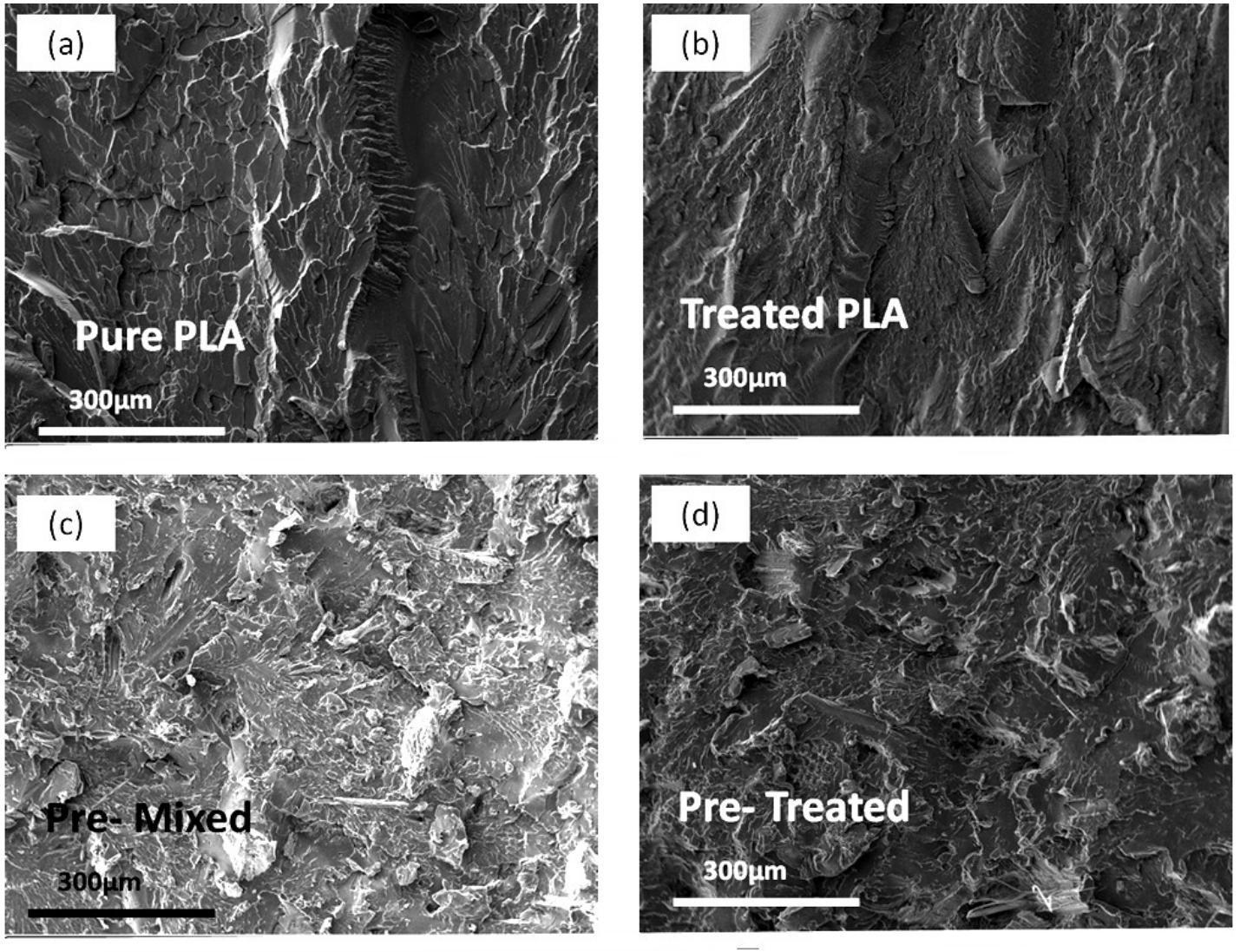

Figure 5- 25: SEM images of Treated with silane, (a) Pure PLA, (b) Treated PLA (c) Pre-Mixed wood PLA/wood Composites, (d) Pre-Treated wood PLA/wood Composites

5.5 Dynamic Mechanical Analysis (DMA)

5.5.1 PLA – Wood flour Composites

The viscoelastic properties of PLA and PLA + wood flour composites were investigated using DMA. As shown in Figure 5- 26, addition of non-dried wood flour increased the storage modulus and the highest increment was for an addition of 40 (wt %) non-dried wood in the PLA matrix. Table 5- 12 shows the dynamic modulus for neat PLA and PLA + non-dried wood composites at different temperatures.

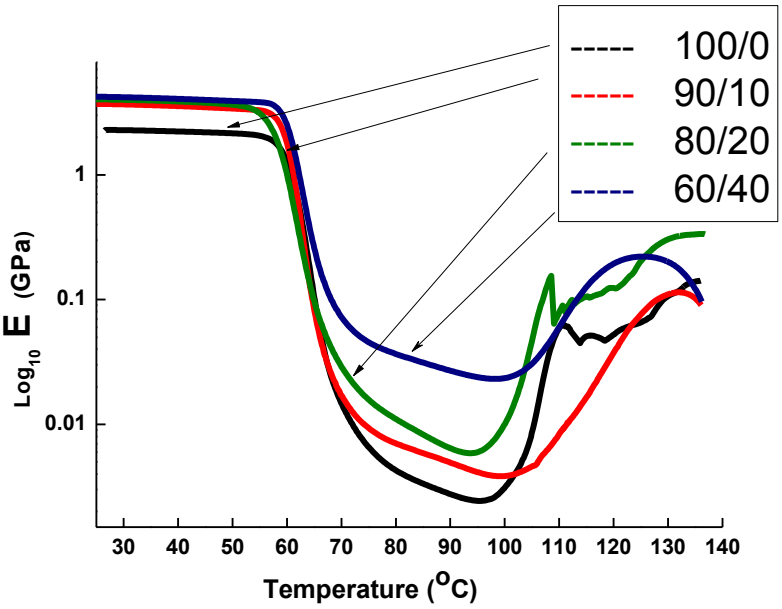

Figure 5- 26: Storage modulus of PLA and PLA+ non-dried wood composite as a function of temperature

It is clear from Figure 5- 26 that there is continuing drop in storage modulus with increasing temperature but again increasing around 100°C and this is an indication of recrystallisation (cold crystallization). The drop in storage modulus is less with the incorporation of 40(wt %) wood into PLA compared with a lower wood content in the PLA. This might be useful in resisting softening and heat distortion of PLA.

From Table 5- 12, it is clear that at 30°C, the storage modulus increased from 2.28 (GPa) to 4.19 (GPa) as non-dried wood was increased from 0 to 40 (wt %). There is

about 85 (%) improvement in storage modulus when 40 (wt %) non-dried wood is added to the PLA matrix. From the table it is also clear that the increase in storage moduli of the composites follows the same trend at 40°C as well. This result is also an indirect confirmation of the increase in tensile modulus of the PLA with the addition of wood flour obtained during tensile testing shown in Figure 5- 8.

Table 5- 12: The flexural modulus of PLA and PLA + non-dried wood composites

PLA / wood	Storage Modulus (30°c)	Storage Modulus (40°c)
(wt%)	(GPa)	(GPa)
100 / 0	2.28	2.18
90 / 10	3.67	3.55
80 / 20	3.99	3.87
60 / 40	4.19	4.07

The effect of mixing dried wood into the PLA matrix is shown in Figure 5- 27 and summarised in table 5-13. Figure 5- 27 suggests that addition of dried wood has increased the storage modulus significantly. Table 5-13 shows that at 30°C the storage modulus for pure PLA is 2.28 (GPa) which is increased to 4.19 (GPa) when the dried wood content increases from 0 to 40 (wt %). This is again reconfirmation of the increment in tensile modulus caused due to addition of dried wood in the PLA matrix. Reinforcement causes about 86 % improvement in storage modulus when 40 (wt%) is added to neat PLA which is almost the same as improvement caused due to the addition of non-dried wood. This indicates that there is no significant difference in PLA composite reinforced with dried or non-dried wood and confirms the findings from figure 5-8 & 5-9. It is evident from Figure 5- 27 that softening of PLA composites starts above 50°C and then gradually continues with increasing temperature. But modulus starts increasing again at about 100°C indicating cold crystallization behaviour.

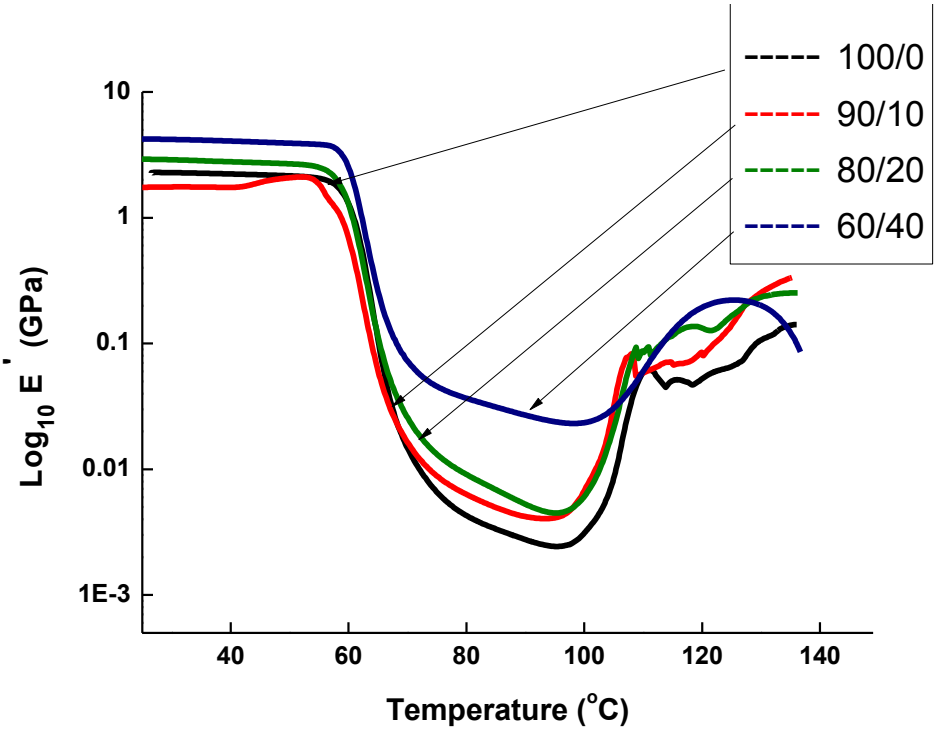

Figure 5- 27: Storage modulus of PLA and PLA + dried wood composite as a function of temperature

It was observed that the addition of 10 (wt %) dried wood to PLA matrix has caused a reduction in storage modulus compared to neat PLA. According to the results the modulus with 10 (wt %) of dried wood flour drops down from 2.28 (GPa) to 1.78 (GPa) at 30°C. Table 5- 13 is shown below, detailing the flexural modulus at different temperature for PLA and PLA-wood composites

Table 5- 13: The flexural modulus of PLA and PLA+ dried -wood composites.

PLA / wood (wt %)	Storage Modulus (30°c) (GPa)	Storage Modulus (40°c) (GPa)
100 / 0	2.28	2.19
90 / 10	1.78	1.69
80 / 20	2.87	2.82
60 / 40	4.19	4.01

The loss factor (Tan δ) which is the ratio of loss modulus to storage modulus is shown in Figure 5- 28 and Figure 5- 29 for PLA -non-dried and PLA-dried wood composites respectively. The addition of wood did not affect the glass transition temperature significantly. The glass transition temperature as computed from *Tan δ* peaks is about 66 °C for PLA and 65.8 ° C, 64.4 ° C, 66 ° C for 10, 20 and 40 (wt%) non-dried wood respectively.

Figure 5- 28 suggests that the area of integration under the *Tan δ* curve decreased with increasing non-dried wood content, indicating the damping capability in PLA + non-dried wood composite. *Tan δ* response exhibits a reduced damping capability and implies an increase in brittle behaviour with the addition of non-dried wood because of the reduction in the ability to dissipate energy as also found by Pilla et al.[97]. They also investigated the properties of PLA + recycled wood fibre composites and found the increase in modulus with the addition of wood into PLA matrix resulting an increase in brittleness of the composite. The increase in the brittle nature of PLA with the addition of non-dried wood also reflects what was found in the tensile properties, such as decrease in tensile strength and strain at break.

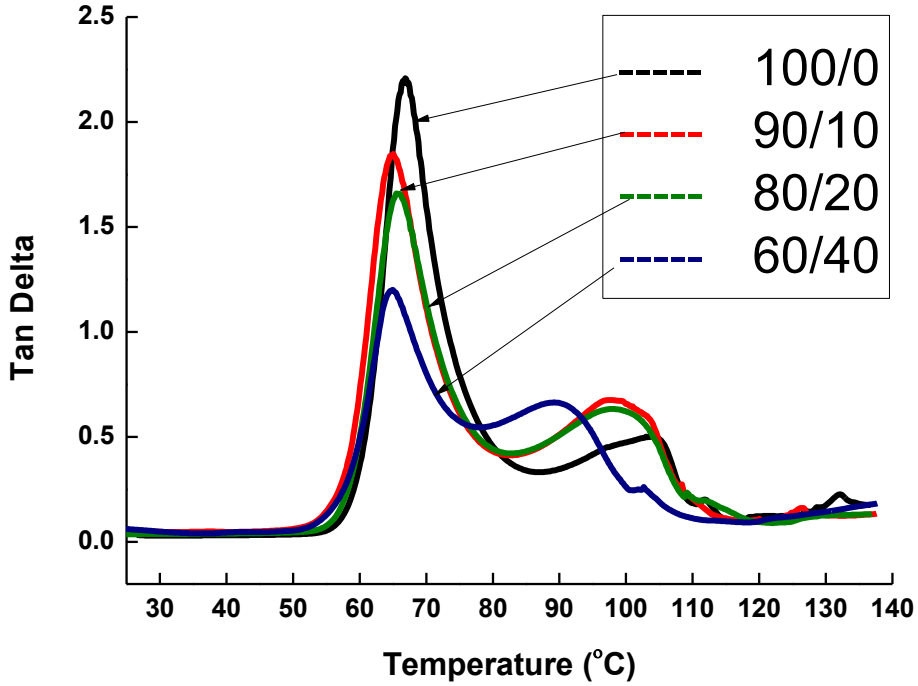

Figure 5- 28: Loss factor (Tan δ peak) of PLA + non-dried composite as function of temperature

Tan δ curves for PLA and PLA+ dried-wood are shown in Figure 5- 29. These results are the same as for the non-dried wood. Hence this result again shows no effect of drying the wood flour on PLA properties.

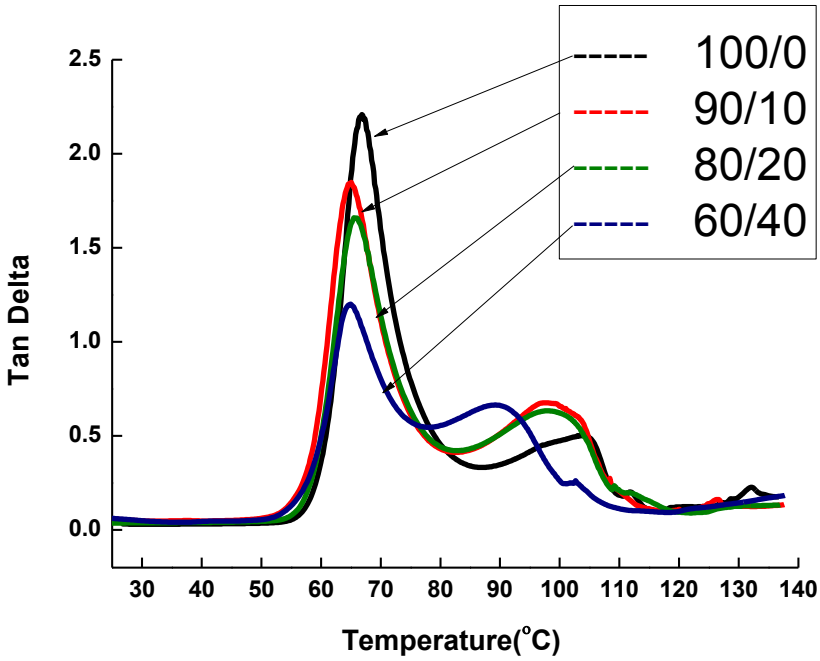

Figure 5- 29: Loss factor (Tan δ peak) of PLA + dried -wood composite as function of temperature

5.5.2 PLA + Wood flour + Copolymer Composites

Copolymer was added to PLA and PLA +wood flour composite and analyzed to characterize the viscoelastic properties.

5.5.2.1 PLA + Copolymer

The storage modulus of PLA + copolymer is shown in Figure 5- 30. Storage modulus (flexural modulus) is shown in Table 5- 14. From the table it is clear that storage modulus was affected significantly by the addition of different levels of copolymer. At 30°C the storage modulus of PLA is 2.28 (GPa) and this was reduced to 1.86 (GPa) and 1.81 (GPa) respectively with the addition of 5 and 10 (wt %) copolymer.

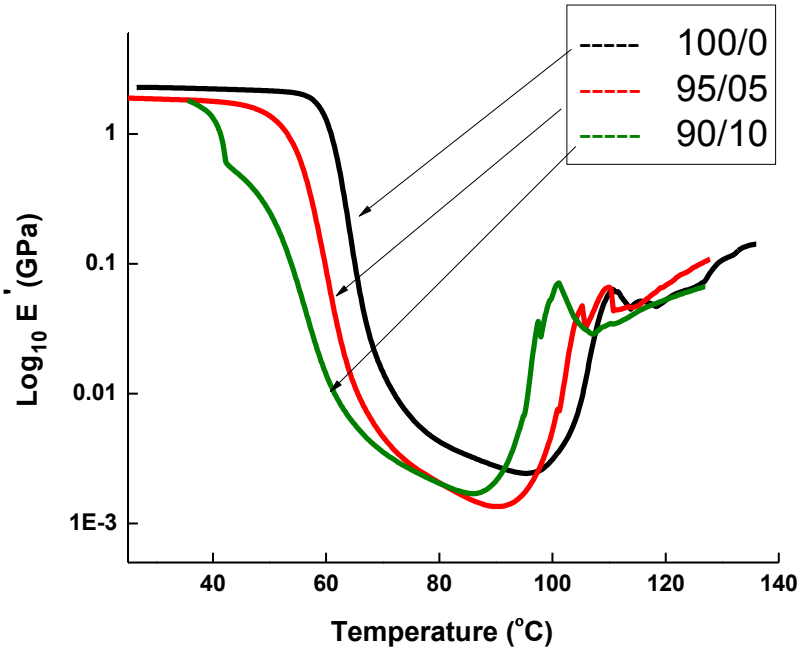

Figure 5- 30: Storage modulus of PLA and PLA + copolymer as a function of temperature

Table 5- 14: Storage modulus of PLA and PLA + copolymer

PLA / copolymer (wt %)	Storage Modulus (30°c) (GPa)	Storage Modulus (40°c) (GPa)
100 / 0	2.28	2.19
95 / 5	1.86	1.78
90 / 10	1.81	1.31

The loss factor Tan δ is also shown in Figure 5- 31. It shows that significant changes have occurred in the PLA matrix with the addition of copolymer. Tan δ peaks have been shifted to lower temperature as the content of copolymer increased from 0 to 10 (wt%), representing a decrease in the glass transition temperature. The glass transition temperature reduced from 66°C to 58°C as copolymer increased from 0 to 10 (wt %). Figure 5- 31 suggests that the area of integration under the Tan δ curves is increased with the addition of copolymer compared with neat PLA, indicating an improvement in the damping capability of PLA. This observation conflicts with findings from tensile testing (Table 5- 10) which show that addition of copolymer

causes a decrease in percent strain at break, symptomatic of a more brittle response of the sample. It is also seen that sample storage modulus drops down with the addition of copolymers but starts increasing again around 90°C. This is an indication of the early start of cold crystallization compared with neat PLA.

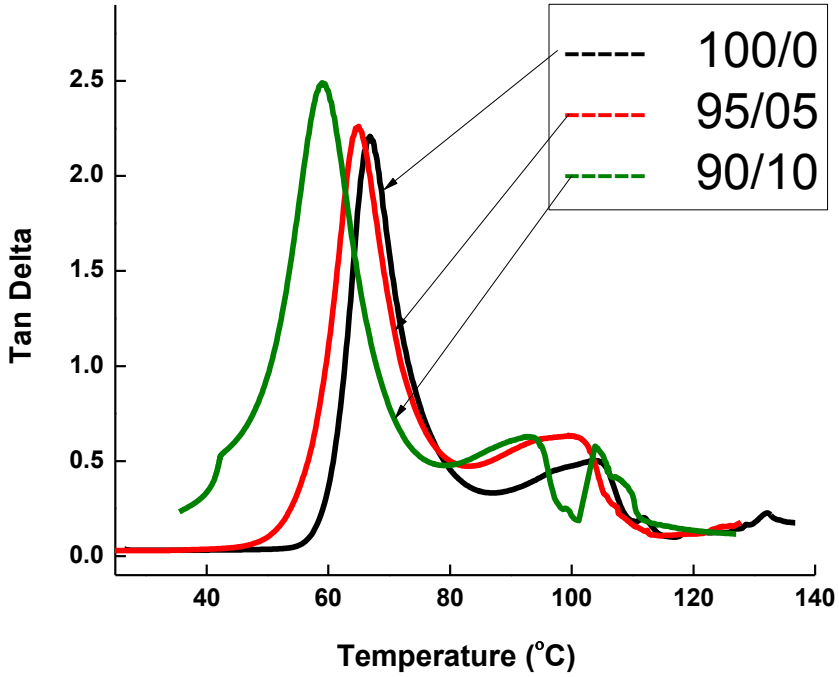

Figure 5- 31: Loss factor (Tan δ peak) of PLA + copolymer as function of temperature

5.5.2.2 PLA + 10 (wt %) wood + Copolymer

Figure 5- 32 shows the dynamic modulus of the PLA and PLA + 10 (wt%) wood + copolymer composites. It is possible to see from the figure that the modulus of PLA is increased with the incorporation of 10 (wt%) wood flour and also 5 (wt%) copolymer. But modulus is reduced significantly with the incorporation of 10 (wt%) copolymer into PLA + 10 (wt%) wood flour. The softening of PLA and PLA +10 (wt%)wood flour composites starts around 60 ° C.

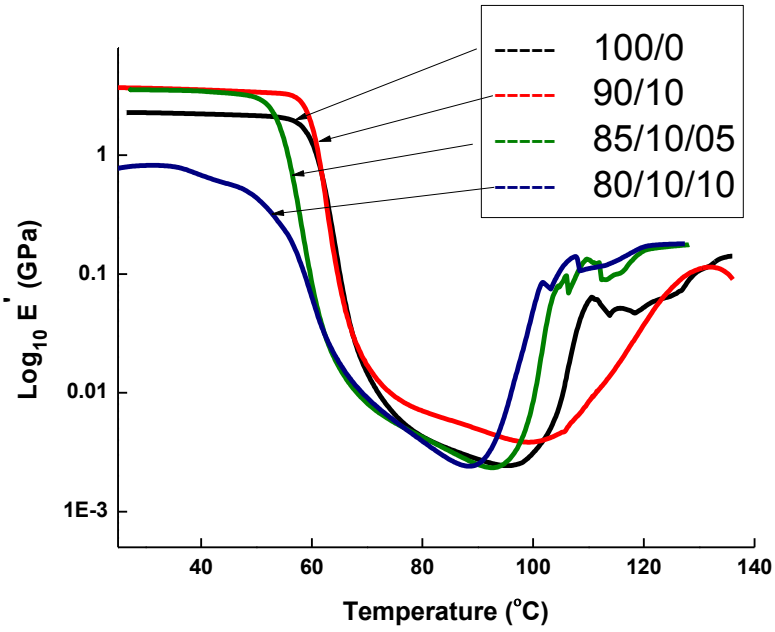

Figure 5- 32: Storage modulus of PLA and PLA + 10 (wt %) wood + CP as a function of temperature

Analysis of storage modulus of PLA and PLA + 10 (wt%) wood + copolymer is shown in Table 5- 15.

Table 5- 15: Storage modulus of PLA and PLA +10 (wt %) + copolymer

PLA / wood / copolymer (wt %)	Storage Modulus (30°c) (GPa)	Storage Modulus (40°c) (GPa)
100 / 0 /0	2.28	2.19
90 / 10 / 0	3.67	3.55
85 / 10 / 5	3.55	3.46
80 / 10 / 10	2.05	1.89

From the table it is clear that copolymer has a significant effect on PLA wood composites. Storage modulus increased from 2.28 (GPa) to 3.67 (GPa) with the incorporation of 10 (wt%) wood flour and slightly decreased to 3.5 (GPa) with the incorporation of 5 (wt%) copolymer into the composites. Storage modulus drops down significantly to 1.89 (GPa) with incorporation of 10 (wt%)copolymer into the composite. The storage modulus again starts increasing at a temperature around 90 ~ 100 ° C due to the effect of cold crystallization [17, 120].

Figure 5- 33 shows tan δ for PLA and PLA +10 (wt%)wood flour composites and the effect of copolymer on the loss factor. It is clear from the figure that incorporation of 10(wt%)wood flour doesn't make any significant difference to the glass transition temperature but the inclusion of copolymer does reduce the glass transition temperature of PLA +10 (wt%) wood flour composites. The area of integration under the *Tan δ* curve is also reduced due to the incorporation of copolymer suggesting a decrease in damping capability of the PLA + wood flour composite.

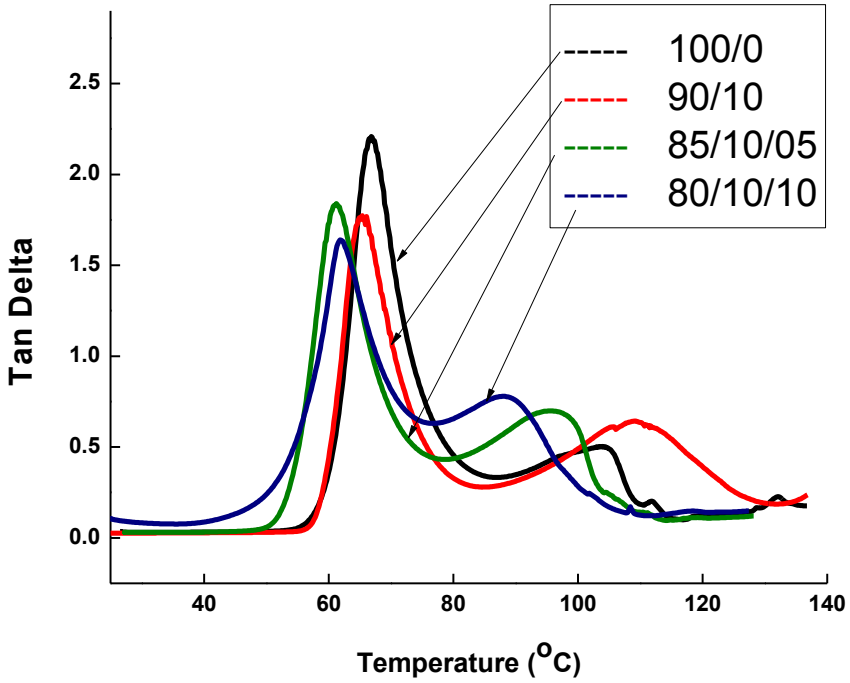

Figure 5- 33: Loss factor (Tan δ peak) of PLA + 10 (wt %) wood + copolymer as function of temperature

5.5.2.3 PLA + 20 (wt %) wood + Copolymer

Figure 5- 34 shows the effect of copolymer and the addition of 20 (wt%)wood flour as reinforcement on storage modulus. It is clear from the figure that storage modulus increases with the addition of 20 (wt%) wood flour into the PLA matrix. It is clear that storage modulus drops around 60°C but starts rising again due to the cold crystallization process at higher temperature (90 ~95 ° C).

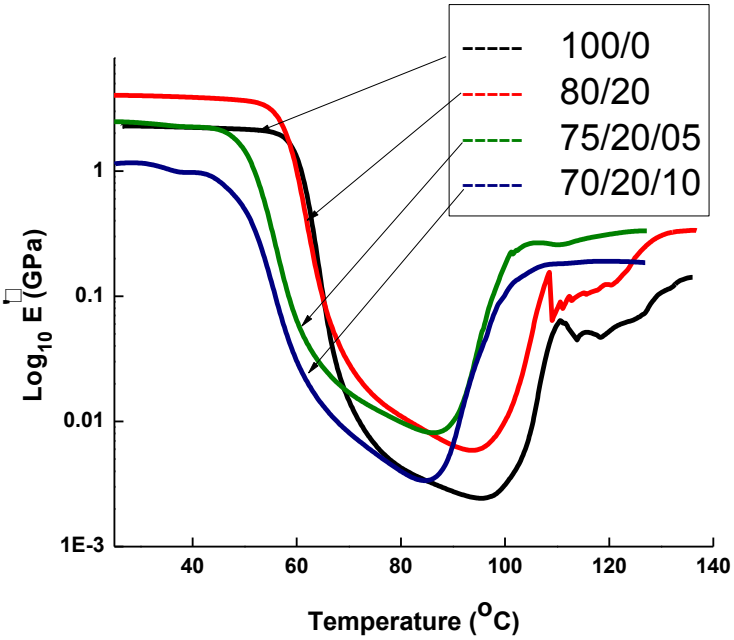

Figure 5- 34: Storage modulus of PLA + 20 (wt %) wood + copolymer as function of temperature

Table 5- 16 shows the storage modulus of PLA +20 (wt %) wood + copolymer at different temperatures. The storage modulus is measured at 30°C and 40°C during DMA testing. At 30°C storage modulus increases from 2.28 (GPa) to 3.99 (GPa) compared with neat PLA due to addition of 20 (wt %) wood flour. But with the incorporation of the copolymer dynamic modulus reduces. Storage modulus drops off significantly from 2.28 to 1.15 (GPa) as copolymer increases from 0 to 10 (wt %).

Table 5- 16: Storage modulus of PLA and PLA +20 (wt %) + copolymer

PLA + wood + copolymer (wt%)	Storage Modulus (30°c) (GPa)	Storage Modulus (40°c) (GPa)
100 / 0 /0	2.28	2.19
80 / 20	3.99	3.87
75 / 20 / 5	2.42	2.24
70 / 20 / 10	1.15	0.97

The loss factor (*Tan δ*) is shown in Figure 5- 35. Wood flour does not affect the glass transition temperature itself, but incorporation of copolymer has led to a reduction in the glass transition temperature. The Tan δ peaks have shifted quite significantly to lower temperature indicating a decrease in the glass transition temperature compared with neat PLA. Also the area of integration under the *Tan δ* peaks is reduced showing decreased damping capability of the composite and enhanced brittle nature of PLA + 20 (wt%) wood flour composite.

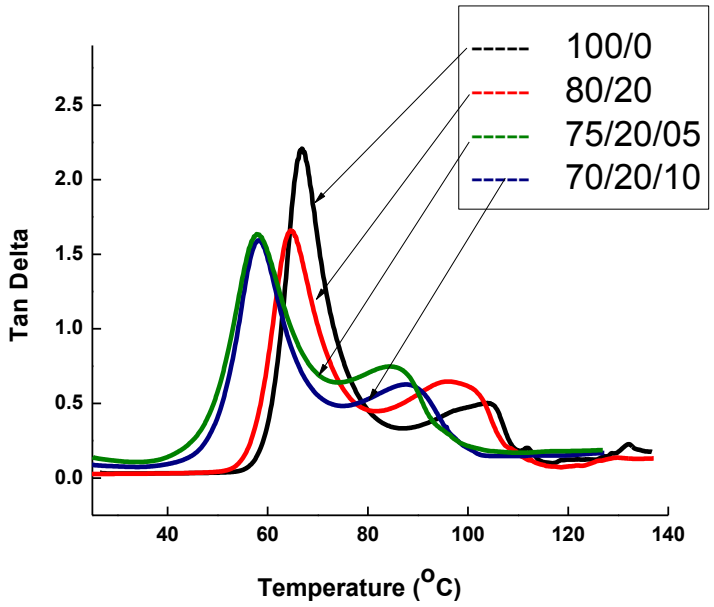

Figure 5- 35: Loss factor (Tan δ peak) of PLA + 20 (wt%) wood + copolymer as function of temperature

5.5.2.4 PLA + 40 (wt %) wood + Copolymer

Viscoelastic properties of PLA and PLA + 40 (wt %) wood flour + copolymer are shown in Figure 5- 36. It is clear from the figure that addition of 40 (wt %) wood increases the storage modulus of PLA significantly. The figure clearly shows that PLA + 40 (wt %) composite seems to soften at a lower temperature in the presence of copolymer. In the presence of 5 and 10 (wt %) copolymer PLA + 40 (wt %) wood composites soften around 45 ~ 48 °C, whereas previously softening started at 55 ~ 60°C. On the other hand cold crystallization starts at lower temperatures when compared to neat PLA and PLA + wood composite.

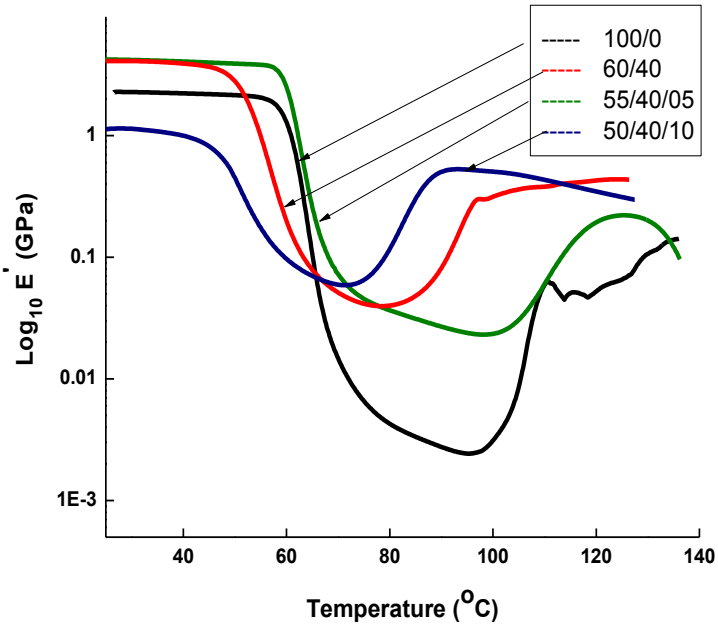

Figure 5- 36: Storage modulus of PLA and PLA +40 (wt %) + copolymer

The storage modulus is shown in Table 5- 17. Storage modulus jumps up from 2.28 to 4.19 (GPa) with 40 (wt %) wood flour compared to neat PLA at a temperature of 30° C. The storage modulus decreased from 4.10 to 1.13 (GPa) when the amount of the copolymer increases from 5 to 10 (wt %).

Table 5- 17: Storage modulus of PLA and PLA +40 (wt %) + copolymer

PLA + wood + copolymer (wt %)	Storage Modulus (30°c) (GPa)	Storage Modulus (40°c) (GPa)
100 / 0 /0	2.28	2.19
60 / 40 / 0	4.19	4.07
55 / 40 / 5	4.10	3.91
50 / 40 / 10	1.13	1.01

It is also clear from loss factor analysis (Figure 5- 37) that *Tan δ* peaks shift towards lower temperature as copolymer is added to PLA+40(wt%) wood flour composite, indicative of decreasing the glass transition temperature. It is evident that the

addition of 40 (wt%) wood flour to the PLA matrix, reduces the area of integration under the *Tan δ* curve, suggestive of decreasing the damping capability resulting in a more brittle material. Incorporation of copolymer further decreases the area under the *Tan δ* curve which agrees with the findings from tensile testing, resulting in reduced strain at break and enhanced brittle nature of the composite.

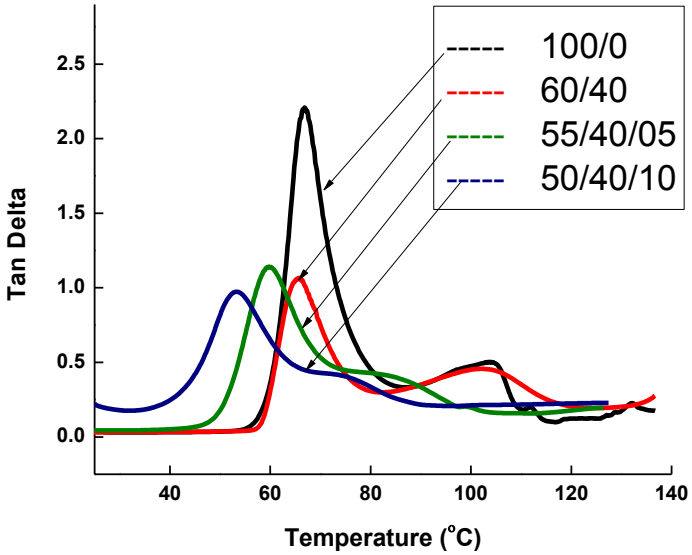

Figure 5- 37: Loss factor (Tan δ peak) of PLA + 40 (wt %) wood + copolymer as function of temperature

5.5.3 PLA –Wood Composites (Silane Treated)

Viscoelastic behaviour of silane treated pure PLA and PLA–wood composites is shown in Figure 5- 38. It is clear that silane treatment does affect the viscoelastic properties of the PLA and its composites reinforced with silane treated wood fibres. The silane treatment of pure PLA improves the storage modulus from 2.3 to 2.7 (GPa) compared to neat PLA. Incorporating pre-treated wood fibres into the PLA matrix, gave improved flexural modulus compared to neat PLA.

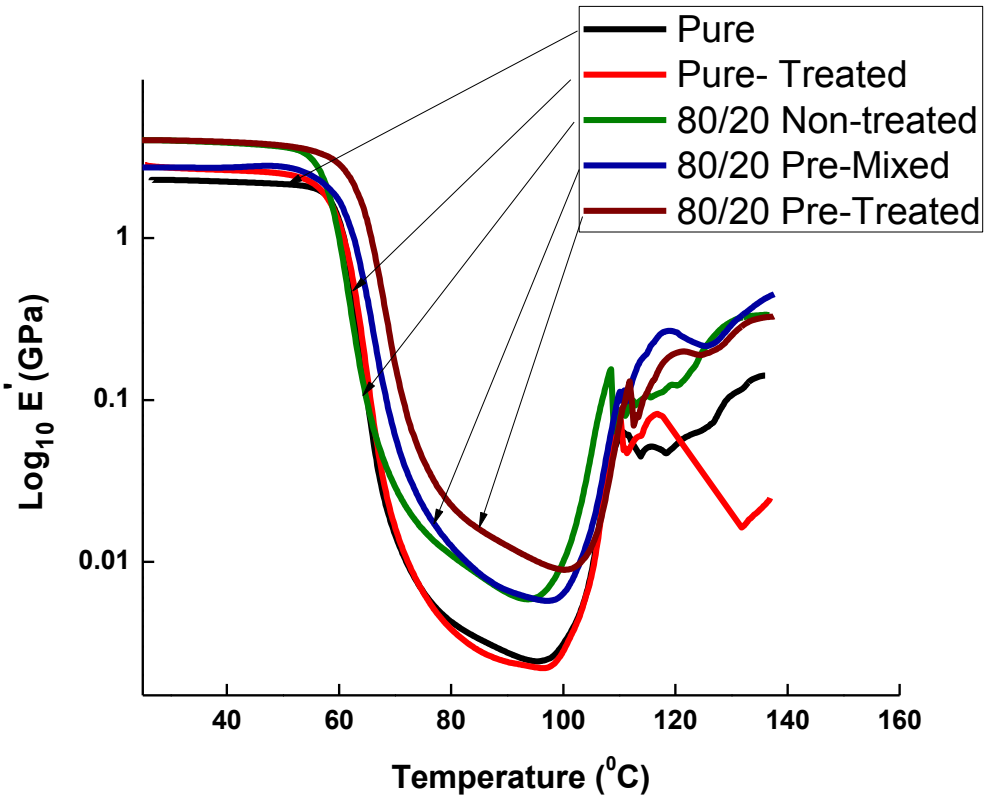

Figure 5- 38: Storage Modulus of PLA and silane treated PLA –Wood Composites as a function of Temperature

The storage modulus for pure PLA and silane treated PLA –wood composites are summarized in Table 5- 18.

Table 5- 18: Storage modulus of PLA and silane treated PLA – wood composites

PLA / Wood (wt %)	Storage Modulus (30°c) (GPa)	Storage Modulus (40°c) (GPa)
100/0 (pure)	2.3	2.2
100/0 (Pure Treated)	2.7	2.6
80/20 (Non-Treated)	3.9	3.8
80/20 (Pre-Mixed)	2.7	2.6
80/20 (Pre-Treated)	4.0	3.9

The effect of silane coupling agent on loss factor (*Tan δ) of* PLA- wood composites is shown in Figure 5- 39. It is clear from loss factor analysis (Figure 5- 39) that there is no significant shift in the peak of *Tan δ* peak when the treated wood fibres is added to the PLA matrix, suggesting no significant change in glass transition temperature. Area under the curve of the *Tan δ* peak of the treated PLA increases with the silane treatment , indicating the effectiveness of the silane treatment. An increase in the area under the curve of the *Tan δ* peak indicates the improvement in the damping capability of the materials. It is also evident that the addition of silane treated wood in the PLA matrix, reduces the area of integration under the *Tan δ* curve, suggestive of decreasing the damping capability resulting in a more brittle material. Incorporation of treated wood following two different procedures, makes no significant change to the behaviour of the PLA- wood composites and results in a degraded weak fragile composite.

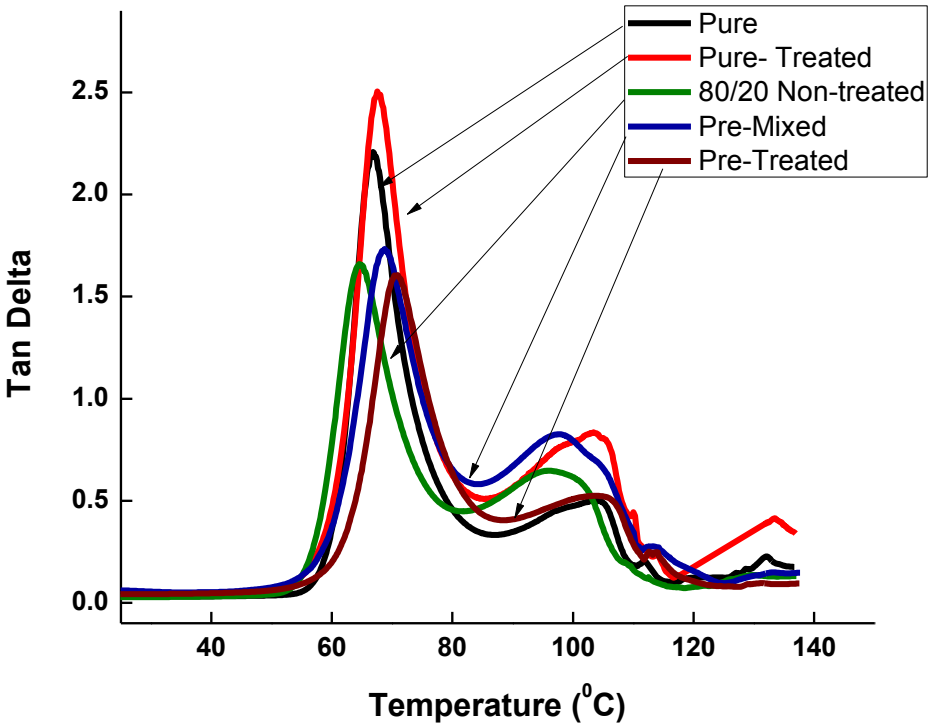

Figure 5- 39: Loss factor (*Tan δ)* of PLA and treated PLA –Wood Composites as a function of Temperature

5.6 Conclusions

From these experimental results, the following conclusions can be drawn:

5.6.1 PLA

PLA is an almost amorphous polymer with a small amount of crystalline content which has a melting temperature around 155 (^oC) to 160 (^oC). The glass transition temperature is around 55 (^oC). PLA starts crystallizing at higher temperature around 100 (^oC). There is a unique double peak observed in the melting endothermic.

5.6.2 PLA / wood

From the DSC results there was found to be no significant improvement in glass transition temperature, melting temperature and overall crystallinity of the composites. The Young's modulus of the PLA composites increased significantly from 4.1 to 8.7 (GPa) when increasing amount of wood fibre was added but the tensile strength reduces. The storage modulus significantly increased from 2.3 to 4.2 (GPa) when the content of wood fibres was increased from 0 to 40 (wt %) and the area under the tan delta curve reduced, thus the composites exhibited brittle failure.

5.6.3 PLA /wood /copolymer

The glass transition temperature decreased from 54 to 48 (^oC) when the content of copolymer increased from 0 to 10 (wt %). The Young's modulus of the composites increased further by adding the lower amount of the copolymer but reduced at higher loading. The tensile strength increased as the content of copolymer increased from 0 to 10(wt %) when compared to pure PLA/wood composites. The peak of tan delta shifts towards the lower temperature as the content of copolymer increased from 0 to 10 (wt %) reconfirming the DSC results and the area under the tan delta curve also reduced by increasing the amount of copolymer.

5.6.4 PLA /wood /silane coupling agent

There is no improvement observed in the properties of the PLA /wood composites with coupling agent.

Chapter 6 PLA – Flax Composites

In this chapter, flax fibre was combined with PLA to create composite materials with various different ratios of flax and PLA. The composites were tested to measure the mechanical and thermal properties. The experimental results obtained are presented, with significant features indicated and interpreted. The PLA/Flax composites were prepared with the following (weight %) of Flax fibres; 0, 10, 20, 30.

In the second phase, the focus was shifted to improve the toughness of the PLA-Flax composites and hybrid composites were prepared with the incorporation of epoxidised natural rubber (ENR) into the PLA- Flax composites. Three sets of samples were prepared; with 10 and 20 (wt %) of ENR into the PLA-flax composites as well as the introduction of a flax and ENR masterbatch into the PLA. Analysis and experimental results are described in details below.

6.1 Thermal Properties

6.1.1 PLA – Flax

Figure 6- 1 shows the DSC second heating curves of neat PLA and PLA/Flax composites at the heating rate of 10 (^{o}C/min). The glass transition (Tg), cold crystallization (Tcc) and melting temperatures (Tm) are obtained directly from the thermograms. It is observed that the cold crystallization peaks for PLA/flax composites are displaced to lower temperatures and that the rate of crystallization is increased by nucleating effect. Two significant endothermic peaks have been observed in the melting endotherm of the PLA composites compared to pure PLA. It indicates that there are two different forms of crystallographic structures produced in the composite samples, which are referred to as α and β.

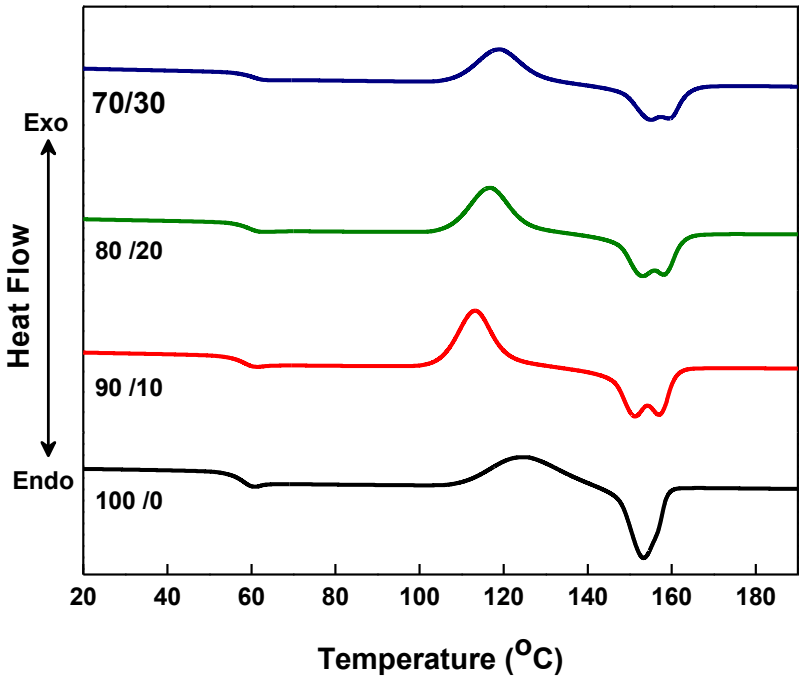

Figure 6- 1: DSC second heating curves of neat PLA and PLA/Flax composites

Table 6- 1 summarises the values obtained for PLA/flax composites, glass transition (Tg), cold crystallization (Tcc), and melting temperatures (T_m), and the % crystallinity of PLA in the composites. It is clear that incorporation of flax has increased the glass transition temperature by 4 (°C) and has decreased the cold crystallization temperature from 127 and 113 (°C).

It is also observed that the T_m of α crystals increases by 2-3 (°C) for all composites while the T_m for β crystals increases with increasing flax fibre content. It is noted also that the % cold crystallization increases with flax content. These indicate that flax fibres produce a nucleating effect on the crystallization of the PLA. However, the values of PLA crystallization are too small to determine a meaningful conclusion. Also the cooling curve of the DSC gives no exothermic peak, as shown in Figure 6- 2.

Table 6- 1: Thermal properties of PLA - Flax Composites.

Sample codes	Tg (°C)	Tcc (°C)	Tm (°C)		Cold Crystallization (%)	Crystallinity (%)
			α	β		
100 /0	54 ± 0.7	127 ± 1.4	155 ± 1.5	----	22 ± 1.2	2.0 ± 0.8
90 / 10	58 ± 0.5	113 ± 0.5	157 ±0.5	151 ± 0.5	26 ± 3.0	2.2 ± 2.1
80 / 20	57 ± 1.0	115 ± 2.0	157 ± 0.5	152 ± 1.0	32 ±2.3	2.7 ± 2.3
70 / 30	58 ± 0.0	118 ± 1.0	158 ± 0.5	154 ± 1.0	28 ± 0.8	5.8 ± 1.4

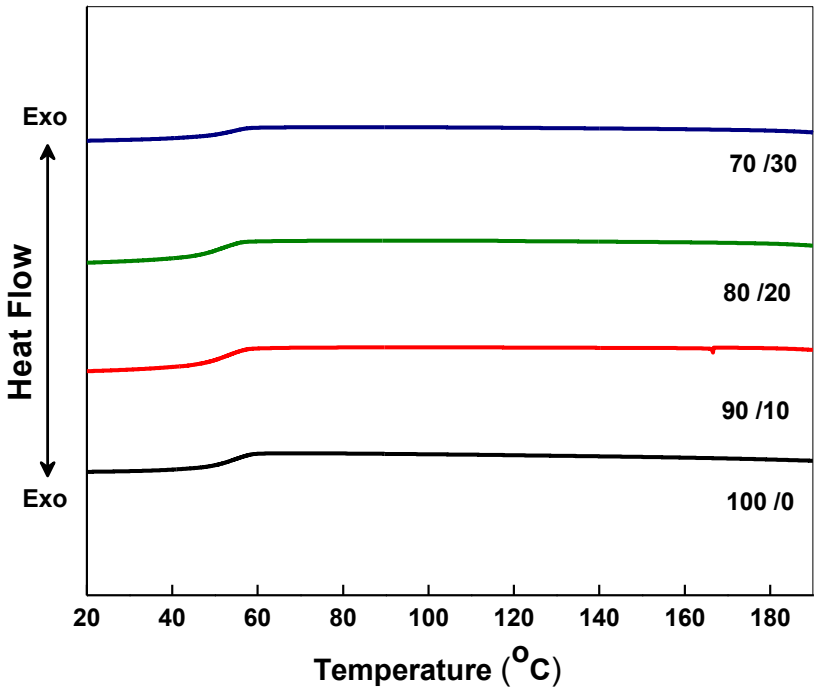

Figure 6- 2: DSC cooling curves of neat PLA and PLA/Flax composites

6.1.2 PLA-FLAX-ENR

Figure 6- 3 shows the DSC scans for pure PLA and PLA/Flax/ENR50 blend without annealing and the data are tabulated in Table 6-2. It can be seen from the scaned curves that glass transitions is not affected significantly by the incorporation of ENR50 compared to PLA/Flax composites. The Tg of the PLA/Flax/ENR50 blends is located at the same temperature range (57~59(°C). It is also observed that there is no

effect on the cold crystallization temperature. Significantly with the incorporation of ENR50 into the PLA/Flax composites, there is only one melting peak observed during the melting endotherm compared with two for the pure PLA/flax composites. Table 6-2 tabulates the measurement of glass transition temperature (Tg), cold crystallization temperature (T_{cc}), melting temperature (T_m), and % crystallinity of PLA/Flax composites. It is clear from the table that the Tg is not affected with the incorporation of ENR50. The exothermic cold crystallization peaks appears between 125 and 130 (°C) and centred at 127 (°C) followed by the melting endothermic peak between 154 and 158 (°C).

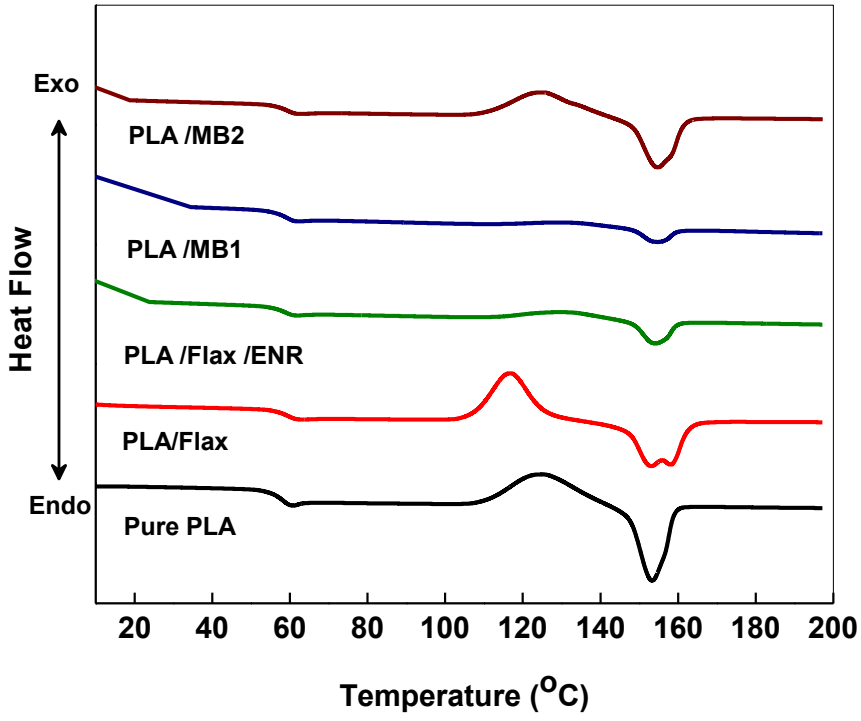

Figure 6- 3: DSC curve for Pure PLA, PLA-Flax and PLA-FLAX-ENR50 blends during second heating without annealing

Jaratrotkamjorn et al. [121] have also studied the melt blending of PLA with natural rubber and reported that the Tg of the PLA was not affected when blended with ENR50. They reported that Tg for PLA/ ENR50 blends in their report is around 58°C when mixed with 10 (wt %) which is very close to the observed value.

Table 6-2: Thermal properties of pure PLA, PLA/flax and PLA/flax/ENR blends during second heating without annealing.

Sample Description	Tg (°C)	Tcc (°C)	Tm (°C)		Cold Crystallization (%)	Crystallinity Xc (%)
			α	β		
Pure PLA	54 ± 0.7	127 ± 1.4	155 ± 1.5	----	22 ± 1.2	2 ± 0.8
PLA /Flax	57 ± 1.0	115 ± 2.0	157 ± 0.5	152 ±1.0	32 ±2.3	3 ± 2.3
PLA/Flax/ENR	58 ±0.8	130 ± 0.6	154 ± 0.8	----	9 ± 0.7	4 ± 0.5
PLA /MB1	59 ± 0.6	131 ± 0.4	154 ± 0.7	----	3.2 ± 0.6	4 ± 0.5
PLA /MB2	58 ± 0.7	125 ± 0.5	154 ± 0.8	-----	18 ± 0.7	5 ± 0.7

Figure 6- 4 shows the DSC heating scans of the annealed samples and the results are summarized. The samples for PLA and PLA /Flax blends with ENR50 were annealed at 120 (°C) for 20 (min) during the cooling cycle of the compression moulding. Observations were recorded based on the first DSC heating scan. The results show that there is no evident crystallization peak during the DSC heating scan, which clearly confirms that all samples crystallized during the annealing process. The samples undergo a melting endotherm and all the samples reveal two melting peaks. However the peaks at higher temperature are more prominent in all samples containing ENR50.

Sarasua et al.[122] have also studied the crystallization and melting behaviour of PLA and have explained the double-peak melting point. Accordingly a more perfect crystalline form corresponds to higher temperature than that at lower temperature. Later Zhang et al.[123] have studied the phase transformation and double melting behaviour of polylactide using the wide –angle X-ray diffraction (XRD) and DSC. They confirmed the formation of **α´**- crystal structure, corresponding to the melting endotherm at lower temperature and its transformation to **α** – crystal structure at higher temperature. In this work the two different melting peaks are identified as **α**

for the higher temperature melting endotherm and **β** corresponds to the lower temperature melting endotherm.

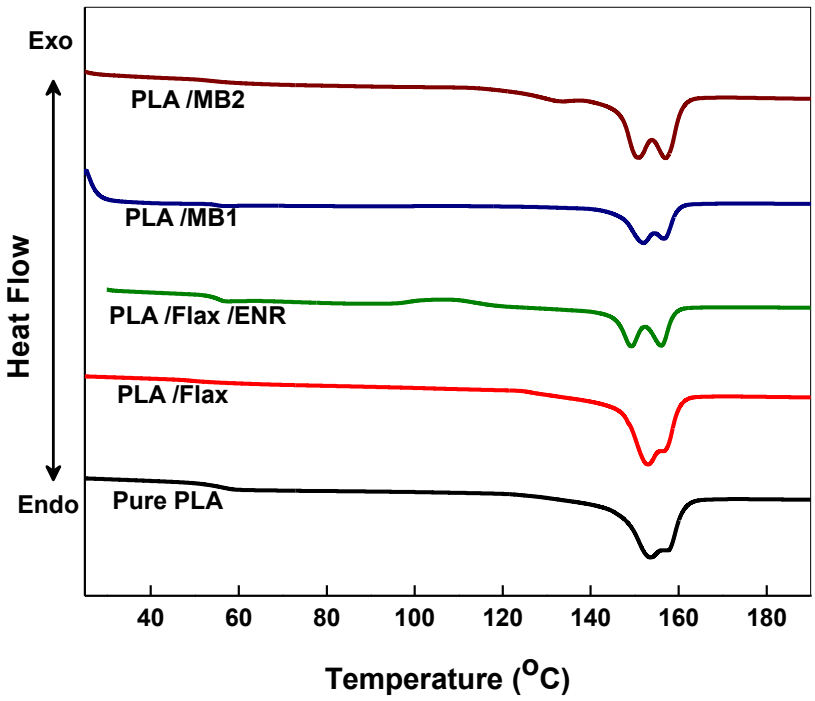

Figure 6- 4: DSC curve for Pure PLA, PLA/Flax and PLA/FLAX/ENR50 blends during first heating after annealing.

The thermal properties and the crystallinity developed in pure PLA and PLA/flax/ENR blends during the annealing process are summarised in Table 6- 3. These indicate that the melting peak for the **α** form appears at 156 - 157 (°C) for sample corresponding to crystallinity developed during the melt blending process, whereas the peak at about 150-153 (°C) corresponds to the melting of crystals generated during the annealing process. It is evident from the analysis that the annealing process promotes the crystallization of PLA due to chain alignment. The heat treatment significantly increased the crystallinity of the pure PLA and the PLA blends respectively. The annealing process caused the improvement in overall crystallinity for pure PLA, PLA/Flax and PLA/Flax/ENR blends significantly from 2 to 31 (%), 3 to 45 (%) and 4 to 30 (%) respectively.

Table 6- 3: Thermal properties and the crystallinity of pure PLA, PLA/flax and PLA/flax/ENR50 blends during first heating after annealing.

Sample Description	Tg (°C)	Tcc (°C)	Tm (°C)		Cold Crystallization (%)	Crystallinity Xc (%)
			α	β		
PLA	56 ± 0.4	----	153 ± 0.8	----	----	31 ± 0.6
PLA /Flax	53 ± 0.0	----	153 ± 0.3	----	----	45 ± 1.4
PLA/Flax/ENR	55 ± 0.3	108 ±0.8	156 ± 0.2	150± 0.8	7.0 ± 0.2	29 ± 0.4
PLA /MB1	55 ± 0.4	----	157 ± 0.3	152 ± 0.4	----	31 ± 0.6
PLA /MB2	52 ± 0.3	-----	157 ± 0.6	150 ± 0.5	-----	30 ± 0.8

6.1 Mechanical Properties

6.1.1 PLA - Flax

The summary of the results of the tensile tests is shown in Table 6- 4. All the results represent the average values based on 7 ~ 10 samples. It is clear from the data that flax reinforcement leads to increase of the modulus while the tensile strength of the composites is decreased. The tensile strength decreased from 43 ± 3.1 to 38 ± 3.4 (MPa) when the content of flax fibres increased from 0 to 30 (wt %). A significant drop in the tensile strength of the composite is observed at lower loading than at higher loading compared to the Pure PLA. As the content of flax increased, the tensile strength is improved. Osman et al. [17] reported a similar decrease in tensile strength while Bax and Mussig [113] reported the increase in tensile strength of the PLA composites when reinforced with flax.

Table 6- 4: Tensile Properties for PLA/flax composites.

Sample codes PLA/Flax	Tensile Strength (MPa)	Tensile Modulus (GPa)	Elongation to break (%)
100/0	43 ± 3.1	4.1 ± 0.6	4.1 ± 0.5
90/10	24 ± 2.3	6.1 ± 0.5	2.7 ± 0.6
80/20	26 ± 1.7	7.2 ± 0.8	1.8 ± 0.5
70/30	38 ± 3.4	8.5 ± 0.4	2.2 ± 0.3

Figure 6- 5 shows the variation of tensile modulus of PLA composites reinforced with flax fibres which clearly show the modulus increases with the content of flax. The Young's modulus increased from 4.1 to 8.5 GPa as the flax content increased from 0 to 30 (wt %). Other researchers have also reported the reinforcing effect in PLA composites, when the flax fibres are incorporated. Osman et al. [17] have made a comparative analysis of incorporating flax fibres in Polypropylene (PP) and PLA. They have reported an increase in Young's modulus of PLA from 3.4 to 8.3 when the content of flax increased from 0 to 30 (wt %), while the modulus of PP increased from 1.6 to 7.6 (GPa) when the content of flax increased from 0 to 40 (wt %). Bax and Mussig [113] , have reported that Young's modulus of PLA/Flax composites increased from 3.1 to 6.3 when the content of flax fibres increased from 0 to 30 (wt%).

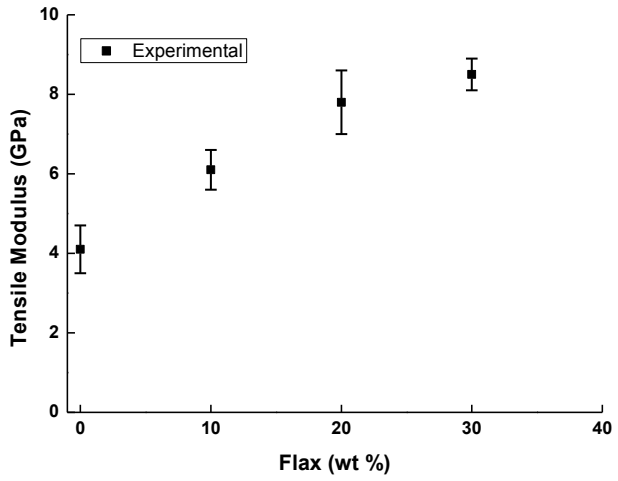

Figure 6- 5: Young's modulus of PLA - Flax composites

6.1.2 Comparison between predicted and experimental tensile properties

Figure 6- 6 shows the comparative experimental and theoretical response of Young's modulus of the PLA, flax and ENR composites as a function of fibre volume fraction. Due to the complex nature of this system, the predicted response of the composites properties is calculated using a general rule of mixtures, described earlier in chapter 3.

In calculating the predicted value of the Young's modulus of the various PLA/Flax composites from the rule of mixtures, the following values have been used; the modulus of the matrix (PLA) is 4.1 (GPa) as measured experimentally. There were quite different values reported in literature for young's modulus of the flax fibres. Two different research groups have reported 70 (GPa) as the modulus value of flax [124, 125]. Bax and Mussig have reported 15 (GPa) as Young's modulus of flax in their review of impact and tensile properties of PLA and its composites [113]. The modulus of the flax fibres is taken as 27 (GPa) also reported by two different research groups [119, 126]. The volume fraction of the filler is calculated from the weight fractions of the flax using equation 3.8 explained in previous chapters. The value of the density of PLA is taken as 1.24 (g/cm^3), while the density of flax is taken as 1.47 (g/cm^3) [126].

Very close correlation between the theoretical and experimental values was clearly observed when the contents of flax are increased from 0 to 20 (wt %) as shown in Figure 6- 6, but when content of flax increased up to 30 (wt %), a significant difference is observed between the experimental and the predicted values. It can be seen from the R^2 value of 0.8, that there is not good agreement between the experimental data and predictions from the rule of mixtures. The difference in comparative analysis between the experimental and predicted values could be due to agglomeration at higher loading.

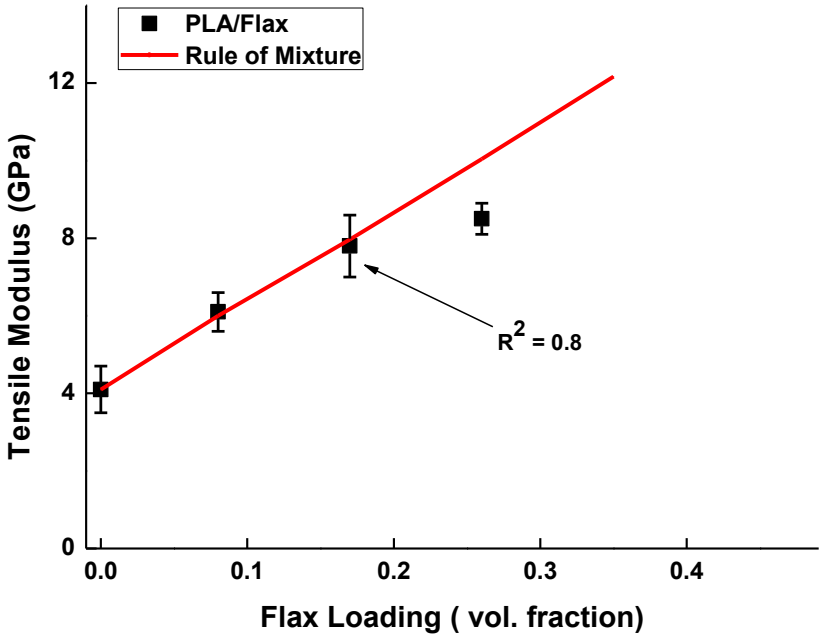

Figure 6- 6: Effect of flax content on tensile modulus as a function of volume fraction of flax

6.1.3 PLA /FLAX /ENR

The tensile properties of PLA composites containing various loading levels of flax and ENR blends are shown in Figure 6- 7, which shows the rigid and brittle behaviour of pure PLA with a low elongation at break of 4 (%) and it breaks soon after yielding without necking. Addition of flax with the PLA makes it more brittle and it fails at very low elongation to break of 2 (%). Annealing of the blend of Flax, ENR and PLA matrix did not change the brittle fracture properties of the composites. It is clear that the behaviour of the annealed composites obtained by direct mixing of PLA, Flax and ENR shows the same brittle failure as composites obtained by quenching PLA and Flax. Again the low compatibility of the PLA with the natural fibres due to the hydrophilic nature of the fibres, leads to a composite with poor mechanical properties. In this case the presence of ENR couldn't improve the incompatibility between the matrix and the fibres as confirmed by the brittleness of the composites.

However the incorporation of Flax and ENR masterbatch into the PLA matrix does change the brittle fracture of PLA to a ductile fracture with the formation and propagation of a neck. The addition of the rubber particles significantly lowers the tensile strength due to the softening effect in the composites together with void formation. The role of epoxidized natural rubber is evident in the annealed samples when the mixing of PLA, Flax and ENR is carried in a two step process (PLA + masterbatch ENR/Flax) in order to prevent the direct contact between the flax fibres and the PLA matrix.

It is very interesting to observe the large increase in ductility with incorporation of the masterbatch into the PLA matrix. The elongation to break increased from 4 to 14 (%) when the content of ENR50 increased from 0 to 20 (wt %). Addition of masterbatch1 into the PLA matrix has significantly increased the elongation to break as compared to masterbatch2. In this particular case, the amount of the ENR50 and the mixing methodology are the two key factors in improving the mechanical properties of PLA composites. It seems that avoiding direct contact between the PLA and flax helps to improve the ductility of PLA and composites. The increase in the elongation to break, suggests that the elastomeric component of the composite affects yielding of the matrix. In addition, the samples are also observed to undergo stress whitening in the neck zone during yielding.

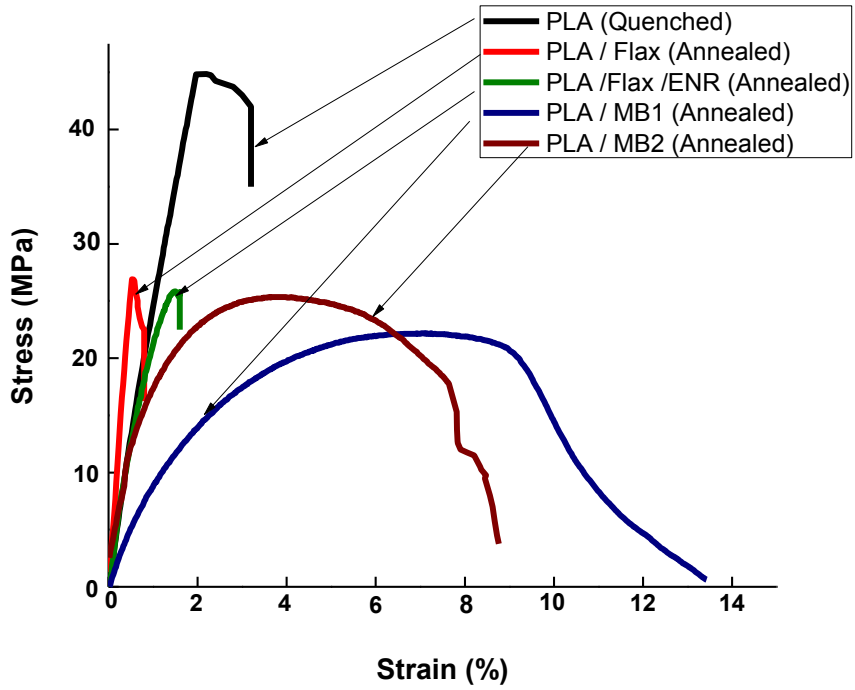

Figure 6- 7: Tensile curves of the mechanical properties of PLA /Flax /ENR blends

The tensile properties for annealed PLA, flax and ENR composites are summarised in Table 6- 5 below. It can also be seen from the table when compared with Table 6- 4 that tensile strength of pure PLA significantly reduced when annealed. The tensile strength reduced from 43 to 18 (MPa) and the Young's modulus increased from 4.1 ± 0.6 to 6.4 ± 0.8 (GPa), thus the crystallization of PLA makes the composites more brittle. It is also observed that tensile strength of the PLA/flax composites decreased from 24 to 20 (MPa) when annealed. Young's modulus increased from 6.1 ± 0.8 to 8.2 ± 2.8 (GPa) when the PLA/flax samples are annealed. Young's modulus is decreased from 8.2 ± 2.8 to 3.8 ± 0.6 (GPa) when the content of ENR50 increased from 0 to 20 (wt %) along with 20 (wt %) of flax fibres and the tensile strength increased from 20 to 27 (MPa). There is no significant change observed in the elongation to break when the flax and ENR are blended together with PLA.

From the table it is clear that when the masterbatch of flax and ENR50 is introduced into the PLA matrix, elongation to break significantly improves. The elongation to break is increased from 2.1 to 13 (%) when the content of masterbatch 1 increased from 0 to 40 (wt %), containing amount of 20, 20 (wt %) of flax and ENR50 respectively compared to pure PLA. It is observed that tensile strength increases from 18 ± 3.2 to 24 ± 1.7 (MPa). The incorporation of flax and ENR masterbatch 1 also caused a reduction in the Young's modulus from 6.4 ± 0.8 to 2.2 ± 0.4. The same behaviour was also seen when the content of flax and ENR masterbatch 2 increased from 0 to 30 (wt %) containing amount of 20, 10 (wt %) of flax and ENR50 respectively in the composite. This indicates that the mixing of flax and ENR masterbatch into the PLA has improved the ductile behaviour of the composites.

Table 6- 5: Mechanical properties of PLA, PLA/flax and PLA /flax /ENR blends when annealed

Sample Description (Annealed)	Tensile Strength (MPa)	Young's Modulus (GPa)	Elongation to break (%)
PLA (100/0)	18 ± 3.5	6.4 ± 0.8	2.1 ± 0.7
PLA/Flax (80/20)	20 ± 2.7	8.2 ± 2.8	4.5 ± 0.8
PLA /Flax/ENR (60/20/20)	27 ± 0.6	3.8 ± 0.6	2.2 ± 0.4
PLA /MB1 (60/40)~(60/20/20)	24 ± 1.7	2.2 ± 0.4	13.6 ± 1.6
PLA /MB2 (70/30)~(60/20/10)	28 ± 2.4	3.4 ± 0.8	8.1 ± 1.2

Other workers have also studied the fracture behaviour and toughening of polylactides with natural rubber. Bitinis et al. [127] have studied the structure and properties of polylactides and natural rubber blends. They have reported that the incorporation of natural rubber into the PLA matrix significantly affected the tensile properties. It was reported that Young's modulus and tensile strength drop with the addition of natural rubber. The Young's modulus and tensile strength decreased from 3.1 ± 0.04 to 1.8 ± 0.08 (GPa) and 63.1 ± 1.1 to 25 ± 0.9 (MPa) respectively when the natural rubber content increased from 0 to 20 (wt %). They have also reported that elongation to break has significantly improved from 3.3 ± 0.4 to 73 ± 14 (%) when 20 (wt %) of rubber content is incorporated.

Zhang et al. [128] have also studied the toughening behaviour of polylactide with epoxidised natural rubber (ENR 20 & ENR50) and reported improvement in the mechanical properties of the blends. They also reported a significant increase in elongation to break with the incorporation of ENR into the PLA matrix. Ishada et al. [129] have also investigated the toughening behaviour of polylactides by melt blending with rubbers. They reported a reduction in tensile properties (modulus, strength) and increase in elongation to break (%) compared to pure PLA when melt blended with rubbers.

6.2 Morphological Properties

The micrographs of flax fibres are shown in Figure 6- 8. The average diameter of the flax fibres was recorded as 16 ‘microns’ using SEM. The initial average length of flax fibres about 6 ~ 8 (cm) as shown in Figure 6- 8 (a) and was reduced by grinding in a high shear mixer.

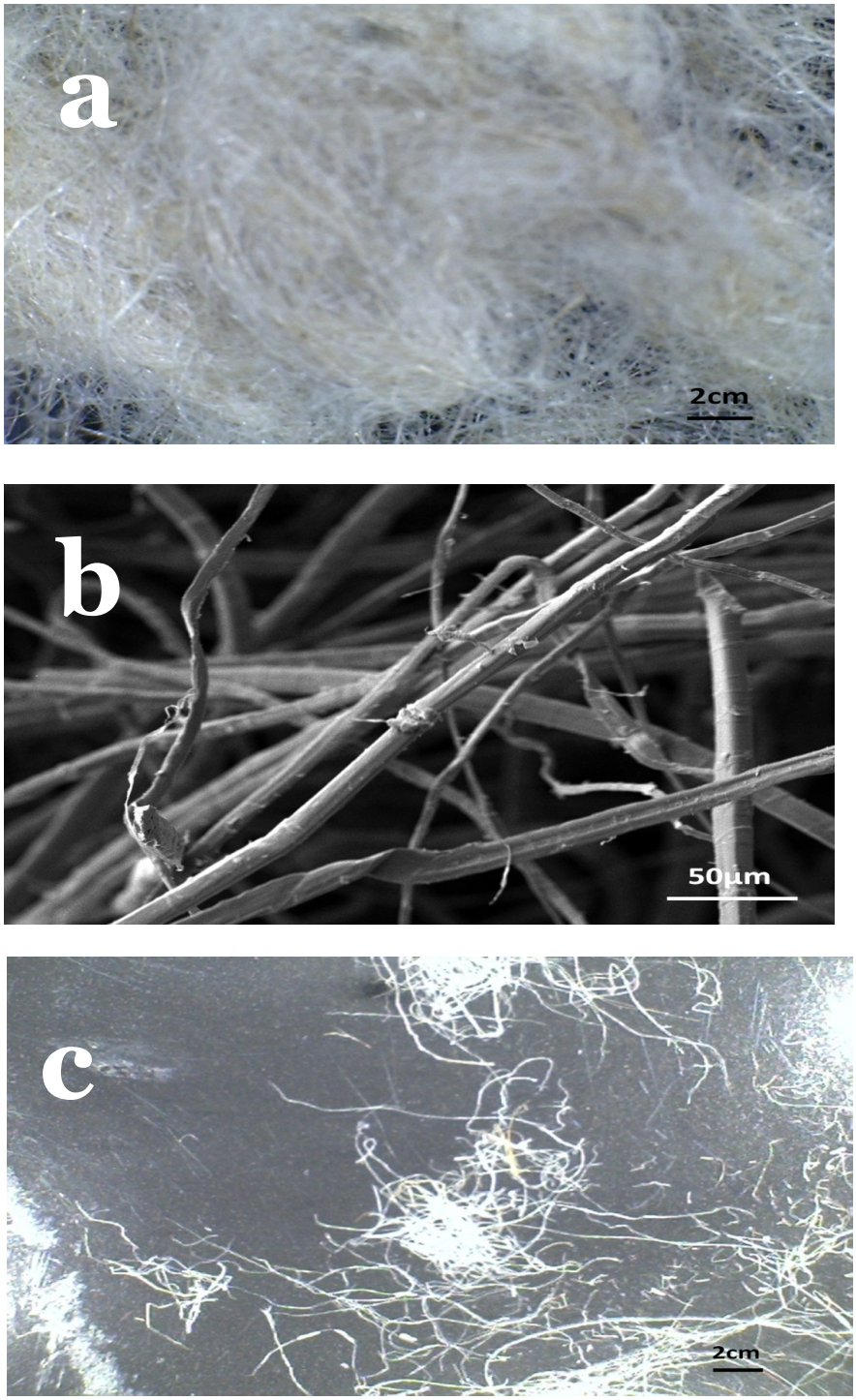

Figure 6- 8: Overview of the Flax fibres; (a) Flax fibres before grinding, (b) SEM analysis, and (c) Flax fibres after grinding

It was interesting to find that the flax fibres seem shorter after grinding and appeared degraded during the shredding process. An enlarged view of the shredded flax fibres is given in Figure 6- 9 and cracks on the rough surface can be clearly observed on the outer periphery.

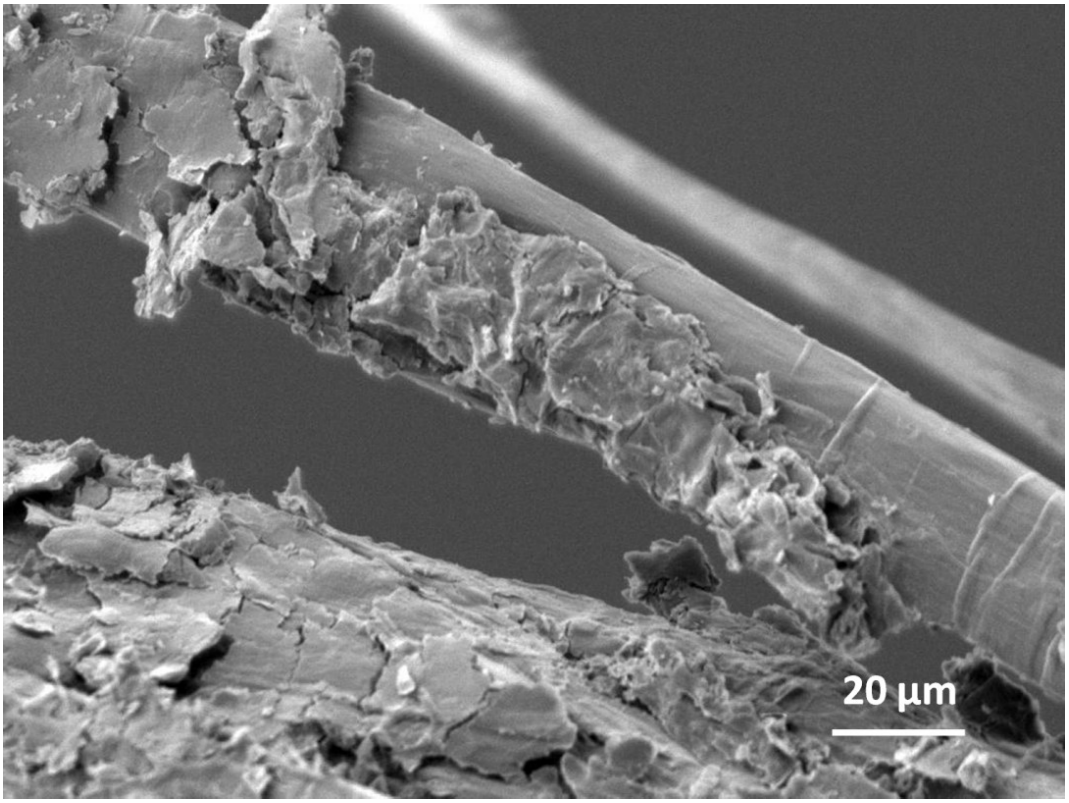

Figure 6- 9: Electronically scanned microscopic view of the shredded flax fibres

Figure 6- 10 shows the SEM images of the fractured surface for PLA /flax composites. The microscopy of fractured surfaces after tensile testing revealed a good distribution of the flax fibres the matrix. It can be seen in the images that the surface morphology of the composites shows a very rough topography, with voids where the fibres have been pulled out. It is evident that the average length of the pulled-out fibres is not greater than 20 µm which indicates the weak points on the composite surface. The pulled out fibres can be seen from the micrographs to be in higher frequency compared to fibres that were broken. This shows poor adhesion between the PLA matrix and flax fibres. Wong et al.[130] have investigated the morphology of PLA/flax composites and similar observations were reported. Generally these micrographs confirm the brittle nature of the failure in the tensile test and there is evidence of pull out flax fibres on the surface.

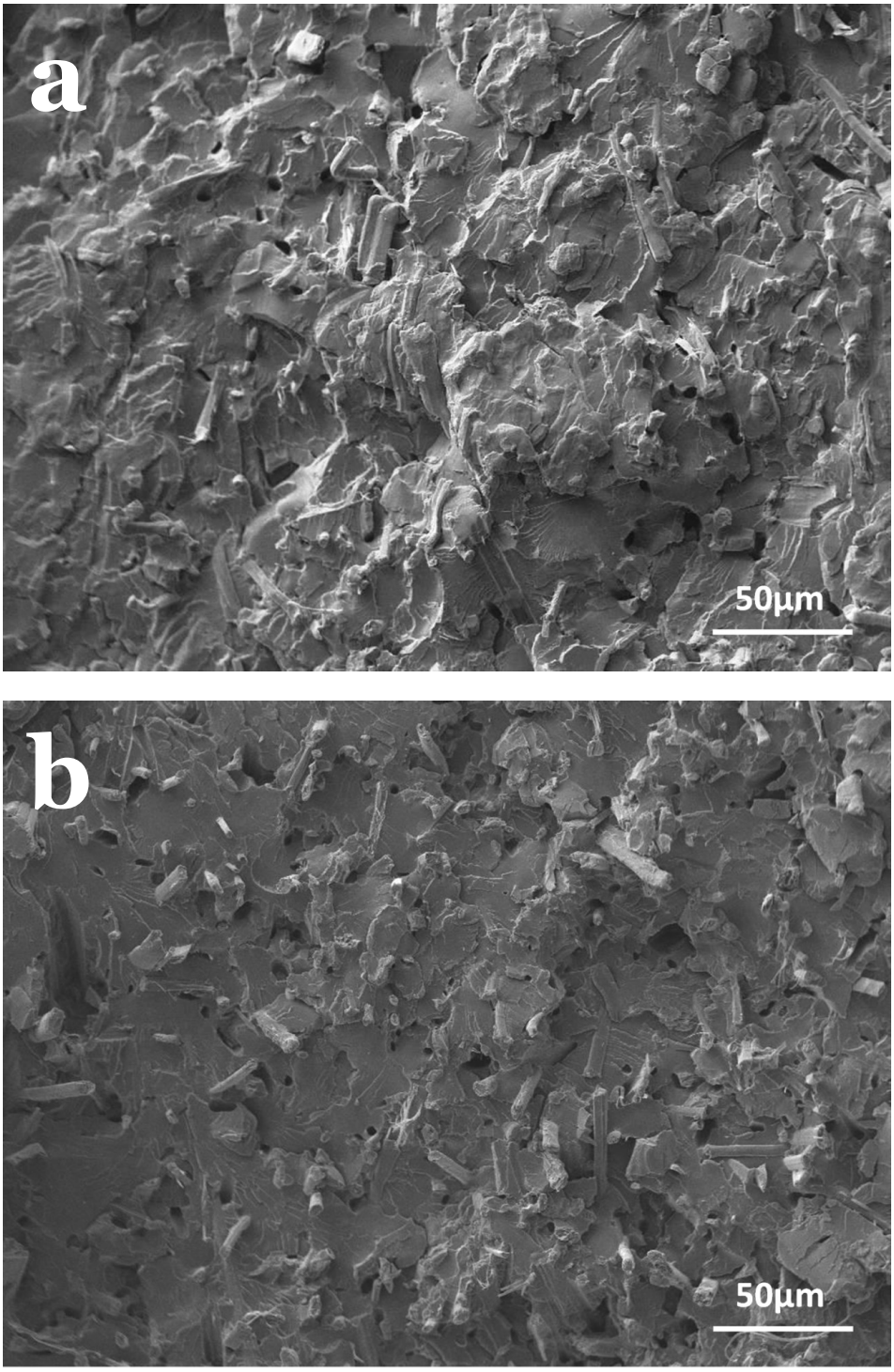

Figure 6- 10: overview of fracture surface of PLA and Flax composites with a mass proportion: (a) 90 /10, (b) 70/30

Figure 6- 11 shows the SEM images of the composite fracture surface of PLA/flax composites toughened with ENR when annealed. The ENR and flax fibres are not well distributed in the PLA matrix and the presence of long fibres pulled –out can be clearly observed from the micrographs, which shows poor adhesion between the flax,

fibres and the matrix. It is also notable to see the ENR particles seem broken on the composite surface as shown in the Figure 6- 11 (b). Two different phases can be seen clearly on the surface, suggesting that the fracture cracks ran along the interface between the PLA matrix and the ENR particle due to poor mechanical adhesion.

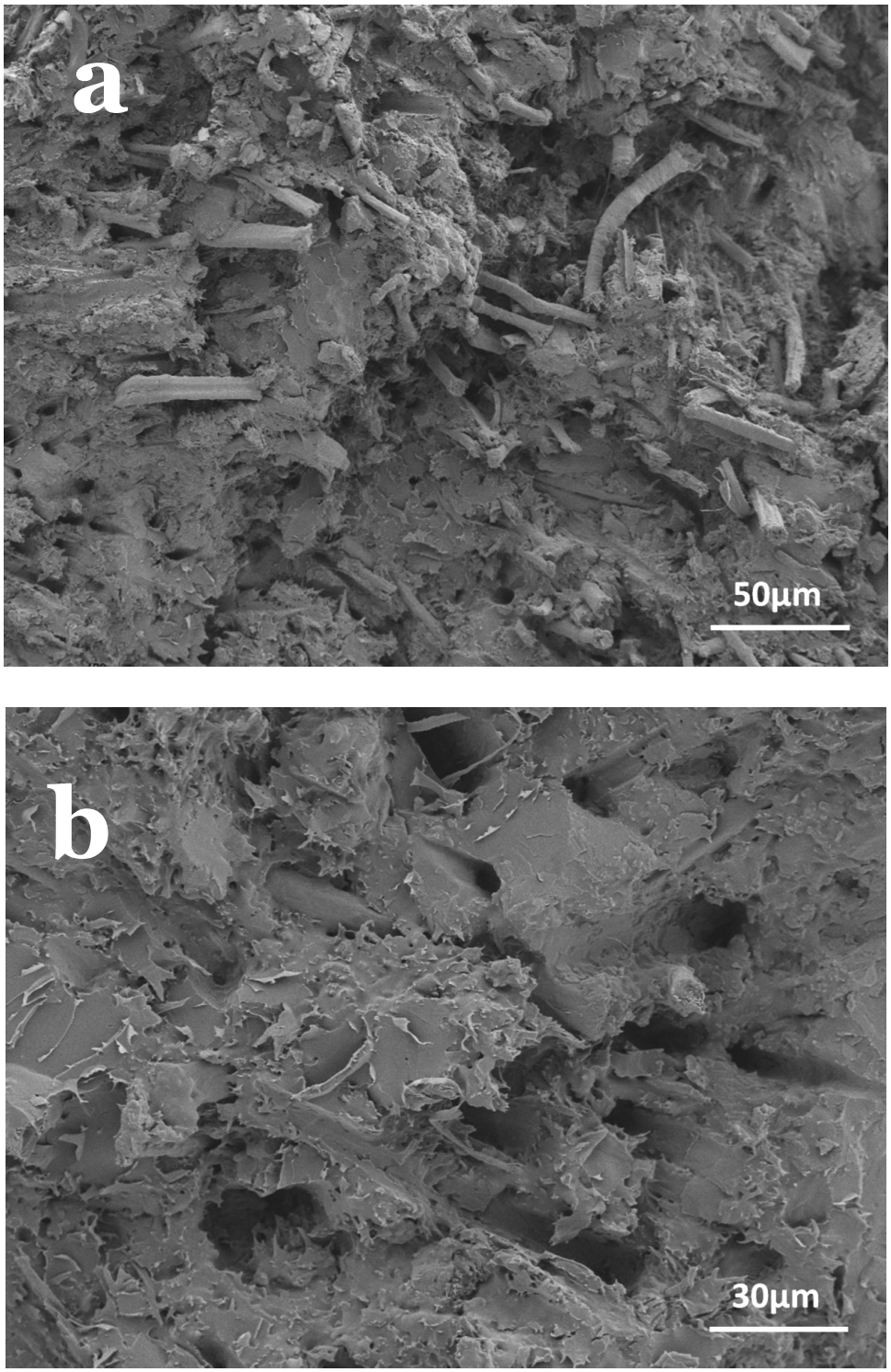

Figure 6- 11: Overview of tensile fracture surface of PLA/Flax/ENR blends with a mass proportion: 60/20/20

SEM micrographs of the fractured surfaces of the PLA composites produced from a masterbatch of flax and ENR are shown in Figure 6- 12. The fractured surface morphology suggests uniform distribution of flax-ENR masterbatch in the PLA matrix. The effect of the masterbatch can be analyzed from these micrographs which clearly signify the dominance of ENR and seems to be strongly bonded with the PLA matrix compared to flax fibres previously described. The flax fibre is covered with layers of ENR and there is no visible phase separation on the surface.

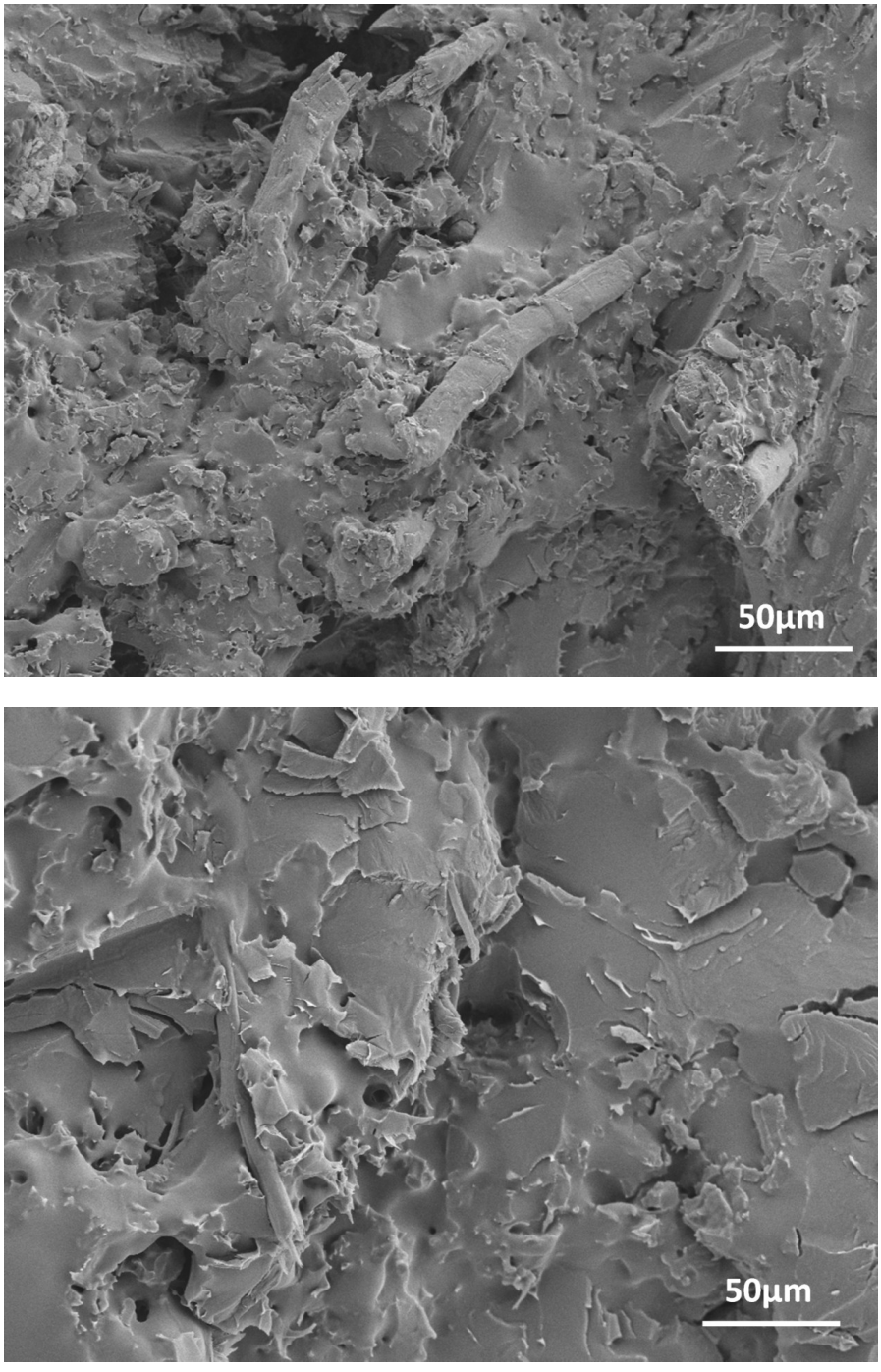

Figure 6- 12: Overview of tensile fracture surface of annealed PLA /masterbatch composites.

6.3 Thermo-mechanical Properties

6.3.1 PLA - Flax

Figure 6- 13 shows the dynamic modulus curves of the non-annealed PLA and PLA/flax composites as a function of temperature. It can be seen from the figure that the modulus of the PLA composites is increased with the incorporation of the flax fibres. This effect is much greater in the rubbery plateau region. The Tg seems to be shifted towards higher temperature only for 30 (wt %) of flax fibre contents. At the temperatures above the rubbery plateau, the modulus curves are decreasing and start increasing again as the temperature increases which results from the crystallization of the PLA.

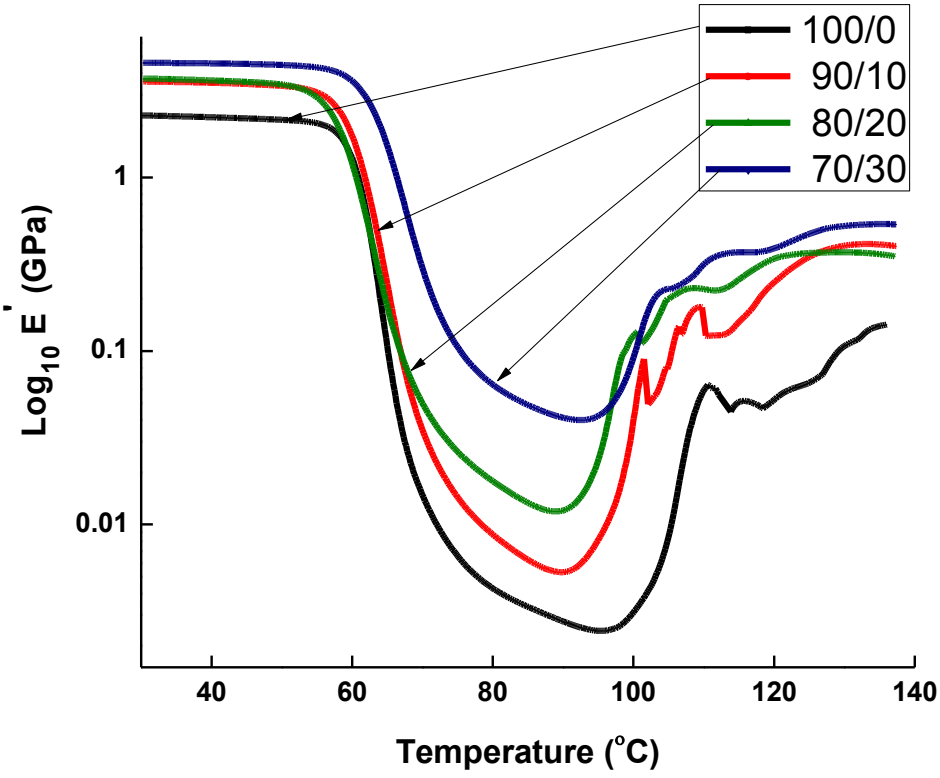

Figure 6- 13: Storage Modulus of PLA and PLA/ flax composites as a function of temperature (quenched)

The values of the storage modulus in flexural mode for PLA and PLA/flax composites at 30°C and 40°C are given in Table 6- 6. It can be seen from the table that measured values increase from 2.3 (GPa) for PLA up to 3.6, 3.7 and 4.6 (GPa) on the addition of

10, 20 and 30 (wt %) flax respectively, bringing a significant improvement in the flexural modulus. Improvement in the modulus with the incorporation of flax into PLA can also be taken as indirect verification of increase in Young's modulus found in tensile testing.

Table 6- 6: Thermo-mechanical Properties of quenched PLA and PLA /flax Composites

Sample codes	Glass Transition Tg (^oC)	Storage Modulus (Flexure) @ 30^oC (GPa)	Storage Modulus (Flexure) @ 40^oC (GPa)
100/0	66	2.3	2.2
90/10	68	3.6	3.5
80/20	68	3.7	3.6
70/30	69	4.6	4.5

Figure 6- 14 shows the tan δ curves as a function of temperature for PLA and PLA/flax composites. It is interesting to note that the position of the tan δ peak does change slightly towards higher temperature with the incorporation of the flax, which indicates the improvement in glass transition temperature of the composites. The area under the curve also decreased when the content of flax fibres increased.

The peak of tan δ and value of storage modulus at 30 (^oC) as a function of the content of flax are shown in Figure 6- 15. It is clear from Figure 6- 15 (a & b) that the peak of tan δ decreased and the storage modulus increased significantly with the addition of flax fibres. The decrease in peak of tan δ and area under the curve indicates the drop in damping ability of the PLA-flax composites when compared to pure PLA. It also shows that the brittleness of the composites increased with addition of the flax fibres which was also indentified in tensile testing of the samples.

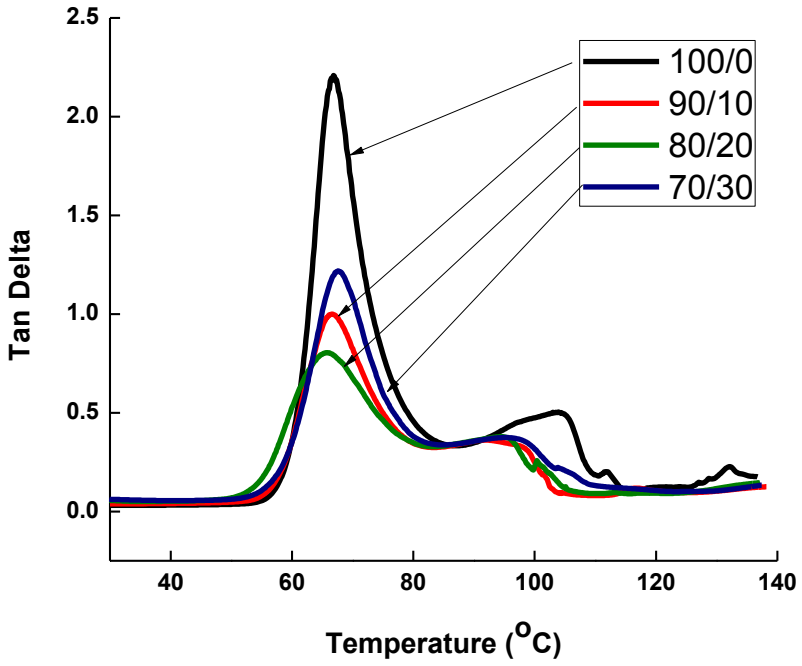

Figure 6- 14: Tan delta for PLA /Flax composites as a function of temperature

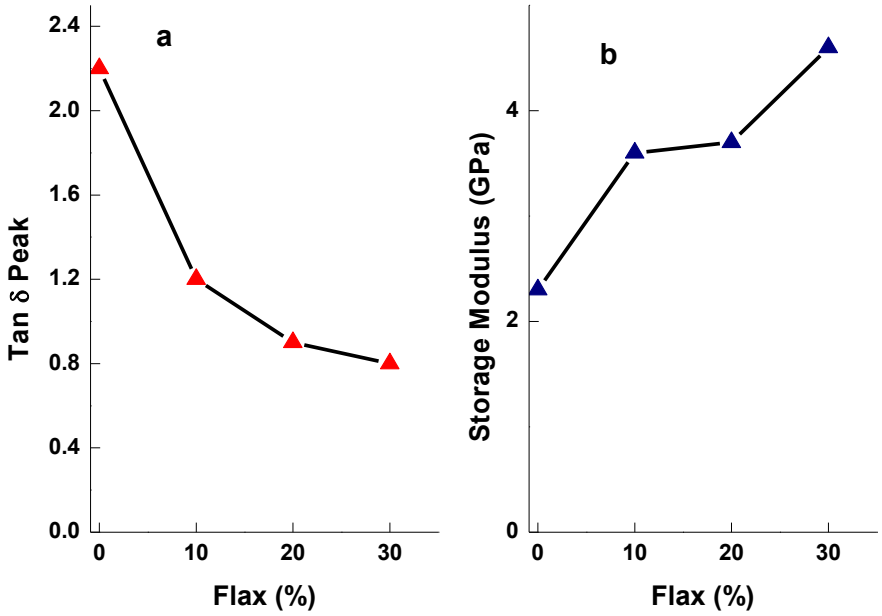

Figure 6- 15: (a) Tan δ Peak vs. contents of Flax, (b) Storage modulus vs. contents of Flax @ 30(°C) for non- annealed samples

6.3.2 PLA - Flax – ENR

Figure 6- 16 shows the temperature dependent variations of the storage modulus (**E´**) recorded for pure PLA and its composites when annealed at 120 (°C). As observed in the DSC analysis, PLA is normally amorphous but can be semi crystalline at specific temperatures as the crystallization occurs around 100 - 120 (°C). Therefore it can be seen from the curves of dynamic modulus that the thermal properties of PLA increased with the incorporation of flax and ENR when subjected to heat treatment. It is clear from the figure that the values of **E´** for PLA and PLA/flax composites drop slightly in the rubbery zone and level off, thus giving improvement in the heat distortion temperature (HDT) of the composites when compared to non-crystallized samples in Figure 6- 13.

Composites of PLA, flax and ENR start softening above Tg around 60 (°C) but the modulus starts to increase again around 80 (°C) because the PLA is crystallising. This increase in storage modulus indicates the crystallized contents in the blends compare to non-annealed PLA, flax and ENR composites. The rise in the modulus indicates improvement in heat distortion temperature (HDT) of the blends compared to pure PLA.

Comparative analysis of the storage modulus for PLA and different blends after annealing is summarized in Table 6- 7 below. The table lists the glass transition temperature calculated from the peak of tan δ and values of storage modulus at different temperatures. It is evident from the table that when 20 (wt %) flax is incorporated, the storage modulus increased distinctly from 2.6 to 2.7 (GPa) at 30 (°C) when the contents of flax increased from 0 to 20 (wt %). With the inclusion of ENR and flax blends into the PLA, there is a decrease in the storage modulus. It is observed that storage modulus decreased from 2.6 to 1.6, 1.1 and 1.5 (GPa) for PLA/flax/ENR, PLA/MB1 and PLA/MB2 blends respectively when compared to pure PLA.

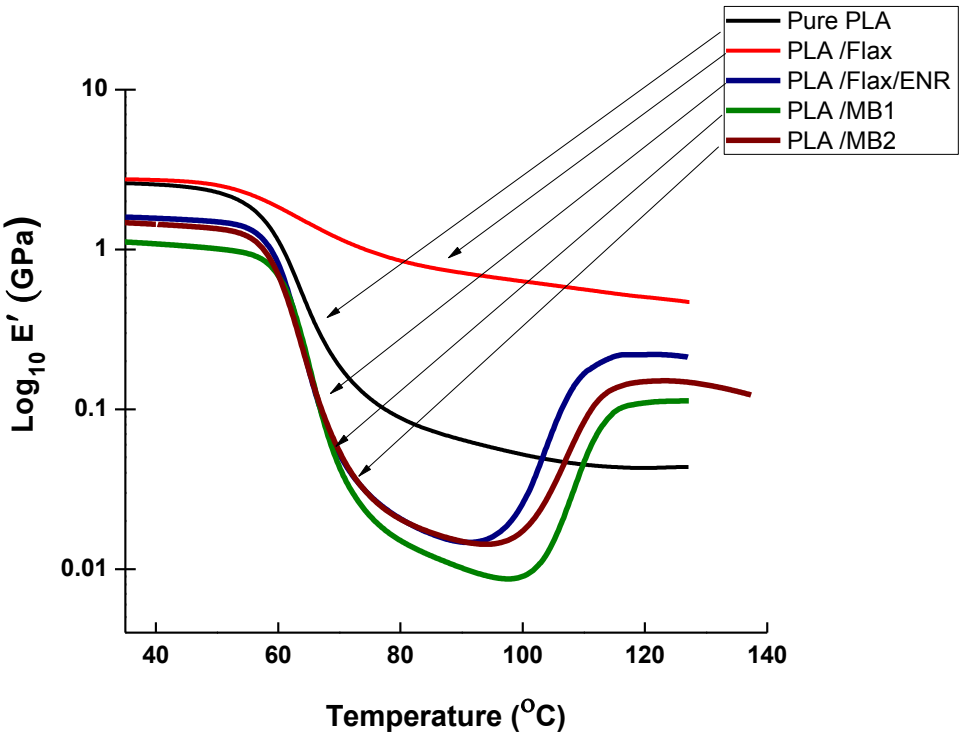

Figure 6- 16: Dependence of storage Modulus versus temperature for pure PLA and PLA/flax/ENR blends

Table 6- 7: Thermo-mechanical Properties of pure PLA and PLA /flax /ENR blends Composites (annealed Samples)

Sample description (annealed) (wt%)	Glass Transition Tg (°C)	Storage Modulus @ 30°C (GPa)	Storage Modulus @ 40°C (GPa)
PLA (100/0)	66	2.6	2.5
PLA/Flax (80/20)	66	2.7	2.6
PLA /Flax/ENR (60/20/20)	66	1.6	1.5
PLA /MB1 (60/40)~(60/20/20)	67	1.1	1.0
PLA /MB2 (70/30)~(60/20/10)	66	1.5	1.4

In Figure 6- 17 the tan delta curves are shown for different crystallized samples. These curves show that there is no significant change in the position of the tan delta. It is evident from the figure that tan delta peak for crystallized PLA/flax composites is broadened and lower compared to crystallized PLA, but the area under the curve is reduced which indicates lowering the damping capability of the composites. It is observed that the incorporation of the flax and ENR into the PLA, the area of

integration under the *Tan δ* curve increased. The incorporation of masterbatch of flax and ENR into the PLA increased the area of integration under the *Tan δ* curves further.

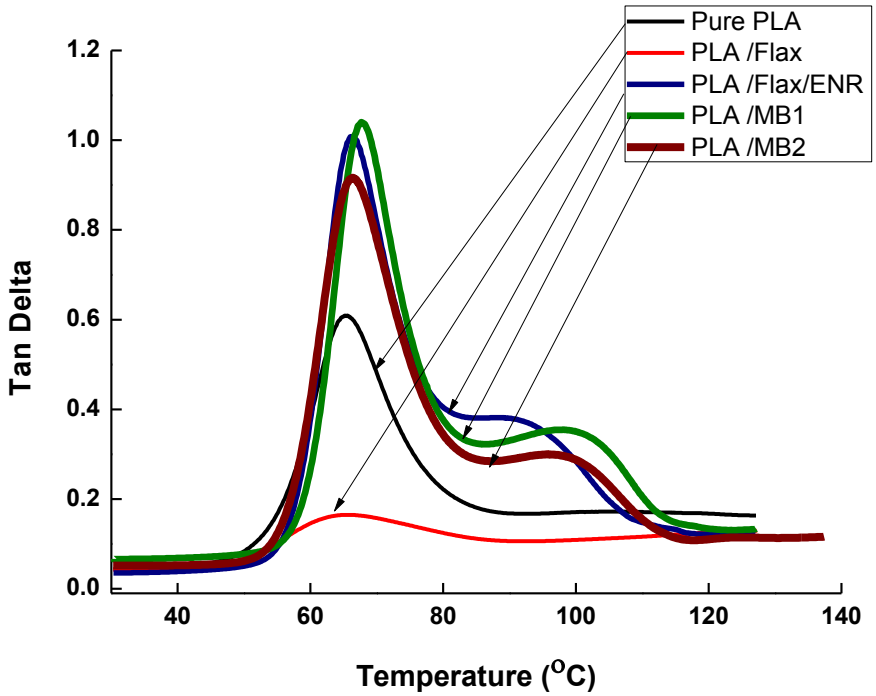

Figure 6- 17: Tan delta for annealed PLA and PLA /flax/ ENR composites as a function of temperature

Figure 6- 18 (a & b) shows the peak of tan delta and values of storage modulus at 30(°C) for different annealed samples. From Figure 6- 18 (a) it is clear that the peak of tan delta is decreased initially with the incorporation of flax but when flax and ENR are incorporated into PLA, the peak of Tan delta increased considerably. On the other hand the value of modulus increased initially with flax but with the addition of ENR the modulus decreased significantly. This shows the damping capability in the composites is improved with the hybrid reinforcement. This is attributed to the incorporation of flax and ENR that affects the mobility of the polymer chains when compared to non-crystallised samples. These observations also underline the analysis of tensile testing for crystallised samples.

The dissimilarity observed in quantitative measurements of storage and Young's modulus for the same samples is due to the nature of the test primarily, and to the difference in deformation rate between tensile and dynamic test. Therefore, findings observed during dynamic analysis for all the systems reinforce the tensile observations and can supplement the thermal characterization of different composite systems.

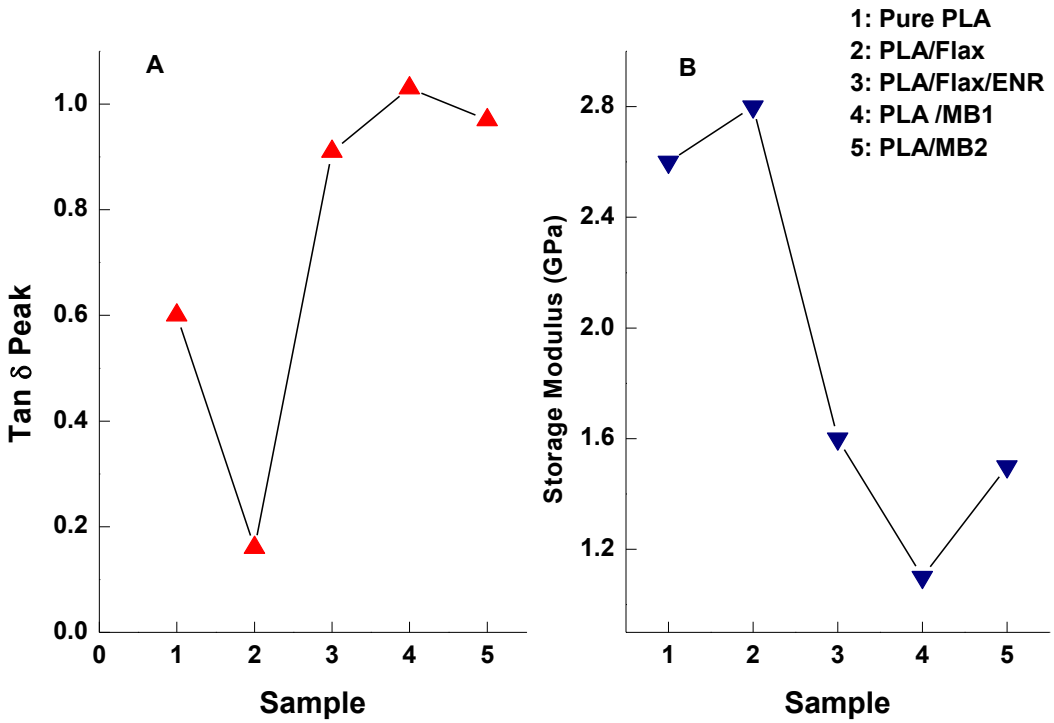

Figure 6- 18: (a) Tan δ Peak for different annealed samples
(b) Storage Modulus for different annealed @ 30°C for annealed samples

6.4 Conclusions

According to the results obtained from the experiments, the following conclusions can be drawn:

6.4.1 PLA/Flax

From the DSC results there was found to be no significant change in thermal properties on adding increasing amounts of flax fibres to PLA. The Young's modulus

of the PLA composites increased significantly from 4.1 to 8.1 (GPa) when the content of flax increased from 0 to 30 (wt %). The tensile strength and elongation to break reduced as the content of flax increased and the composites exhibit brittle failure. The storage modulus also increased from 2.2 to 4.6 (GPa) when the content of flax increased from 0 to 30 (wt %) with a reduction in the area under the tan delta curve.

6.4.2 PLA/Flax/ENR

DSC results show that the thermal properties remained unchanged, but significant improvement is observed in overall crystallinity of the composites for the annealed samples when compared to un-annealed. The Young's modulus decreased with the addition of ENR and the elongation to break improved from 2 to 13 (%) when the content of flax and ENR50 masterbatch increased from 0 to 40 (wt %), exhibiting a ductile failure when compared to pure PLA. Storage modulus decreased and area under the tan delta increased when the loading of ENR increased from 0 to 20 (wt %), thus increasing the damping ability of the composites. This confirmed that the ENR/flax masterbatch improved the toughness of PLA.

Chapter 7 PLA - Talc Composites

PLA -talc composites are investigated in this chapter. The aim of the study is to examine how talc influences the crystallisation of PLA, investigating the dispersion of the talc in the PLA matrix and to model the effect of talc on the mechanical properties i.e. tensile modulus (Young's modulus) of the composites.

Two different grades of talc were incorporated into PLA to see the effect of particle size on the composite properties. Talc 1 has a median particle size less than one micron (0.9 μm) and Talc 2 has median particle size of 2.2 microns (μm). In the first phase of the project, PLA /Talc composites were prepared with the following weight % of talc; 0, 10, 20, 30. The talc was melt compounded and processed with PLA at the given addition level. The morphology, thermal properties and mechanical properties of these blends have been investigated.

7.1 Thermal Properties

The DSC profiles are shown in figures 7.1 - 7.2 for PLA /Talc1, while figures 7.3- 7.4 show the thermal properties for PLA /Talc2 composites. The heating scans for PLA / Talc 1 (Figure 7- 1) show the glass transition temperature and the exothermic and endothermic peaks derived from cold crystallization of the amorphous phase and the melting peak respectively. The second heating scans of the various composites are given in Figure 7- 1.

It can be seen from the figure that the melting temperature (T_m) of the pure PLA is about 155°C, as indicated by the single peak in Figure 7- 1. In the presence of the talc filler, the melting of the crystalline phase is characterized by a double peak, which becomes more pronounced with a higher concentration of talc. The double peak denotes two different crystalline or spherulitic forms. The second peak is around 150°C signifying a less thermally stable phase

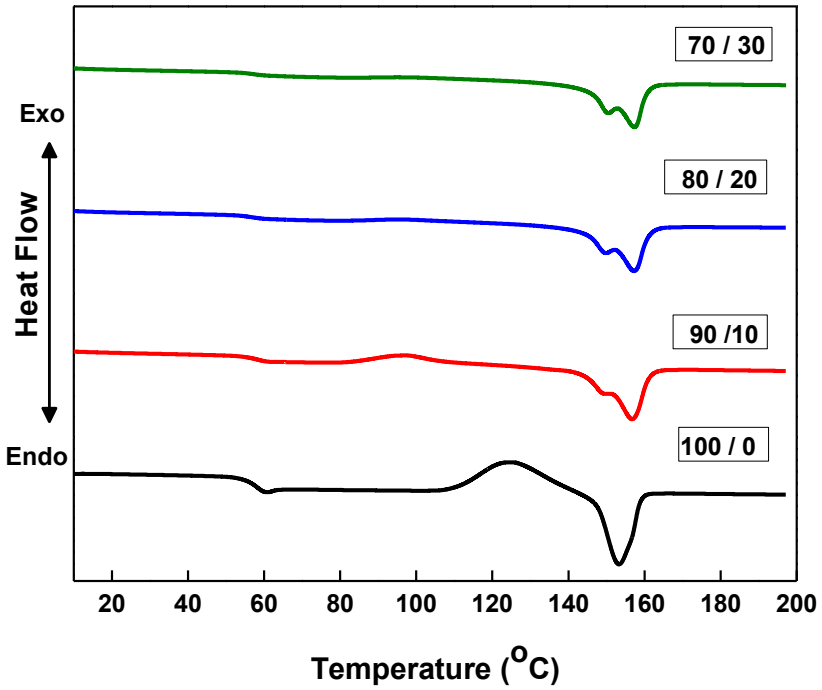

Figure 7- 1: DSC Heating Scans of PLA / Talc 1 Composites

Other workers have also reported a double peak in the melting endotherm of PLA for both pure PLA [131] and PLA composites [84]. Nofer et al. [132] also studied the crystallization kinetics of linear and long-chain-branched polylactide and reported double peaks in the melting endotherm of polylactides. They also investigated the melting behaviour of polylactide with a double peak. They suggested that the peak that appears at low- temperature can be related to the endothermic reaction of metastable or deficient crystals formed at the start of the cold crystallization process, while the melting peak that appears at higher temperature is related to the perfect crystal structure formed at the later stages of cold crystallization.

One of the other possible explanations for the double peak melting endotherm is that two different crystals or spherulites form because in the presence of talc the PLA has increased tendency to crystallize. In the case of two different spherulite forms, one may be formed during composite preparation and the second might be formed during sample preparation, because both times the PLA composite is processed above its melting point.

Data from the heating scans for PLA /Talc 1 composites are summarized in Table 7- 1. It can be seen that there is a slight increase in the glass transition temperature (Tg) of the PLA from 54 °C to 57 °C on the addition of the talc filler, presumably due to a constraint on free volume of the polymer by the introduction of a platy filler. The cold crystallization temperature (T_c) is reduced from 127°C for the pure PLA to 96°C for the PLA/talc composites indicating a nucleating effect by the talc filler. However, the extent of cold crystallization is greatly reduced – from 22% for pure PLA to 5.6% for the 90/10 composite and then down to 0.7 (%) and 0 (%) for the 80/20 and 70/30 composites respectively.

Also included in the table, data on the (%) crystallinity is calculated using equation 4-2 described in chapter 4 earlier. It is seen that the pure PLA is essentially amorphous with a crystallinity of only 2 (%), whereas addition of 10 (wt %) of talc increases the crystallinity from 2 to 25 (%). The addition of 30 (wt %) talc gives only a slight further increase in crystallinity up to 27 (%). It is clear from these data that talc acts as a nucleating agent for the crystallization of PLA.

Table 7- 1: Glass Transition, Crystallization and Melting temperatures of PLA / Talc 1 Composites

Sample codes	Tg (°C)	Tcc (°C)	Tm (°C)		Cold Crystallization (%)	Crystallinity (%)
			α	β		
100/0	54 ± 0.7	127 ± 1.4	155 ± 1.5	----	22 ± 1.2	2 ± 0.8
90/10	58 ± 1.0	96 ± 1.0	156 ± 0.5	149 ± 0.1	7.0 ± 0.6	25 ± 0.5
80/20	57 ± 0.5	95 ± 0.4	157 ± 0.5	155 ± 0.5	0.7 ± 0.1	25 ± 0.9
70/30	57 ± 0.4	----	157 ± 0.2	150 ± 0.3	-----	27 ± 0.1

Further evidence is provided by the DSC cooling scans shown in Figure 7- 2. Here it can be seen that pure PLA is amorphous, with no crystallisation peak, whereas addition of talc gives rise to an exothermic crystallisation peak in the cooling scan. Increasing the talc content gives rise to a more pronounced crystallisation exotherm.

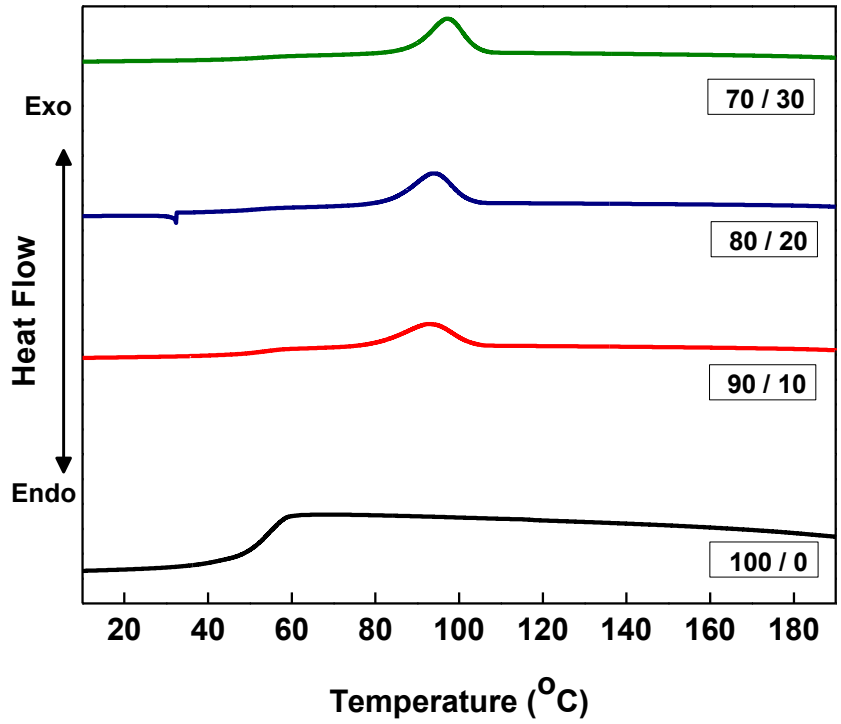

Figure 7- 2: DSC Cooling Scans of PLA / Talc 1 Composites

It is well known that talc acts as a nucleating agent when added to isotactic polypropylene homopolymer or copolymer[106], where it has been shown to increase the crystallization temperature and nucleation density and reduce the spherulite size. Harris and Lee [111] have also reported that talc can act as a nucleating agent to control the crystallinity of PLA and hence improve mechanical properties. The reason for the specific role of talc (as opposed to other inorganic fillers) in promoting spherulite nucleation of polypropylene has been attributed [103] to matching of the (001) talc plane with a specific crystallographic direction in the isotactic polypropylene and it is proposed that hexagonal rings on the talc surface form hydrogen bonds with methyl groupings in the PP. In a similar way, it is likely that crystallographic matching would account for the role of talc in promoting crystallinity in PLA.

The second heating scans of the DSC profiles for PLA /Talc2 composites are shown in Figure 7- 3. The figure shows the glass transition temperature, and the exothermic

and endothermic peaks derived from cold crystallization of the amorphous phase and the melting peak respectively. The thermal behaviour of the PLA /Talc2 composites indicates the same effect as the PLA/Talc1 composites, thus confirming the thermal analysis results described earlier. The analysis of the PLA /Talc2 composites is summarized in Table 7-2.

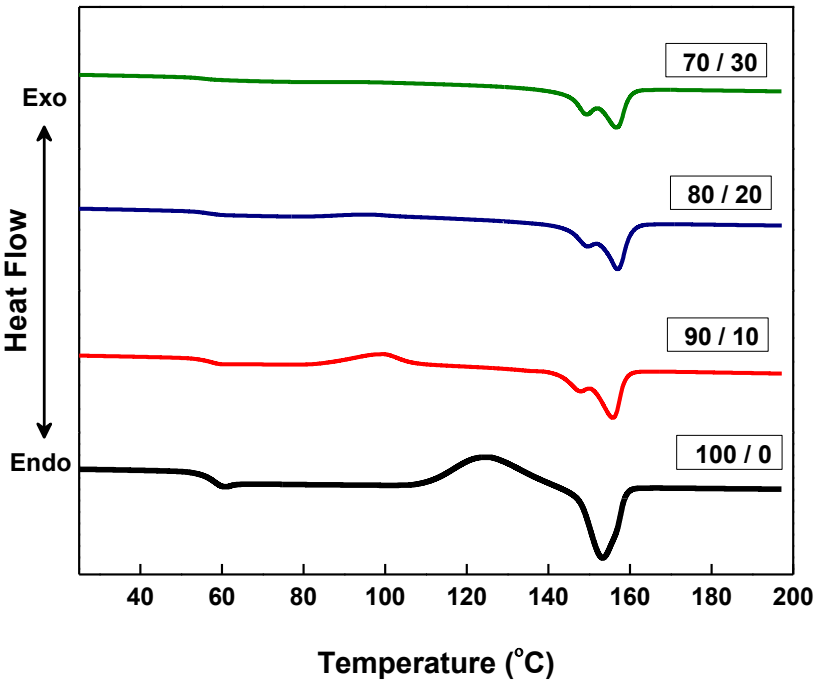

Figure 7- 3: DSC Heating Scans of PLA / Talc 2 Composites

Table 7-2: Glass Transition, Crystallization and Melting temperatures of PLA/Talc2 Composites

Sample codes	Tg (°C)	Tcc (°C)	Tm (°C)		Cold Crystallization (%)	Crystallinity (%)
			α	β		
100 /0	54 ± 0.7	127 ± 1.4	155 ± 1.5	----	22 ± 1.2	2 ± 0.8
90 / 10	57 ± 1.0	98 ± 1.0	157 ± 0.5	148 ± 0.5	8.3 ± 18	17 ± 0.2
80 / 20	56 ± 0.4	94 ± 0.5	156 ± 0.0	150 ± 0.0	1.24 ± 0.5	24 ± 0.9
70 / 30	56 ± 0.5	----	156 ± 0.5	149 ± 0.5	----	28 ± 0.4

It can be seen that talc 2 also nucleates the essentially amorphous pure PLA. Inclusion of 10 (wt %) of talc increases the crystallinity to 17 (%). Further

incorporation of 30 (wt %) talc gives a significant further increase in crystallinity up to 28 (%). There is no significant difference observed in the increase of crystallinity of the PLA when the two different grades of talc are incorporated. Further evidence of crystallization can be seen in the cooling scans of DSC profiles for PLA /Talc 2 composites, shown in Figure 7- 4. In comparison to pure PLA which has no exothermic peak, the PLA/Talc composites have an evident exothermic peak in the cooling scans.

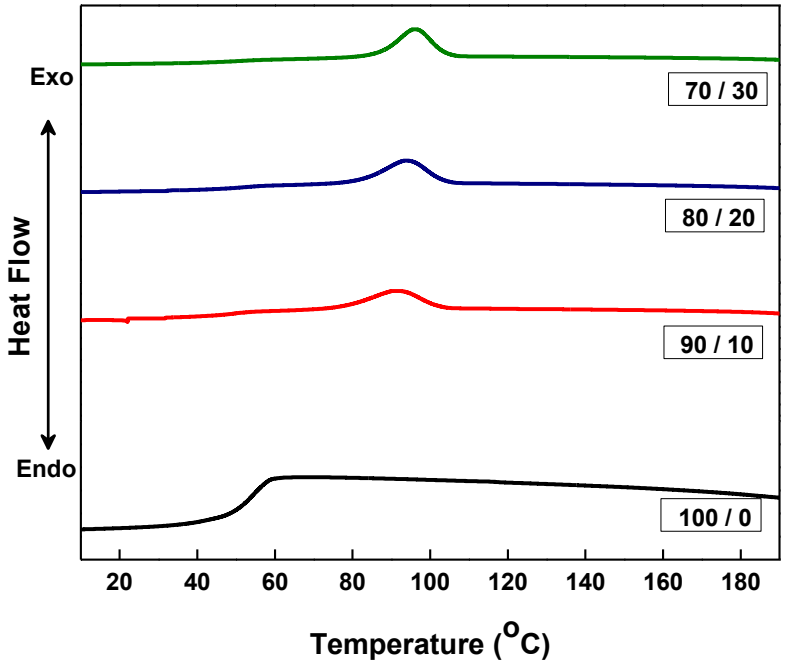

Figure 7- 4: DSC Cooling Scans of PLA / Talc 1 Composites

7.2 Mechanical Properties

The effect of particle loading on mechanical properties and the summary of the tensile properties of PLA and PLA/ Talc composites are shown in Table 7- 3.

Table 7- 3: Tensile properties of PLA/talc composites

Sample codes	Tensile Strength (MPa)	Tensile Modulus (GPa)	Elongation to break (%)
100 / 0	43 ± 3.1	4.1 ± 0.6	4.1 ± 0.5
PLA – Talc 1			
90 / 10	38 ± 2.4	5.8 ± 0.5	3.0 ± 0.8
80 / 20	41 ± 2.6	7.0 ± 0.7	2.0 ± 0.3
70 / 30	44 ± 3.7	9.8 ± 0.8	2.0 ± 0.6
PLA – Talc 2			
90 / 10	35 ± 3.1	5.2 ± 0.5	3.0 ± 0.8
80 / 20	36 ± 2.8	7.4 ± 1. 2	3.2 ± 0.2
70 / 30	40 ± 1.7	9.2 ± 0.7	2.7 ± 0.6

It can be inferred from Table 7- 3, that incorporation of talc into PLA has no significant effect on the tensile strength of the composites. Tensile strength is reduced initially when Talc 1 is incorporated into PLA in low concentration but afterwards increased gradually when loading of the filler increased from 10 to 30 (wt%). The same kind of behaviour is also observed when Talc 2 is incorporated into PLA. Conclusively the talc has no significant effect on the tensile strength of the composites compared with neat PLA when the contents of the different grades of talc increased from 0 to 30 (wt %).

It can be analysed from the Table 7- 3 that all samples exhibited brittle failure. There is found to be a reduction in elongation to break of the samples from 4 % for pure PLA to 2.0% for PLA/talc composites. A reduction in elongation to break implies that the composites have become more brittle with the talc addition. Other workers have also reported a drop in % elongation when talc is added to PLA based composites [84]. The most likely reason for the drop is that the addition of platy filler to a brittle polymer is causing stress concentration and crack initiation and therefore reducing toughness.

The effect of particle loading on Young's modulus as a function of volume fraction is given in Figure 7- 5 for PLA and PLA / Talc composites. It can be seen from the figure that the tensile modulus of the PLA is greatly influenced by the addition of talc. The tensile modulus of neat PLA obtained from the tensile testing machine is 4.1 ± 0.6 (GPa). The modulus of the composites is increased from 4.1 to 9.8 (GPa) when the content of Talc 1 increased from 0 to 30 (wt %), and significant improvement in Young's modulus of the composites was recorded compared to neat PLA. It was also observed that when Talc 2 is incorporated into neat PLA at the same addition level, the Young's modulus increased from 4.1 to 9.2 (GPa), also bringing considerable improvement to the modulus of the composites and a linear increase relative to the content of the talc.

It is suggested that the improvement in tensile modulus, bringing a stiffening effect into the PLA-Talc composites, is an indication of mechanical adhesion between the matrix and the filler. It is also noticeable that the structure of the talc is platy, therefore the reinforcing and stress transformation capability are dependent on the adhesion between the matrix and the filler. It can be seen from Figure that Talc1 having fine particle size (0.9 μm) seems to be dispersed effectively in the matrix and increased the modulus compared with Talc 2, having less fine structure.

Fowlks and Narayan [109] also found improvement in the modulus of PLA with the incorporation of talc. They have reported that the modulus is increased from 3.6 to 7.0 (GPa) when the content of talc increased from 0 to 40 (wt %) bringing about 48 (%) improvement. Whaling et al. [80] have also found the same behaviour when talc is incorporated into biopolymers. They improved the tensile modulus of neat Poly (3-hydroxybutyrate) (PHB) by 70 (%) when the talc content increased from 15 to 50 (wt %).

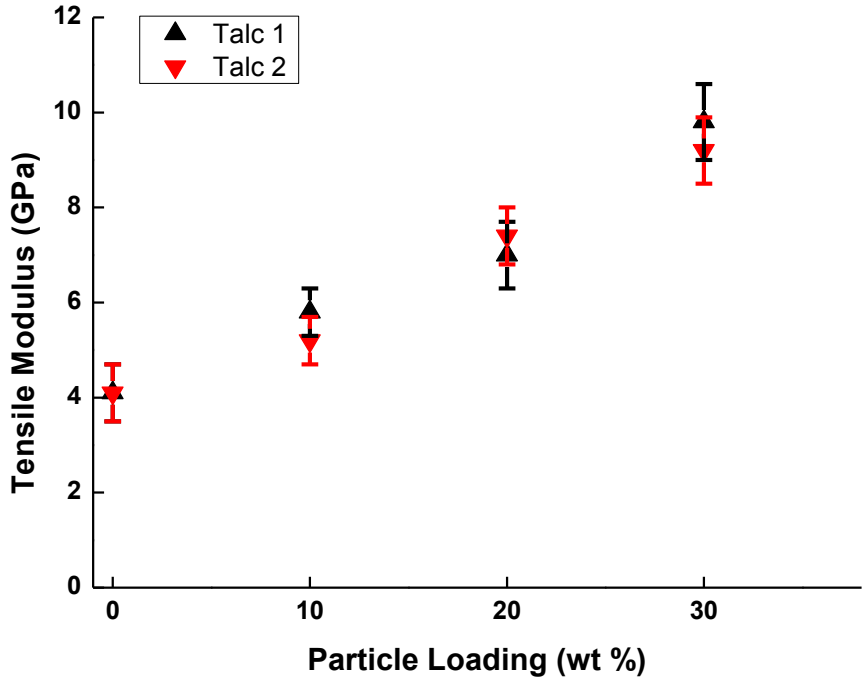

Figure 7- 5: Young's modulus of PLA/ Talc composites

7.3 Comparison between theoretical and experimental tensile properties

Different theoretical models can be applied to predict the reinforcing effect on Young's modulus of particulate composites. Due to the platy structure of the filler, the geometrical parameters of the filler will affect the properties of the composite. Of particular importance is the aspect ratio (L/D) of the filler, which is the ratio of length (L) to a thickness (D) of the filler particles. The Halpin-Tsai equation [133] takes into account the effect of filler geometry in predicting the modulus of the composite materials. The Halpin-Tsai equation is given in equation 7-1 below.

$$\frac{E_c}{E_m} = \frac{\left(1 + AB\phi_f\right)}{\left(1 - B\phi_f\right)} \text{ ---------- (7-1)}$$

Where, E_c is the Young's modulus of the composite, E_m is the Young's modulus of the matrix, E_f is the Young's modulus of the filler, φ_f is the volume fraction of the filler, A=2(L/D) and B=(R-1)/(R+A), where $R=E_f/E_m$. In calculating the predicted value of the Young's modulus of the various PLA/talc composites from the Halpin Tsai equation, the following values have been used: E_m is 4.1 (GPa) as measured, E_f is taken as 70 (GPa) which is the elastic modulus of other silicate fillers (such as glass), φ_f is calculated from the weight fraction using the values of the density of PLA of 1.24 (g/cm^3) and the density of talc as 2.8 (g/cm^3). The aspect ratio of the talc was measured from the TEM cross-sections shown in Figure 7- 6. The TEM morphology of the composites was analyzed using the imageJ® software.

ImageJ® is a Java based image processing and analysis tool which is used for editing, analyzing and modifying images, especially morphology based images like TEM or SEM micrographs. ImageJ® is also able to calculate angles and distances and creates density histograms and line profile plots. It supports the standard image processing functionalities such as contrast manipulation, sharpening, smoothing, edge detection and median filtering. It also has the ability to do geometric transformation like scaling and rotation.

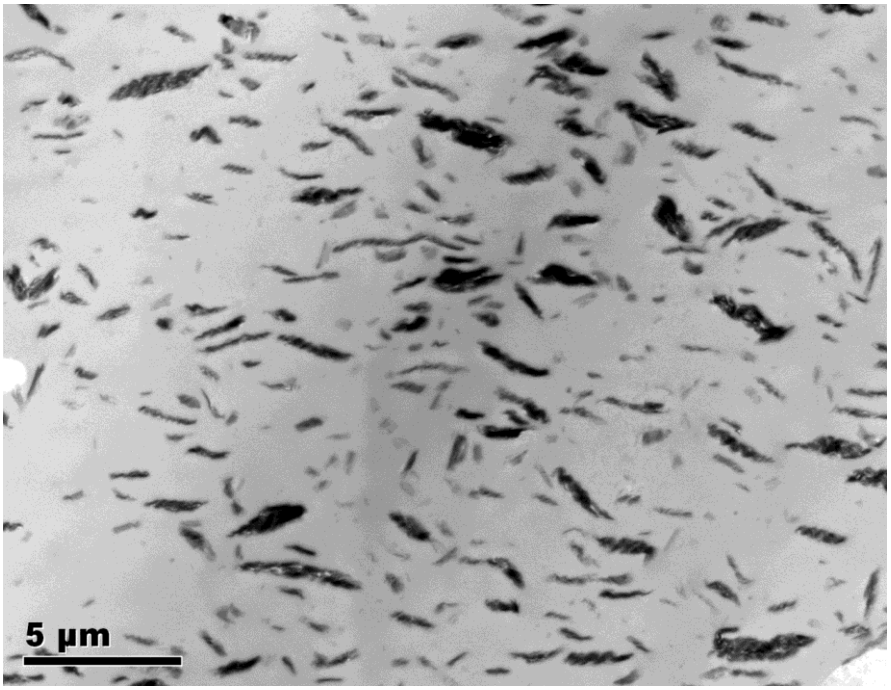

Figure 7- 6: TEM Micrographs of PLA / Talc Composites (90/10)

The percentile frequency of the talc particles as a function of aspect ratio is shown in Figure 7- 7.

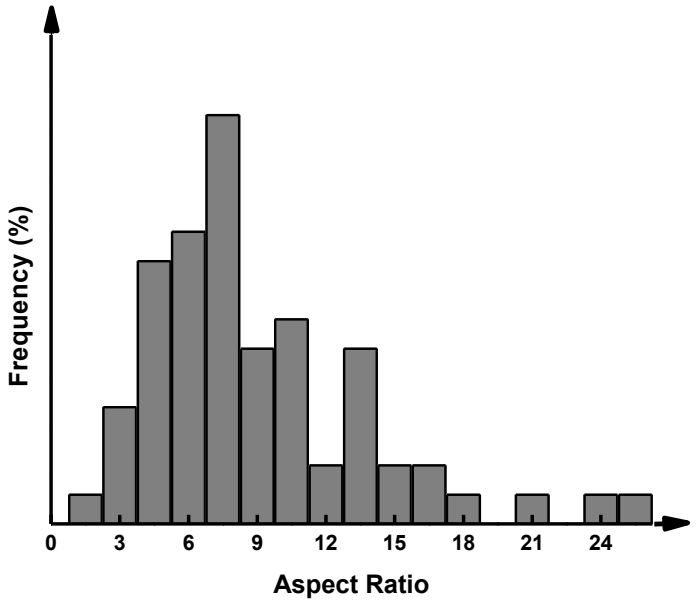

Figure 7- 7: Aspect ratio frequency of the talc particles

ROM tool of the ImageJ® was used to calculate the aspect ratio of each particle from TEM analysis. The scale was readjusted with the known distance according to the TEM image micro scale in the ImageJ®. Length and thickness of each particle were analysed and the median aspect ratio was calculated based on this analysis. The average aspect ratio was found to be 8, as shown in Figure 7- 7. There was no difference observed in the aspect ratio both the talc types.

Experimental measurements of the tensile modulus of the PLA/talc composites are plotted in Figure 7- 8 and Figure 7- 9. The figures show the superimposition of these data on the theoretical prediction of the Halpin Tsai model. There is seen to be a good fit between the Halpin Tsai prediction and the experimental data for PLA/Talc1 composites shown in Figure 7- 8. Figure 7-9 shows the comparison of the experimental response data with the theoretical response based on the Halpin-Tsai equation for PLA/talc2 composites. The correlation between the experimental and the theoretical responses was verified by the multiple coefficient of determination, R^2 [87, 88]. It can be seen that with the R^2 values of 0.96 and 0.94, that there is good

agreement between the experimental data and the prediction from Halpin –Tsai model.

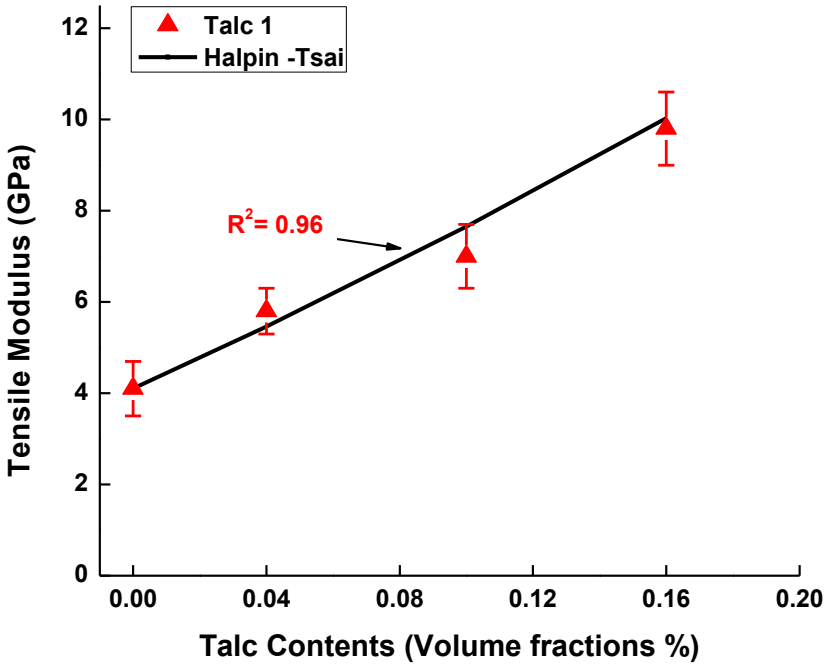

Figure 7- 8: Comparison of Experimental Data with the Haplin –Tsai Model

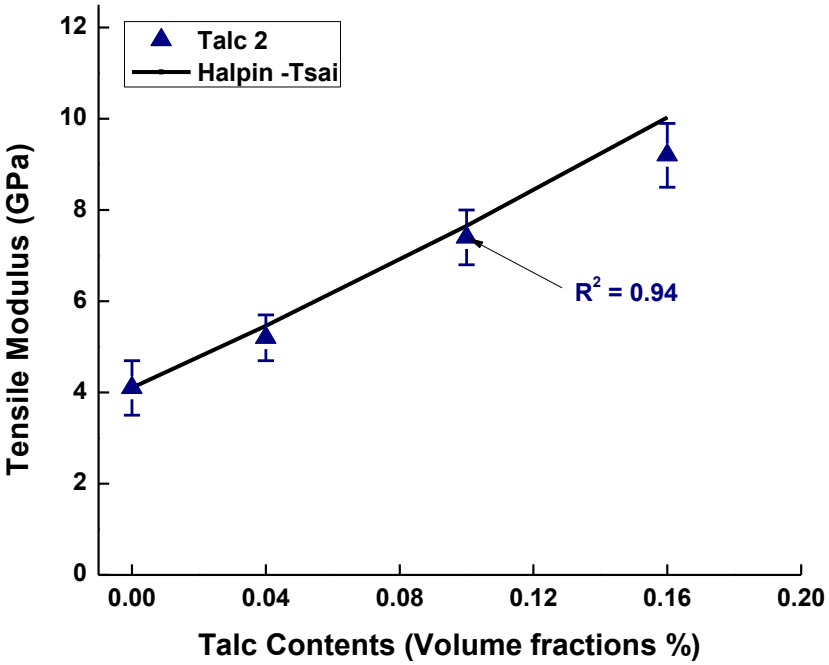

Figure 7- 9: Comparison of Experimental Data with the Haplin –Tsai Model

7.4 **Morphology of PLA/Talc Composites**

The morphology of the pure talc is shown in the scanning electron micrographs in Figure 7- 10 (a , b) & (c , d) for Talc 1 and Talc 2 respectively. It can be seen to have a plate-like shape, which dominates the morphology. The two types of talc have median diameters of 0.9 and 2.2 μm, both of which are in the category of ultra-fine talc.

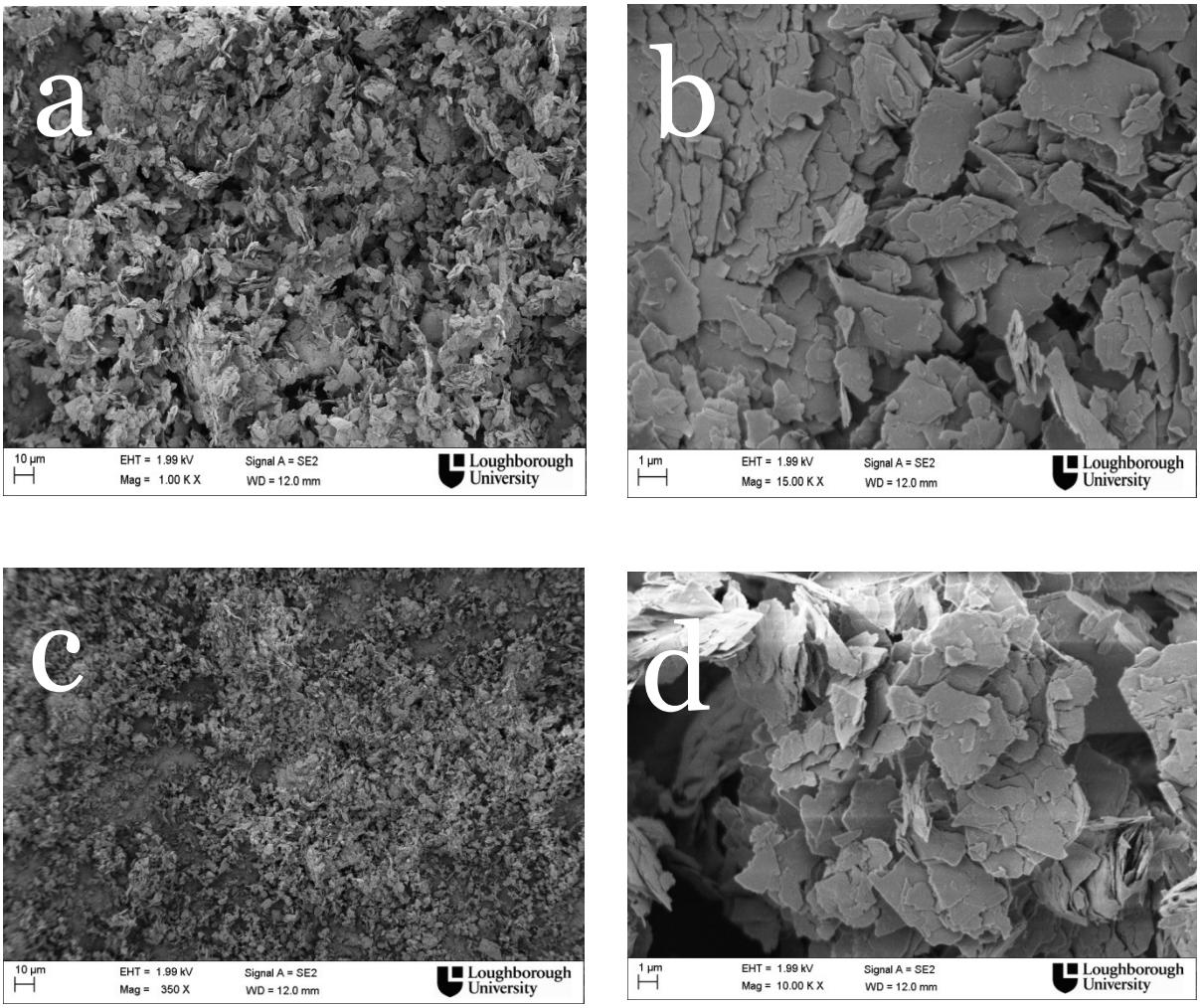

Figure 7- 10: SEM morphology of pure talc; Talc 1= (a), (b); Talc 2 = (c), (b)

The morphology and microstructure of composite materials play a significant role in prediction of the macroscopic properties. The PLA/talc microstructure was examined

using backscattered electrons to effectively observe the size, dispersion, and orientation of the talc particles in the PLA matrix. Figure 7- 11 shows backscattered electron images of the surfaces of the compression molded pure PLA and PLA/Talc1 composites containing 10 (wt %), 20 (wt %) and 30 (wt %) of talc respectively. The backscattered analysis is strongly dependent on the average atomic number of the samples. Because of the atomic number contrast in the backscattered electron image, it is possible to see the distribution of the talc particles in the PLA matrix. Talc, having a higher average atomic number than PLA, which is revealed as light particles in the micrographs.

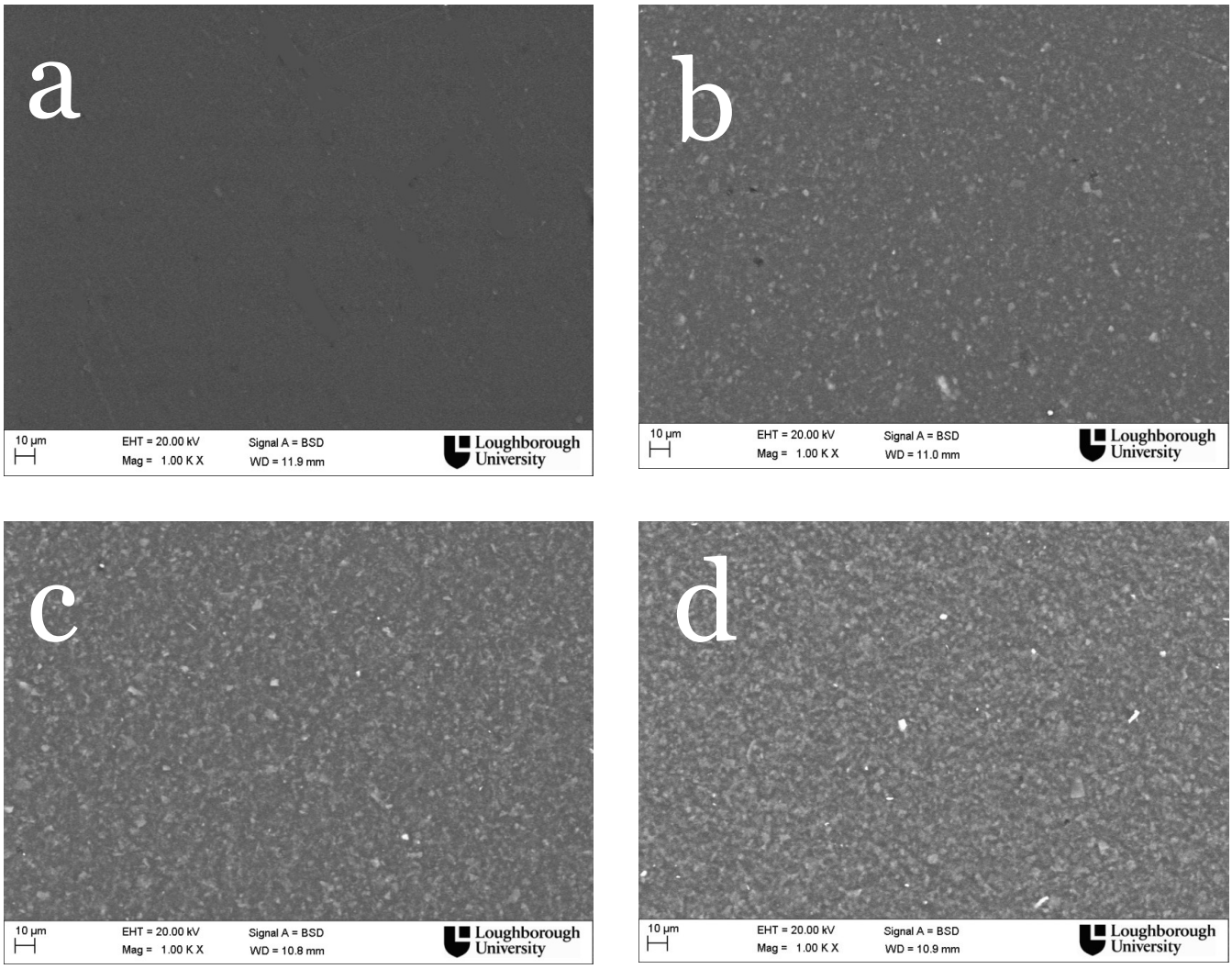

Figure 7- 11: Backscattered SEM micrograph of PLA / Talc 1 composite (a) Pure PLA, (b) 90/10 , (c) 80/20, (d) 70 /30

Backscattered SEM morphology for PLA/Talc 2 is shown in Figure 7- 12. It is assumed from these images that talc particles are distributed uniformly in the PLA matrix. The difference in the particle size of the talc is evident from these images compared to Figure 7- 11 given above.

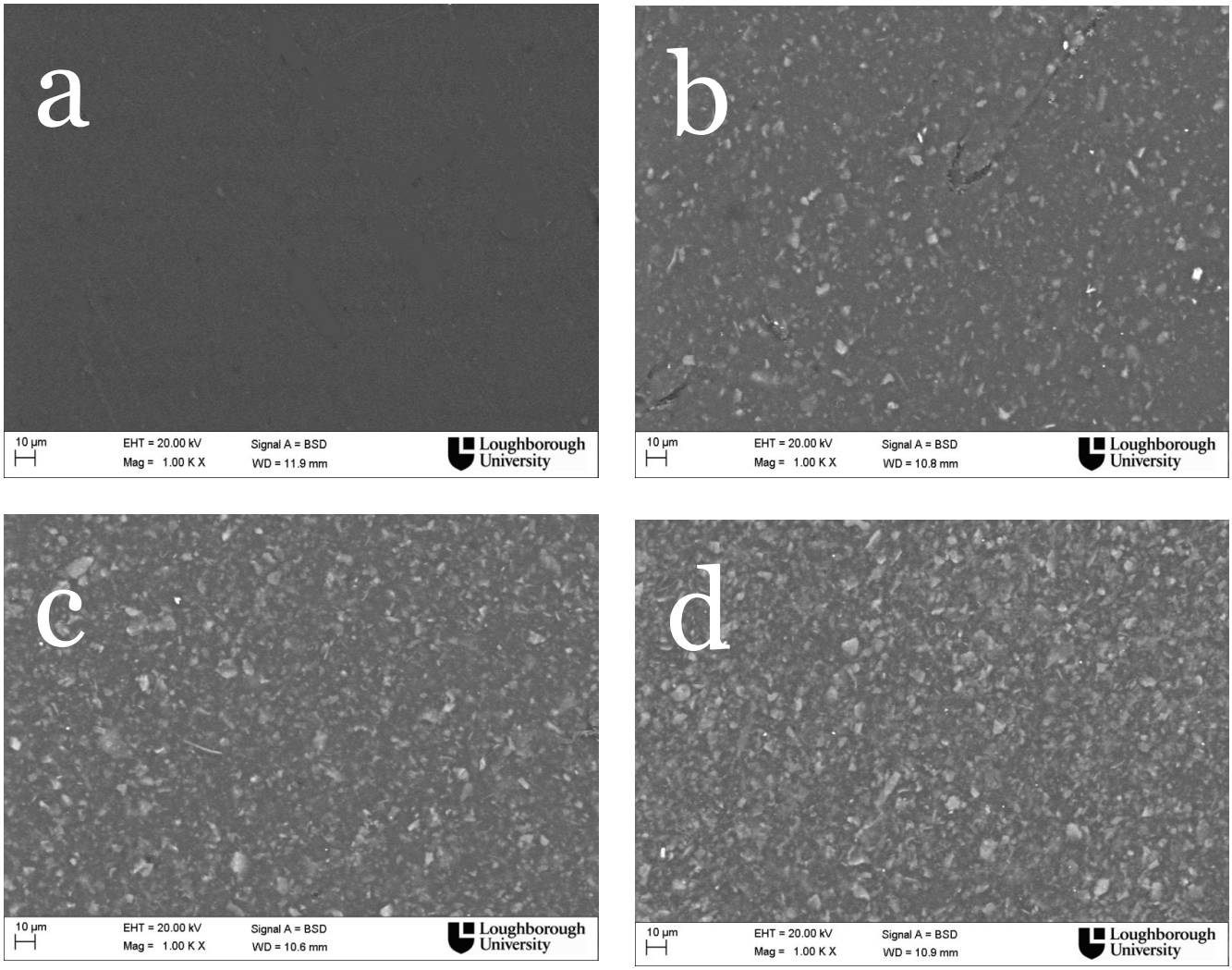

Figure 7- 12: Backscattered SEM micrograph of PLA / Talc 2 composite
(a) Pure PLA, (b) 90/10 , (c) 80/20, (d) 70 /30

Generally the backscattered analysis of the composite surfaces indicates even distribution of the talc in the matrix. These images show that the talc particles are uniformly distributed in the matrix and have tended to align parallel to the sample surface.

Transmission Electron Microscopy (TEM) was used to characterize the morphology of the PLA /talc composites. The TEM picture of pure PLA is shown in Figure 7- 13.

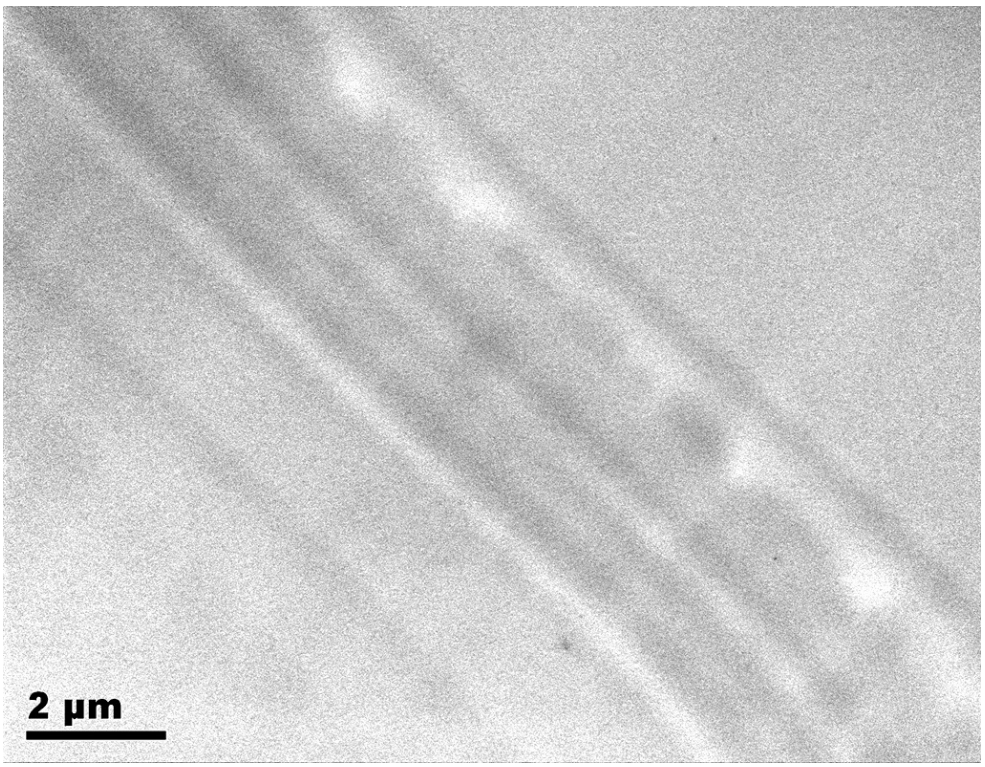

Figure 7- 13: TEM Micrographs of pure PLA

The TEM micrographs of cross-sections through the samples containing 10 (wt %) and 30 (wt %) micro Talc1 and Talc2 are shown in Figure 7- 14 (a, b) and Figure 7- 15 (a, b) respectively. In these micrographs, the talc particles are in black and the PLA matrix is the light gray background. It is observed from these images that the talc particles are well distributed within the polymer matrix and have predominantly aligned along the flow direction of the polymer melt. It appears that particles of talc 1 are more uniformly dispersed in the PLA matrix compared with talc 2. Some evidence of agglomeration is also observed in Figure 7- 15, where platy shapes of coarse particles are joined together and restricting the homogeneous dispersion of the filler in the matrix. This contributes to a reduction in toughness , because it has been shown in that the toughness decreases with the addition of coarse particles, also reported by DePolo and Baird [134].

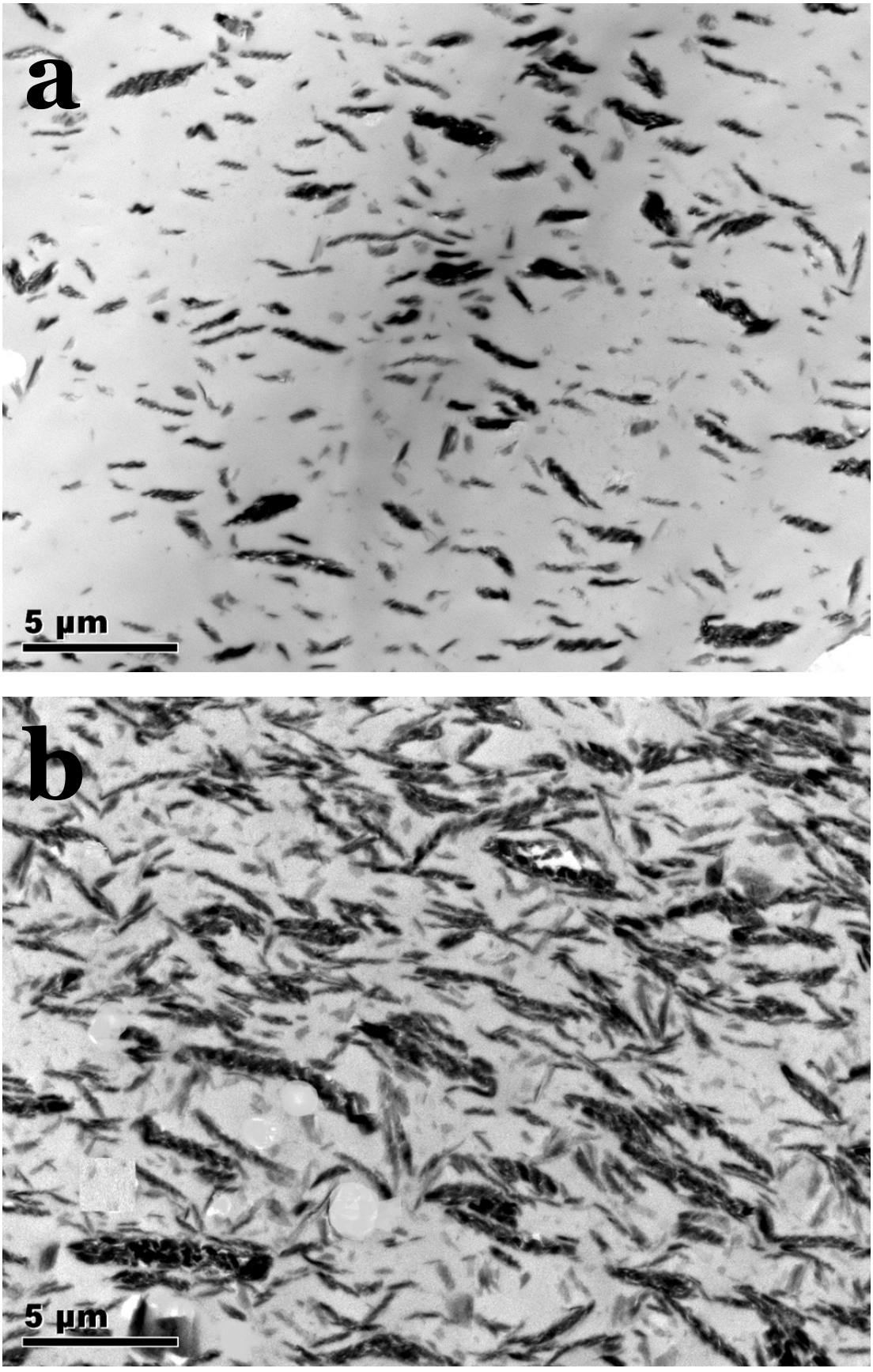

Figure 7- 14: TEM Micrographs of PLA / Talc1 Composites (a) 90/10, (b) 70/30

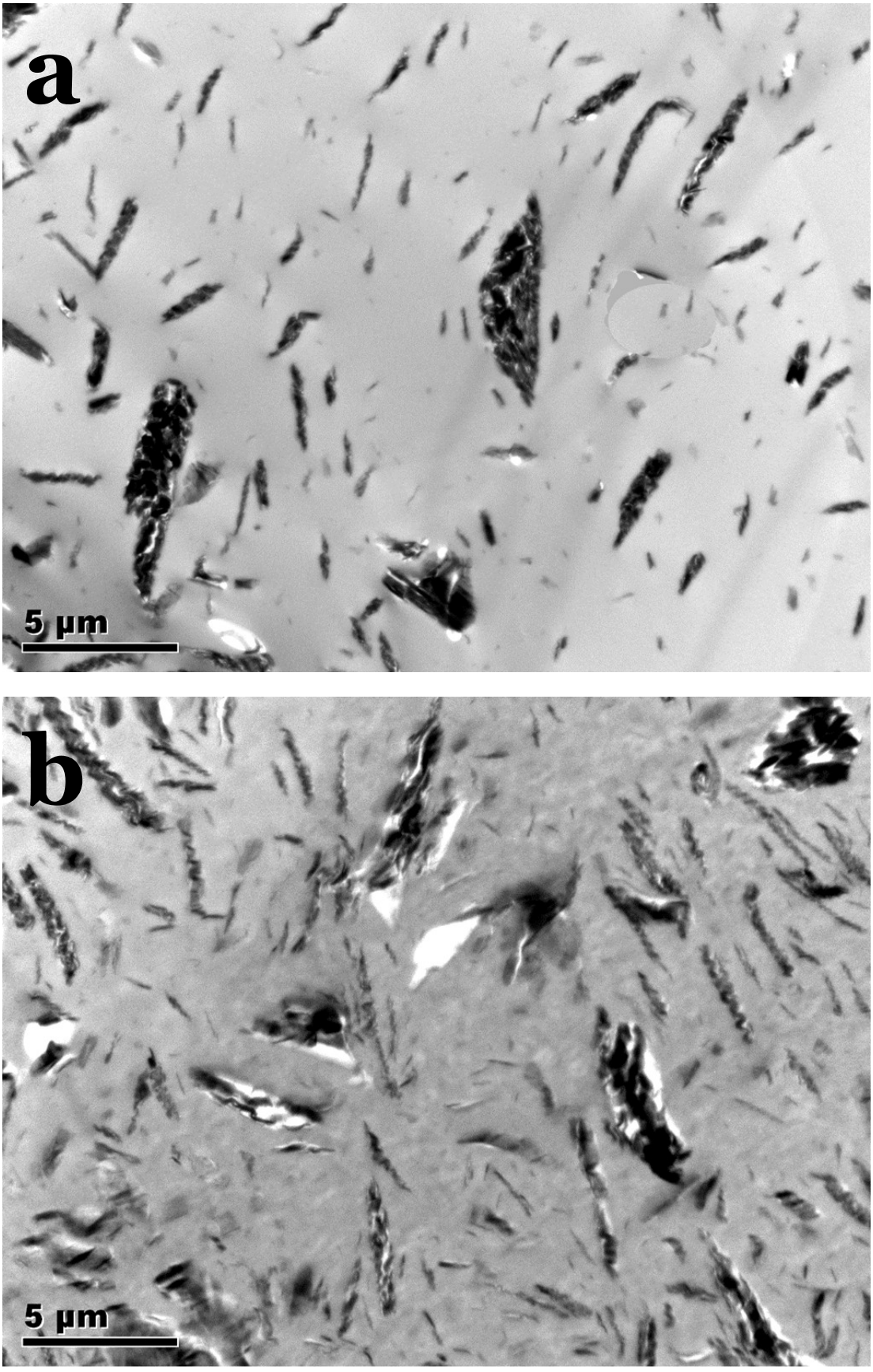

Figure 7- 15: TEM Micrographs of PLA / Talc2 Composites (a) 90/10, (b) 70/30

Fracture surfaces of the PLA/talc composites containing different concentrations of Talc 1 and Talc 2 at a loading level of 10 (wt%) and 30 (wt%) are shown in Figure 7- 16 (a, b) and Figure 7- 17 (a, b) respectively. These images suggest good dispersion of talc into the PLA matrix, resulting in a homogeneous composite.

Generically these micrographs confirm the brittle nature of the failure in the tensile test. There is evidence of pull out of some talc particles from the surface. The talc was not coated with any coupling agent, so although it is well distributed because of its relatively hydrophobic surface, overall there is not good surface adhesion between the talc and the polymer matrix.

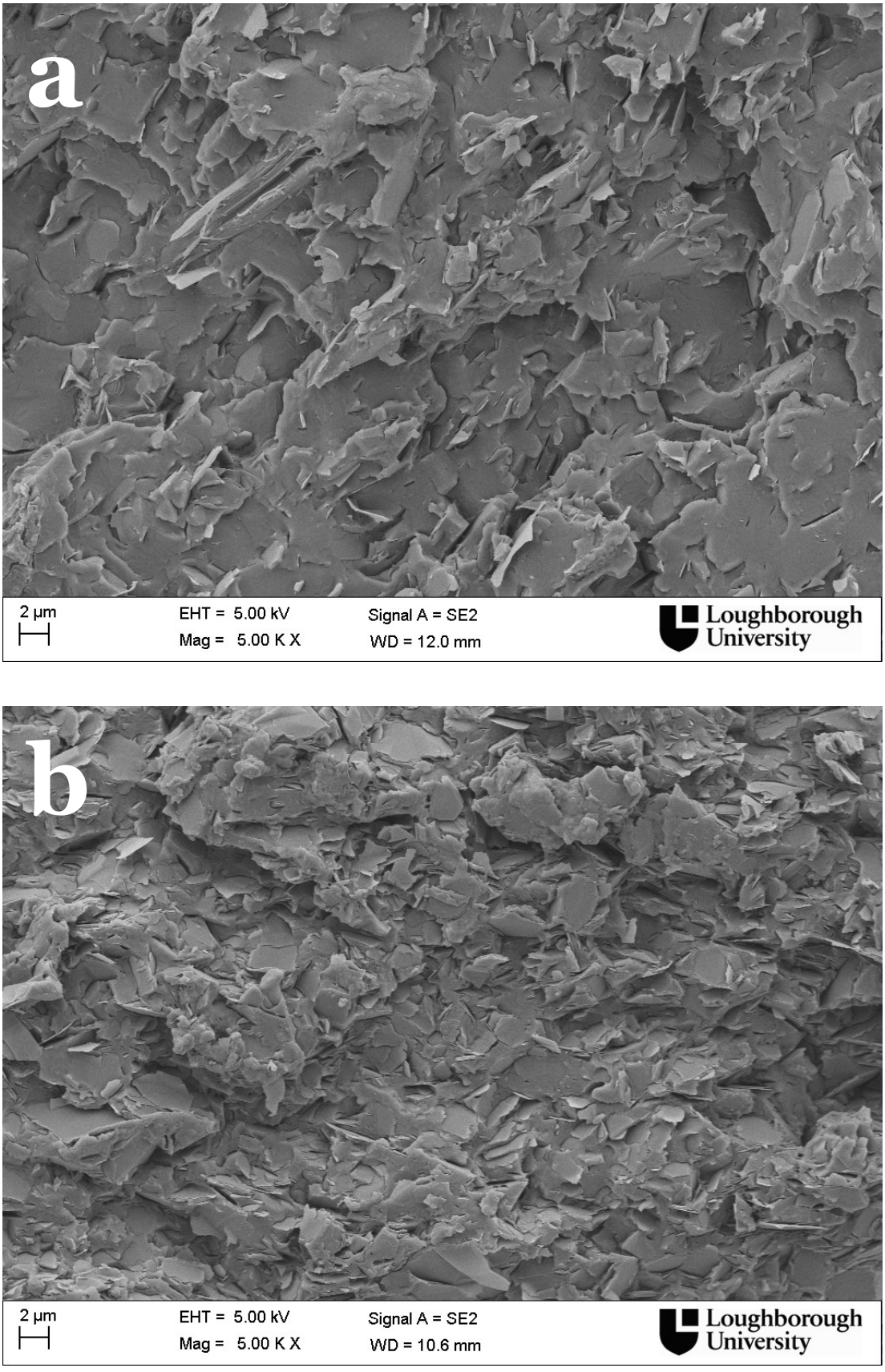

Figure 7- 16: SEM Images of tensile –fractured surfaces of a PLA / Talc1 Composites: (a) 90 / 10 , (b) 70 / 30

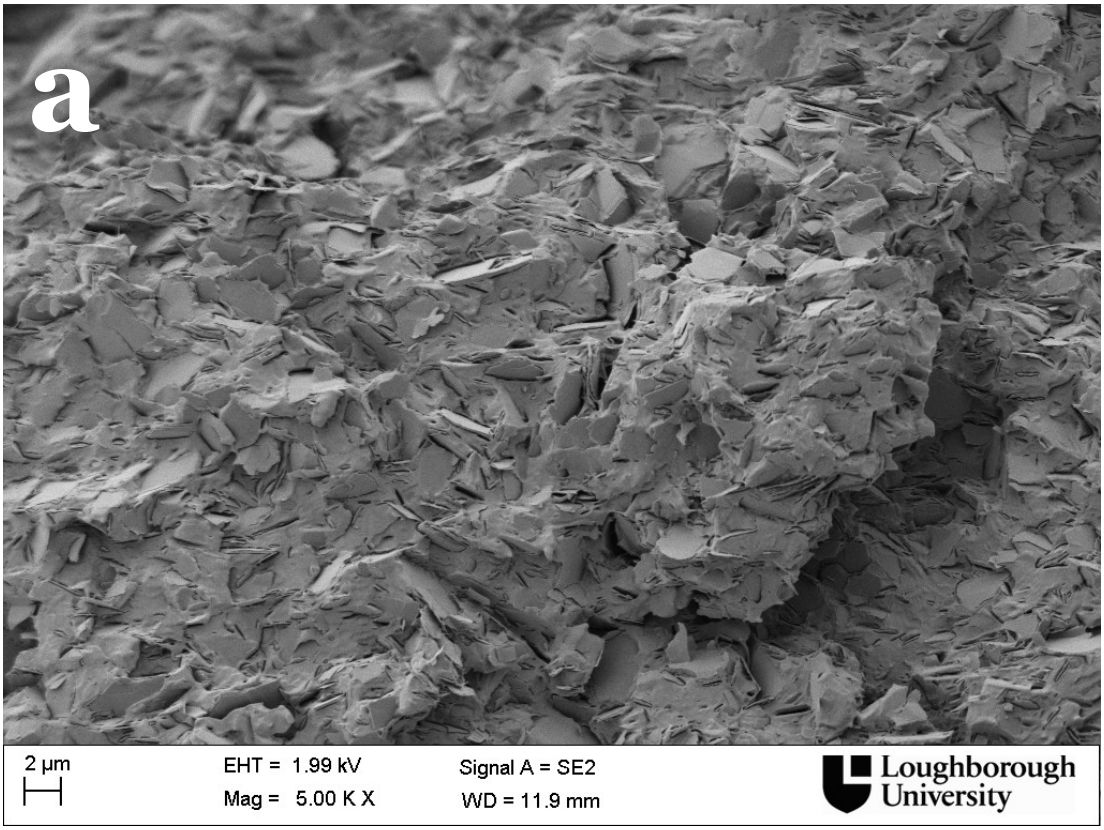

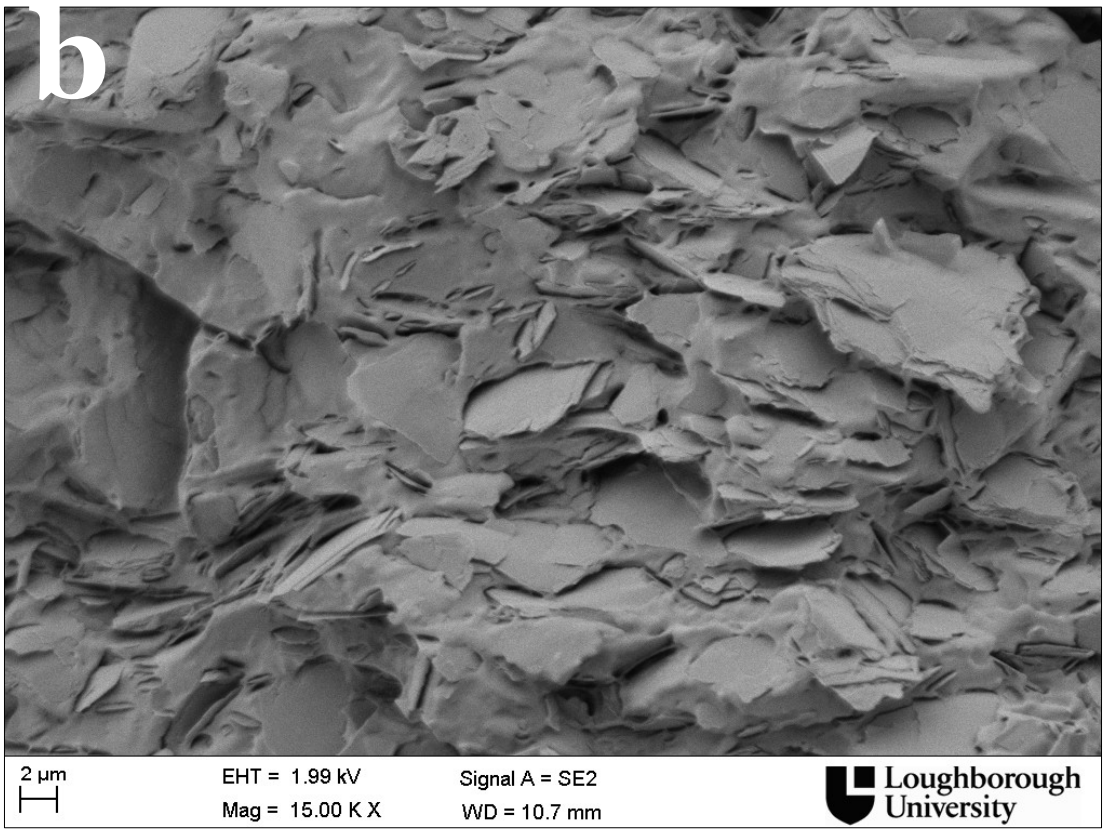

Figure 7- 17: SEM Images of tensile –fractured surfaces of a PLA / Talc2 Composites: (a) 90 / 10 , (b) 70 / 30

7.5 Dynamic Mechanical Properties

The temperature dependence of the dynamic storage modulus of PLA and PLA /Talc1 composites is given in Figure 7- 18 which is a plot of the logarithm of the storage modulus as a function of temperature. It is clear from the plot that the addition of talc to the PLA matrix gives a very significant increase in the storage modulus of the samples, depending on the amount of talc added.

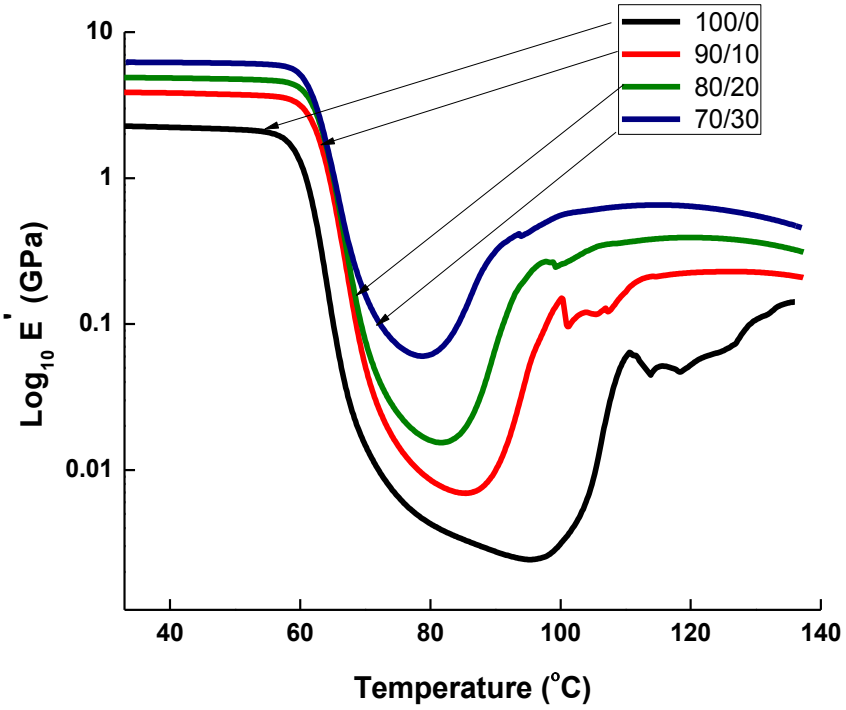

Figure 7- 18: Storage Modulus as a Function of Temperature for PLA/Talc 1 Composites

The figure shows that the storage moduli of the PLA and PLA/Talc 1 composites remain almost constant at temperatures below the glass transition temperature (up to about 60°C) and then drop at the Tg, as would be expected for an amorphous polymer. It is seen that for all the samples, as the temperature continues to increase, the drop in storage modulus is arrested and the modulus starts to increase again. This is due to the recrystallisation of the PLA. The extent to which this happens is determined by the amount of talc present: the greater the amount of talc, the lower the temperature at which recrystallisation takes place. This confirms the earlier

observations made in the DSC tests that talc acts as a nucleating agent for the crystallization of PLA. This observation has implications for the softening and heat distortion of PLA. The fact that talc acts as both a reinforcing filler and a nucleating agent for recrystallisation of PLA, implies that it is a useful additive to increase the heat distortion temperature (HDT) of PLA.

Figure 7- 19 shows the plot of Tan Delta (Tan δ) as a function of temperature for PLA and PLA /Talc 1 composites. Tan δ is the loss factor, which is the ratio of the loss modulus to the storage modulus. It describes the extent of viscous dissipation of energy in a polymer and is related to molecular motion. There is a particularly strong damping at the glass transition because the large increase in volume that occurs above Tg allows space for molecular motion to take place. Hence the main peak in the Tan δ versus the temperature plot corresponds to the Tg of the polymer.

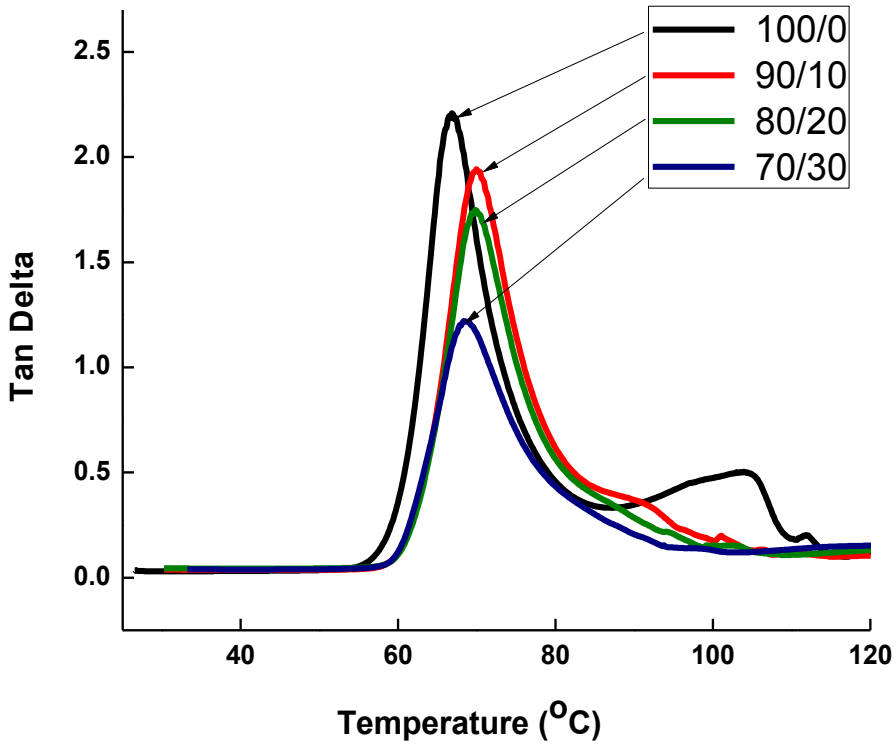

Figure 7- 19: Tan Delta as a Function of Temperature for PLA and PLA /Talc1 Composites

It can be observed from Figure 7- 19 that the peak position is significantly shifted towards higher temperature when Talc 1 is added to the PLA matrix. As in the case of the DSC results, this small increase in Tg on the addition of significant amounts of talc to PLA can be interpreted in terms of a constraint on the mobility of the polymer chains by the addition of a platy filler. Another observation which is made from Figure 7- 19 is that the area under the Tan δ peaks decreases with increasing talc content and this implies a reduced damping capability in the composites with increasing talc addition. This also ties in with the reduction in elongation-to-break found in the mechanical (tensile) property measurements.

The values of the flexural storage modulus for PLA and PLA /Talc 1 composites at 30°C and 40°C are given in Table 7- 4. It can be seen from the table that measured values increase from 2.3 (GPa) for PLA up to 3.9, 4.9 and 6.3 (GPa) on the addition of 10, 20 and 30 (wt %) Talc1 respectively, bringing a significant improvement in the flexural modulus. The improvement in the storage modulus was in line with the increase in the tensile moduli discussed above. The storage modulus of neat PLA obtained from DMA is not equal to the tensile modulus, which can be attributed to the nature and application of stresses in both tests, also reported by Whaling et al. [80] .

Table 7- 4: Thermo-mechanical Properties of PLA and PLA /Talc1 Composites

Sample codes	Glass Transition Tg (°C)	Storage Modulus (Flexure) @ 30°C (GPa)	Storage Modulus (Flexure) @ 40°C (GPa)
100/0	66	2.3	2.2
90 /10	67	3.9	3.8
80 /20	67	4.9	4.8
70 /30	69	6.3	6.2

Figure 7- 20 shows the temperature dependence of the storage modulus of PLA and PLA/talc 2 composites, in the form of logarithm of the storage modulus as a function of temperature. The storage modulus increases linearly with increasing content of the talc in the composites. As described earlier, a continuous drop in modulus is observed with increasing temperature. The sharp transition curve is observed around 60^{o}C, but again increasing around 80 –100 ^{o}C, indicating recrystallisation (i.e. cold crystallization). This is useful in resisting softening and heat distortion of PLA. It is also evident that cold crystallization starts at a lower temperature with the increasing content of the filler in PLA, thus accelerating the crystallization process, a confirmation of DSC findings in Table 7-3. Huda et al. [110] have also studied the effect of talc and recycled wood on PLA and PP and reported the same kind of viscoelastic behaviour of the composites.

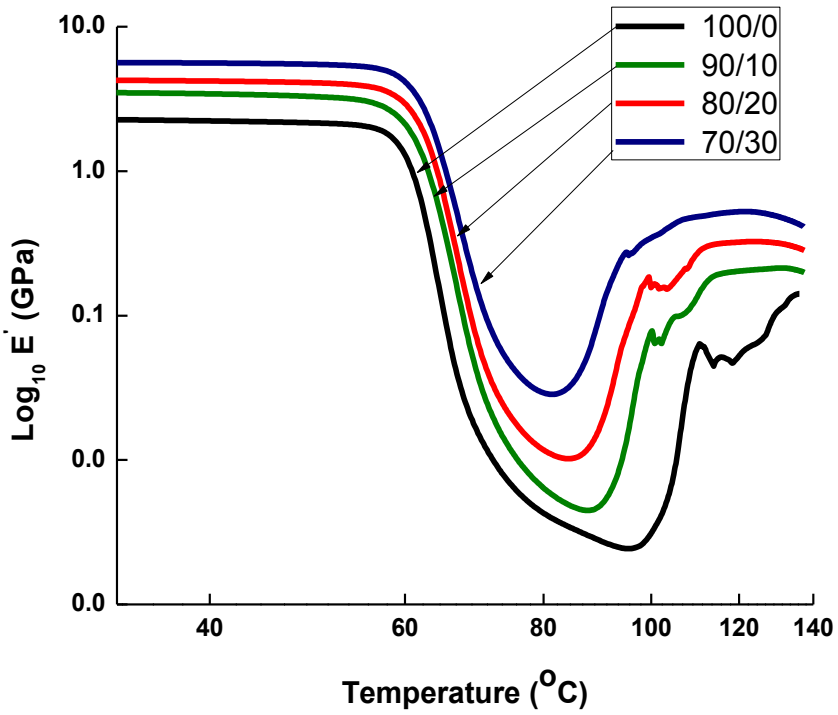

Figure 7- 20: Storage Modulus as a Function of Temperature for PLA / Talc 2 Composites

The effect of temperature on the loss factor (*Tan δ*) for pure PLA and PLA /Talc 2 composites is shown in Figure 7- 21 The peak of *Tan δ* decreases with the increasing talc level and shows a slight shift towards higher temperature. It is also evident from the figure that the area of integration under the Tan δ curve decreased with the increasing talc content, indicating a decrease in the damping campability of the composite. It can be deduced that Talc 2 has a similar effect to Talc 1 on thermo-mechanical properties of the polylactic acid composites.

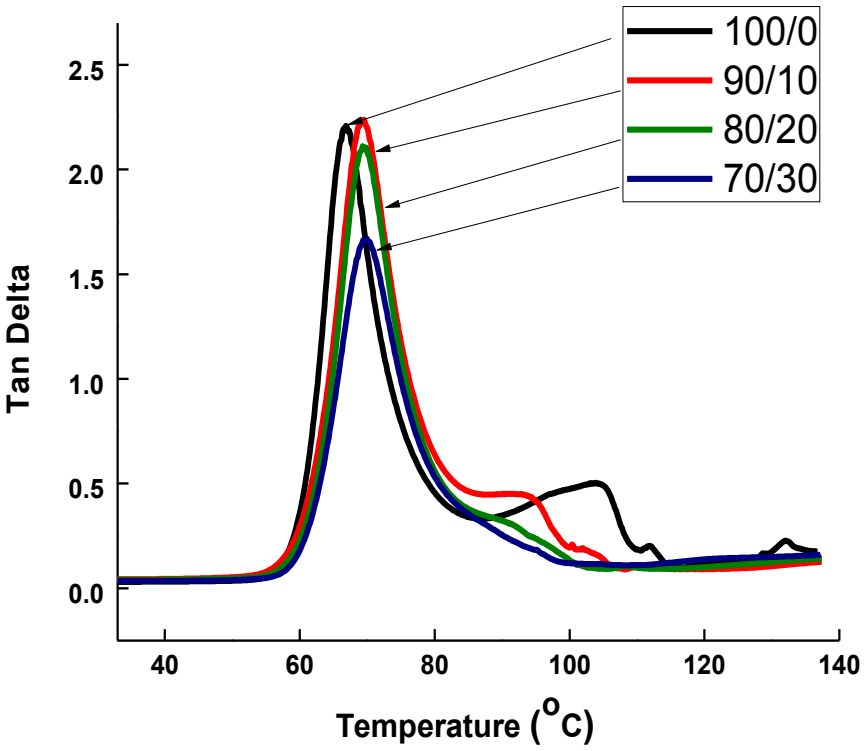

Figure 7- 21: Tan Delta as a Function of Temperature for PLA/Talc 2 Composites

The values of the storage modulus in flexural mode for PLA and PLA/Talc 2 composites at 30°C and 40°C are given in Table 7- 5. It can be seen from the table that measured values increase from 2.3 GPa for PLA up to 3.5, 4.3 and 5.6 GPa on the addition of 10, 20 and 30 (wt%) Talc2 respectively, bringing a significant improvement in the flexural modulus. Improvement in the modulus of PLA- Talc composites when Talc 1 is incorporated into the PLA matrix is higher compared with

Talc 2. The Glass transition temperature is also given in the Table 7- 5, calculated as the peak of the Tan delta curve given in Figure 7- 21 above. There can be seen to be a slight but significant increase in Tg.

Table 7- 5: Thermo-mechanical Properties for PLA and PLA /Talc 2 Composites

Sample codes	Glass Transition Tg (^oC)	Storage Modulus (Flexure) @ 30^oC (GPa)	Storage Modulus (Flexure) @ 40^oC (GPa)
100/0	66	2.3	2.2
90 /10	67	3.5	3.4
80 /20	69	4.3	4.2
70 /30	69	5.6	5.5

7.6 **Conclusions**

According to the results obtained from the experiments, the following conclusions can be drawn;

The talc was found to be acting as a nucleating agent for crystallization of PLA and overall crystallinity significantly improved. The crystallinity of the PLA increased from 2 to 30 (%) when the content of talc increased from 0 to 30 (wt %). It was also observed that talc has accelerated the cold crystallization of PLA and the crystallization temperature decreased from 127 to 96 (^oC) when the content of talc increased from 0 to 30 (wt %).

There was significant improvement in Young's modulus of the composites with increasing talc addition and these results were found to fit the Halpin Tsai model. The Young's modulus increased from 4.1 to 9.8 (GPa) when the content of talc increased from 0 to 30 (wt %). The elongation to break reduced as the content of talc increased and the composite exhibits brittle failure.

Thermo-mechanical tests confirmed that the combination of increased crystallinity and storage modulus leads to improvement in the heat distortion properties. The storage modulus increased from 2.2 to 6.3 (GPa) with increasing content of talc.

Chapter 8 Conclusions and Further Work

8.1 Conclusions

The objective of this research was to investigate PLA as a matrix in a composite system where natural fibres (wood, flax) and mineral fillers (talc) are used as reinforcement, and to measure the properties of the composites produced. From this research the following conclusions are summarised.

8.1.1 PLA- Wood Composites

Wood fibres were used as reinforcement in the form of flour, to characterise the mechanical and thermal properties of PLA- wood composites. Different levels of wood flour content were incorporated into the PLA matrix. Non-dried wood (NDW) flour and dried –wood (DW), both were mixed to see the difference in terms of mechanical and thermal properties in the first phase. In the second phase, copolymer (CP) was mixed with PLA-wood composites to facilitate the penetration of polymer matrix into the fibre. In the third phase the effect of fibre treatment on mechanical properties of PLA-wood composites was investigated.

According to the results obtained from the experiments, the following conclusions can be drawn;

1. PLA is an almost amorphous polymer with a small amount of crystalline content which has a melting temperature around 155^{o}C to 160 ^{o}C. Glass transition temperature is around 55 ^{o}C. PLA starts cold crystallization at higher temperature around 100^{o}C. There is unique double peak observed in the melting endotherm.

2. Wood flour enhances the crystallinity of PLA but PLA-wood composites behave in a more brittle way as strain at break reduced as levels of wood increased from 0 to 40 (wt%). Incorporation of non-dried and dried wood flour increases the elastic and flexural modulus significantly but tensile

strength reduces as the level of wood flour content increased compared to neat PLA. Young's modulus of PLA increased from 4.1 to 8.7 (GPa) when the content of wood increased from 0 to 40(wt %). The experimental values from tensile testing were compared with theoretical response based on Halpin-Tsai equation, with a reasonable agreement. Loss factor (Tan δ peak) lies in the same temperature zone with incorporation of wood fibre resulting in a decrease in area of integration under the Tan δ curve. This indicates the brittle behaviour of PLA– wood composite and reduces the damping capability of the resulting material.

3. Addition of dried or non-dried wood did not make any significant difference in terms of mechanical or thermal properties; findings from both experiments were quite similar.

4. SEM images suggest that wood fibres are homogeneously mixed within the PLA matrix, and most of the fibres break during the tensile testing showing good adhesion between the fibres and the matrix. All the samples exhibit brittle failure as seen by fracture surface morphology examination under SEM.

5. Various contents of copolymer were added to reduce the viscosity of the PLA matrix and to ease the penetration of the matrix into the narrow lumens of wood particles and fill the hollow regions in PLA wood composites. The mechanical and thermal properties of PLA were affected by incorporation of copolymer into PLA- wood flour composite to a great extent. Glass transition temperature reduced from 55^{o}C to 48^{o}C compared to neat PLA. PLA-wood-copolymer composites start crystallizing at lower temperature during cold crystallization compared to neat PLA-wood composite. Young's modulus increased due to incorporation of copolymer but reduced at higher loading. Tensile strength of PLA - wood - copolymer reduced compared to neat PLA but was still better than the neat PLA - wood composite. Incorporation of copolymer into PLA - wood composite affected the Tan δ peak, it shifted towards lower temperature, showing decrease in glass transition temperature and reducing the area of integration under the Tan δ curve.

6. The wood fibres were subjected to two different procedures during the silane chemical treatment, in an attempt to improve the interfacial strength and mechanical properties of wood fibres and PLA matrix composites. The wood fibres were treated with 3 (wt %) of silane agent coupling mixing with acetone compared to the fibre (wt %). It was observed that the average tensile strength and young's modulus of the silane treated wood based PLA composites decreased compared to neat PLA- wood composites. Discolouration of the PLA- wood composites was observed compared to non-treated. The reduction in average tensile strength and young's modulus could be due to the degradation of silane, occurring during processing. It was also thought that the amount of the silane coupling agent used was believed to be more than the recommended amount of silane, which might have decoupled the interface between the fibres and matrix rather than improve the interfacial strength between the wood and the PLA.

8.1.2 PLA- Flax Composites:

Flax fibres were used to reinforce PLA. Different loading of flax fibres were incorporated into the PLA matrix and their properties was investigated. In order to improve the toughness of the PLA-flax composites, epoxidised natural rubber (ENR) was incorporated. New formulations based on PLA-Flax-ENR composites were developed and their properties were analysed.

According to the results obtained from the experiments, the following conclusions can be drawn;

1. The PLA-flax composites exhibited the same thermal properties as compared with PLA- wood composites. The glass transition temperature for PLA -flax composites is around 54 (^{o}C) and an exothermic peak appears around 100 (^{o}C) corresponding to cold crystallization. The melting peak (endothermic peak) occurs at 150 to 160 (^{o}C). A double peak appears in the melting endotherm indicating two different entities: either different crystalline structures or

spherulites. These peaks become clearer as the content of flax increases from 0 to 30 (wt %).

2. The heat treatment significantly affects the crystallization behaviour of PLA composites. In order to balance the mechanical properties of the fibres and the matrix, the PLA-flax-ENR composites were annealed at 120 (^{o}C) during compression moulding. The crystallinity of PLA-flax-ENR composites increased from 3 to 35 (%) with annealing for 20 minutes. DSC analysis confirmed the effect of heat treatment.

3. Incorporation of flax fibres increases the elastic and flexural modulus significantly but tensile strength reduces as the level of flax content increased compared to neat PLA. Young's modulus of PLA increased from 4.1 to 8.5 (GPa) when the content of flax increased from 0 to 30 (wt %). The experimental values compared with the theoretical values based on the rule of mixtures. Addition of flax fibres brings stiffening effect into the PLA composites and causes reduction in the elongation at break and tensile strength of the composites.

4. Morphological analysis of fractured surface for PLA – flax composites showed a uniform distribution of the fibres in the matrix. Most of the fibres break clearly but fibre pull-out was also observed and believed to be one of the reasons for reduced tensile strength.

5. Integral blending of ENR into the PLA and Flax composites did not affect the mechanical properties of the composites and the samples exhibit brittle failure. The morphology show separate phases which is an indicative of poor adhesion between the ingredients of the composites.

6. Introducing a masterbatch (pre-mixed) of flax and ENR into the PLA matrix in order to avoid the direct exposure of the flax fibres into the PLA significantly affects the mechanical properties of the composites. Rubber mixing method seems to be more effective in order to improve the toughness of the PLA- Flax composites. Incorporating flax–ENR masterbatch into PLA

gives better toughening mechanism than the integral blending of ENR with PLA and flax.

7. The elongation to break was significantly improved and elastic modulus was reduced with introduction of the flax and ENR into the PLA. The strain at break increased from 2 to 14 (%), while Young's modulus reduced from 4.1 to 2.2 (GPa) when a masterbatch of flax and ENR mixed with PLA compared to integral mixing of ENR, flax and PLA. Improvement in the strain at break and area under the stress-strain curve, thus shows improvement in the toughness of the composites. This also indicates better interaction between the flax and PLA.

8. The DMA results showed a very significant increase in the storage modulus of the samples, depending on the amount of flax added. Above Tg there is an increase in modulus for samples containing flax fibres. Also the area under the tan delta curve also reduced, indicating the stiffening effect in the composites. The area under the tan delta curve reduced, thus the damping capability of the composites decreased and reconfirms the tensile results.

9. The storage modulus curves for annealed samples decrease slightly above Tg and level off again, thus suggesting an improvement in heat distortion properties of the composites. This is because the sample has crystallized.

10. The incorporation of masterbatch of flax and ENR into the annealed samples decreased the storage modulus and the position of the peak of the tan delta curve remained unchanged, thus showing no significant change in Tg. The area under the curves increased with incorporation of ENR, thus the damping capability of the composites increased compared to PLA- flax composites. Hence investigating the viscoelastic properties of the composites reinforced the results obtained from tensile testing.

8.1.3 PLA – Talc composites

Talc has been used as reinforcing filler in the PLA matrix, in order to investigate the thermal, tensile (mechanical), thermo-mechanical and morphological properties of

PLA- talc composites. Two different types of talc with different particle sizes were incorporated into the PLA matrix. The effect of talc and particle size on the crystallization behaviour and mechanical properties of PLA/talc composites were studied at weight ratios of 100/0, 90/10, 80/20 and 70/30. The following conclusions have been drawn.

1. The DSC heating scans showed that the cold crystallization temperature (T_c) was reduced from 127 (°C) for the pure PLA to 96 (°C) for the PLA/talc composites demonstrating a nucleating effect by the talc filler. Pure PLA was found to be essentially amorphous with a crystallinity of only 2 (%), whereas the crystallinity increased to 25 (%) after addition of talc. For both types of talc, same effect was observed in thermal properties.

2. As talc was found to be a nucleating agent for PLA composites, this was further evidenced by the DSC cooling scans: pure PLA was amorphous, with no crystallisation (exothermic) peak, whereas addition of talc gave rise to an exothermic crystallisation peak in the cooling scan.

3. Morphology of the composites was observed by both scanning and transmission electron microscopy. The talc particles were seen to be uniformly distributed and predominantly aligned along the flow direction of the polymer melt.

4. The aspect ratio of the ultra-fine talc particles dispersed in the PLA matrix was measured from the transmission electron micrographs and found to be an average value of 8.

5. All samples exhibited brittle failure in tensile testing. There was a significant increase in Young's modulus from a value of 4.1 (GPA) for the pure PLA up to 5.8, 7.0 and 9.8 (GPa) on the addition of 10, 20 and 30 (weight %) of talc respectively.

6. There was found to be a good fit between these data and the theoretical prediction from the Halpin Tsai model.

7. The DMA results showed a very significant increase in the storage modulus of the samples, depending on the amount of talc added. Above Tg there is an increase in modulus for samples containing talc, due to the recrystallisation of the PLA caused by the nucleating effect of the talc. The results indicate that talc is a useful additive to increase the heat distortion temperature (HDT) of PLA because it acts as both reinforcing filler and a nucleating agent.

8. It was observed that ultra fine (0.9μm) talc has a more effective reinforcement capability compared with the higher particle size (2.2μm), but not different in affecting the thermal and thermo-mechanical properties.

8.2 Further Work

1. To study the effect of copolymers in combination with the plasticiser or liquid ester on the mechanical and thermal properties of PLA- wood composites.

2. To study the toughening effect of ENR on the mechanical properties of PLA-wood composites.

3. To study the optimised effect of Silane coupling agent on the properties of PLA-wood composites.

4. To study the rheological characteristics of PLA and its composites.

5. To study the effect of stearic acid coating of talc on the PLA –talc composites.

6. To study the mechanism by which talc acts as a nucleating agent for PLA.

References

1. A.K, Mohanty , M. Mishra, and L.T.D. Drzal, *Sustainable Bio-Composites from Renewable Resources: Opportunities and Challenges in the Green Materials World*. Journal of Polymer and the Environment, 2002. **10**(1 / 2): p. 254 - 262.

2. A.K. Mohanty, M. Misra , and L.T. Drzal *Poly Lactic acid Technology*, in *Natural Fibres, Biopolymers, and Biocomposites*2005, CRC: Michigan , USA. p. 527 - 578.

3. E.Vink, K. Rábago, D. Glassner, and P. Gruber, *Applications of life cycle assessment to NatureWorks™ polylactide (PLA) production*. Polymer Degradation and Stability, 2003. **80**(3): p. 403-419.

4. R. Auras, B. Harte, and S. Selke, *An overview of polylactides as packaging materials*. Macromol Biosci, 2004. **4**(9): p. 835-64.

5. M. Okada, C*hemical Synthesis of biodegradable Polymers*. Progress in Polymer Science, 2002. **27**: p. 87 -133.

6. D.R. Witzke, *Introduction to Properties, Engineering and prospects of Polylactide Polymers*, in *Materials* 1997, Michigan State University: USA.

7. R.E. Drumright, P.R. Gruber , and D.E. Henton, *Polylactic Acid Technology*. Advanced Materials, 2000. **12**(23): p. 1841 -1846.

8. V.K.Velde, and P. Kiekens, *Biopolymers: overview of several properties and consequences on their applications*. Polymer Testing, 2002. **21**: p. 433 - 442.

9. J.Pandey, S. Ahn, C. Lee, A. Mohanty, and M. Misra, *Recent Advances in the Application of Natural Fiber Based Composites*. Macromolecular Materials and Engineering, 2010. **295**(11): p. 975-989.

10. E.S. Stevens, *Green Plastics : An Introduction to the New Science of Biodegradable Plastics*2001: Princeton University Press.

11. R. Auras, L. Lim, S. Selke, and H. Tsuji, *Poly(lactic acid) - Synthesis, Structures, Properties, Processing, and Applications*, ed. R.F. Grossman and D. Nwabunma2010, New Jersey.: John Wiley & Sons. 522.

12. L.S.Nair, and C.T. Laurencin, *Biodegradable polymers as biomaterials*. Progress in Polymer Science, 2007. **32**(8-9): p. 762-798.

13. A.K, Mohanty, M. Mishra, and G. Hinrichsen, *Biofibres- biodegradable polymers and biocomposites- An Overview*. Macromolecular Materials and Engineering, 2000. **276 / 277**: p. 1-24.

14. M. García, I. Garmendia, and J. García, *Influence of natural fiber type in eco-composites*. Journal of applied polymer science, 2008. **107**(5): p. 2994-3004.

15. R.A. Auras, B. Harte, S. Selke, and R. Hernandez, *Mechanical, Physical, and Barrier Properties of Poly(Lactide) Films*. Journal of Plastic Film and Sheeting, 2003. **19**(2): p. 123-135.

16. M. Avella, A. Buzarovska, M.E. Errico, G. Gentile, and A. Grozdanov, *Eco-Challenges of Bio-Based Polymer Composites*. Materials, 2009. **2**(3): p. 911-925.

17. K. Oksman, M. Skrifvars, and J.F. Selin, *Natural fibres as reinforcement in polylactic acid (PLA) composites*. Composites Science and Technology, 2003. **63**(9): p. 1317-1324.

18. C.N. Cutter, *Opportunities for bio-based packaging technologies to improve the quality and safety of fresh and further processed muscle foods*. Meat Sci, 2006. **74**(1): p. 131-142.

19. R.C. Hardmen, *Biopolymers : Making Materials Nature's Way* 1993, U.S. Congress, Office of technology.

20. M.A. Hubbe, *Bioresources : From here to Sustainability*. Bioresources 2006. **1**(2): p. 1- 149.

21. D. Garlotta, *A Literature Review of Poly(Lactic Acid)*. Journal of Polymers and the Environment, 2001. **9**(2): p. 63 - 84.

22. J. Christophe, and P. Coszach, *PLA : A potential solution to plastic waste dilemma*. Macromolecular Symposia, 2000. **153**: p. 287 - 303.

23. P. Skelton, *Biopolymer packaging in UK grocery market*, 2006, Materials change for a better environment.

24. M. Murariu, A.D.S. Ferreira, E. Duquesne, L. Bonnaud, and P. Dubois, *Polylactide (PLA) and Highly Filled PLA - Calcium Sulfate Composites with Improved Impact Properties*. Macromolecular Symposia, 2008. **272**(1): p. 1-12.

25. D.M. Bigg, *Mechanical Properties of Particulate Filled Polymers*. Physical Composites, 1987. **8**(2).

26. J.S. Bergstrom, and M.C. Boyce, M*echanical behavior of particle filled elastomers*. Rubber Chemical Technology, 1999. **72**(633 - 656).

27. D. Plackett, T. Løgstrup Andersen, W. Batsberg Pedersen, and L. Nielsen, *Biodegradable composites based on l-polylactide and jute fibres*. Composites Science and Technology, 2003. **63**(9): p. 1287-1296.

28. R. Mani, and M. Bhattacharya, *Properties of injection moulded blends of starch and modified biodegrdabe polyesters*. European Journal, 2001. **37**: p. 515 - 526.

29. M.S. Huda, L.T. Drzal, M. Misra, A.K. Mohanty, K. Williams, and D.F. Mielewski, *A study on biocomposites from recycled newspaper fiber and poly (lactic acid)*. Industrial & engineering chemistry research, 2005. **44**(15): p. 5593-5601.

30. J. Markarian, *Biopolymers present new market opportunities for additives in packaging*. Plastics, Additives and Compounding, 2008. **10**(3): p. 22-25.

31. F. Vilaplana, E. Strömberg, and S. Karlsson, *Environmental and resource aspects of sustainable biocomposites*. Polymer Degradation and Stability, 2010. **95**(11): p. 2147-2161.

32. A.C.Albertsson, and S. Karlsson, *Aspects of biodeterioration of inert and degradable polymers*. International biodeterioration & biodegradation, 1993. **31**(3): p. 161-170.

33. M. Wollerdorfer, and H. Bader, *Influence of natural fibres on the mechanical properties of biodegradable polymers*. industrial Crops and Products, 1998. **8**: p. 105 -112.

34. Y. Ikada, and H. Tsuji, *Biodegradable polyesters for medical and ecological applications*. Macromolecular Rapid Communications, 2000. **21**: p. 117 - 132.

35. R. Mehta, V. Kumar, H. Bhunia, and S.N. Upadhyay, *Synthesis of Poly(Lactic Acid): A Review*. Journal of Macromolecular Science, Part C: Polymer Reviews, 2005. **45**(4): p. 325-349.

36. W. Amass, A. Amass, and B. Tinghe, *A Review of Biodegradable Polymer : Uses, Current Developments in the Synthesis and Characterization of biodegradable Polyester, Blends of Biodegradable Polymers and Recent Advances in Bidegradation Studies.* Polymers International, 1998. **47**: p. 89 - 144.

37. L. Avérous, and F. Le Digabel, *Properties of biocomposites based on lignocellulosic fillers.* Carbohydrate Polymers, 2006. **66**(4): p. 480-493.

38. S. Taj, M.A. Munawar, and S. Khan, *Review : Natural fibres reinforced polymer composites* Proc. Pakistan Academic Society 2007. **44**(2): p. 129 - 144.

39. B. Gupta, N. Revagade, and J. Hilborn, *Poly(lactic acid) fiber: An overview.* Progress in Polymer Science, 2007. **32**(4): p. 455-482.

40. J. Slager, and A.J. Domb, *Biopolymer stereocomplexes.* Advanced Drug Delivery Reviews, 2003. **55**(4): p. 549-583.

41. J. Burlet, M.-C. Heuzey, C. Dubois, P. Wood-Adams, and J. Brisson. *Thermal stabilization of high molecular weight l-polylactide.* in ANTEC. 2005.

42. R.Auras, B. Harte, and S. Selke. P*olylactides. a new era of biodegradable polymers for packaging application.* in ANTEC. 2005.USA.

43. C. HUA, D. VlPUL, A. RICHARD, C. CROSS, and P.M. STEPHEN, *Effects of Physical Aging, Crystallinity, and Orientation on the Enzymatic Degradation of Poly(Lactic acid).* Journal of Polymer Science: Part B: Physics, 1996. **34**: p. 2701 - 2708.

44. H. Tsuji, and Y. Ikada, *Blends of Aliphatic Polyesters. 1. Physiacal properties and morphologies of solution -Cast blends from Poly(DL-lactide) and Poly (c-caprolactone).* Journal of applied polymer science, 1996. **60**: p. 2367 - 2375.

45. R. Auras, *Polylactic acid based biocomposites* in *Engineering*2004, Michigan State University: East Lashing

46. J.J.KOLSTAD, *Crystallization Kinetics of Poly(i-lactide-co-meso-lactide).* Journal of applied polymer science, 1996. **62**: p. 1079 - 1091.

47. R.J. Young, and P.A. Lovell, *Introduction to Polymers.* Vol. 2nd Edition. 1991, Montreal, Canada: CRC Press.

48. T.M. Ovitt, and G.W. Coates, *Stereoselective ring-opening polymerization of rac-lactide with a single-site, racemic aluminum alkoxide catalyst: Synthesis of stereoblock poly (lactic acid).* Journal of Polymer Science Part A: Polymer Chemistry, 2000. **38**(S1): p. 4686-4692.

49. T.M. Ovitt, and G.W. Coates, *Stereochemistry of lactide polymerization with chiral catalysts: new opportunities for stereocontrol using polymer exchange mechanisms.* Journal of the American Chemical Society, 2002. **124**(7): p. 1316-1326.

50. B.M. Chamberlain, M. Cheng, D.R. Moore, T.M. Ovitt, E.B. Lobkovsky, and G.W. Coates, *Polymerization of lactide with zinc and magnesium β-diiminate complexes: stereocontrol and mechanism.* Journal of the American Chemical Society, 2001. **123**(14): p. 3229-3238.

51. Di Lorenzo, M.L., *Crystallization behavior of poly (L-lactic acid).* European Polymer Journal, 2005. **41**(3): p. 569-575.

52. A. Celli, and M. Scandola, *Thermal properties and physical ageing of poly (l-lactic acid).* Polymer, 1992. **33**(13): p. 2699-2703.

53. B. Kalb, and A. Pennings, *General crystallization behaviour of poly (L-lactic acid).* Polymer, 1980. **21**(6): p. 607-612.

54. P. Badrinarayanan, K.B. Dowdy, and M.R. Kessler, *A comparison of crystallization behavior for melt and cold crystallized poly (l-Lactide) using rapid scanning rate calorimetry*. Polymer, 2010. **51**(20): p. 4611-4618.

55. F. De Santis, R. Pantani, and G. Titomanlio, *Nucleation and crystallization kinetics of poly (lactic acid)*. Thermochimica Acta, 2011. **522**(1): p. 128-134.

56. T. Ke, and X. Sun, *Melting behavior and crystallization kinetics of starch and poly (lactic acid) composites*. Journal of Applied Polymer Science, 2003. **89**(5): p. 1203-1210.

57. H. Li, and M.A. Huneault, *Effect of nucleation and plasticization on the crystallization of poly (lactic acid)*. Polymer, 2007. **48**(23): p. 6855-6866.

58. S. Saeidlou, M.A. Huneault, H. Li, and C.B. Park, *Poly (lactic acid) Crystallization*. Progress in Polymer Science, 2012.

59. M. Ajioka, K. Enomoto, K. Suzuki, and A. Yamaguchi, *The Basic Properties of Poly(lactic Acid) Produced by the Direct Condensation Polymerization of Lactic Acid*. Journal of Environmental Polymer Degradation, 1995. **3**(4): p. 225 -235.

60. I. Engelberg, and J. Kohn, *Physico-mechanical properties of degradable polymers used in medical applications: a comparative study*. Biomaterials, 1991. **12**: p. 292 -304.

61. D.W. Grijpma, H. Altpeter, M.J. Bevis, and J. Feijen, *Improvement of the mechanical properties of poly(D,L-lactide) by orientation*. Polymer International, 2002. **51**: p. 845 - 851.

62. A.C. Renouf-Glauser, J. Rose, D.F. Farrar, and R.E. Cameron, *The effect of crystallinity on the deformation mechanism and bulk mechanical properties of PLLA*. Biomaterials, 2005. **26**(29): p. 5771-82.

63. G. Perego, D. Cella, and C. Bastioli, *Effect of Molecular Weight and Crystallinity on Poly(lactic acid) Mechanical Properties*. Journal of applied polymer science, 1996. **59**: p. 37-43.

64. D. Grijpma, A.J. Nijenhuls, P. Wijk Van, and A.J. Pennings, *High impact strength as-polymerized PLLA*. polymer Bulletin, 1992. **29**: p. 571 - 578.

65. S. Park, M. Todo, and K. Arakawa, *Effect of annealing on the fracture toughness of poly(lactic acid)*. JOUrnal of Materials Science, 2004. **39**: p. 1113-1116.

66. M. John, and S. Thomas, *Review : Biofibres and biocomposites*. Carbohydrate Polymers, 2008. **71**(3): p. 343-364.

67. P.A. Fowler, J.M. Hughes, and R.M. Elias, *Review: Biocomposites: technology, environmental credentials and market forces*. Journal of the Science of Food and Agriculture, 2006. **86**(12): p. 1781-1789.

68. M. Jacob, and S. Thomas, *Biofibres and Biocomposites*, 2000, School of Chemical Science, Mahatma Gandhi University: India.

69. X.Y. Liu, and G. Dai, *Surface modification and micromechanical properties of jute fiber mat reinforced polypropylene composites*. eXPRESS Polymer Letters, 2007. **1**(5): p. 299-307.

70. A.K. Bledzki, S. Reihmane, and J. Gussan, *Properties and modification methods for vegetable fibres for natural fiber composites*. Journal of applied polymer science, 1996. **59**(1329 -1336).

71. A.A. Shah, F. Hasan, A. Hameed, and S. Ahmed, *Biological degradation of plastics: a comprehensive review*. Biotechnol Adv, 2008. **26**(3): p. 246-65.

72. S. Taj, M.A. Munawar, and S. Khan, *Review : Natural fiber reinforced polymer composites*. Proc. Pakistan Academic Society, 2007. **44**(2): p. 129 - 144.

73. L.H. Pawel, Zadorecki., and P. Flodin, *Cellulose Fiber-Polyester Composites With Reduced Water Sensitivity (1) - Chemical treatment and Mechanical properties.* Polymer Composites, 1987. **8**(3): p. 199 -203.

74. M.D. Beg, *The Improvement of Interfacial Bonding, Weathering and Recycling of Wood Fibre Reinforced Polypropylene Composites*, in *Materials and Process Engineering* 2007, The University of WAIKATO: New Zealand p. 194.

75. A.C.E.Dent, C.R. Bowen, R. Stevens, M.G. Cain, and M. Stewart, *Tensile Strength of Active Fibre Composites – Prediction and Measurement*. Ferroelectrics, 2008. **368**(1): p. 209-215.

76. L.R. Mathews, and R.D. Rawlings, *Composite Materials: Engineering and Science*1999, England: CRC.

77. K. Kalaprasad, K. Joseph , S. Thomas, and C. Pavithran, *Theoretical modelling of tensile properties of short sisal fibre-reinforced low-density Polyethylene composites*. Journal of Materials Science, 1997. **32**: p. 4261 -4267.

78. P.V. Joseph, G. Mathew, K. Joseph, S. Thomas, and P. Pradeep, *Mechanical properties of short sisal fiber-reinforced polypropylene composites: Comparison of experimental data with theoretical predictions*. Journal of applied polymer science, 2003. **88**(3): p. 602-611.

79. K. Joseph, R.D.T. Filho, B. James, S. Thomas, and L.H.d. Carvalho, A *review on sisal fiber reinforced polymer composites*. Reviews in Agricultural Sciences., 1999. **3**(3): p. 367 -379.

80. A. Whaling, R. Bhardwaj, and A.K. Mohanty, *Novel Talc-Filled Biodegradable Bacterial Polyester Composites*. Industrial & Engineering Chemistry Research, 2006. **45**: p. 7497 - 7503.

81. B.L. Shah, S.E. Selke, M.B. Walters, and P.A. Heiden, *Effects of wood flour and chitosan on mechanical, chemical, and thermal properties of polylactide.* Polymer Composites, 2008. **29**(6): p. 655-663.

82. S.Y. Fu, X.-Q. Feng, B. Lauke, and Y.-W. Mai, *Effects of particle size, particle/matrix interface adhesion and particle loading on mechanical properties of particulate–polymer composites.* Composites Part B: Engineering, 2008. **39**(6): p. 933-961.

83. S.Y. Fu, X Hu, and C.Y. Yue, *A new model for the transverse modulus of unidirectional fiber composites*. Journal of Materials Science, 1998. **33**: p. 4953 - 4960.

84. S. Jain, M.M. Reddy, A.K. Mohanty, M. Misra, and A.K. Ghosh, *A New Biodegradable Flexible Composite Sheet from Poly(lactic acid)/Poly(ε-caprolactone) Blends and Micro-Talc.* Macromolecular Materials and Engineering, 2010. **295**(8): p. 750-762.

85. T.B. Lewis, and L.E. Nielsen, *Dynamic Mechanical Properties of Particulate- Filled Composites* Journal of applied polymer science, 1970. **14**: p. 1449 - 1471.

86. M.A. Sawpan, *Mechanical Performance of Industrial Hemp Fibre Reinforced Polylactide and Unsaturated Polyester Composites*, in *Materials and Process Engineering* 2009, The University of WAIKATO: Hamilton , New Zealand. p. 229.

87. S.K. Sinha, and M.C. Wang, *Artificial Neural Network Prediction Models for Soil Compaction and Permeability*. Geotechnical and Geological Engineering, 2007. **26**(1): p. 47-64.

88. A.J. Rice, *Mathematical Statistics and Data Analysis*. Vol. 3rd Edition. 2007, USA: Brooks /Cole. 621.

89. F.P. La Mantia, and M. Morreale, *Green composites: A brief review*. Composites Part A: Applied Science and Manufacturing, 2011. **42**(6): p. 579-588.

90. A.N. Netravali, and S. Chabba, *Composites get greener*. Materials Today, 2003. **6**(4): p. 22-29.

91. K.G, Satyanarayana, G.G.C. Arizaga, and F. Wypych, *Biodegradable composites based on lignocellulosic fibres—An overview*. Progress in Polymer Science, 2009. **34**: p. 982 -1021.

92. N. Graupner, A.S. Herrmann, and J. Müssig, *Natural and man-made cellulose fibre-reinforced poly(lactic acid) (PLA) composites: An overview about mechanical characteristics and application areas*. Composites Part A: Applied Science and Manufacturing, 2009. **40**(6-7): p. 810-821.

93. M.S. Huda, L.T. Drzal, and A. Mohamed, *Wood fiber reinforced poly(lactic acid) composites*, in *5th Annual SPE Automotive Composites Conference*2005, SPE: Troy, Michigan

94. A.K. Bledzki, A.K. and J. Gassan, *Composites reinforced with cellulose based fibres*. Progress in Polymer Science, 1999. **24**: p. 221 - 274.

95. Y. Li, Y., Y.W. Mai, and L. Ye, *Sisal fiber andits composites: a review of recent developments*. Composite Science and Technology, 2000. **60**: p. 2037 -2055.

96. S.Y. Lee, I.A. Kang, G.H. Doh, H.G. Yoon, B.D. Park, and W. Qinglin, *Thermal and Mechanical Properties of Wood Flour/Talc-filled Polylactic Acid Composites: Effect of Filler Content and Coupling Treatment*. Journal of Thermoplastic Composite Materials, 2008. **21**(3): p. 209-223.

97. S. Pilla, S. Gong, E. O'Neill, L. Yang, and R.M. Rowell, *Polylactide-recycled wood fiber composites*. Journal of applied polymer science, 2009. **111**(1): p. 37-47.

98. K. Manjula Dilkushi Silva, K. Tarverdi, R. Withnall, and J. Silver, *Incorporation of wheat starch and coupling agents into poly (lactic acid) to develop biodegradable composite*. Plastics, Rubber and Composites, 2011. **40**(1): p. 17-24.

99. I.E. Zhang, and X. Sun, *Mechanical Properties of Poly(lactic acid)/Starch Composites Compatibilized by Maleic Anhydride*. Biomacromolecules, 2004. **5**: p. 1446 - 1451.

100. M.S. Huda, L. Drzal, A. Mohanty, and M. Misra, *Chopped glass and recycled newspaper as reinforcement fibres in injection molded poly(lactic acid) (PLA) composites: A comparative study*. Composites Science and Technology, 2006. **66**(11-12): p. 1813-1824.

101. I. Ahmed, P.S. Cronin, E.A. Abou Neel, A.J. Parsons, J.C. Knowles, and C.D. Rudd, *Retention of mechanical properties and cytocompatibility of a phosphate-based glass fiber/polylactic acid composite*. J Biomed Mater Res B Appl Biomater, 2009. **89**(1): p. 18-27.

102. X. Hu, H.-S. Xu, and Z.-M. Li, *Morphology and Properties of Poly(L-Lactide) (PLLA) Filled with Hollow Glass Beads*. Macromolecular Materials and Engineering, 2007. **292**(5): p. 646-654.

103. E. Ferrage, F. Martin, A. Boudet, S. Petit, G.Fourty, F. Jouffret, *Talc as nucleating agent of polypropylene: morphology induced by lamellar particles addition and interface mineral-matrix modelization*. Journal of Materials Science, 2002. **37**(8): p. 1561-1573.

104. B. Chen, and J.R.G. Evans, *Elastic moduli of clay platelets*. Scripta Materialia, 2006. **54**(9): p. 1581-1585.

105. M.S. Huda, L.T. Drzal, A.K. Mohanty, and M. Misra, *The effect of silane treated- and untreated-talc on the mechanical and physico-mechanical properties of poly(lactic acid)/newspaper fibres/talc hybrid composites*. Composites Part B: Engineering, 2007. **38**(3): p. 367-379.

106. B. Fillon, A. Thierry, B. Lotz, and J.C. Wittmann, *Efficiency Scale for Polymer Nucleating-Agents*. Journal of Thermal Analysis, 1994. **42**(4): p. 721-731.

107. S.N. Maiti, and K.K. Sharma, *Studies on polypropylene composites filled with talc particles: Part 1 Mechanical Properties.* Journal of Materials Science, 1992(27).

108. M. Murariu, L. Bonnaud, P. Yoann, G. Fontaine, S. Bourbigot, and P. Dubois, *New trends in polylactide (PLA)-based materials: "Green" PLA–Calcium sulfate (nano)composites tailored with flame retardant properties.* Polymer Degradation and Stability, 2010. **95**(3): p. 374-381.

109. A.C. Fowlks, and R. Narayan, *The effect of maleated polylactic acid (PLA) as an interfacial modifier in PLA-talc composites*. Journal of Applied Polymer Science, 2010. **118**(5): p. 2810-2820.

110. M.S. Huda, L.T. Drzal , and M. Misra *A Study on Biocomposites from Recycled Newspaper Fiber and Poly(lactic acid).* Industrial & Engineering Chemistry Research, 2005. **44**: p. 5593 - 5601.

111. A.M Harris, and E.C. Lee, *Improving mechanical performance of injection molded PLA by controlling crystallinity*. Journal of applied polymer science, 2008. **107**(4): p. 2246-2255.

112. D.D Kee, and Q. meng, *Mechanical and thermal roperties of pla/clay/wood nanocomposites*. Polymer research online, 2006.

113. B. Bax, and J. Müssig, *Impact and tensile properties of PLA/Cordenka and PLA/flax composites.* Composites Science and Technology, 2008. **68**(7-8): p. 1601-1607.

114. S. Pilla, S. Gong, E. O'Neill, R.M. Rowell, and A.M. Krzysik, *Polylactide-pine wood flour composites.* Polymer Engineering & Science, 2008. **48**(3): p. 578-587.

115. A.P.Mathew, K. Oksman, and M. Sain, *Mechanical properties of biodegradable composites from poly lactic acid (PLA) and microcrystalline cellulose (MCC).* Journal of applied polymer science, 2005. **97**(5): p. 2014-2025.

116. S.S. Ray, K. Yamada, A. Ogami, M. Okamoto, and K. Ueda, *New Polylactide/Layered Silicate Nanocomposite: Nanoscale Control Over Multiple Properties.* Macromolecular Rapid Communication, 2002. **23**(16): p. 943 - 947.

117. A.P. Mathew, K. Oksman, and M. Sain, *The effect of morphology and chemical characteristics of cellulose reinforcements on the crystallinity of polylactic acid.* Journal of applied polymer science, 2006. **101**(1): p. 300-310.

118. T. Tabi, I.E. Sajo, A.S. Luyt, and J.G. Kavacs, *Crystalline structure of annealed polylactic acid and its relation to processing*. eXPRESS Polymer Letters, 2010. **4**(10): p. 659-668.

119. A. Ashori, *Wood-plastic composites as promising green-composites for automotive industries!* Bioresour Technol, 2008. **99**(11): p. 4661-7.

120. S. Huda, L.T. Drzal, A.K. Mohanty, M. Misra, K. Williams, and D.F. Mielewski. *Mechanical, Thermal and Morphological Studies of Poly (lactic acid) PLA/Talc/Recycled Newspaper Fiber Hybrid 'Green'Composites*. 2005.

121. R.Jaratrotkamjorn, C. Khaokong, and V. Tanrattanakul, *Toughness enhancement of poly(lactic acid) by melt blending with natural rubber*. Journal of Applied Polymer Science, 2012: p. 5027-5036.

122. J.R Sarasua, R.E. Prud'homme, M. Wisniewski, L.A. Borgene, and N. Spassky, *Crystallization and Melting Behavior of Polylactides.* Macromolecules, 1998. **31**: p. 3895 - 3905.

123. J. Zhang, K. Tashiro, H. Tsuji, and J.A. Domb, *Disorder-to-Order Phase Transition and Multiple Melting Behavior of Poly(L-lactide) Investigated by Simultaneous Measurements of WAXD and DSC.* Macromolecules, 2008. **41**: p. 1352 - 1357.

124. T. Mukherjee, and N. Kao, *PLA Based Biopolymer Reinforced with Natural Fibre: A Review*. Journal of Polymers and the Environment, 2011. **19**(3): p. 714-725.

125. Andersons, J., E. Spārniņš, and R. Joffe, *Stiffness and strength of flax fiber/polymer matrix composites*. Polymer Composites, 2006. **27**(2): p. 221-229.

126. P.K.Bajpai, I. Singh, and J. Madaan, *Development and characterization of PLA-based green composites: A review*. Journal of Thermoplastic Composite Materials, 2012.

127. N. Bitinis, R. Verdejo, P. Cassagnau, and M.A. Lopez-Manchado, *Structure and properties of polylactide/natural rubber blends*. Materials Chemistry and Physics, 2011. **129**(3): p. 823-831.

128. C. Zhang, W. Wang, Y. Huang, Y. Pan, L. Jiang, Y. Dan, Y. Luo, and Z. Peng, *Thermal, mechanical and rheological properties of polylactide toughened by expoxidized natural rubber*. Materials & Design, 2013. **45**: p. 198-205.

129. S. Ishida, R. Nagasaki, K. Chino, T. Dong, and Y. Inoue, *Toughening of Poly(L-lactide) by Melt Blending with Rubbers*. Journal of Applied Polymer Science, 2009. **113**(1): p. 558-566.

130. S. Wong, A.R. Shanks, and A. Hodzic, *Poly(L4actic acid) Composites With Flax Fibres Modified by Plasticizer Absorption*. Polymer Engineering and Science, 2003. **43**(9): p. 1566 - 1575.

131. T. Tabi, I.E. Sajo, F. Szabo, A.S. Luyt, and J.G. Kovacs, *Crystalline structure of annealed polylactic acid and its relation to processing*. eXPRESS Polymer Letters, 2010. **4**(10): p. 659-668.

132. M. Nofar, W.L. Zhu, C.B. Park, and J. Randall, *Crystallization Kinetics of Linear and Long-Chain-Branched Polylactide*. Industrial & engineering chemistry research, 2011. **50**(24): p. 13789-13798.

133. L. Mascia, *Thermoplastics: Materials Engineering*. Second ed1989, London: Elsevier Applied Science.

134. W.S. DePolo, and D.G. Baird, *Particulate reinforced PC/PBT composites. I. Effect of particle size (nanotalc versus fine talc particles) on dimensional stability and properties*. Polymer Composites, 2009. **30**(2): p. 188-199.